1-1-2017

Biochemical and Molecular Assessment of Toxicity of Primaquine Metabolites on Erythrocytes

Jagrati Jain
University of Mississippi

BIOCHEMICAL AND MOLECULAR ASSESSMENT OF TOXICITY OF PRIMAQUINE METABOLITES ON ERYTHROCYTES

A dissertation
presented in partial fulfillment of the requirements
for the Degree of Doctor of Philosophy
in the Department of BioMolecular Sciences
Division of Pharmacology
School of Pharmacy
The University of Mississippi

By

JAGRATI JAIN

August 2017

ABSTRACT

The 8-aminoquinoline (8AQ) antimalarial drug primaquine (PQ) is the only drug for prevention of malaria relapse. Moreover, PQ also has gametocytocidal activity against *Plasmodium falciparum*. However, clinical use of PQ has been limited due to its hemolytic toxicity, especially in glucose-6-phosphate dehydrogenase deficient (G6PDd) individuals. Phenolic and quinone metabolites generated via cytochrome P_{450}-dependent pathways appear to be responsible for hemolytic effects of PQ. However, the mechanism for the hemolytic toxicity of PQ is still poorly understood.

To explore the mechanism, targets, and pathways for toxicity of PQ, normal and G6PDd human erythrocytes were treated with the potential hemotoxic metabolites of PQ namely, 5-hydroxy-primaquine (5-HPQ), 5,6-orthoquinone primaquine (5,6-OQPQ) and 6-methoxy-8-hydroxylaminoquinoline (MHQ). The early and late biomarkers of hemotoxicity were investigated to explore the mechanism of PQ toxicity. 5-HPQ, 5,6-OQPQ, and MHQ caused marked increase in methemoglobin formation and generated robust oxidative stress in both normal and G6PDd human erythrocytes. However, these metabolites depleted reduce glutathione (GSH) levels selectively in G6PDd human erythrocytes. Treatment with 5,6-OQPQ also induced eryptosis in G6PDd erythrocytes, as determined by phosphatidylserine exposure (Annexin V binding).

This study was further extended to investigate the role of NRH-quinone oxidoreductase 2 (NQO2) in PQ-induced hemolytic toxicity. NQO2, has a potential function in metabolic detoxification or activation of quinones and quinone-based drugs. Co-treatment of erythrocytes

with NQO2 inhibitors potentiated the hemotoxic response of PQ metabolites. The computational docking studies suggested stronger interactions of PQ metabolites with NQO2 compared to melatonin (the NQO2 inhibitor) and menadione (the NQO2 substrate). Together these results suggest that NQO2 might have a protective role against PQ-induced hemolytic toxicity.

The PQ metabolite, 5,6-OQPQ was further evaluated for the effects on the non-targeted global metabolomic profile of normal and G6PDd human erythrocytes. The GSH-methionine-glutamate pathway metabolites were greatly affected by G6PD deficiency. Treatment with 5,6-OQPQ also significantly modified GSH-methionine-glutamic acid pathway in erythrocytes. Treatment also increased the levels of antioxidant and hemolysis related markers in erythrocytes.

These studies provide a better insight into the pathophysiology of hemolytic toxicity caused by PQ in the G6PDd population.The new knowledge generated would provide rational bases for controlling toxicity of PQ and designing 8AQ analogs with better safety and therapeutic profiles.

DEDICATION

This work is dedicated to my husband, daughter, siblings, and parents. Without their continuous support, encouragement, and inspiration I would not have accomplished what I accomplished today.

LIST OF ABBREVIATIONS

2’7’-dichlorofluorescein diacetate (DCFDA)

4-hydroxy-2-,3-trans-nonenal (HNE)

5,6-orthoquinone primaquine (5,6-OQPQ)

5-hydroxy-primaquine (5-HPQ)

5-methyldeoxycitidine (MDC)

6-methoxy-8-hydroxylaminoquinoline (MHQ)

6-methyltetrahydropterin (MTH)

Acquired immunodeficiency syndrome (AIDS)

Adenosine diphosphate (ADP)

Adenosine monophosphate (AMP)

Adenosine triphosphate (ATP)

Alkoxyl radicals ($RO^{\cdot}$)

Analysis of Variance (ANOVA)

Asparagine (Asn)

Aspartic acid (Asp)

Asymmetric dimethylarginine (ADMA)

Beta-citryl-glutamic acid (BCGA)

Catalase (CAT)

Cytosine monophosphate (CMP)

Dapsone (DDS)

Dapsone hydroxylamine (DDSNOH)

Data-dependent acquisitions (DDA)

Deoxycytidine monophosphate (dCMP)

Dihydronicotinamide riboside (NRH)

Extra precision (XP)

Flavin adenosine dinucleotide (FAD)

Flavin adenosine dinucleotide dihydrogen (FADH2)

Fluorescence isothiocyanate (FITC)

Glucose-6-phosphate dehydrogenase deficient (G6PDd)

Glutamic acid (GLU)

Glutamine (GLN)

Glutathione peroxidase (GPx)

Glutathione reductase (GR)

Glycerophosphocholine (GPC)

Guanosine diphosphate (GDP)

Human liver microsomes (HLM)

Human metabolome database (HMDB)

Hydrogen peroxide (H_2O_2)

Hydroxyl radical ($OH^{\cdot}$)

Hypochlorous acid (HClO)

Immunoglobulin (Ig)

Injection time (IT)

Inosine monophosphate (IMP)

Institutional review board (IRB)

Liquid chromatography (LC)

Lysophosphatidylcholines (LPC)

Malondialdehyde (MDA)

Mass spectrometry (MS)

Melatonin (Mel)

Methemoglobin (MtHb)

Methionine (Met)

Molecular oxygen (O_2)

Mouse liver microsomes (MLM)

NADPH-quinone oxidoreductase 1 (NQO1)

Nicotinamide adenine dinucleotide (NAD)

Nicotinamide adenine dinucleotide hydrogen (NADH)

Nicotinamide adenine dinucleotide phosphate (NADP)

Nicotinamide adenosine dinucleotide phosphate hydrogen (NADPH)

Nicotinamide mononucleotide (NMN)

Nitric oxide radical ($NO^{\cdot}$)

Nitrofurantoin (NFT)

NRH-quinone oxidoreductase 2 (NQO2)

Oxidized glutathione (GSSG)

Ozone (O_3)

Part per million (ppm)

Phenyl Alanine (Phe)

Phosphate buffered saline glucose (PBSG)

Phosphatidylserine (PS)

Primaquine (PQ)

Principle Components Analysis (PCA)

Prostaglandin-E2 (PGE2)

Protein Database (PDB)

Quercetin (Quer)

Reactive oxygen species (ROS)

Reduced glutathione (GSH)

Resveratrol (Res)

RFU- Relative fluorescence unit.

S-(1,2-Dicarboxyethyl) Glutathione (DCE-GS)

S-Adenosylhomocysteine (SAH)

S-Adenosyl-methionine (SAM)

Serine (Ser)

Singlet oxygen ($^1O_2$)

Superoxide dismutase (SOD)

Superoxide ion radical ($O^{\cdot -}{}_2$)

Symmetric dimethylarginine (SDMA)

Tris(2-carboxyethyl)phosphine hydrochloride (TCEP)

Tryptophan (TRP)

Two Dimensional (2D)

Ultra-high-performance liquid chromatography (UHPLC)

Valine (Val)

ACKNOWLEDGMENTS

First of all, I would like to thank my advisor, Dr. Babu L. Tekwani for his guidance, support, and encouragement during my Ph.D. I am grateful for him to share his wisdom with me. He taught me to analyze my work critically and has also provided perceptive discussions about the research. I have learned so much from him, which will be invaluable for my future scientific career.

I want to express my profound and sincere gratitude and thank my dissertation and original research proposal committee members, Dr. Kristie Willett, Dr. Larry Walker, Dr. John Rimoldi and Dr. Shabana Khan for their suggestion, guidance and their valuable time. I am thankful to all of you for being an integral part of my committee. I am grateful to Dr. Larry Walker and consider myself fortunate to have had an opportunity to work with him. I am indebted to Dr. Kristie Willett for all her support and care which helped me to stay focused during my program.

The collaboration with other scientific group has added significant value to this work. My sincere thanks are to Dr. Alexandra Rutledge (Department of Chemistry, Vanderbilt University, Nashville, TN 37235, USA) for the valuable help for metabolomics analysis as well as analysis and interpretation of the data. I also want to thank to the metabolomics core at the Vanderbilt University for the research facility.

I thank Dr. Pankaj Pandey and Dr. Robert Doerksen for their help in computational studies and Dr. Dhammika Nanayakkara for providing primaquine metabolites. I am pleased to thank, Dr. Ziaeddin Madar, Dr. Asok Dashmahapatra, Dr. Anthony Verlangeire, Dr. Tracy Brooks and Dr.

John Matthews for intensifying my interest in pharmacology and for providing a sound knowledge in the subject. I am thankful to Ms. Jennifer Michael and Ms. Sherrie Gussow for their help with administrative paperwork. I would also like to thank the University Library (Pharmacy Science Library) for their extensive collections, as without them my research would have been a tough task.

None of above would have been possible without the love and support of my family. I am thankful to my parents, sister, and brother who have provided a perennial source of love, concern, support, and strength which has been invaluable throughout my education. I have been fortunate to have a wonderful husband "Surendra Jain" who has been supportive and has expressed unwavering faith in me. I sincerely appreciate the love, care, generosity and understanding he showed towards me during past five years. I do not have enough words to express my feelings and level of respect I hold for him, but as always, I am sure he will understand what I mean. Also, I am thankful to my lovely little princess "Aanya" for the love and affection she shows for me.

I am grateful to all the faculty, staff, and graduate students in the Department of BioMolecular Sciences and the National Centre for Natural Product Research (NCNPR). Finally, I want to acknowledge U. S. Department of Defense for the primary source of funding for my research.

TABLE OF CONTENTS

LIST OF TABLES

LIST OF FIGURES

CHAPTER 1

DRUG-INDUCED OXIDATIVE HEMOLYTIC ANEMIA

1.1. INTRODUCTION

The pathophysiological and toxic manifestations caused due to treatment with a drug in the blood cells are clinically referred as drug-induced hematologic disorders. The drug-induced hematologic disorders can affect all types blood cells including leukocytes, erythrocytes, and platelets. Reduction in all three cell-types with a hypoplastic bone marrow, due to a drug-treatment is referred as drug-induced aplastic anemia. The reduction in leukocytes alone due to a drug-treatment is known as drug-induced agranulocytosis. The decrease in platelet counts due to drug exposure is called drug-induced thrombocytopenia (Kamakshi 2014). Decrease in hematocrit primarily due to hemolytic reactions or an accelerated removal of red blood cells is known as hemolytic anemia.

Drug treatments can affect erythrocytes by causing various hemolytic anemias, comprising drug-induced immune hemolytic anemia, drug-induced megaloblastic anemia and drug-induced oxidative hemolytic anemia (Kamakshi 2014). Hemolysis is the removal of damaged erythrocytes from the circulation before their normal life span (120 days). Hemolysis can remain asymptomatic for a lifetime and most often represents as anemia when erythrocytosis cannot balance the rate of erythrocytes destruction. The clinical manifestation of hemolytic anemia are dark urine. cholelithiasis, isolated reticulocytotic or jaundice (Dhaliwal et al. 2004).

In drug-induced immune hemolytic anemia, the body generated immunoglobin G or immunoglobulin M (IgM) (or both) against the erythrocytes, and these antibodies bind to antigens on the surface of erythrocytes. The binding of antibodies and antigens triggers the destruction of erythrocytes via the complement and mononuclear phagocytic systems (Garratty 2012). Th drugs which directly or indirectly affect DNA synthesis cause megaloblastic hemolysis. In this type of hemolytic anemia, the development of megaloblasts, the precursor of erythrocytes, is abnormal in bone marrow (Scott and Weir 1980). The drugs which produce oxidative stress and have potential to undergo redox cycling cause drug-induced oxidative hemolytic anemia. Such type of anemia is commonly seen in a genetic condition of glucose 6 phosphate dehydrogenase (G6PD) enzyme deficiency (Winterbourn 1985; Fibach and Rachmilewitz 2008).

Drug-induced hemolytic anemia can be intravascular or extravascular. In intravascular hemolysis, the destruction of erythrocytes occurs in the circulation, and the content of erythrocytes is released into the vascular compartment. The common causes of intravascular hemolysis are complement fixation, immune complex deposition, infectious agent, membrane damage and membrane trauma due to oxidative damage. The second type of hemolysis is extravascular hemolysis and is relatively more common than intravascular hemolysis. In extravascular hemolysis, the damaged erythrocytes that contain membrane alterations are eliminated from the circulation by macrophages of the liver and spleen (Dhaliwal et al. 2004; Kamakshi 2014).

1.2. GLUCOSE 6 PHOSPHATE DEHYDROGENASE DEFICIENCY

G6PD deficiency is the most common enzymopathy with more than 400 million cases in worldwide and is frequent in malaria endemic countries (Youngster et al. 2010; Mason et al. 2007). G6PD deficiency is an X-linked hereditary disorder caused due to a mutation in G6PD gene

(Cappellini and Fiorelli 2008; Youngster et al. 2010). G6PD deficiency has more than 400 allelic variants (Nkhoma et al. 2009), and PQ causes hemolysis in all variants (Mason et al. 2007). G6PD enzyme deficiency is highly prevalent in Africa, southern Europe, the middle east, southeast Asia, and the central and southern Pacific islands. However, due to migrations, this deficiency is relatively prevalent in North and South America and parts of northern Europe (Cappellini and Fiorelli 2008). The clinical manifestations of hemolytic toxicity depend mainly on the amount of oxidative stress and severity of the patient's G6PD genetic defect (Cappellini and Fiorelli 2008; Kamakshi 2014). The most common G6PD variants are the Mediterranean variant and African variant. A Mediterranean variant is the most severe G6PDd variant and is mainly found in Europe, west and central Asia, and northern India. African variant is the mildest variant. This variant is predominant in sub-Saharan Africa and African-Americans. (Cappellini and Fiorelli 2008)

G6PD enzyme participates in the pentose phosphate pathway, which is the sole source for production of NADPH, glutathione recycling in erythrocytes, and is essential for the function of catalase (Figure 1.1) (Nkhoma et al. 2009; Mason et al. 2007; Cappellini and Fiorelli 2008; Judith Recht 2014). NADPH, GSH, and catalase constitute primary antioxidant defense system in human erythrocytes (Judith Recht 2014). The G6PDd erythrocytes have limited capability to regenerate NADPH and recycle GSH. Oxidative stress may exhaust the cellular GSH in G6PDd erythrocytes due to compromised efficiency to produce NADPH. The later events may cause cellular and molecular changes in erythrocytes, which may lead to hemolytic anemia in the G6PDd population treated with drugs causing oxidative stress (Mason et al. 2007).

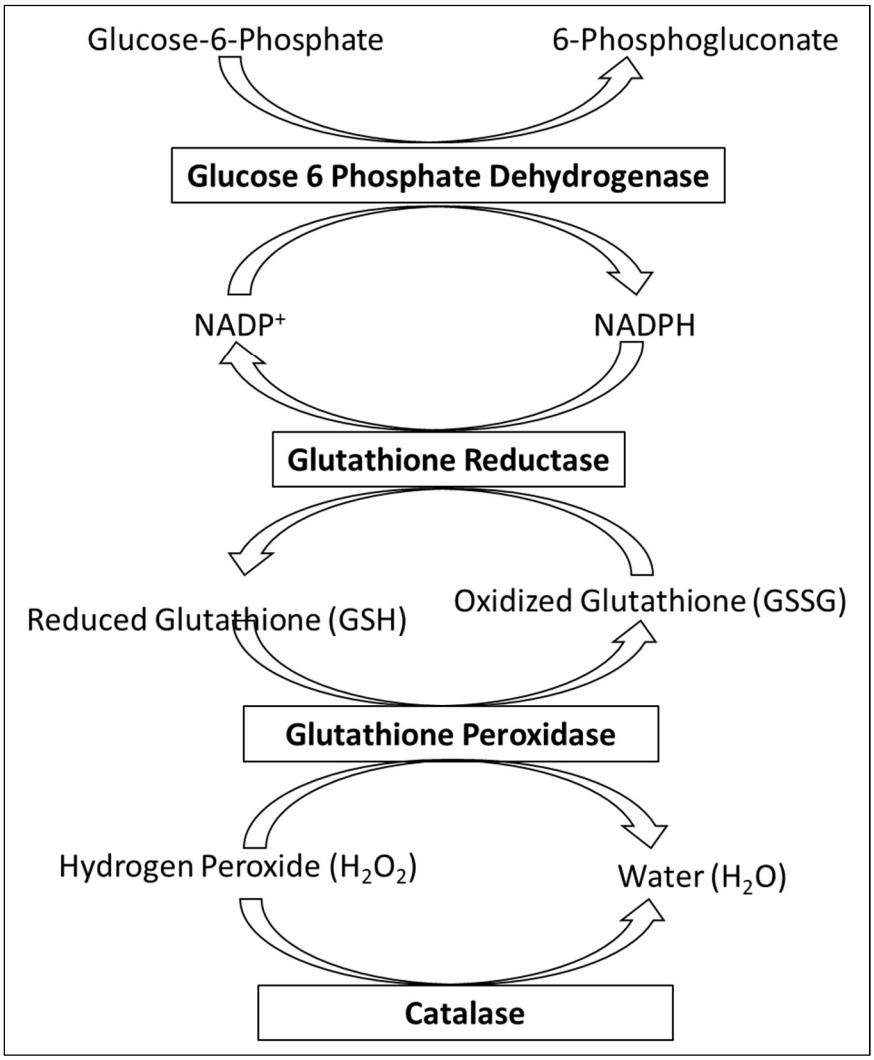

Figure 1.1: Role of glucose 6 phosphate dehydrogenase (G6PD) and other antioxidant enzymes against oxidative stress. NADP- Nicotinamide adenine dinucleotide phosphate. NADPH- Nicotinamide adenine dinucleotide phosphate hydrogen. (Youngster et al. 2010)

1.3. OXIDATIVE STRESS IN ERYTHROCYTES

1.3. 1. Reactive oxygen species

The oxidative status of cells is regulated by the equilibrium between pro-oxidants and antioxidants. Reductants donate electrons, and oxidants accept electrons. Prooxidants act as reactive oxygen species (ROS) and are classified into nonradicals and radicals. The radicals have at least an unpaired electron, which is responsible for high reactivity. Radicals either accept or donate an electron to gain stability. The radicals react rapidly with other molecules and thus have a short half-life. The most common radicals in biological systems are alkoxyl radicals ($RO^{\cdot}$), hydroxyl radical ($OH^{\cdot}$), nitric oxide radical ($NO^{\cdot}$), superoxide ion radical ($O^{\cdot -}_2$), and one form of singlet oxygen ($^1O_2$). The non-radical ROS life span varies from seconds to hours. Non-radical reactive oxygen species include the aldehydes, hypochlorous acid (HClO), hydrogen peroxide (H_2O_2), organic peroxides, ozone (O_3) and molecular oxygen (O_2) (Fibach and Rachmilewitz 2008; Winterbourn 1985). The properties of common ROS are described in Table 1.1.

Table 1.1: Characteristics of common reactive oxygen species (ROS) (Winterbourn 1985).

ROS	Characteristics
Hydrogen peroxide (H_2O_2)	Oxidizing Compound, Permeable to membranes Cause lipid peroxidation React with heme protein and thiols
Hypochlorous acid (HClO)	Oxidizing Compound Permeable to membranes Forms protein crosslinks Selectively react with thioester and thiols
Singlet oxygen ($^1O_2$)	Excited state and high-energy form of oxygen, React with majority of biomolecules
Hydroxyl radical ($OH^{\cdot}$)	Lead to protein denaturation, lipid peroxidation, and enzyme inactivation Highly reactive with majority of biomolecules
Superoxide ($O^{\cdot -2}$)	Form hydroxyl radical via Fenton reaction Limited membrane permeability and biological reactivity Oxidizes and reduces hemoglobin

1.3.2. Antioxidant enzymatic system

The primary function of endogenous antioxidative enzymes is to maintain the redox balance during oxidative stress in the cells/erythrocytes. The main endogenous antioxidative enzymes are superoxide dismutase (SOD), glutathione peroxidase (GPx), glutathione reductase (GR) and catalase (CAT) in the erythrocytes. All these enzymes provide protection against ROS via scavenging superoxide radicals and hydrogen peroxide, changing them to less reactive species (Figure 1.2. and 1.3) (Pandey and Rizvi 2010; Fibach and Rachmilewitz 2008).

SOD catalyzes the conversion of superoxide anion (O^{-2}) to hydrogen peroxide (H_2O_2). As mentioned earlier, H_2O_2 is ROS and not a radical, though it is quickly converted to hydroxyl radical ($^{\bullet}OH$) by Fenton reaction. The hydroxyl radicals are extremely reactive with many biomolecules and are responsible for most of the cellular damage. SOD is one of the most important endogenous antioxidant enzymes and protects cells from ROS (Pandey and Rizvi 2010; Fibach and Rachmilewitz 2008; Winterbourn 1985).

Glutathione peroxidase (GPx) counteracts hydrogen peroxide (H_2O_2) by using hydrogens from two GSH (reduced glutathione) molecules and forming two water molecules and one GSSG (oxidized glutathione). The enzyme glutathione reductase (GR) then recycles GSH from GSSG using NADPH as a source of hydrogen (Pandey and Rizvi 2010; Fibach and Rachmilewitz 2008).

Catalase enzyme is another vital part of the enzymatic defense system in the cell. Catalase is the most active enzyme present in nature (Pandey and Rizvi 2010). The enzyme shows high affinity for H_2O_2 and thus degrade H_2O_2 into water rapidly before it can diffuse to the other parts of erythrocytes. Catalase offers highly energy efficient mechanism to remove H_2O_2. Therefore, during energy deprivation environment, catalase neutralize H_2O_2 in an energy efficient manner

which results in the net gain of reducing equivalents and cellular energy. Hence, the activity of catalase is a critical biomarker of oxidative stress (Pandey and Rizvi 2010; Fibach and Rachmilewitz 2008)

Superoxide dismutase (SOD):

Superoxide + Hydrogen $\Longrightarrow$ Oxygen + Hydrogen peroxide

Catalase:

Hydrogen peroxide $\Longrightarrow$ Oxygen + Water

Glutathione Reductase (GR):

Hydroxyl radicals + Reduced glutathione $\Longrightarrow$ Oxidixed glutathione + Water

Figure 1.2: Neutralization of reactive oxygen species by the endogenous antioxidant system in erythrocytes (Fibach and Rachmilewitz 2008).

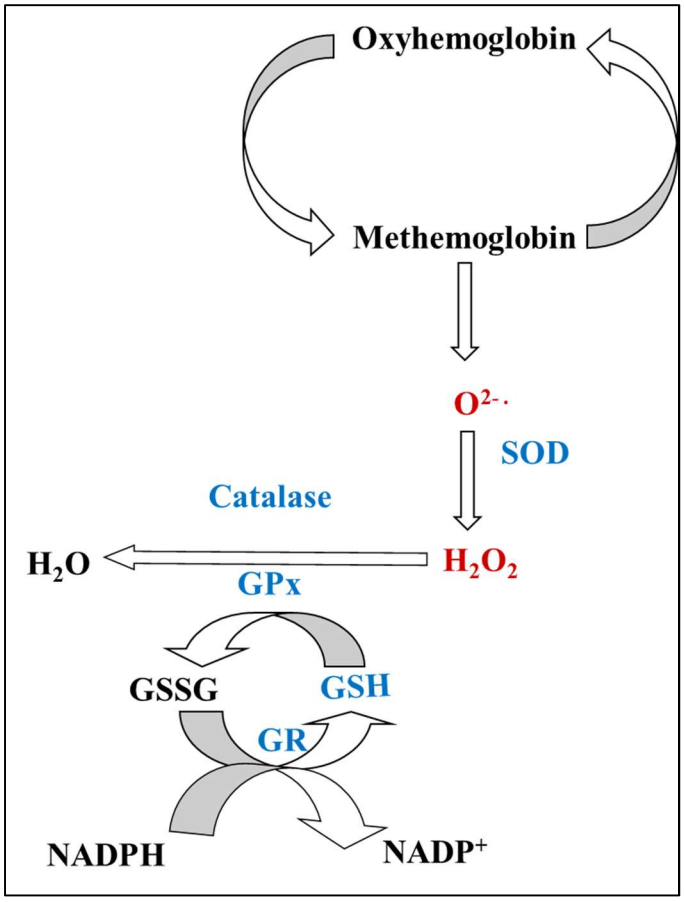

Figure 1.3: Combined action of the endogenous antioxidant system (blue) to detoxifies reactive oxygen species (red) by endogenous in erythrocytes (Fibach and Rachmilewitz 2008). **O^{-2}:** Superoxide anion; **H_2O_2:** Hydrogen peroxide; **SOD:** Superoxide dismutase; **GPx:** Glutathione peroxidase; **GR:** Glutathione reductase; **GSH:** Reduced glutathione; **GSSG:** Oxidized glutathione.

1.3.3. Oxidation of hemoglobin

Hemoglobin is a solid source of generation of superoxide radicals in erythrocytes. There is a transfer of an electron between the heme iron and oxygen in oxygenated hemoglobin. When hemoglobin is oxygenated, the heme iron stays in the Fe^{2+} ferrous state. Though when hemoglobin auto-oxidizes, methemoglobin and superoxide radicals are formed. In normal physiological condition, the formation of methemoglobin (approximately, 3%) produces superoxide continuously and subsequently generates hydrogen peroxide and oxygen as byproducts of dismutation reaction. Hence, normal erythrocytes have a huge amount of the reducing enzyme SOD. To restore hemoglobin function, methemoglobin is reduced by the NADH methemoglobin reductase and NADH methemoglobin reductase (Gordon-Smith 1980; Winterbourn 1985).

Due to excessive oxidation of hemoglobin, the globin protein of hemoglobin is denatured, condensed and precipitated. These denatured globin proteins in the hemoglobin are called, “heinz bodies.” The interaction between the xenobiotic (drug having oxidation properties) and hemoglobin is the crucial process, which is characterized by methemoglobin and heinz body formation and both of them are important biomarkers of oxidative hemolytic anemia (Gordon-Smith 1980; Winterbourn 1985).

1.3.4. Oxidation of erythrocytes membrane

The membranes in erythrocytes contain lipid bilayer. Due to the oxidative stress, the lipid peroxidation occurs. Lipid peroxidation, a free-radical chain reaction is augmented by ROS. During this process, unstable carbon radicals are generated from the fatty acids and rearrange to produce short alkanes and conjugated dienes. These short alkane and conjugated dienes then react

oxygen to form peroxyl radicals, and through abstraction of hydrogen abstraction, lipid hydroperoxides are formed. The oxidation products are highly reactive and undergo for further oxidation and form secondary oxidation products like 4-hydroxy-2-,3-trans-nonenal (HNE), malondialdehyde (MDA), or isoprostanes. The second oxidation products can lead to form protein cross-linking and thus denatures the protein. Thus, the formation of MDA is frequently used as a biomarker to examine the oxidative damage on lipids (Gordon-Smith 1980; Fibach and Rachmilewitz 2008; Pandey and Rizvi 2010).

1.3.5. Eryptosis

The suicidal death of erythrocytes is called eryptosis. It is a coordinated signaling pathway of certain events, which cause disposal of defective erythrocytes. As erythrocytes do not contain mitochondria and nucleus, they are devoid of the classical apoptotic pathway and apoptotic characteristics such as mitochondrial depolarization and condensation of nuclei. Also, the signaling pathways, which lead to eryptosis, are different from classical pathways of apoptosis (Figure 1.4). However, eryptosis shares some traits of apoptosis-like cell shrinkage, cell membrane blebbing, and exposure of phosphatidylserine (PS) on the cell surface. Moreover, like apoptosis, in eryptosis, the defected cells are engulfed and degraded by macrophages (Lang et al. 2012). Eryptosis is commenced by complex signaling pathways, which are comprised of: 1) increase in intracellular free calcium ion concentration, ceramide and, prostaglandin-E2 (PGE2); 2) activation of caspases, kinases, ionic channels and calpain protease and 3) externalization of phosphatidylserine to the erythrocytes surface. Eryptosis can be caused due to osmotic shock, mechanical damage of erythrocytes and agents that induce energy depletion or generate oxidative

stress. The elevation of eryptosis is correlated with metabolic disease, genetic disorders and bacterial and viral infections (Aguilar-Dorado et al. 2014).

Different eryptosis stimulators including oxidative stress, energy depletion, and hyperosmotic shock cause activation of Ca^{2+} permeable non-selective cation channels and trigger the intake of Ca^{2+} in erythrocyte. The increase in intraerythrocytic Ca^{2+} activates protease calpain, a cysteine endopeptidase, which degrades protein and ultimately promotes cell membrane blebbing. Moreover, the increment in cytosolic Ca^{2+} stimulates degeneration of phospholipid asymmetry of the cell membrane and causes phosphatidylserine exposure at the outer membrane leaflet of the erythrocyte. Externalization of PS is a signal to circulating macrophages to come and engulf the affected cells (Lang et al. 2006; Lang and Lang 2015).

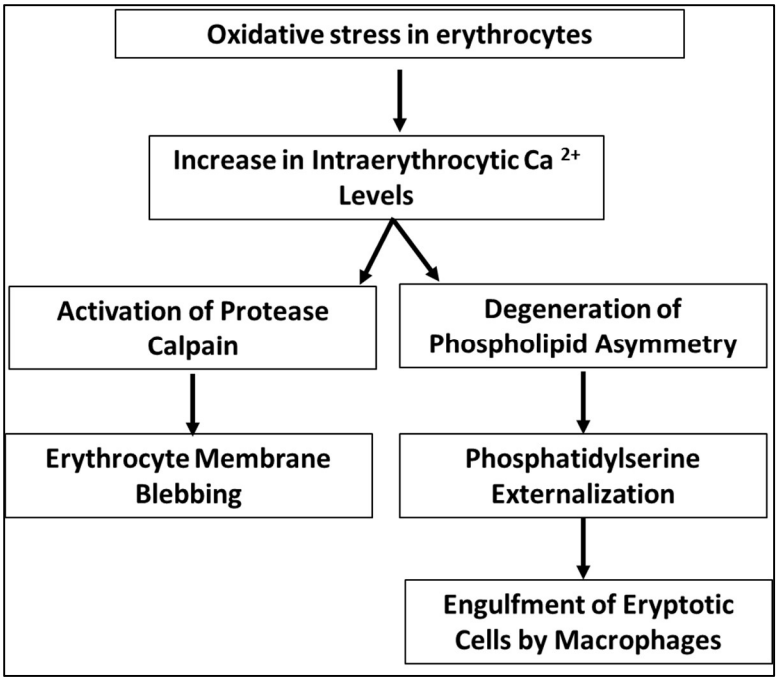

Figure 1.4: Major events of eryptosis pathway (Lang and Lang 2015).

1.3.6. Pathway of oxidative stress in erythrocytes

In, erythrocytes the hemoglobin is converted to methemoglobin via auto-oxidation or in the presence of xenobiotic (usually drug which has redox and oxidative potential). During formation of methemoglobin, superoxide anions are formed. SOD converts superoxide anions to hydrogen peroxide, and hydrogen peroxide is detoxified via enzyme catalase. Apart from SOD and catalase, other endogenous antioxidants present in erythrocytes take care of ROS. However, if these endogenous antioxidants failed to detoxify ROS, damage to macromolecules, like lipid peroxidation, denaturation of hemoglobin and formation of heinz body and protein cross-linking occur which is irreversible and this leads to the lysis of erythrocytes (Pandey and Rizvi 2010; Gordon-Smith 1980; Winterbourn 1985). The pathway of oxidative stress leading to hemolytic toxicity is described in Figure 1.5.

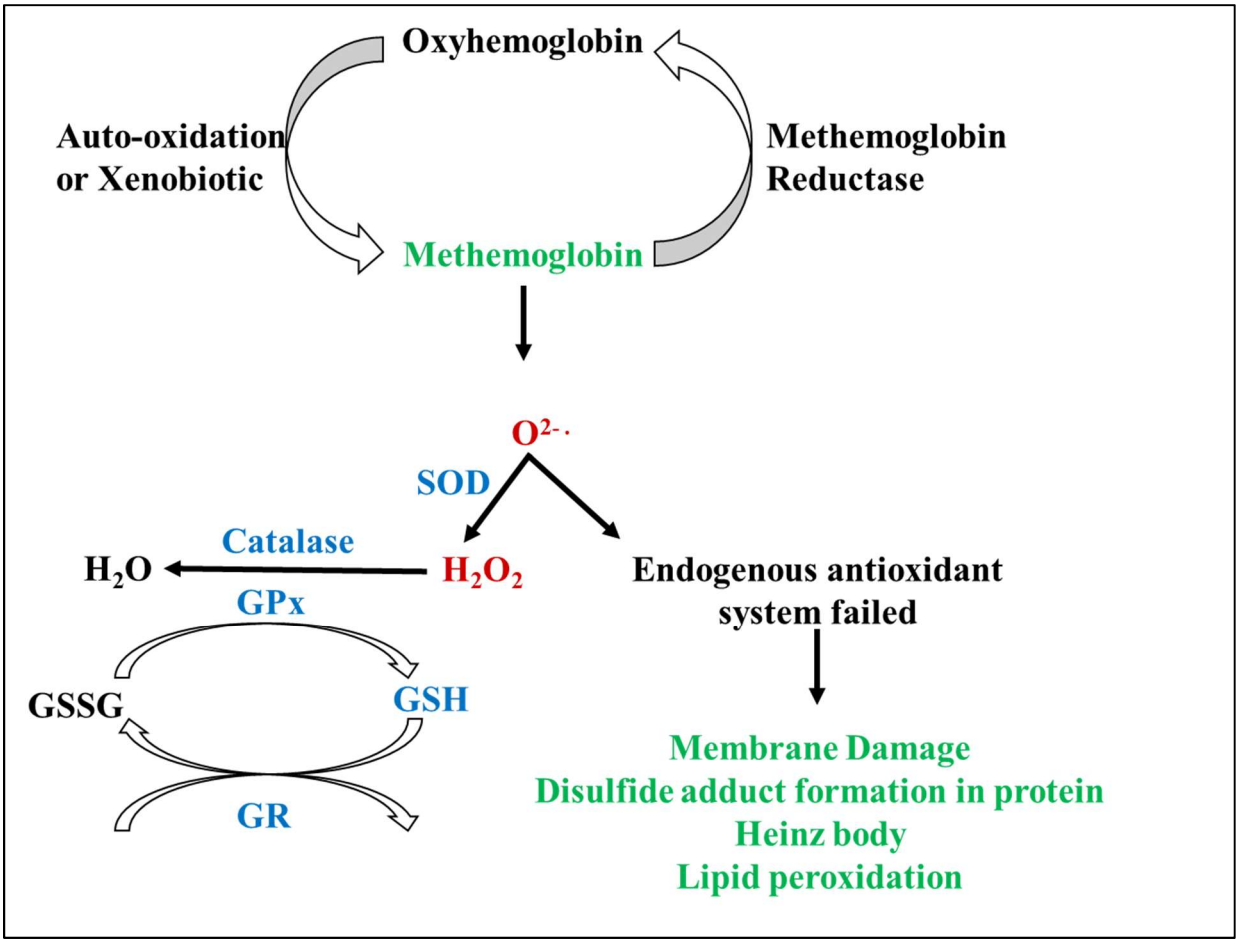

Figure 1.5: Pathway leading to hemolysis caused by oxidative stress (Pandey and Rizvi 2010). The reactive oxygen species (red) are detoxified through the endogenous antioxidant system (blue). If the endogenous antioxidant system is failed to neutralize reactive oxygen species, macromolecule damage occurs. **O^{-2}:** Superoxide anion; **H_2O_2:** Hydrogen peroxide; **SOD:** Superoxide dismutase.

1.4. DRUGS ASSOCIATED WITH OXIDATIVE HEMOLYTIC ANEMIA

1.4.1. Ascorbic acid

Ascorbic acid (Figure 1.6) is given at higher doses to treat severe deficiency such as scurvy. High doses of ascorbic acid aid in the prevention of colds, the improved wound healing, and treatment of cancer (Vilter 1980). Literature reports incidents of hemolysis after higher doses of ascorbic acid in G6PDd erythrocytes (Rees et al. 1993; Udomratn et al. 1977; Huang et al. 2014). In vivo studies were done to investigate the effect of higher doses of ascorbic acid on G6PDd human erythrocytes. At larger doses, ascorbic acid-induced hemolysis of G6PDd human erythrocytes (Udomratn et al. 1977). Though at therapeutic dosages, there are no confirmations to disregard the use of ascorbic acid in patients with a G6PDd population (Youngster et al. 2010).

Literature also reports oxidative hemolysis caused by higher doses of ascorbic acid in patients having normal erythrocytes with no genetic defect (Ibrahim et al. 2006) and with hemoglobinopathies like sickle cell anemia and thalassemia (Arruda et al. 2013). Contrast to hemolytic incidences of ascorbic acid; reports also showed that ascorbic acid decreased the phenylhydrazine-induced oxidative hemolysis by inhibiting methemoglobin and heinz bodies formation caused by phenylhydrazine in erythrocytes (Claro et al. 2006; Biswas et al. 2005). Thus, the controversial effect of ascorbic acid is observed on hemolysis, and the exact mechanism and clinical significance of these findings are still unclear.

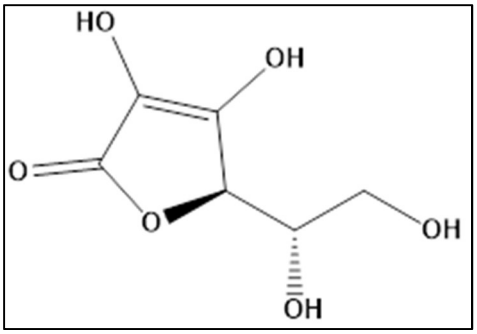

Figure 1.6: Structure of Ascorbic acid

1.4.2. Dapsone

Dapsone (DDS), an antibacterial and antiprotozoal agent, is used for the treatment of various disease conditions including dermatitis herpetiformis, *Pneumocystis pneumonia* in acquired immunodeficiency syndrome (AIDS) patient, leprosy, malaria and inflammation (Wolf et al. 2000; Ganesan et al. 2010). Several clinical reports confirm the hemotoxicity of DDS (Deps et al. 2012; Cha et al. 2016; Pamba et al. 2012; Barclay et al. 2011; Mitsides et al. 2014).DDS metabolites produced in the liver are believed to cause hemotoxic reactions (Figure 1.7). Earlier studies on the CYP-mediated metabolism of DDS had shown that CYP2C9, CYP2C19, CYP2E1, and CYP3A4, are mainly involved in the metabolism of DDS (Li et al. 2003; Ganesan et al. 2010).

Dapsone causes hemotoxicity in normal as well as G6PDd populations and the mechanisms seem to induce changes to the membranes of erythrocyte membrane (McMillan et al. 2005). ROS is produced this drug, induces binding of oxidized and denatured hemoglobin to the cytoskeleton membrane of erythrocytes. These oxidative changes in the erythrocytes' membrane lipids have been demonstrated to accelerate the removal of the damaged erythrocytes by macrophages, leading to hemolytic injury (McMillan et al. 2005).

Dapsone hydroxylamine (DDSNOH), is a potent hemotoxic metabolite of DDS (Grossman and Jollow 1988; McMillan et al. 1995) and has been linked to hemolytic toxicity of DDS in several in vitro and in vivo studies (Mitra et al. 1995; McMillan et al. 1995; Grossman et al. 1995; Grossman et al. 1992; McMillan et al. 1998). CYP2C9 and CYP2C8 isoforms of CYP enzymes cause the formation of dapsone hydroxylamine (Ganesan et al. 2010). DDSNOH induces methemoglobin, generates oxidative stress in human erythrocytes (Kramer et al. 1972; Albuquerque et al. 2015). It further depletes GSH, forms disulfide-linked hemoglobin polymers and disulfide-linked hemoglobin adducts on certain membrane skeletal proteins in rat and human erythrocytes (Grossman et al. 1992; McMillan et al. 1995). The literature suggests that the hemotoxicity associated with DDS depends on the metabolism of DDS, though exact metabolism and hemotoxic pathways of DDS are still unclear.

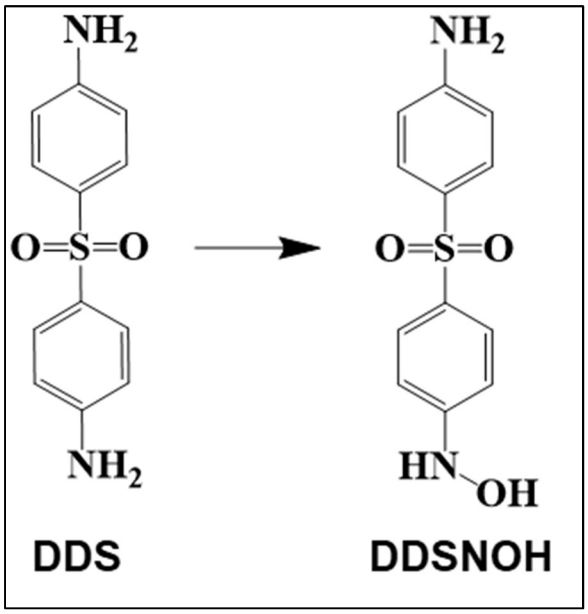

Figure 1.7: Metabolism of DDS to DDSNOH

1.4.3. Metformin

Metformin (Figure 1.8.A) is an antidiabetic drug and, is used in first-line therapy for type II diabetes. There have been 14 million Americans which were administered metformin between 2010 and 2012, indicating the widespread use of metformin among the diabetic population (Ruggiero et al. 2016). Metformin-induced hemolytic anemia in G6PDd patients have been reported in the literature (Ruggiero et al. 2016; Meir et al. 2003; Blum et al. 2011; Packer et al. 2008; Kirkiz et al. 2014; Kamakshi 2014). Though the metformin-induced hemolysis is rare, and metformin is not incorporated in the list of drugs unsafe in G6PDd population, and it still is important to consider seriously. There is not known mechanism of metformin-induced hemolysis and a definitive association between G6PD enzyme activity, and metformin-induced hemolytic anemia is not known (Ruggiero et al. 2016). In practice, it would be not practical to screen patients started on metformin for G6PD deficiency; though a patient with known G6PD deficiency should be observed carefully, or prescription of metformin in patients with known G6PD deficiency need to be avoided (Ruggiero et al. 2016). No studies has been to understand the mechanism of hemotoxicity associated with metformin.

1.4.4. Methylene blue

Methylene blue (methylthioninium chloride) (Figure 1.8.B) is a compound with multiple uses. It is mainly used for the treatment of methemoglobinemia induced by drugs. In addition, it is used for the treatment of various infections and poisoning in vivo. In vitro, it is used as a dye to stain tissues, bacterial cells, and DNA (McDonagh et al. 2013). Methylene blue is an effective therapy to reduce methemoglobin back to hemoglobin. However, methylene blue is linked with

adverse hemolysis reactions in G6PDd individuals. Thus, methylene blue is contraindicated or advised precaution for use in G6PDd individuals due to a risk of hemolytic anemia (Youngster et al. 2010; Kamakshi 2014; McDonagh et al. 2013).

Methylene blue causes reduction in methemoglobinemia via biliverdin reductase B (BLVRB) enzyme (Skold et al. 2011; Curry 1982; Wright et al. 1999). Methylene blue is reduced to leukomethylene blue by BLVRB enzyme, and during this reduction, BLVRB enzyme accepts electrons from NADPH (Curry 1982). Leukomethylene blue acts as an electron donor and reduces methemoglobin back to hemoglobin and converts to methylene blue in a redox cycle reaction (Curry 1982; Wright et al. 1999). On the contrary, methylene blue is an oxidizing agent; it can cause methemoglobinemia at high concentrations. Methylene blue causes hemolysis by oxidizing hemoglobin, oxidizing GSH to GSSG and forming heinz bodies (Sills and Zinkham 1994; Kelner and Alexander 1985). However, the exact pathway of methylene blue-induced hemolysis is still unknown.

The mechanism of action of methylene blue to reduced methemoglobin back to hemoglobin depends on the intracellular capacity for NADP/NADPH recycling of the erythrocytes. The pentose phosphate pathway is the only source of NADPH in erythrocytes, methylene blue treatment to reduce methemoglobin back to hemoglobin relies on G6PD enzyme activity. Moreover, methylene blue has been linked to exacerbating oxidative stress in G6PDd erythrocytes. Thus, methylene blue is an inappropriate treatment option for methemoglobinemia in G6PD-deficient individuals (McDonagh et al. 2013).

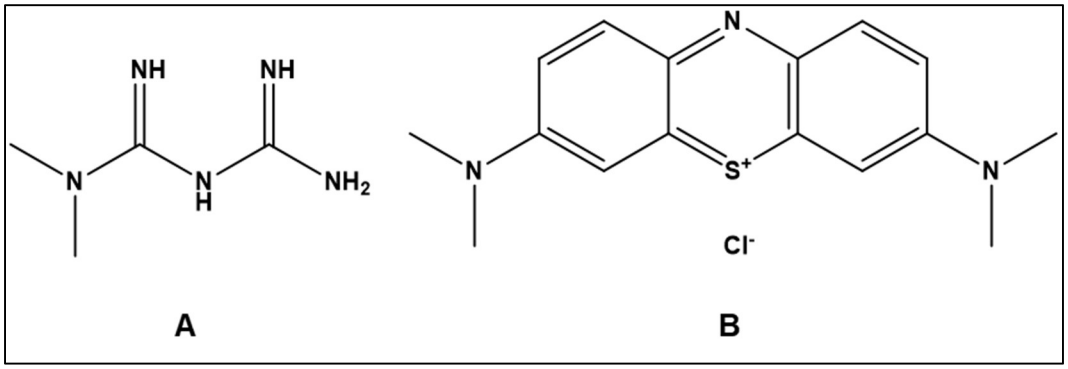

Figure 1.8: Structure of (A) metformin and (B) Methylene blue.

1.4.5. Nitrofurantoin

Nitrofurantoin (NFT) is the drug of choice for treatment and prophylaxis of acute uncomplicated lower urinary tract infections because of minimum resistance, the lower tendency of collateral damage and high efficacy (Colgan and Williams 2011; Gupta et al. 2011; Shakti and Veeraraghavan 2015). NFT also causes severe hemolytic anemia in glucose-6-phosphate dehydrogenase (G6PD) deficient populations. This limits the use of NFT for these patients (Gait 1990; Shakti and Veeraraghavan 2015). Moreover, evidence shows the hydroxylation of NFT (Jonen 1980) and formation of aminofurantoin metabolite of NFT in rat (Aufrere et al. 1978). In addition, aminofurantoin, a reductive metabolite of NFT is detected in human urine as well (Hoener and Patterson 1981). Thus, aminofurantoin is the only known human metabolite of NFT. However, recent data suggest that nitrofurantoin is metabolized through CYP450 system and generate 1-aminohidantoin in rat (Aracena et al. 2014). These data suggest that metabolism of NFT occurs through both reductive and oxidative pathway. However, the knowledge about the pathways for metabolism of NFT, namely type of CYP isoforms and identity of the metabolites, is still unclear and incomplete.

A preliminary study with normal blood cells showed that NFT increased methemoglobin formation and hydrogen peroxide generation, whereas cellular levels of GSH and ATP were decreased (Dershwitz et al. 1985). NFT reversibly inhibits glutathione reductase (GR) in rat hemolysates, hepatocytes and human hemolysates (Buzard et al. 1960; Rossi et al. 1988). The redox cycling and nitro reduction ability of NFT is known to be associated with its hepatic and pulmonary toxicity. The one electron reduction of the 5-nitro group in NFT, produces nitro radical anions and furthermore generates superoxide, hydrogen peroxide (H_2O_2) and highly reactive hydroxyl radical (Figure 1.9). Thus, the potential of NFT for the formation of ROS seems to cause cytotoxicity but is not the only factor to cause toxicity (Minchin, Ho, and Boyd 1986; Wang et al. 2008). The mechanism of hemolytic toxicity of NFT in G6PDd patient is still unknown, but in normal erythrocytes, the challenge with NFT is that it increases MtHb formation and H_2O_2 generation with decreases in cellular levels of GSH and ATP (Dershwitz et al. 1985). However, no investigations have been done in G6PDd erythrocytes *in vitro* and *in vivo* to follow the hemolytic response and mechanism for the hemolytic toxicity of NFT. Thus, the hemolytic mechanism induced by NFT is still not clear and unknown.

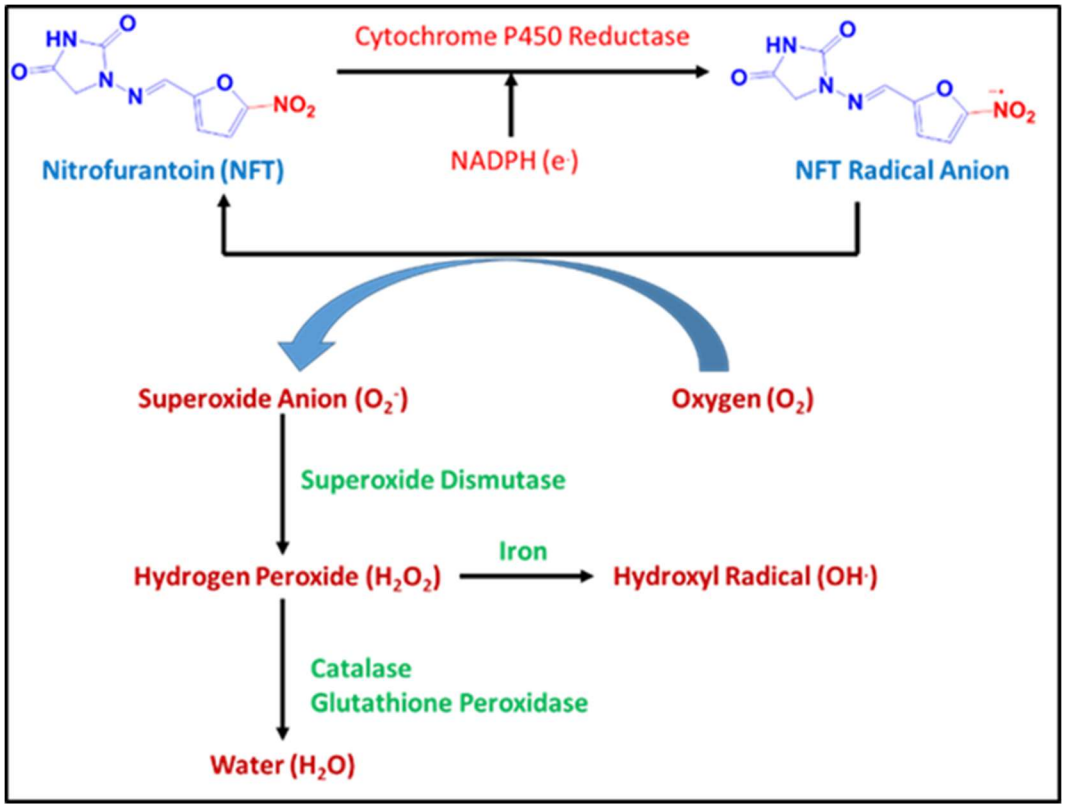

Figure 1.9: Redox cycling of NFT and generation of reactive oxygen intermediates (Wang et al. 2008; Gupta et al. 2011)

1.4.6. Nalidixic acid

Nalidixic acid (Figure 10.A) is an antibacterial belonging to the quinolone class. The likely adverse effect of nalidixic acid in general population is hemolytic anemia. There were three reported cases of hemolysis in G6PDd individuals induced by nalidixic acid and accordingly there is a caution concerning the use of nalidixic acid in G6PDd patients (Youngster et al. 2010).

The photosensitized hemolytic lysis caused by nalidixic acid was investigated by (Fernandez and Cardenas 1990; Fernandez et al. 1987). The nalidixic acid-induced photo-hemolysis was oxygen-dependent. The effects of numerous antioxidants and hydroxyl radical scavengers on nalidixic-induced photo-hemolysis indicated a photo-oxidative step. Furthermore, it was found that the nalidixic acid was the reason of hemolysis, yet the photoproducts for nalidixic acid showed a greater potential of photo-hemolysis rather than nalidixic acid itself (Fernandez et al. 1987; Fernandez and Cardenas 1990). However, the exact mechanism photosensitized hemolytic lysis caused by nalidixic acid is still not complete.

1.4.7. Phenazopyridine

Phenazopyridine (Figure 10.B) is an azo dye and has analgesic properties. It is frequently given with antibacterial therapy for urinary tract infection as it aids to relieve pain and discomfort (urgency, frequency) before antibacterial controls the infection. This drug is available through prescription as well as over the counter (Cornwell and Bartek 1996).

Literature shows that phenazopyridine caused severe hemolysis in G6PDd patients (Tishler and Abramov 1983; Galun et al. 1987). Phenazopyridine has been associated with methemoglobinemia, heinz body formation in erythrocytes in patients with overdose or having

renal insufficiency (Cornwell and Bartek 1996; Yu et al. 2011; Noonan et al. 1983; Terrell et al. 1988). Though it should be noted that hemolysis has been linked with patients with no G6PDd too (Cornwell and Bartek 1996; Yu et al. 2011; Youngster et al. 2010; Terrell et al. 1988). The hemotoxicity of phenazopyridine is linked with its metabolism. A metabolite phenazopyridine namely, 2,3,6-triaminopyridine, autoxidizes at neutral pH and produces superoxide radical and hydrogen peroxide and thus may be responsible for hemolytic anemia caused by phenazopyridine (Munday and Fowke 1994). The knowledge of the mechanism associated with phenazopyridine induced hemolysis is not clear.

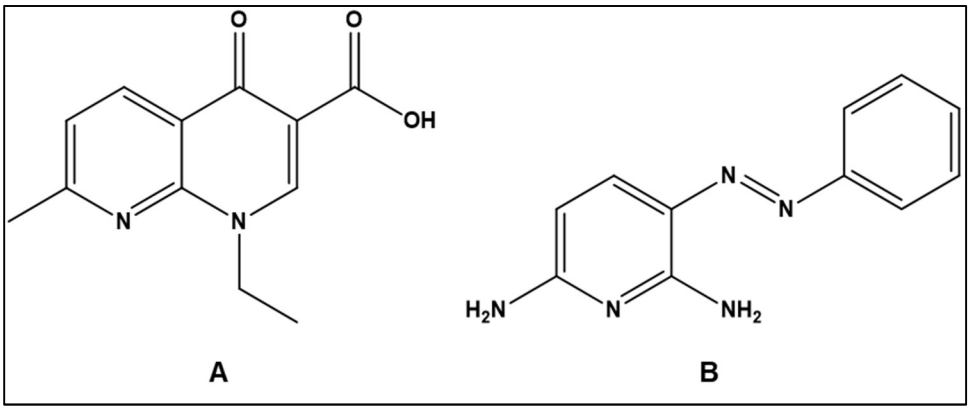

Figure 1.10: Structure of (A) nalidixic acid and (B) phenazopyridine.

1.4.8. Primaquine

Primaquine (PQ), belongs to a drug class 8-aminoqinoline (8-AQ) and is a potential antiprotozoal agent. It is mainly used for prophylaxis and treatment of malaria. PQ is the only drug approved by FDA, and acts against the hard-to-kill liver stage of *Plasmodium vivax* and *P. oval* and used to prevent malaria relapse (Ashley et al. 2014; Tekwani and Walker 2006). Relapses are significantly responsible for the morbidity in *P. vivax and P. ovale* malaria (Leslie et al. 2016). PQ

also acts against mature P5 *P. falciparum* gametocytes and thus WHO recommends PQ for prevention of malaria transmission.

PQ causes severe hemolytic reactions in individuals with a genetic deficiency of glucose-6-phosphate dehydrogenase (G6PD) (Ashley et al. 2014) and the G6PD deficiency was discovered due to PQ-induced hemotoxicity in 1950. The understanding of PQ metabolism has been greatly expanded in the last six years. The metabolism of PQ mainly depends on two metabolizing enzymes, namely CYP 2D6 and MAO-A (Figure 1.11). The in vitro studies of PQ, showed that all CYP isoforms (CYP 2D6, MAO-A, CYP 2C19, and CYP 3A4) have capability to metabolize primaquine to some extent (Pybus et al. 2012). The phenolic metabolites related with redox cycling (Vasquez-Vivar and Augusto 1992) were mainly the products of CYP 2D6 metabolism (Pybus et al. 2012; Fasinu et al. 2014). Further knockout mice studies demonstrated that the formation phenolic metabolites of PQ was reduced in CYP 2D knockout mice (Potter et al. 2015).The MAO-A enzyme causes the formation of a primaquine aldehyde species carboxyprimaquine, which is the most abundant plasma metabolite of PQ in the humans (Pybus et al. 2012; Fasinu et al. 2014).

Several studies have been done to understand the hemolytic toxicity of the PQ in vitro and in vivo (Vasquez-Vivar and Augusto 1992, 1994; Bolchoz et al. 2001; Bolchoz et al. 2002b; Bolchoz et al. 2002a; Bowman et al. 2004; Bowman et al. 2005b; Bowman et al. 2005a; Ganesan et al. 2009; Ganesan et al. 2012). It is well established that the hemolytic anemia and efficacy of PQ is hepatic metabolism-dependent (Ganesan et al. 2012; Ganesan et al. 2009; Fasinu et al. 2014; Pybus et al. 2012; Pybus et al. 2013). The hemotoxic effect of PQ in the presence of human liver microsomes (HLM), mouse liver microsomes (MLM) and recombinant human-CYPs isoforms in normal and G6PDd human erythrocytes was analyzed (Ganesan et al. 2009; Ganesan et al. 2012).

The studies showed that in the presence of HLM, PQ-induced methemoglobin (MtHb) formation, reactive oxygen species (ROS) generation, and depletion in thiols in human erythrocytes (Ganesan et al. 2009; Ganesan et al. 2012). Multiple CYP isoforms (CYP1A2, CYP2E1, CYP2B6, CYP2D6, and CYP3A4) were found to mediate the metabolism of PQ and cause PQ-associated hemotoxicity in human erythrocytes (Ganesan et al. 2009). Recent studies revealed that the production of 5-hydroxy primaquine and other phenolic metabolites of PQ depend on of CYP 2D6-mediated metabolism (Fasinu et al. 2014; Pybus et al. 2012; Pybus et al. 2013; Potter et al. 2015). However, the exact hemotoxic mechanism due to PQ in erythrocytes is still unclear (Marcsisin et al. 2016).

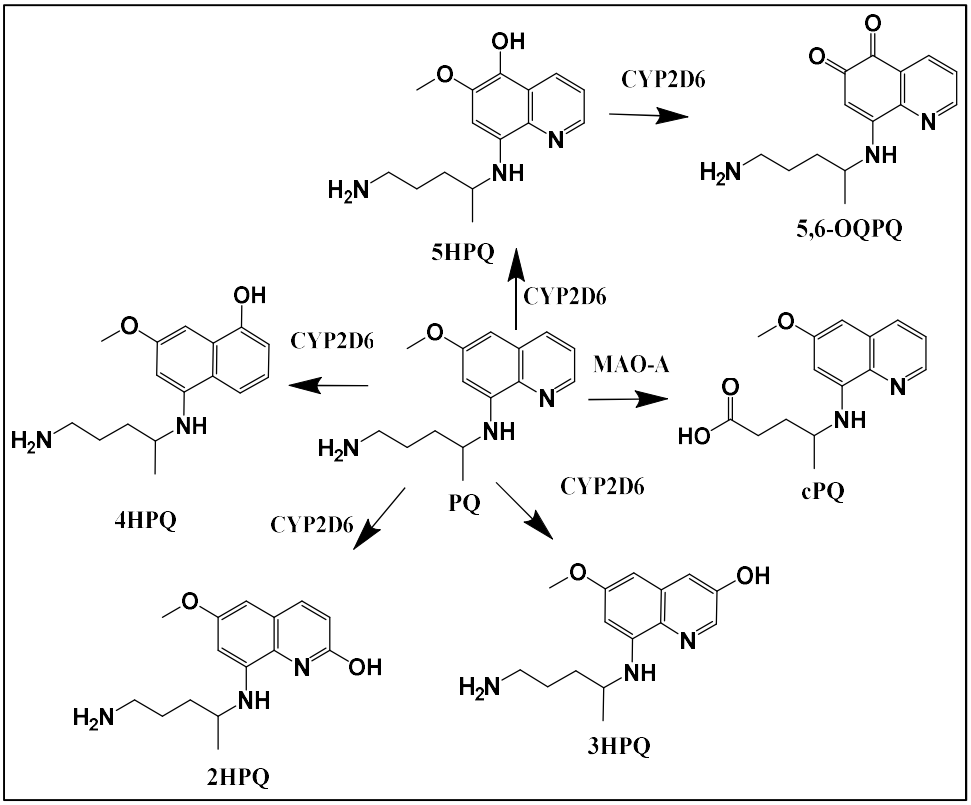

Figure 1.11: Metabolism of PQ via CYP2D6 and MAO-A pathway. cPQ: carboxyprimaquine, (2HPQ): 2-hydroxyprimaquine, 3HPQ: 3-hydroxyprimaquine, 4HPQ: 4-hydroxyprimaquine, 5-HPQ: 5-hydroxyprimaquine and 5,6-OQPQ: 5,6-orthoquinone-primaquine.

1.4.9. Rasburicase

Rasburicase is a recombinant urate oxidase used for the prevention and treatment of hyperuricemia associated with hematological malignancies (Pui 2002; Goth 2008). Rasburicase caused hemolytic anemia in G6PDd patients. Rasburicase has oxidizing potential and converts uric acid with high affinity into allantoin, which is removed by the kidneys. During this conversion, a high concentration of hydrogen peroxide is generated which might is responsible for the hemolysis in G6PDd and catalase enzyme deficiency (Goth 2008; Ibrahim et al. 2017). Moreover, due to the oxidizing property of rasburicase, the ferrous form of iron in erythrocytes is converted to ferric form resulting in the formation of methemoglobin, which makes the heme component incapable of carrying oxygen (Ibrahim et al. 2017). Rasburicase induced robust methemoglobin formation in G6PDd and catalase deficient patient and thus methemoglobin is used as a biochemical marker in laboratories to determine hemolysis caused by this drug (Elinoff et al. 2011; Cheah et al. 2013; Ng et al. 2012; Bucklin and Groth 2013; Ibrahim et al. 2017).

1.4.10. Sulfacetamide

Sulfacetamide is a sulfonamide and have anti-infectious properties. Currently, it is primarily used in topical formulations. Sulfacetamide has the theoretical potential to induce hemolysis in G6PDd patients, but the literature search showed no reported cases. It seems that sulfacetamide can be used safely in G6PDd patients in topical formulations (Youngster et al. 2010).

1.4.11. Sulfamethoxazole

Sulfamethoxazole is used sulfonamide antibacterial and comes in combination with trimethoprim. The combination of trimethoprim and sulfamethoxazole is called cotrimoxazole. Several reports suggest the hemolysis caused trimethoprim-sulfamethoxazole or sulfamethoxazole alone in G6PDd erythrocytes (Chisholm-Burns et al. 2010; Chan and Wong 1975; Reinke et al. 1995; Chan 1997; Chan 1972; Owusu 1972). However, in some clinical studies the effect of trimethoprim-sulfamethoxazole or sulfamethoxazole alone in G6PDd erythrocytes is inconclusive (Chan and McFadzean 1974; Lexomboon and Unkurapiana 1978).

1.4.12. Sulfanilamide

Sulfanilamide is a short-acting sulfonamide with antibacterial properties (Barkan and Goldsmith 1946; Youngster et al. 2010). Several clinical reports suggest that sulfanilamide induces hemolysis in G6PDd erythrocytes and the hemolysis is the cause of oxidative properties and redox potential of this drug (Ali et al. 1999; Barkan and Goldsmith 1946; Naiman 1964; Heeres and Zondag 1961). The oxidant and reduced forms of sulfanilamide have antibacterial potential. Moreover, the reduction and oxidation of sulfanilamide are reversible (Barkan and Goldsmith 1946). In a study, Ali et al. suggested that sulfanilamide caused concentration-dependent GSH depletion selectively in G6PDd erythrocytes as compared to normal erythrocytes (Ali et al. 1999). Early reports suggest the hemolysis in G6PDd erythrocytes individuals, however, the dose is four times higher than the therapeutic dose. No hemolysis reports were found at a therapeutical dose of sulfanilamide in G6PDd population (Youngster et al. 2010).

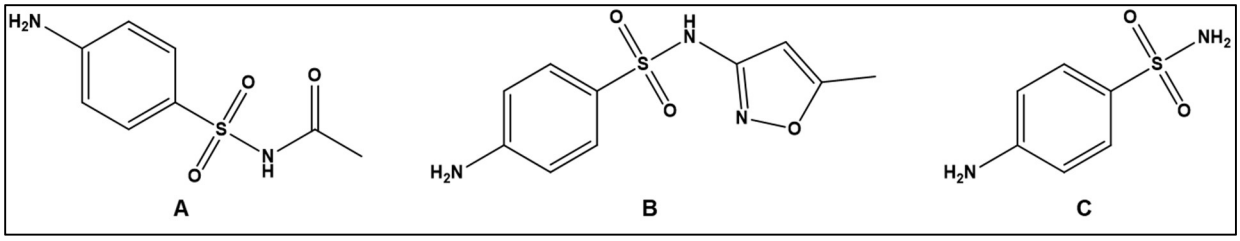

Figure 1.12: Structure of (A) sulfacetamide, (B) sulfamethoxazole and (C) sulfanilamide.

1.5. CONCLUDING REMARKS

The detrimental effects of oxidative stress are caused due to the uncontrolled generation of ROS. ROS play a vital role in hemolysis initiation (Fibach and Rachmilewitz 2008). Drugs that has redox potential and oxidative properties are capable of forming methemoglobin. During methemoglobin formation, superoxide radical and ions are produced (Gordon-Smith 1980; Winterbourn 1985). To detoxify this ROS the endogenous antioxidant enzymes like SOD, GR, GPx and catalase play a crucial role. However, if these endogenous antioxidants are not able to take care of ROS, lipid peroxidation, protein crosslinking and denaturation occurs (Fibach and Rachmilewitz 2008; Pandey and Rizvi 2010). These biochemical, molecular and cellular parameters which are affected and modified during hemolysis caused by oxidative stress serve excellent biomarkers to examine the extent of oxidative damage, and aid to assess hemolysis related changes (Pandey and Rizvi 2010).

The knowledge associated with the mechanism and pathways of drug-induced oxidative hemolysis is limited. Further studies, to identify early and late (eryptotic) hemotoxic marker and studies to understand the oxidative hemotoxic pathway in the erythrocytes are needed to be done.

The knowledge generated by these studies can be used to build a strategy to mitigate drug-induced oxidative hemolysis.

CHAPTER 2

EVALUATION OF EARLY AND LATE BIOCHEMICAL AND CELLULAR CHANGES TRIGGERED BY PRIMAQUINE METABOLITES IN NORMAL AND GLUCOSE-6-PHOSPHATE DEHYDROGENASE DEFICIENT HUMAN ERYTHROCYTES

2.1. INTRODUCTION

Currently, primaquine (PQ), an 8-aminoquinoline (8-AQ), is the sole FDA-approved drug, which acts against the hard-to-kill hypnozoites stage of *Plasmodium vivax* and *P. ovale* and used to prevent malaria relapse (Ashley et al. 2014; Tekwani and Walker 2006). Relapses are significant contributors to infection and morbidity in *P. vivax* and *P. ovale* malaria (Leslie et al. 2016). PQ also acts against mature P5 *P. falciparum* gametocytes and thus WHO recommends PQ for prevention of malaria transmission (Tekwani and Walker 2006; Ashley et al. 2014). 8-AQs also have a potential therapeutic use for treatment of other protozoal infections namely, leishmaniasis and trypanosomiasis as well as pneumocystis infections (Tekwani and Walker 2006). However, PQ causes severe hemolytic reactions in individuals with a genetic deficiency of glucose-6-phosphate dehydrogenase (G6PD) (Ashley et al. 2014). G6PD deficiency is the most common enzymopathy with more than 400 million cases worldwide and is frequent in malaria endemic countries (Mason et al. 2007; Youngster et al. 2010). PQ-induced hemotoxicity in G6PD deficient (G6PDd) population precludes the use of PQ for much- needed malaria control and elimination efforts and necessitates the development of 8-AQ analogs with better safety.

Numerous studies have explored the hemolytic toxicity of the PQ in vitro and in vivo (Vasquez-Vivar and Augusto 1992, 1994; Bolchoz et al. 2001; Bolchoz et al. 2002b; Bolchoz et al. 2002a; Bowman et al. 2004; Bowman et al. 2005b; Bowman et al. 2005a; Ganesan et al. 2009; Ganesan et al. 2012). It is well established that the hemolytic anemia and efficacy of PQ is hepatic metabolism-dependent (Ganesan et al. 2012; Ganesan et al. 2009; Fasinu et al. 2014; Pybus et al. 2012; Pybus et al. 2013). Recent studies revealed that the production of 5-hydroxy-primaquine (5-HPQ) and other phenolic metabolites of PQ depend on of CYP 2D6-mediated metabolism (Fasinu et al. 2014; Pybus et al. 2012; Pybus et al. 2013; Potter et al. 2015). The 5-HPQ is capable of redox cycling back and forth to the corresponding quinone-imine. The 5-HPQ and corresponding quinone-imine species, in the presence of water, form the stable 5,6-orthoquinone primaquine (5,6-OQPQ) (Figure 2.1) (Marcsisin et al. 2016).

Previous studies showed that PQ undergoes hepatic metabolism and induces accumulation of methemoglobin, generates reactive oxygen species (ROS) leading to oxidative stress and also cause depletion of GSH in human erythrocytes (Ganesan et al. 2009; Ganesan et al. 2012). This hypothesis is consistent with several other in vitro studies done with 5-HPQ and 6-methoxy-8-hydroxylaminoquinoline (MHQ) in rat erythrocytes (Bolchoz et al. 2001; Bolchoz et al. 2002a; Bowman et al. 2004; Bowman et al. 2005a). In G6PDd erythrocytes absence of G6PD enzyme compromises the capacity to regenerate NADPH and recycle GSH. The G6PDd erythrocytes also have compromised the ability for detoxification of ROS. Thus, three biomarkers, described above are demonstrated as the potential biochemical markers for hemolytic response in human erythrocytes.

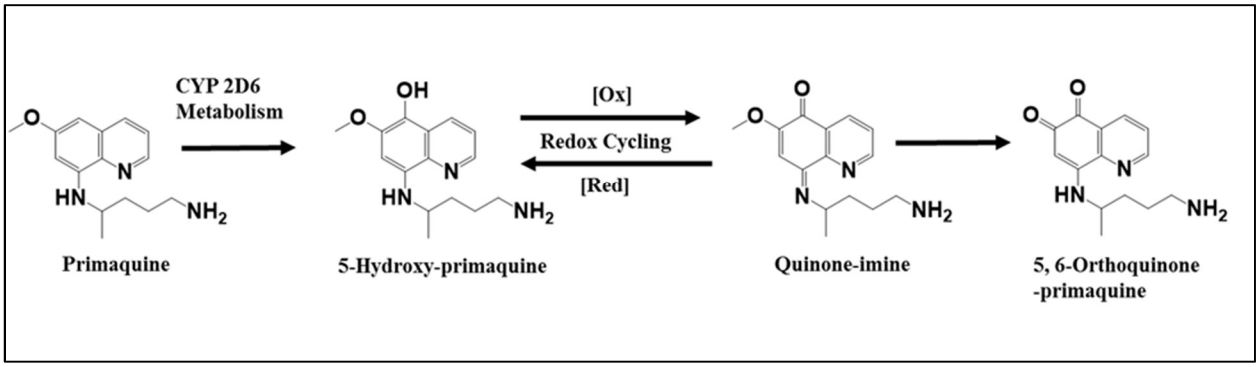

Figure 2.1: Metabolism of PQ to 5-hydroxy-primaquine (5-HPQ) through CYP2D6, and redox cycling of 5-HPQ to its corresponding quinone imine and ortho-quinone. The figure is adapted from (Marcsisin et al. 2016).

Recent reports have shown that the erythrocytes subjected to the hemolytic response due to pathophysiological factors or external insults; undergo specific biochemical and cellular changes. These changes have been collectively referred as eryptosis, which is similar to apoptosis in nucleated eukaryotic cells (Lang et al. 2006; Lang et al. 2012). As erythrocytes do not contain mitochondria and nucleus, they are devoid of the classical apoptotic pathways and apoptotic characteristics such as mitochondrial depolarization and condensation of nuclei. The signaling pathways, which lead to eryptosis, are different from classical pathways of apoptosis. However, eryptosis shares some traits of apoptosis-like cell shrinkage, cell membrane blebbing, and exposure of phosphatidylserine (PS) on the cell surface. Eryptosis could be induced by the agents that cause oxidative stress (Lang et al. 2006; Lang et al. 2012). Exposure to PQ generates severe oxidative stress in erythrocytes (Ganesan et al. 2009), which is presumably triggered by the PQ metabolites produced through CYP-mediated pathways. In normal individuals' presence of a G6PD, the enzyme in pentose phosphate pathway, generate NADPH and formation of GSH is not compromised and thus, oxidative stress has been taken care. Nevertheless, in G6PD deficiency,

the capability of coping with oxidative stress is compromised (Judith Recht 2014). The events involved in eryptosis, commit the damaged erythrocyte to be removed from the circulation through extravascular mechanisms. The exposure of PS on the outer membrane is the ultimate commitment of erythrocyte to be phagocytized by the macrophages (Lang et al. 2012).

2.2. HYPOTHESIS

Phenolic and quinone metabolites, generated through CYP-mediated pathways are responsible for the hemolytic toxicity of PQ. These metabolites cause selective changes in early and late biochemical markers of hemolytic toxicity in G6PDd erythrocytes as compared to normal erythrocytes.

2.3. OBJECTIVE

The purpose of this study was to understand the mechanism of hemolytic toxicity of PQ through evaluation of key biochemical parameters namely, the accumulation of methemoglobin (MtHb), generation of oxidative stress and the levels of reduced glutathione (GSH). These parameters were monitored in normal and G6PDd erythrocytes treated with PQ metabolites. Changes in cellular markers associated with eryptosis were analyzed as late biomarkers of hemotoxic response. The metabolites were tested for a dose-dependent hemolytic response.

2.4. MATERIALS AND METHODS.

2.4.1. Chemicals

2,7-Dichlorofluorescein diacetate (DCFDA), betulinic acid, D-(+)-glucose and tris(2-carboxyethyl)phosphine hydrochloride (TCEP) were purchased from Sigma–Aldrich (St. Louis,

MO, USA). GSH-Glo™ Glutathione Assay kit and Annexin V-FITC Apoptosis Detection kit were purchased from Promega (Madison, WI, USA) and Abcam (Cambridge, MA, USA) respectively. 5-hydroxy-primaquine (5-HPQ), 5,6-orthoquinone-primaquine (5,6-OQPQ) and 6-methoxy-8-hydroxylaminoquinoline (MAQ-NOH or MHQ) were synthesized by Dr. N.P. Dhammika. Nanayakkara at the National Center for Natural Products Research (NCNPR), University of Mississippi (Fasinu et al. 2014). The 5-HPQ is relatively unstable compound and undergo rapid spontaneous oxidation. Time-lapse LC-MS analysis suggested the in the solution 5-HPQ instantly converted to quinone-imine and 5,6-orthoquinone analog. Other reagents used were of highest purity grade available.

2.4.2. Procurement of human blood

Blood was drawn from normal and glucose 6-phosphate dehydrogenase deficient (G6PDd) healthy volunteers under an IRB approved protocol and stored at 4 ^{0}C. To analyze early biomarkers of hemolytic response (MtHb formation, ROS generation, GSH and total glutathione estimation) of 5-HPQ and 5,6-OQPQ, the G6PDd blood taken from an African American male carrying the classic A/A- a combination of electrophoretic variant (Asn126Asp) and deficiency allele (Val68Met) was used. To determine the hemolytic response of MHQ, G6PDd blood was obtained a Caucasian male containing the Ser188Phe Mediterranean mutation was used. To evaluate phosphatidylserine exposure, the late eryptosis response, induced by 5,6-OQPQ, G6PDd blood taken from an African American male carrying the classic A/A- a combination of electrophoretic variant (Asn126Asp) and deficiency allele (Val68Met) was used.

2.4.3. Preparation of erythrocytes for hemotoxicity assays

The normal and G6PDd blood were centrifuged at 4500 g at 4 ◦C for 10 minutes, and buffy coats were removed. The erythrocyte pellets were washed twice with chilled phosphate buffered saline (110 mM sodium chloride, 20 mM disodium hydrogen phosphate and 4 mM potassium dihydrogen phosphate, pH 7.4) with 10 mM glucose (PBSG). The washed erythrocytes pellets were suspended at 50% hematocrit in chilled PBSG.

2.4.4. In vitro hemotoxic assays

The in vitro hemotoxic assays were adapted from an earlier in vitro metabolism-linked hemotoxicity assay (Ganesan et al. 2012; Ganesan et al. 2009). In these assays, different biochemical, molecular and cellular changes, which have been linked to oxidative hemotoxicity were measured. The hemotoxic assays namely, the formation of methemoglobin, generation of ROS, levels of intraerythrocytic GSH and total glutathione were measured as early hemotoxic biomarkers. Externalization of PS on the outer membrane of erythrocytes was measured as a late eryptotic biomarker. The PQ metabolites 5-HPQ, 5,6-OQPQ and MHQ were tested at the concentrations ranging from 3.125 to 25 µM. The structures of PQ, 5-HPQ, 5,6-OQPQ and MHQ are shown in Figure. 2.2

2.4.4.1. Methemoglobin formation assay

The reaction mixture contained 50 µl erythrocytes suspended in PBSG with 50% hematocrit, 2.5 µl of test metabolite (5-HPQ, 5,6-OQPQ or MHQ) and PBSG to make a final volume of reaction mixture to 200 µl. The reaction mixture with appropriate control without test drug was also set up simultaneously. Each assay was set up at least in duplicates. The reaction

mixtures were incubated for 1 hour at 37^{0}C in a shaking water bath. After incubation, samples were kept on ice and methemoglobin levels were measured by a Co-Oximeter (IL-682).

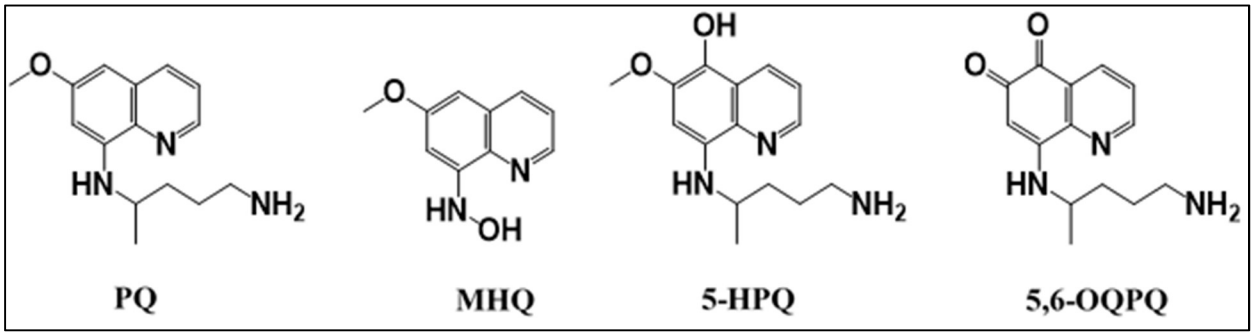

Figure 2.2: Structure of primaquine (PQ) and its metabolites. 5-HPQ (5-hydroxy-primaquine), 5, 6-OQPQ (5, 6-orthoquinone of primaquine) and MHQ (6-methoxy-8-hydroxylaminoquinoline).

2.4.4.2. Reactive oxygen species (ROS) formation (oxidative stress kinetics assay)

This assay was performed in clear flat bottom 96 well plates. The washed normal and G6PDd erythrocytes (50% hematocrit) were loaded with DCFDA, a fluorescent ROS probe. The PBSG washed erythrocytes (50% hematocrit) were incubated with 600 µM DCFDA at 37 ^{0}C for 20 min and centrifuged at 4500 X g for 10 minutes. The DCFDA loaded erythrocytes pellet was resuspended in PBSG to 50% hematocrit and used for the ROS formation assay. The reaction mixtures contained 100 µL DCFDA loaded erythrocytes (50% hematocrit) and 2 µl test drug (3.125 µM - 25 µM). Appropriate control without test drug was also set up at the same time. The plate was read for 2 (every 5 minutes) hours at 37^{0}C on a fluorescence microplate reader for kinetic measurement of fluorescence (excitation 488 nm and emission 535 nm). The data were recorded as relative fluorescence units (RFU), and the time-dependent increase in fluorescence was calculated in Excel software.

2.4.4.3. Estimation of intraerythrocytic reduced glutathione (GSH) and total glutathione levels.

The initial reaction set up for GSH, and total glutathione estimation assay was similar to that for the methemoglobin formation assay described above. The estimation of GSH and total glutathione was done with GSH-Glo™ Glutathione Assay Kit (Promega). To prepare the samples for GSH and total glutathione a 5 µl aliquot was mixed with 20 µl GSH-Glo buffer and kept on ice for at least 20 minutes. The samples were centrifuged at 10650 X g for 10 min at 4 ^{0}C. The supernatants were transferred to separate tubes, and 225 µl of distilled water was added to the supernatants. The samples were vortexed and used for intraerythrocytic GSH and total glutathione determination. Aliquots of 2.5 µl from each sample were transferred to a fresh 96 wells microplate and 25 ml GSH-Glo reagent was added to each well. The plate was incubated for 30 min at 25°C on a shaker. Luciferin detection reagent (25 µl) was added to each well and plate was further incubated for 15 min at room temperature on a shaker. Luminescence was read at 100 integrations on a luminescence microplate reader. Aliquots (2.5 µl each) from the reaction mixtures were mixed with 2.5 µl tris(2-carboxyethyl)phosphine hydrochloride (TCEP) (final concentration 500 µM) and incubated with 25 µl GSH-Glo reagent for 30 min at 25°C on a shaker. TCEP was used to reduce all glutathione into GSH (Winther and Thorpe 2014). The remaining experimental method was similar to the GSH determination assay. Reduced glutathione at 6.25 µM was used as a standard. The data was obtained as relative luminescence unit (RLU). To calculate GSH and total glutathione in blood following formula was used. The concentration of GSH or total glutathione (µmoles/mL blood)

$= (RLU\ of\ corresponding\ treatment * 25 * 2.5 * 50 * 400 * 5)/(RLU\ of\ standard\ X\ 1000\ X\ 1000)$

2.4.4.4. Evaluation of phosphatidylserine exposure (Annexin V binding assay).

The externalization of phosphatidylserine was evaluated by flow cytometric assays using Annexin V-FITC Apoptosis Detection kit, Abcam. The annexin V shows high affinity for exposed phosphatidylserine on the cell surface, and thus it is used as a probe to detect the phosphatidylserine externalization. To prepare the samples, 50 µl of the washed normal and G6PDd erythrocytes (suspended in PBSG with 50% hematocrit) were treated with 2.5 µl metabolite. PBSG was added to make a final volume of reaction mixture to 250 µl. Samples were incubated for 24 hours at 37 ^{0}C in a shaking water bath. After incubation, the aliquots containing 1×10^6 erythrocytes were removed and centrifuged at 4500 X g for 10 min at 4 ^{0}C. The supernatants were removed. The erythrocytes' pellets were resuspended in 500 µL of binding assay buffer and 5 µL Annexin-FITC binding dye was added. The reaction mixtures were incubated for 5 minutes at room temperature in the dark. Annexin V-FITC binding was analyzed by flow cytometry (excitation = 488 nm; emission = 530 nm) using FITC signal detector (FL1). Data were recorded for 10,000 events per sample. Betulinic acid (10 µM) was used as a positive control in this assay. Betulinic acid, a pentacyclic lupane-type triterpene derivative of botulin, is isolated from the bark of *Betula pubescens.* Treatment of human erythrocytes in vitro treatment with betulinic acid induces eryptosis via membrane permeabilization and phosphatidylserine externalization (Macczak et al. 2016). The data was obtained as mean fluorescence and mean fluorescence of M2 population was used for analysis.

2.4.5. Statistical analysis.

Multiple comparisons among groups mean were analyzed by two-way ANOVA followed by Tukey's post hoc tests using GraphPad Prism® version 7.3. The p values <0.05 were considered as significant difference. Data are presented as a mean ± standard error (SE).

2.5. RESULTS

2.5.1. Methemoglobin formation

The washed normal and G6PDd human erythrocytes were incubated with the test compounds at 37 ^{0}C for an hour and then analyzed with Co-oximeter to determine methemoglobin. Exposure of erythrocytes to oxidative reactions converts the Fe^{+2} oxyhemoglobin to Fe^{+3} methemoglobin, which loses the oxygen carrying capacity. The increase in blood methemoglobin levels, referred as methemoglobinemia, is an important diagnostic marker for oxidative stress. Treatment of human erythrocytes with 5-HPQ, 5,6-OQPQ, and MHQ in vitro caused a robust and concentration-dependent increase in methemoglobin formation in normal and G6PDd human erythrocytes (Figure 2.3). Treatment with 5-HPQ produced a significant increase in methemoglobin levels in normal erythrocytes at 12.5 and 25 µM ($p< 0.001$ and $p< 0.001$ respectively), as compared to vehicle control. Similarly, 5-HPQ treatment significantly increased methemoglobin in G6PDd erythrocytes at 6.25, 12.5 and 25 µM ($p< 0.05$, $p< 0.0001$ and $p< 0.0001$ respectively) as compared to vehicle control. The increase in methemoglobin level due to 5-HPQ treatment was almost similar in normal and G6PDd human erythrocytes at all the concentration levels tested, except at 25 µM, which caused a statistically significant increase in methemoglobin in G6PDd erythrocytes compared to normal ($p< 0.01$) (Figure 2.3.A).

Similarly, 5,6-OQPQ treatment also produced concentration-dependent increase in methemoglobin level, which was statistically significant at the concentration levels tested at 6.25, 12.5 and 25 μM as compared to the vehicle control, both in normal ($p< 0.001$, $p< 0.0001$ and $p< 0.0001$ respectively) and G6PDd ($p< 0.0001$, $p< 0.0001$ and $p< 0.0001$ respectively) human erythrocytes (Figure 2.3.B). Again, the increase in methemoglobin level due to 5,6-OQPQ treatment was almost similar in normal and G6PDd human erythrocytes at all the concentration levels tested.

The des-alkylated PQ metabolite MHQ, also produced significant increase in methemoglobin at 6.25, 12.5 and 25 μM, MHQ, as compared to vehicle control, both in normal ($p< 0.001$, $p< 0.0001$ and $p< 0.0001$ respectively) and G6PDd ($p< 0.01$, $p< 0.0001$ and $p< 0.0001$ respectively) human erythrocytes (figure 2.3.C). The methemoglobin formation induced by MHQ was statistically not different in normal and G6PD deficient erythrocytes. However, at the highest concentration, methemoglobin formation induced by MHQ was significantly lower compared to that induced due to the treatment with 5-HPQ and 5,6-OQPQ, both in normal ($p< 0.01$ and $p< 0.0001$ respectively) and G6PDd erythrocytes ($p< 0.0001$ and $p< 0.0001$ respectively).

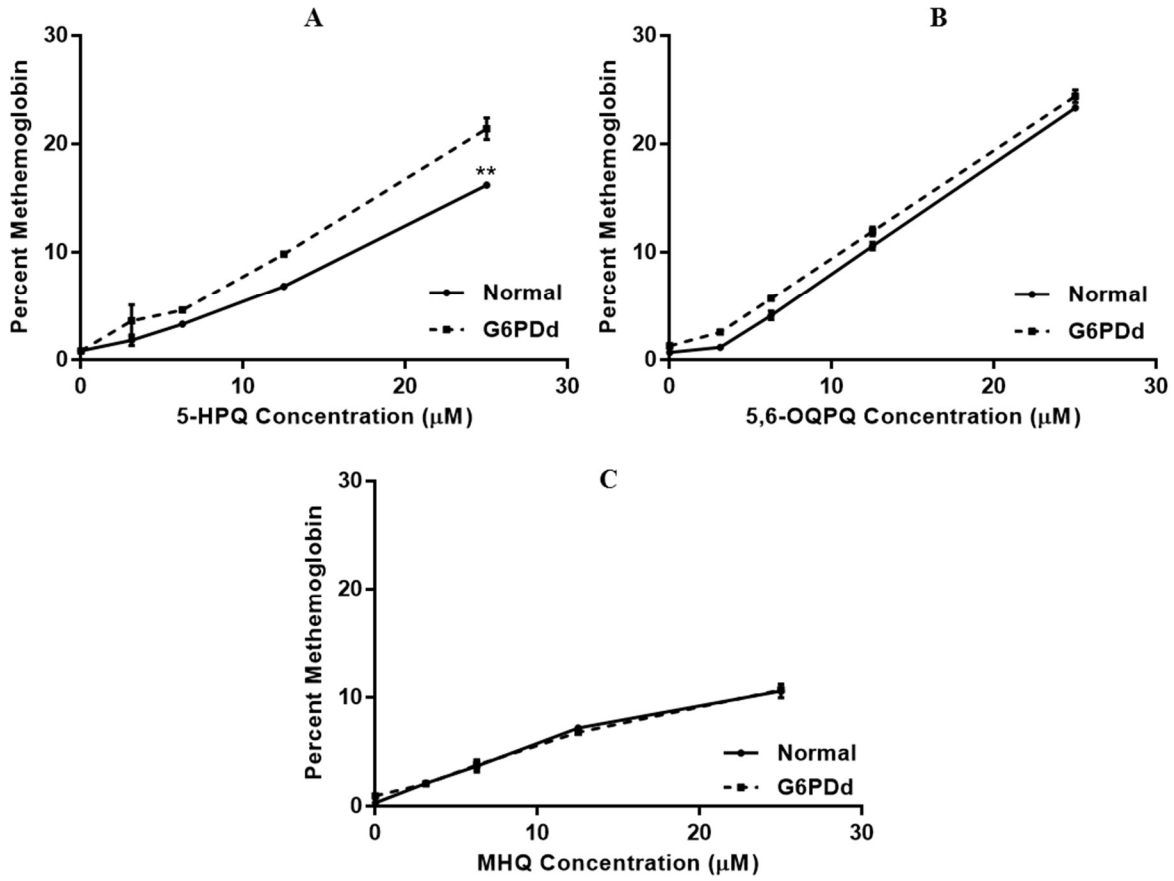

Figure 2.3: Methemoglobin formation in normal and G6PDd human erythrocytes due to treatment with **(A) 5-HPQ**, **(B) 5,6-OQPQ** and **(C) MHQ**. Each data point represents mean ± SE of at least duplicate observations. The results were statistically analyzed with GraphPad Prism® with two-way ANOVA followed by Tukey's multiple comparison test and P values <0.05 were considered as statistically significant. $^{**}p < 0.01$ compared with G6PDd erythrocyte with corresponding concentration.

2.5.2. Generation of reactive oxygen species (ROS)

To determine the effect of 5-HPQ, 5,6-OQPQ and MHQ on oxidative stress, the reactive oxygen species (ROS) generation in both normal and G6PDd human erythrocytes was measured using the fluorescent dye, DCFDA. Like methemoglobin toxicity, all the three metabolites namely, 5-HPQ, 5,6-OQPQ and MHQ generated significant, concentration-dependent ROS in normal and G6PDd human erythrocytes, which is indicated by an increase in fluorescence. Generation of oxidative stress (increase in ROS) due to 5-HPQ exposure was statistically significantl at all the concentrations (3.125 to 25 μM) tested ($p< 0.0001$), in normal human erythrocytes. In G6PDd human erythrocytes, 5-HPQ exposure caused significant increase in oxidative stress at 6.25, 12.5 and 25 μM as compared to vehicle control ($p< 0.01$, $p< 0.0001$ and $p< 0.0001$, respectively) (Figure 2.4). ROS formation caused by 5-HPQ was significantly higher at 3.125, 6.25 and 12.5 μM concentration ($p< 0.05$, $p< 0.01$ and $p< 0.001$, respectively) in normal versus G6PDd erythrocytes (Figure 2.4).

Similar to 5-HPQ, 5,6-OQPQ also generated robust ROS in normal human erythrocytes 3.125, 6.25, 12.5 and 25 μM as compared to vehicle control (0 μM) in normal ($p< 0.05$, $p< 0.01$, $p< 0.0001$ and $p< 0.0001$, respectively). However, in G6PDd human erythrocytes, exposure of 5,6-OQPQ produced significant ROS at 12.5 and 25 μM concentration ($p< 0.001$ and $p< 0.0001$, respectively) (Figure 2.5). 5,6-OQPQ produced considerably higher ROS in normal erythrocytes ($p< 0.01$) as compared to G6PDd human erythrocytes only at 25 μM (Figure 2.5). Generation of oxidative stress (increase in ROS) due to MHQ exposure was statistically significant at all the concentrations (3.125 to 25 μM) tested ($p< 0.0001$), both in normal and G6PDd human erythrocytes (Figure 2.6). However, ROS formation caused by MHQ was not significantly different in normal versus G6PDd erythrocytes (Figure 2.6).

Thus, these data suggest that 5-HPQ, 5,6-OQPQ, and MHQ generated considerable oxidative stress in normal and G6PDd human erythrocytes. MHQ did not produce significantly different oxidative stress in normal as compare to G6PDd human erythrocytes. However, 5-HPQ and 5,6-OQPQ produced statistically higher amount of oxidative stress in normal as compare to G6PDd human erythrocytes (Figure 2.4, 2.5 and 2.6).

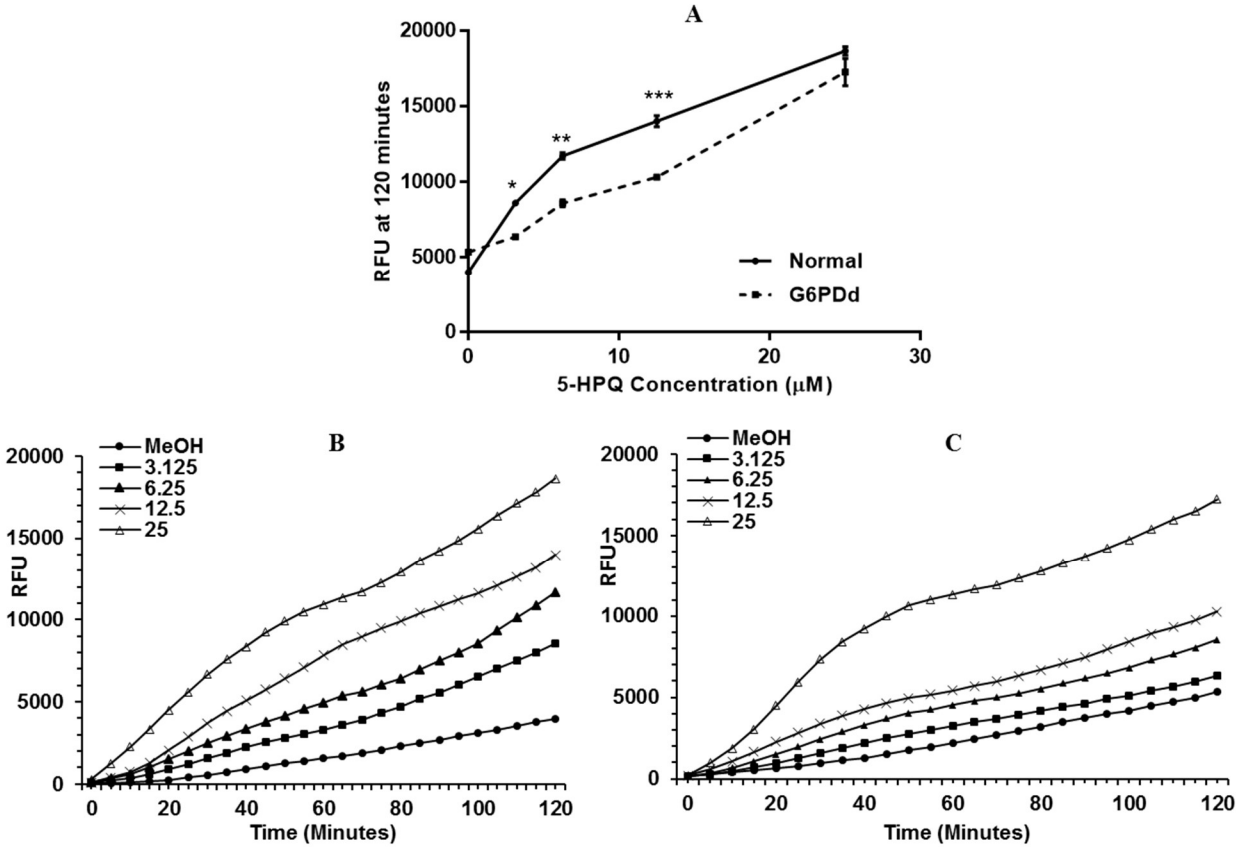

Figure 2.4: Generation of reactive oxygen species**,** shown by increase in fluorescence in DCFDA loaded normal and G6PDd human erythrocytes by 5-HPQ exposure. (A**)** RFU at 120 minutes in normal and G6PDd human erythrocytes exposed to 5-HPQ. Each data point represents mean ± SE of at least duplicate observations. The results were analyzed with GraphPad Prism® with two-way ANOVA followed by Tukey's multiple comparison test and P values <0.05 were considered as statistically significant. Time-dependent increase in fluorescence due to reactive oxygen species generation in (B) normal, and (C) G6PDd human erythrocytes exposed to different concentration of 5-HPQ**.** Each data point is mean of at least duplicate observations. RFU- Relative fluorescence unit.

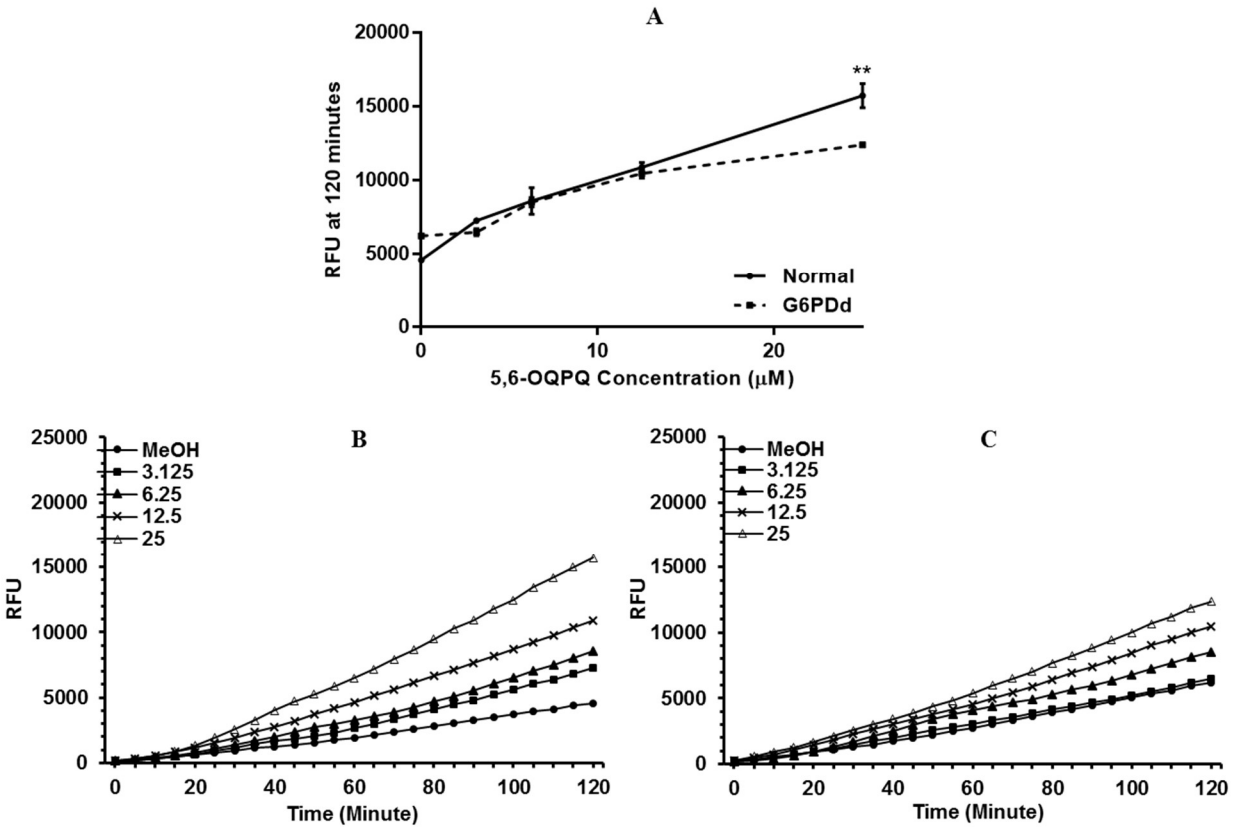

Figure 2.5: Generation of reactive oxygen species**,** shown by increase in fluorescence in DCFDA loaded normal and G6PDd human erythrocytes by 5,6-OQPQ exposure. (A**)** RFU at 120 minutes in normal and G6PDd human erythrocytes exposed to 5-HPQ. Each data point represents mean ± SE of at least duplicate observations. The results were analyzed with GraphPad Prism® with two-way ANOVA followed by Tukey's multiple comparison test and P values <0.05 were considered as statistically significant. Time-dependent increase in fluorescence due to reactive oxygen species generation in (B) normal, and (C) G6PDd human erythrocytes exposed to different concentration of 5,6-OQPQ**.** Each data point is mean of at least duplicate observations. RFU- Relative fluorescence unit.

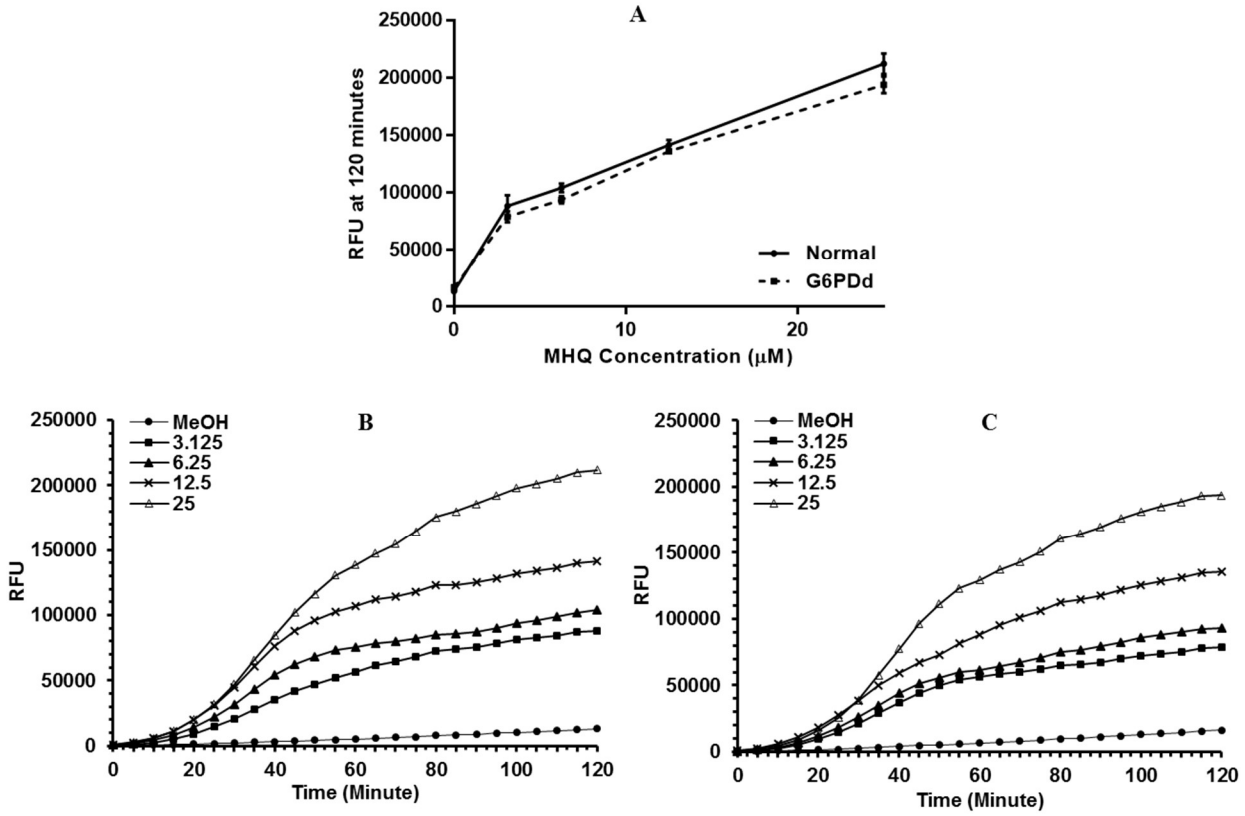

Figure 2.6: Generation of reactive oxygen species**,** shown by increase in fluorescence in DCFDA loaded normal and G6PDd human erythrocytes by MHQ exposure. (A**)** RFU at 120 minutes in normal and G6PDd human erythrocytes exposed to 5-HPQ. Each data point represents mean ± SE of at least duplicate observations. The results were analyzed with GraphPad Prism® with two-way ANOVA followed by Tukey's multiple comparison test and P values <0.05 were considered as statistically significant. Time-dependent increase in fluorescence due to reactive oxygen species generation in (B) normal, and (C) G6PDd human erythrocytes exposed to different concentration of MHQ**.** Each data point is mean of at least duplicate observations. RFU- Relative fluorescence unit.

2.5.3. Estimation of intraerythrocytic reduced glutathione (GSH) levels.

To estimate the effect of 5-HPQ, 5,6-OQPQ and MHQ on the intraerythrocytic GSH level in normal and G6PDd human erythrocytes enzymatic luciferase assay was used. The basal GSH level (vehicle control, 0 µM) in G6PDd human erythrocytes was significantly lower as compared to normal human erythrocytes ($p<0.001$) (Figure. 2.7.A and 2.7.C) suggesting that the depletion in GSH level in G6PDd erythrocytes is because of the genetic defect. Treatment of 5-HPQ increased GSH at 3.125 µM (5.6 %) and decreased GSH at 12.5 µM and 25 µM (5.7% and 10.7% respectively) relative to vehicle control in normal human erythrocytes (Figure. 2.7.B). However, the increase and decrease in GSH level due to treatment in normal erythrocytes was not significant. Treatment of 5-HPQ caused concentration-dependent depletion in GSH level at 3.125 µM, 6.25 µM (40.9%), 12.5 µM (46.8%) and 25 µM (74.7%) in G6PDd human erythrocytes as compared to vehicle control and the depletion in GSH levels were not significant (Figure. 2.7.A and 2.7.B).

Exposure of 5,6-OQPQ, increased GSH at 3.125 µM (5.5%), 6.25 µM (8.4%), 12.5 µM (6.04 %) relative to untreated normal human erythrocytes (Figure. 2.7.D). The increased in GSH level due to treatment in normal erythrocytes was not significant. Exposure of 5,6-OQPQ caused concentration-dependent depletion in GSH level at 3.125 µM (41.7%), 6.25 µM (61%; $p< 0.05$), 12.5 µM (77.8%; $p< 0.01$) and 25 µM (85.1%; $p< 0.01$) in G6PDd human erythrocytes as compare to vehicle control (Figure. 2.7.C and 2.7.D).

MHQ caused, increase in GSH levels at 3.125 µM (62.1%), 6.25 µM (40.6%), 12.5 µM (24.4%) and 25 µM (0.33%) relative to vehicle control in normal human erythrocytes (Figure. 2.7.F). In G6PDd erythrocytes, MHQ increased GSH levels at 3.125 µM (18.7%), 12.5 µM (16%) and 25 µM (21.6%) and depleted GSH levels at 3.125 µM (14,3%) relative to vehicle control in G6PDd human erythrocytes (Figure. 2.7.F). The effect of MHQ in GSH levels in normal and

G6PDd human erythrocytes was not significant (Figure. 2.7.E). Thus, these results indicate that 5,6-OQPQ caused concentration-dependent depletion in GSH level selectively in G6PDd human erythrocytes.

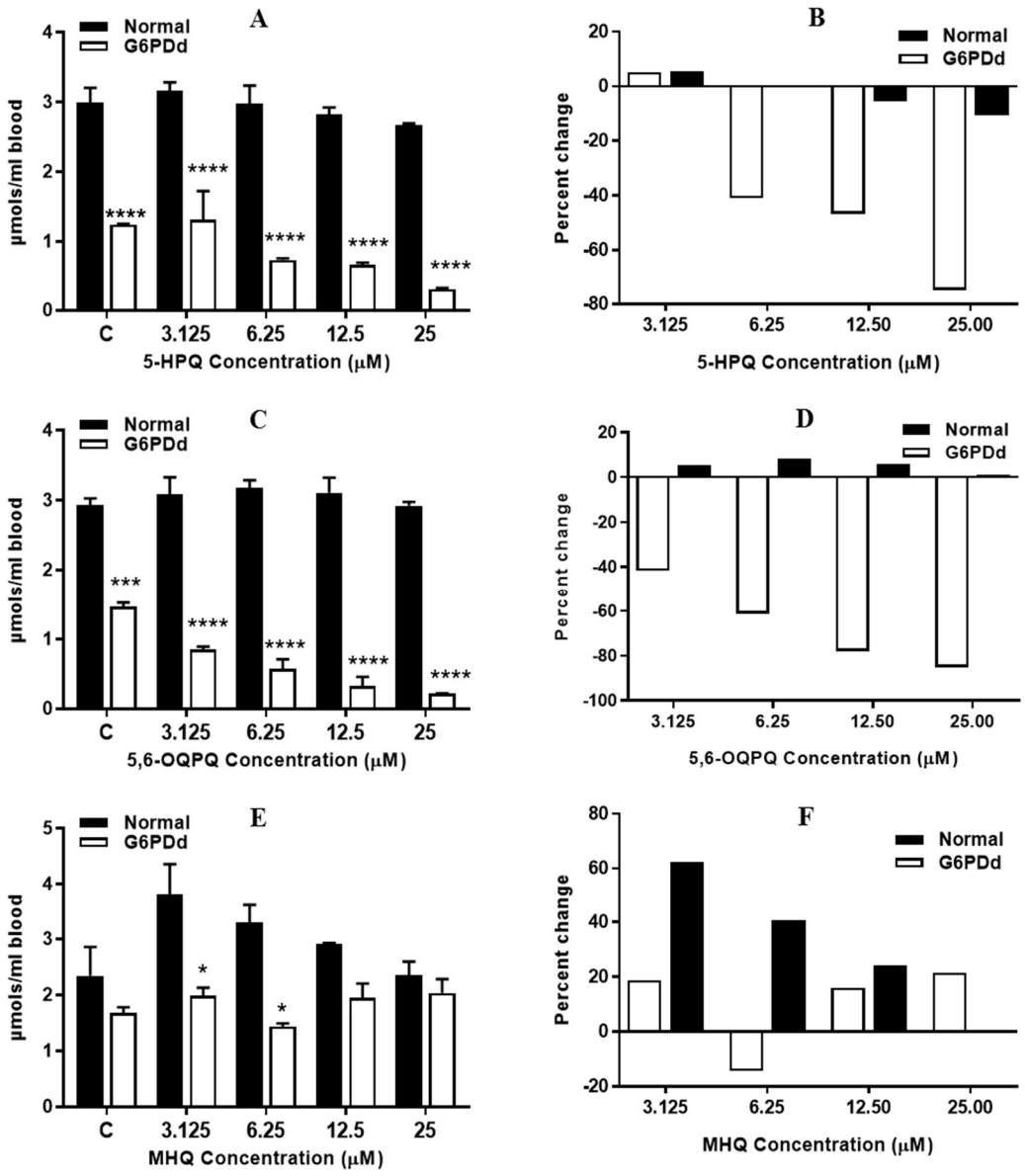

Figure 2.7: Intraerythrocytic GSH levels of normal and G6PDd human erythrocytes treated with (A) 5-HPQ, (C) 5,6-OQPQ and (E) MHQ. Each data point represents mean ± SE of at least duplicate observations. The results were analyzed with GraphPad Prism® with two-way ANOVA followed by Tukey's multiple comparison test and P values <0.05 were considered as statistically significant. $^{*}p < 0.05$, $^{***}p < 0.001$ and $^{****}p < 0.0001$ compared with normal erythrocyte with corresponding concentration**.** Percent change in **i**ntraerythrocytic GSH levels of normal and G6PDd human erythrocytes due to treatment with (B) 5-HPQ, (D) 5,6-OQPQ and (F) MHQ. The percent change in intraerythrocytic GSH levels in treated normal and treated G6PDd erythrocytes are expressed relative to those in vehicle control in normal and G6PDd erythrocytes respectively.

2.5.4. Estimation of intraerythrocytic total glutathione levels.

Total intraerythrocytic glutathione level was also measured by enzymatic luciferase assay using TCEP as reducing agent to thiol (Winther and Thorpe 2014). The results suggest that the basal total intraerythrocytic glutathione levels (vehicle control) were lower in G6PDd human erythrocytes as compared to normal human erythrocytes. However, the difference was not statistically significant (54.7% in Figure 2.8.A, 37.3% in Figure 2.8.C and 34.9% in Figure 2.8.E). Exposure of 5-HPQ increased total glutathione levels at 3.125 µM (4.6%) and decreased total glutathione levels at 6.25 µM (2.8%),12.5 µM (6.9%) and 25 µM (15%) relative to vehicle control in normal human erythrocytes (Figure. 2.8.B). Treatment of 5-HPQ caused an increase in total glutathione levels at 3.125 (67%), 6.25 (5.1%), 12.5 (42.7%) and 25 µM (10.8%) in G6PDd human erythrocytes as compare to vehicle control (Figure 2.8.B). However, the effect of 5-HPQ on total glutathione levels was not significant at any concentration (3.125-25 µM) as compared to vehicle control in normal and G6PDd erythrocytes (Figure 2.8.A and 2.8.B).

Treatment of 5,6-OQPQ, increased total glutathione levels at 3.125 µM (8.1%), 6.25 µM (6.3%) and 25 µM (2.7%) and decreased total glutathione levels at 12.5 µM (1.9%) relative to vehicle control in normal human erythrocytes (Figure. 2.8.D). 5,6-OQPQ caused decrease in total glutathione levels at 3.125 (13.9%), 6.25 (18.9%), 12.5 (7.4%) and 25 µM (7.4%) in G6PDd human erythrocytes as compare to vehicle control (figure. 2.8.D). However, 5,6-OQPQ did not have any significant effect on total glutathione levels at any concentration (3.125-25 µM) as compared to vehicle control in normal and G6PDd erythrocytes (Figure. 2.8.C and 2.8.D).

MHQ caused an increase in total glutathione levels at 3.125 (69.8%), 6.25 (58.3%), 12.5 µM (54.9%) and decreased at 25 µM (3.55%) relative to vehicle control in normal human

erythrocytes (Figure 2.8.F). In G6PDd erythrocytes, MHQ increased total glutathione levels at 3.125 (45,2%), 6.25 (3.9%), 12.5 (37.5) and 25 μM (62.5%) relative to vehicle control in G6PDd human erythrocytes (Figure 2.8.F). Though, the effect of MHQ on total glutathione levels in normal and G6PDd human erythrocytes was not significant as compared to vehicle control (Figure 2.8.E). These results indicate that 5-HPQ, 5,6-OQPQ, and MHQ did not cause significant effect on total glutathione level in normal and G6PDd human erythrocytes.

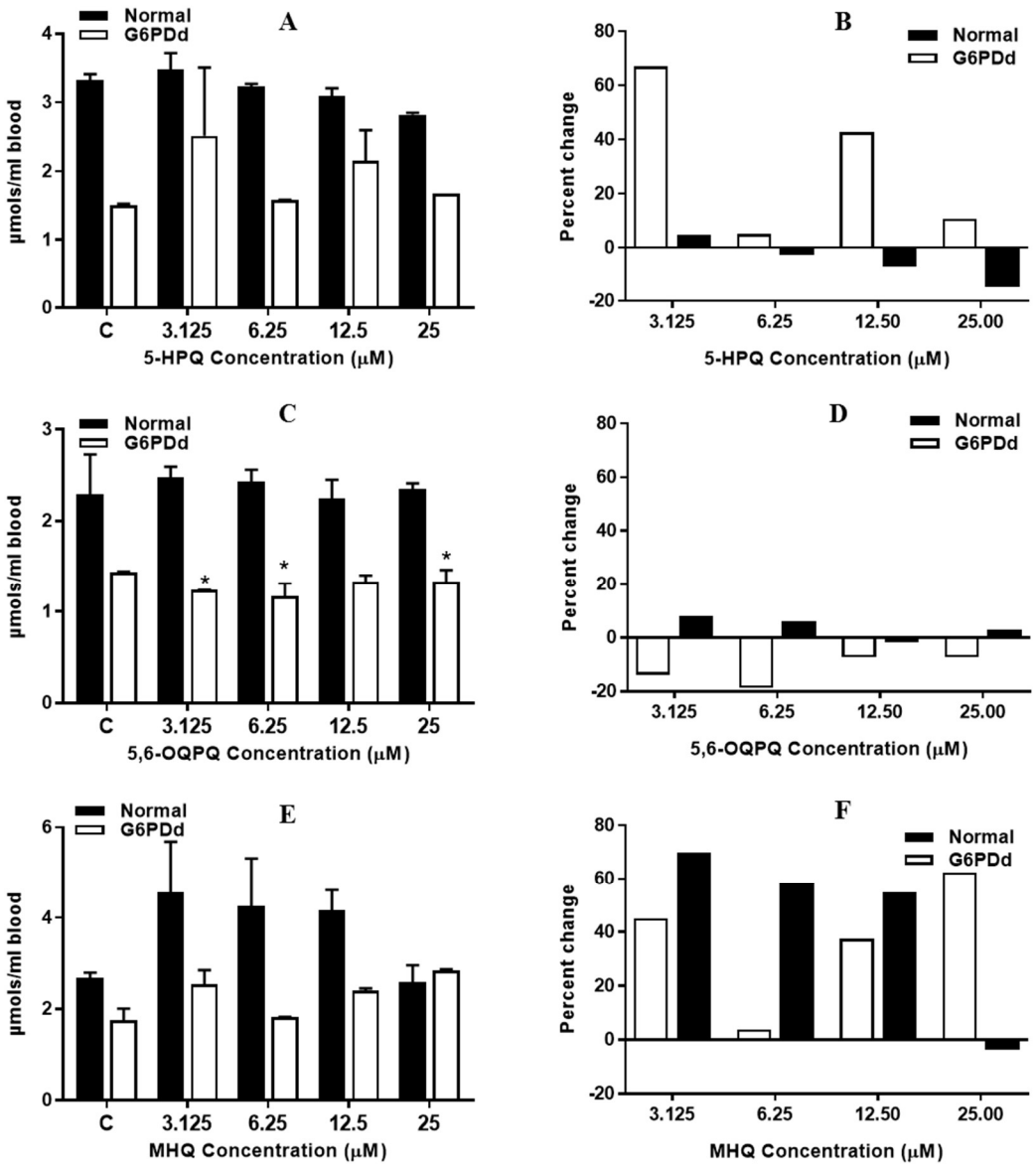

Figure 2.8: Intraerythrocytic total glutathione levels of normal and G6PDd human erythrocytes treated with (A) 5-HPQ, (C) 5,6-OQPQ and (E) MHQ. Each data point represents mean ± SE of at least duplicate observations. The results were analyzed with GraphPad Prism® with two-way ANOVA followed by Tukey's multiple comparison test and P values <0.05 were considered as statistically significant. $^{*}p < 0.05$ compared with normal erythrocyte with corresponding concentration**.** Percent change in **i**ntraerythrocytic total glutathione levels of normal and G6PDd human erythrocytes due to treatment with (B) 5-HPQ, (D) 5,6-OQPQ and (F) MHQ. The percent change in intraerythrocytic GSH levels in treated normal and treated G6PDd erythrocytes are expressed relative to those in vehicle control in normal and G6PDd erythrocytes respectively.

2.5.5. Determination of phosphatidylserine exposure in human erythrocytes.

The flow cytometric assay employing FITC Annexin V binding assay was used to determine phosphatidylserine externalization in normal and G6PDd erythrocytes. Betulinic acid was tested as a positive control in this assay. Translocation of phosphatidylserine on the outer membrane of erythrocytes due to treatment with 5,6-OQPQ (25 μM) and a comparative evaluation of translocation of phosphatidylserine in normal and G6PDd erythrocytes due to 5,6-OQPQ exposure was done. Treatment with betulinic acid caused a significant increase in phosphatidylserine exposure both in normal ($p<0.01$) and G6PDd erythrocytes ($p<0.001$). Treatment with betulinic acid caused statistically more externalization of phosphatidylserine in G6PDd erythrocytes versus normal erythrocytes ($p<0.05$). Treatment with 5,6-OQPQ induced phosphatidylserine externalization in both normal and G6PDd erythrocytes, however, the increase in phosphatidylserine externalization was statistically significant ($p<0.01$) only in G6PDd erythrocytes. Treatment with 5,6-OQPQ induced significantly higher phosphatidylserine externalization in G6PDd as compared to normal erythrocytes ($p<0.01$) (Figure 2.9). Thus, these results suggest that 5,6-OQPQ caused externalization of phosphatidylserine on the outer surface of G6PDd human erythrocytes.

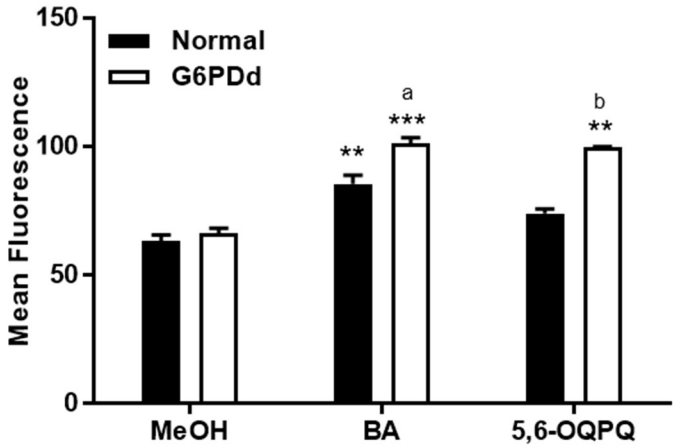

Figure 2.9: Phosphatidyl serine exposure (as analyzed by Annexin V binding) induced by 5,6-OQPQ in normal and G6PDd human erythrocytes. Each data point represents mean ± SE of at least duplicate observations. The results were analyzed with GraphPad Prism® with two-way ANOVA followed by Tukey's multiple comparison test and P values <0.05 were considered as statistically significant. $^{**}p < 0.01$, $^{***}p < 0.01$ compared with corresponding erythrocyte and vehicle control. $^{a}p < 0.05$, $^{b}p < 0.01$ compared with normal human erythrocytes exposed with corresponding treatment.

2.5.6. Comparative hemolytic response of 5-HPQ, 5,6-OQPQ, and MHQ

The methemoglobin formation induced by 5-HPQ, 5,6-OQPQ and MHQ was compared at the highest concentration (25 µM) used in the assay. The results suggest that methemoglobin formation caused by 5,6-OQPQ was significantly higher as compared to that of caused due to 5-HPQ and MHQ in normal ($p< 0.001$ and $p< 0.0001$ respectively). However, in G6PDd erythrocytes, 5,6-OQPQ induced methemoglobin formation was significantly higher as compared to MHQ ($p< 0.0001$) and 5-HPQ ($p> 0.05$). Similarly, 5-HPQ formed significantly higher methemoglobin as compared to MHQ in normal and G6PDd erythrocytes ($p< 0.01$ and $p< 0.0001$ respectively). Thus, these results suggest PQ metabolites formed methemoglobin in the following order: 5,6-OQPQ > 5-HPQ > MHQ in normal and G6PDd erythrocytes (Figure 2.3).

Similarly, oxidative stress generated by 5-HPQ, 5,6-OQPQ and MHQ was compared at the highest concentration (25 μM) used in the assay. The comparison suggests that ROS generation induced by MHQ was significantly higher as compared to that of induced by 5-HPQ ($p< 0.0001$) and 5,6-OQPQ ($p< 0.0001$) in normal and G6PDd erythrocytes. However, 5-HPQ did not generate significantly different ROS as compared to 5,6-OQPQ in normal and G6PDd erythrocytes (Figure 2.4, 2.5 and 2.6). Thus, these results suggest PQ metabolites generates oxidative stress in following order: MHQ > 5-HPQ = 5,6-OQPQ in normal and G6PDd erythrocytes.

The depletion in GSH levels caused by 5-HPQ, 5,6-OQPQ, and MHQ was also compared at the highest concentration (25 μM) used in the assay in G6PDd erythrocytes only since metabolites did not have any significant depletion in normal erythrocytes. Treatment of 5-HPQ and 5,6-OQPQ caused depletion (74.7% and 85.1%; $p< 0.01$ respectively) in GSH levels in G6PDd human erythrocytes as compare to vehicle control. However, MHQ caused 18.7% increase in G6PDd erythrocytes. However, the GSH depletion caused by 5,6-OQPQ was significant.

2.6. DISCUSSION

PQ treatment to G6PD individuals causes severe hemolysis accompanied with dark urine and mild jaundice (Ashley et al. 2014; Clayman et al. 1952; Hockwald et al. 1952). The clinical manifestations of hemolytic toxicity depend mainly on the dose of PQ and severity of the patient's G6PD genetic defect (Ashley et al. 2014; Cappellini and Fiorelli 2008). Various groups studied both in vitro and in vivo hemotoxic effects of PQ (Hong et al. 1992; Vasquez-Vivar and Augusto 1992, 1994; Morais Mda and Augusto 1993; Bolchoz et al. 2001; Bolchoz et al. 2002b; Bolchoz et al. 2002a; Bowman et al. 2004; Bowman et al. 2005b; Bowman et al. 2005a; Ganesan et al. 2009; Ganesan et al. 2012; Garg et al. 2011). The efficacy and hemolytic toxicity of PQ depend

on hepatic metabolism (Ganesan et al. 2009; Ganesan et al. 2012; Xuan et al. 2016). Although numerous studies have been done in last two decades, to understand the underlying mechanism of PQ-induced hemolysis still, the metabolite (s) and pathway (s), which are responsible for the hemolytic toxicity is not clear and inadequate.

Ganesan et al. analyzed the hemotoxic effect of PQ in the presence of human liver microsomes (HLM), mouse liver microsomes (MLM) and recombinant human-CYPs isoforms in normal and Glucose-6-Phosphate Dehydrogenase-deficient (G6PDd) human erythrocytes (Ganesan et al. 2009; Ganesan et al. 2012). The studies showed that in the presence of HLM, PQ-induced methemoglobin (MtHb) formation, reactive oxygen species (ROS) generation, and depletion in thiols in human erythrocytes (Ganesan et al. 2009; Ganesan et al. 2012). Multiple CYP isoforms (CYP2E1, CYP2B6, CYP1A2, CYP2D6, and CYP3A4) were found to mediate the metabolism of PQ and cause PQ-associated hemotoxicity in human erythrocytes (Ganesan et al. 2009). Recent studies revealed that the production of 5-HPQ and other phenolic metabolites of PQ depend on of CYP2D6-mediated metabolism (Fasinu et al. 2014; Pybus et al. 2012; Pybus et al. 2013; Potter et al. 2015).

The current studies mentioned in this chapter suggest that 5-HPQ and MHQ are hemotoxic metabolites of PQ. 5-HPQ and MHQ produced a robust generation of methemoglobin and oxidative stress in normal and G6PDd human erythrocytes. 5-HPQ caused depletion of GSH selectively in G6PDd human erythrocytes. However, MHQ did not cause depletion in GSH levels in either human erythrocytes. The results found in our studies regarding 5-HPQ and MHQ hemotoxicity are consistent with previous studies done on 5-HPQ and MHQ on rat erythrocytes (Bolchoz et al. 2001; Bolchoz et al. 2002b; Bolchoz et al. 2002a; Bowman et al. 2004; Bowman et al. 2005b; Bowman et al. 2005a). These studies suggested that 5-HPQ caused methemoglobin

formation, depletion of GSH (Bowman et al. 2004) and generation of ROS in rat erythrocytes (Bowman et al. 2005b), and MHQ resulted in oxidation of GSH (Bolchoz, Morrow et al. 2002), and generated oxidative stress (Bolchoz, Gelasco et al. 2002) in rat erythrocytes (Bolchoz, Budinsky et al. 2001, Bolchoz, Gelasco et al. 2002, Bolchoz, Morrow et al. 2002). Although, our result did not show the effect of MHQ on GSH depletion/oxidation since the concentration of MHQ used by Bolchoz et al. was 350 μM. Our studies also explored the hemotoxic mechanism of 5,6-OQPQ, the spontaneously transformed product of 5-HPQ, which has been identified only recently (Fasinu et al. 2014). The results showed that 5,6-OQPQ caused concentration-dependent generation of methemoglobin and oxidative stress in normal and G6PDd human erythrocytes and also induced concentration-dependent depletion of GSH selectively in G6PDd human erythrocytes. The comparative hemolytic response of 5-HPQ, 5,6-OQPQ, and MHQ suggest that 5,6-OQPQ formed the highest amount of methemoglobin, followed by 5-HPQ and MHQ in normal and G6PDd erythrocytes. MHQ generated highest oxidative stress as compared to 5-HPQ and 5,6-OQPQ in normal and G6PDd erythrocytes. 5-HPQ and 5,6-OQPQ generated the almost similar amount of oxidative stress in normal and G6PDd erythrocytes. Furthermore, 5,6-OQPQ caused higher GSH depletion followed by 5-HPQ and MHQ in G6PDd erythrocytes.

5,6-OQPQ caused externalization of phosphatidylserine on the outer surface of G6PDd human erythrocytes suggesting the involvement of eryptosis in PQ-induced hemotoxicity. However, previous studies showed that eryptosis might not be involved in removing damaged erythrocytes, which occur due to PQ hemotoxicity (Ganesan et al. 2012). However, in this study (Ganesan et al. 2012), the erythrocytes were incubated with PQ alone in the presence of human liver microsomes only for 3 hours. The short exposure time of 3 hours may not be sufficient to

trigger cellular changes in erythrocytes. Unlike current studies, where erythrocytes were incubated with 5,6-OQPQ for 24 hours.

In conclusion, the current in vitro studies described here infers that 5-HPQ, 5,6-OQPQ, and MHQ are hemotoxic metabolites of PQ and cause a concentration-dependent hemotoxic response by forming methemoglobin, generating oxidative stress in normal and G6PDd human erythrocytes. 5,6-OQPQ depleted GSH and caused externalization of phosphatidylserine selectively in G6PDd human erythrocytes. Exposure of PS on the outer membrane is the ultimate commitment of erythrocyte to be phagocytized by macrophages. Thus, these results suggest that eryptotic pathway triggers the removal of damaged erythrocytes from the circulation in the G6PDd population on exposure to PQ.

CHAPTER 3

THE ROLE OF NRH-QUINONE OXIDOREDUCTASE 2 IN HEMOLYTIC TOXICITY OF PRIMAQUINE METABOLITES.

3.1. INTRODUCTION & RATIONALE

NRH-quinone oxidoreductase 2 (NQO2) is a cytosolic and ubiquitously expressed FAD-linked oxidoreductive enzyme, catalyzes mandatory two-electron reductions of quinone to hydroquinones without accumulating semiquinones and free radicals (Foster et al. 2000; Vella et al. 2005). Thus, NQO2 seems to be the detoxification enzyme for quinones (Graves et al. 2002). However, earlier reports suggest that NQO2 is also capable of causing metabolic activation of quinones (Ferry et al. 2010). In addition, to reduction of quinone, NQO2 stabilizes the p53 tumor suppressor (Khutornenko et al. 2010). NOQ2 gene is expressed in heart, liver, kidney, brain and erythrocytes. Furthermore, only NQO2 is present in human erythrocytes and NADPH-quinone oxidoreductase 1 (NQO1) is absent (Graves et al. 2002).

Human erythrocytic NQO2 is the only potential protein target identified for PQ (Ki-1.04±0.38 μM) (Graves et al. 2002). Previous kinetics studies demonstrated that PQ preferentially binds to the oxidized state of NQO2. PQ shows competitive inhibition against the electron donating co-factor dihydronicotinamide riboside (NRH), and reduces FAD to $FADH_2$ (Leung and Shilton 2013). Ping-pong mechanisms can explain the inhibition of NQO2 by PQ and reduction mechanism of NQO2. According to this mechanism, NQO2 protein has a unique catalytic site for

the substrate and co-substrate. First, the co-substrate (an electron donor) occupies the site, releases and converts the FAD to $FADH_2$. After that, the substrate (an electron acceptor) enters the catalytic site and is reduced (Leung and Shilton 2013; Vella et al. 2005; Kwiek et al. 2004).

NQO2 belongs to thioredoxin family of enzymes and is distinctive as it uses dihydronicotinamide riboside (NRH) as a reducing coenzyme instead of NADH or NADPH. Nicotinamide riboside, the oxidized form of the NRH, participates in NAD metabolism, although the cellular source of the NRH, is still not known, and it is unclear why NQO2 uses NRH (Leung and Shilton 2013; Long and Jaiswal 2000). Melatonin (Mel) (IC_{50} = 41.5±1.5μM), resveratrol (Res) (IC_{50} = 0.143±0.05 μM) and quercetin (Quer) (IC_{50} = 1.4±0.1 μM) are potent inhibitors of NQO2 (Figure 3.1) (Ferry et al. 2010; Boutin et al. 2005). As mentioned earlier, that NQO2 is the only target identified for PQ and redox cycling of quinone and quinone-imine metabolites has been implicated in hemotoxicity of PQ (Marcsisin et al. 2016). It is also known that in erythrocytes only NOQ2 is present and NQO1 is absent, and NQO2 participates in quinone activation/detoxification (Graves et al. 2002; Foster et al. 2000; Vella et al. 2005; Ferry et al. 2010). It seems NQO2 might have a role in PQ-induced hemolytic toxicity. Thus, in the current study, Mel, Res and Quer, the inhibitors of NQO2 were used as probes to investigate the function of NQO2 in PQ metabolites-induced hemolytic toxicity.

Docking studies are a powerful tool to gain an understanding of interactions between the protein and ligands (Grinter and Zou 2014; Huang and Zou 2010). With docking studies, the binding mode and binding affinity between protein and ligand are determined and is important to understand the overall mechanism and function of the protein-ligand complex (Huang and Zou 2010). Thus, the molecular docking between human NQO2 protein crystal structure (PDB id 4FGJ) and metabolites of PQ was performed using Schrödinger software suite.

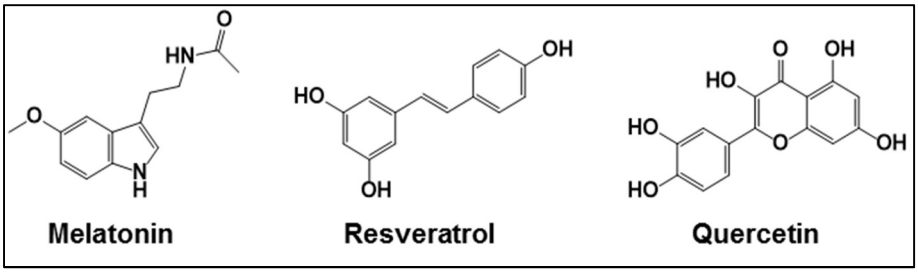

Figure 3.1: Structures of NQO2 inhibitors.

3.2. HYPOTHESIS

The oxidative phenolic and quinone metabolites of PQ interact with NQO2, which modulates redox cycling of PQ metabolites and their potential to cause hemolytic toxicity.

3.3. OBJECTIVE

The purpose of this study was to investigate the function of NQO2, a cytosolic flavoprotein enzyme involved in metabolic detoxification/activation of quinones, in PQ-induced hemolytic anemia. In this study, the hemolytic toxicity of PQ metabolites was evaluated in the presence of NQO2 inhibitors, namely melatonin (Mel), resveratrol (Res) and quercetin (Quer) on normal and G6PDd human erythrocytes. Further, the interactions between human NQO2 protein crystal structure (PBD: 4FGJ) and metabolites of PQ were analyzed using computational docking approach.

3.4. MATERIALS AND METHODS.

3.4.1. Chemicals

Melatonin, resveratrol, and quercetin were purchased from Sigma–Aldrich (St. Louis, MO, USA). The information of remaining chemicals and kits were given in Chapter 2.

3.4.2. Procurement of human blood

Blood was drawn from normal and glucose 6-phosphate dehydrogenase deficient (G6PDd) healthy volunteers under an IRB approved protocol and stored at 4^0C. To analyze the effect of NQO2 inhibitors in early biomarkers of hemolytic response (MtHb formation, ROS generation, GSH and total glutathione estimation) of 5-HPQ and 5,6-OQPQ, the G6PDd blood taken from an African American male carrying the classic A/A- a combination of electrophoretic variant (Asn126Asp) and deficiency allele (Val68Met) was used. To determine the effect of NQO2 inhibitors in the hemolytic response of MHQ, G6PDd blood was obtained a Caucasian male containing the Ser188Phe Mediterranean mutation was used. To evaluate the effect of quercetin on phosphatidylserine exposure, the late eryptosis response, induced by 5,6-OQPQ, G6PDd blood taken from an African American male carrying the classic A/A- a combination of electrophoretic variant (Asn126Asp) and deficiency allele (Val68Met) was used.

3.4.3. Preparation of erythrocytes for hemotoxicity assays

Similar to chapter 2 section 2.4.3

3.4.4. In vitro hemotoxic assays

The in vitro hemotoxic assays were similar to mentioned in chapter 2 section 2.4.4. The concentration of NOQ2 inhibitors (melatonin, resveratrol, and quercetin) used was 100 μM.

3.4.4.1. Methemoglobin formation assay

The reaction mixture contained 50 µl erythrocytes suspended in PBSG with 50% hematocrit, 2.5 µl of test NQO2 inhibitor (Mel, Res, and Quer), 2.5 µl of test metabolite (5-HPQ, 5,6-OQPQ or MHQ) and PBSG to make a final volume of reaction mixture to 250 µl. Remaining method is similar to "methemoglobin formation assay" mentioned in chapter 2 section 2.4.4.1.

3.4.4.2. Reactive oxygen species (ROS) formation (oxidative stress kinetics assay)

The reaction mixtures contained 100 µL DCFDA loaded erythrocytes (50% hematocrit), 2 µl test NQO2 inhibitor, 2 µl test metabolite and PBSG to make a final volume of reaction mixture to 200 µl. The test NOQ2 inhibitor was first incubated with erythrocytes for 10 minutes at 37^0C and then the test metabolite was added. Remaining method is similar to "ROS formation assay" mentioned in chapter 2 section 2.4.4.2.

3.4.4.3. Estimation of intraerythrocytic reduced glutathione (GSH) and total glutathione levels

The method is similar to "estimation of intraerythrocytic reduced glutathione (GSH) and total glutathione levels" mentioned in chapter 2 section 2.4.4.3.

3.4.4.4. Evaluation of phosphatidylserine exposure (Annexin V binding assay)

To prepare the samples, 50 µl the washed normal and G6PDd erythrocytes (suspended in PBSG with 50% hematocrit) were treated with 2.5 µl test NQO2 inhibitor and 2.5 µl test metabolite. PBSG was added to make a final volume of reaction mixture to 250 µl. The test NOQ2 inhibitor was first incubated with erythrocytes for 10 minutes at 37^0C and then the test metabolite

was added. Samples were incubated for 24 hours at 37 ^{0}C in a shaking water bath. The method was similar to "evaluation of phosphatidylserine exposure (Annexin V binding assay)" mentioned in chapter 2 section 2.4.4.4.

3.4.5. Computational methods

The crystal structure of human NQO2 enzyme was downloaded from the protein data bank [PDB ID: 4FGJ] (Leung and Shilton 2013). Protein structure was preprocessed for adding missing hydrogens, adjusting bond orders, proper ionization, and refined using protein preparation wizard in Schrödinger software suite v2016-1 (Schrödinger 2016a). We kept water molecules in the crystal structure near 5Å of ligand binding site. There was no missing side chain; however, alternate positions were found for few residues [MET116 (chain A), GLU153 (chain A), SER164 (chain A), MET116 (chain B), SER134 (chain B)] including PQ. We used the highest average occupancy position of these residues as well as for PQ. The PROPKA program was used to predict the protonation states for protein residues at pH 7.0. Finally, a restrained minimization considering hydrogens only was performed using OPLS3 (Optimized Potentials for Liquid Simulations) force field. All the ligands, PQ, PQ metabolites (5-HPQ, 5,6-OQPQ, and MHQ), menadione and melatonin (Mel) were sketched using Maestro, and ionizable compounds were converted to their most probable charged forms at physiological pH 7.4 and energy minimized using LigPrep module implemented in the Schrödinger software (Sastry et al. 2013; Schrödinger 2016b). Furthermore, the grid was prepared considering co-crystal ligand (primaquine) as the centroid of the active site in the NQO2 protein. A scaling factor of 1.0 was applied to the van der Waals radii and docking study was performed using Glide software considering extra precision (XP) docking method (Friesner et al. 2006). The protein was kept rigid while ligands were flexible during docking. 5

poses for each ligand were kept. Default settings were used for all remaining parameters if not reported elsewhere. The best poses were ranked based on Emodel scores [a mathematical combination of the Glide-score, the ligand strain ($E_{internal}$), and the Coulomb and van der Waals energies]. Further binding free energy (Prime MM-GBSA) of the best protein-ligand complexes was calculated using Prime module of the Schrödinger software. The docking score and interaction profile between protein and ligands were further analyzed (Friesner et al. 2006; Sastry et al. 2013).

Menadione is a known substrate of NQO2 (Ferry et al. 2010). PQ, Mel and menadione were used as a reference compound in this study so that the glide gscore and interaction profile of these reference compound can be compared with PQ metabolites. The knowledge generated through this analysis would help to understand that how the PQ metabolites bind/interact with the protein, whether PQ metabolites bind like an inhibitor or like a substrate.

3.4.6. Statistical analysis.

Similar to chapter 2 section 2.4.5.

3.5. RESULTS

3.5.1. Methemoglobin formation

The washed normal and G6PDd human erythrocytes were incubated with the test compounds at 37^0C for an hour and then analyzed with co-oximeter to determine methemoglobin. Exposure of erythrocytes to oxidative reactions converts the Fe^{+2} oxyhemoglobin to Fe^{+3} methemoglobin, which loses the oxygen carrying capacity. The elevation in blood methemoglobin levels, referred as methemoglobinemia, is an important diagnostic marker for oxidative stress. Co-

treatment of human erythrocytes with NQO2 inhibitors (Mel, Res, and Quer) caused a robust elevation in metabolites (5-HPQ, 5,6-OQPQ, and MHQ) induced- methemoglobin formation.

Mel caused significant increase in 5-HPQ-induced methemoglobin formation in both normal and G6PDd erythrocytes at 6.25, 12.5 and 25 μM concentration of 5-HPQ (Figure 3.2.A and 3.2.B). Res and Quer considerably increased in 5-HPQ-induced methemoglobin formation in both normal and G6PDd erythrocytes at all concentration (3.125-25 μM) of 5-HPQ (3.2.C and 3.2.D, 3.2.E and 3.2.F). These results indicate that all three NQO2 inhibitors (Mel, Res, and Quer) increased 5-HPQ-induced methemoglobin.

Mel, Res, and Quer caused a significant increase in 5,6-OQPQ-induced methemoglobin formation in both normal and G6PDd erythrocytes at all concentrations (3.125-25 μM) of 5,6-OQPQ (Figure. 3.3). These results suggest that NQO2 inhibitors (Mel, Res, and Quer) augment methemoglobinemia induced by 5,6-OQPQ.

Mel, Res, and Quer significantly increased MHQ-induced methemoglobin formation in both normal and G6PDd erythrocytes at all concentrations (3.125-25 μM) of 5,6-OQPQ (Figure. 3.4). These results show that NQO2 inhibitors (Mel, Res, and Quer) augment methemoglobinemia induced by MHQ.

Thus, the results indicate that NQO2 inhibitors (Mel, Res, and Quer) intensified methemoglobinemia induced by PQ metabolites (5-HPQ, 5,6-OQPQ, and MHQ) in normal and G6PDd erythrocytes. Moreover, Quer alone caused a significant increase in methemoglobin accumulation (Figure 3.2.E, 3.2.F, 3.3.E, 3.3.F, 3.4.E and 3.4.F) and suggested that Quer forms methemoglobin in normal and G6PDd erythrocytes.

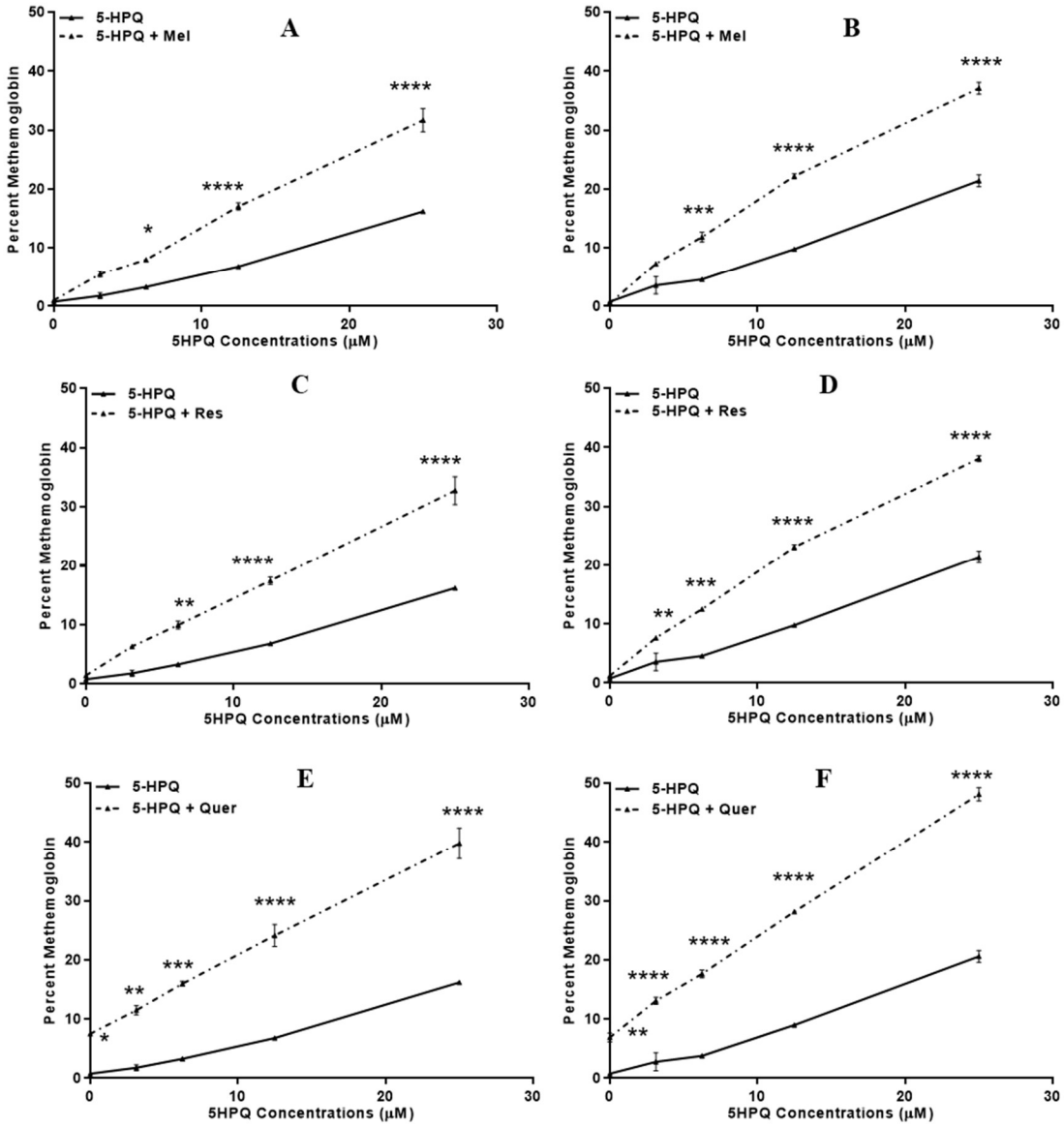

Figure 3.2: Methemoglobin formation due to treatment with 5-HPQ (A, B, C, D, E and F), 5-HPQ + Mel (A and B), 5-HPQ + Res (C and D) and 5-HPQ + Quer in (E and F) normal and (B, D and F) G6PDd human erythrocytes. Each data point represents mean ± SE of at least duplicate observations. The results were statistically analyzed with GraphPad Prism® with two-way ANOVA followed by Tukey's multiple comparison test and P values <0.05 were considered as statistically significant. *p < 0.05, **p < 0.01, ***p < 0.001, ****p < 0.0001 compared with 5-HPQ-treated erythrocytes at corresponding concentration.

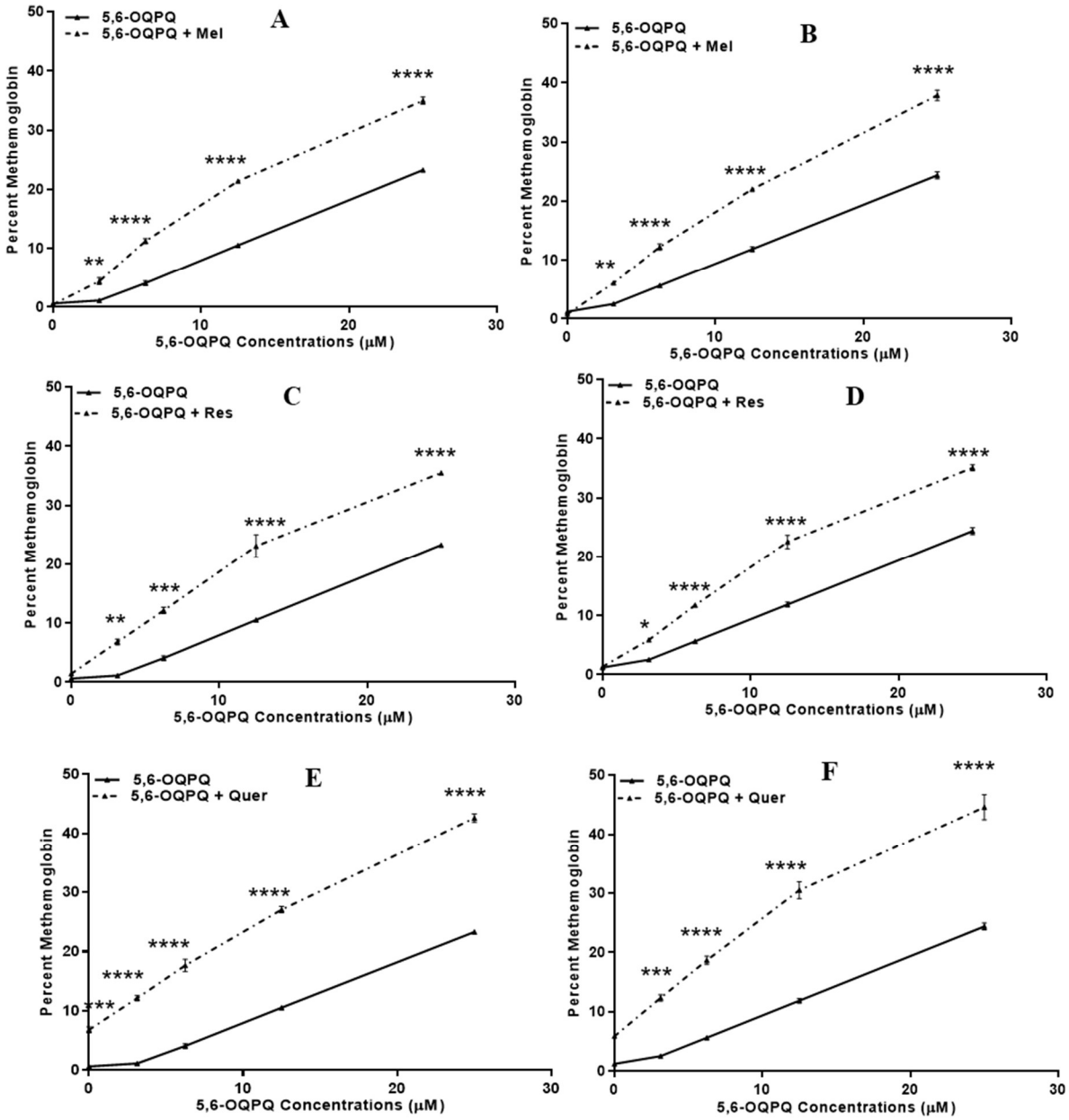

Figure 3.3: Methemoglobin formation due to treatment with 5,6-OQPQ (A, B, C, D, E and F), 5,6-OQPQ + Mel (A and B), 5,6-OQPQ + Res (C and D) and 5,6-OQPQ + Quer in (E and F) normal and (B, D and F) G6PDd human erythrocytes. Each data point represents mean ± SE of at least duplicate observations. The results were statistically analyzed with GraphPad Prism® with two-way ANOVA followed by Tukey's multiple comparison test and P values <0.05 were considered as statistically significant. *p < 0.05, **p < 0.01, ***p < 0.001, ****p < 0.0001 compared with 5,6-OQPQ -treated erythrocytes at corresponding concentration.

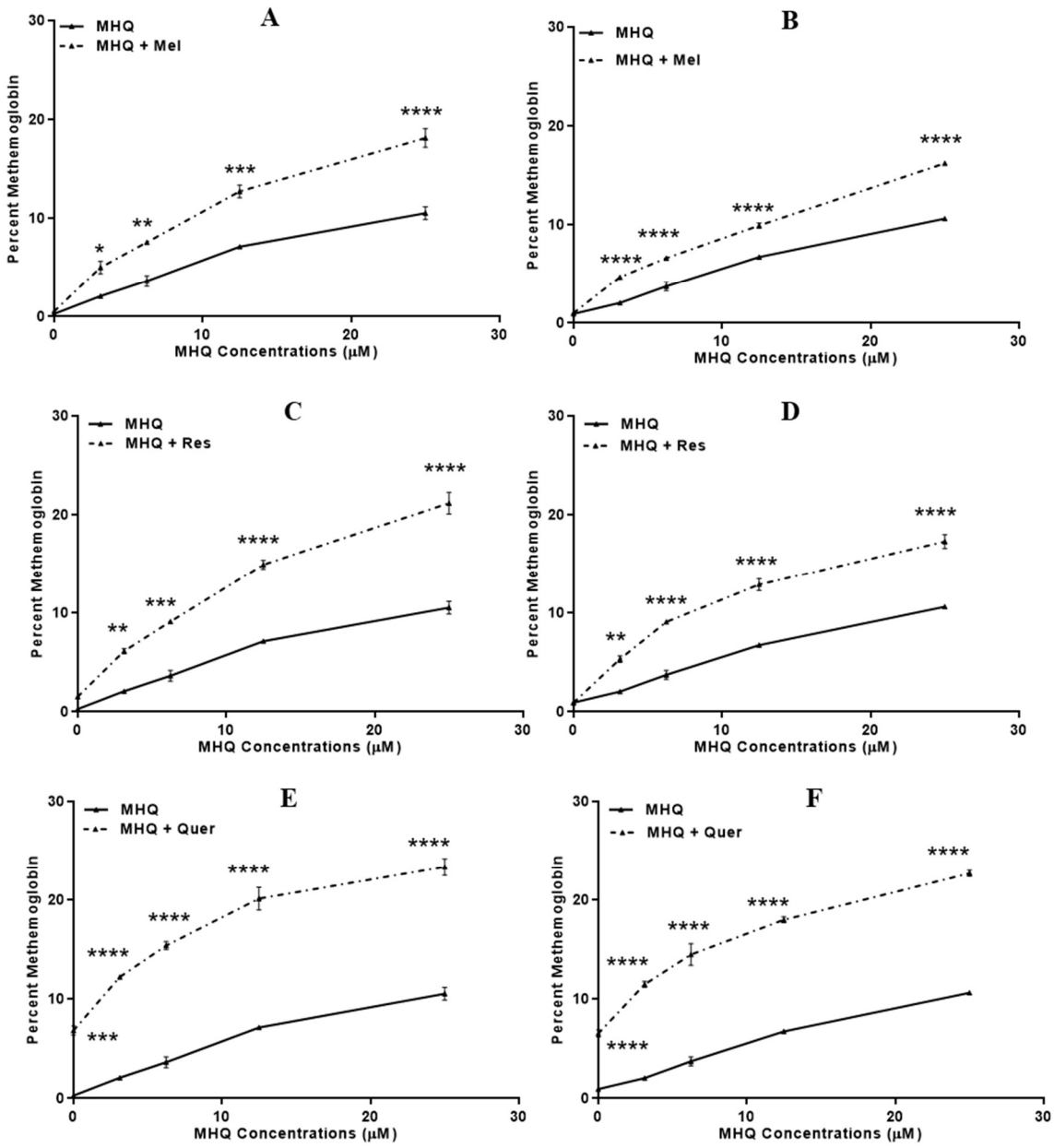

Figure 3.4: Methemoglobin formation due to treatment with MHQ (A, B, C, D, E and F), MHQ + Mel (A and B), MHQ + Res (C and D) and MHQ + Quer in (E and F) normal and (B, D and F) G6PDd human erythrocytes. Each data point represents mean ± SE of at least duplicate observations. The results were statistically analyzed with GraphPad Prism® with two-way ANOVA followed by Tukey's multiple comparison test and P values <0.05 were considered as statistically significant. *p < 0.05, **p < 0.01, ***p < 0.001, ****p < 0.0001 compared with MHQ-treated erythrocytes at corresponding concentration.

3.5.2. Generation of reactive oxygen species (ROS)

To determine the effect of NQO2 inhibitors (Mel, Res, and Quer) on oxidative stress caused by PQ metabolites (5-HPQ, 5,6-OQPQ, and MHQ), the reactive oxygen species (ROS) generation in both normal and G6PDd human erythrocytes was measured using the fluorescent dye, DCFDA. Co-treatment of Mel increased generation of oxidative stress (increase in ROS) caused by 5-HPQ in normal and G6PDd human erythrocytes at all the concentrations, (3.125-25 µM) of 5-HPQ (Figure 3.5.A and 3.5.B). Res partially subsided ROS generated by 5-HPQ in normal erythrocytes and G6PDd human erythrocytes at all the concentrations (3.125-25 µM) of 5-HPQ (Figure 3.5.C and 3.5.D). Quer had a dual effect on 5-HPQ-induced ROS generation in both erythrocytes. Quer increased ROS induced by a lower concentration of 5-HPQ in normal (3.125 µM) and G6PDd (3.125 and 6.25 µM) erythrocytes (Figure 3.5.E and 3.5.F). However, Quer partially attenuated ROS caused by the higher concentration of 5-HPQ in normal (12.5 and 25 µM) and G6PDd (25 µM) erythrocytes (Figure 3.5.E and 3.5.F). Additionally, treatment of Quer alone produced a significant increase in ROS in normal and G6PDd erythrocytes as compared to vehicle control (Figure 3.5.E and 3.5.F).

Co-exposure of Mel with 5,6-OQPQ potentiated oxidative stress generated due 5,6-OQPQ alone in normal and G6PDd human erythrocytes at all the concentrations (3.125-25 µM) of 5,6-OQPQ (Figure 3.6.A and 3.6.B). Res partially attenuated oxidative stress produced by 5,6-OQPQ in G6PDd erythrocytes at 25 µM concentrations of 5,6-OQPQ (Figure 3.6.D). Similarly, Res partially attenuated oxidative stress produced by 5,6-OQPQ in normal erythrocytes. However, the effect of Res is not statistically significant (Figure 3.6.C). Quer increased ROS induced by 5,6-OQPQ in normal and G6PDd at 3.125 - 12.5 µM concentrations of 5,6-OQPQ (Figure 3.6.E and

3.6.F). Furthermore, exposure of Quer alone generated a significant increase in ROS in normal and G6PDd erythrocytes as compared to vehicle control (Figure 3.6.E and 3.6.F).

Co-exposure of Mel with MHQ potentiated oxidative stress generated due to MHQ alone in normal and G6PDd human erythrocytes at all the concentrations (3.125 - 25 µM) of MHQ (Figure 3.7.A and 3.7.B). Res and Quer partially attenuated oxidative stress produced by MHQ alone in normal and G6PDd human erythrocytes at all the concentrations (3.125 - 25 µM) of MHQ (Figure. 3.7).

Thus, the results indicate that Mel potentiates oxidative stress induced by PQ metabolites (5-HPQ, 5,6-OQPQ, and MHQ) in normal and G6PDd erythrocytes. However, in normal and G6PDd erythrocytes, Res partially attenuate oxidative stress generated by PQ metabolites (5-HPQ, 5,6-OQPQ, and MHQ). Quer had the ability to generate oxidative stress in normal and G6PDd erythrocytes. Like Res, Quer also partially attenuate PQ-metabolites-induced oxidative stress in human erythrocytes.

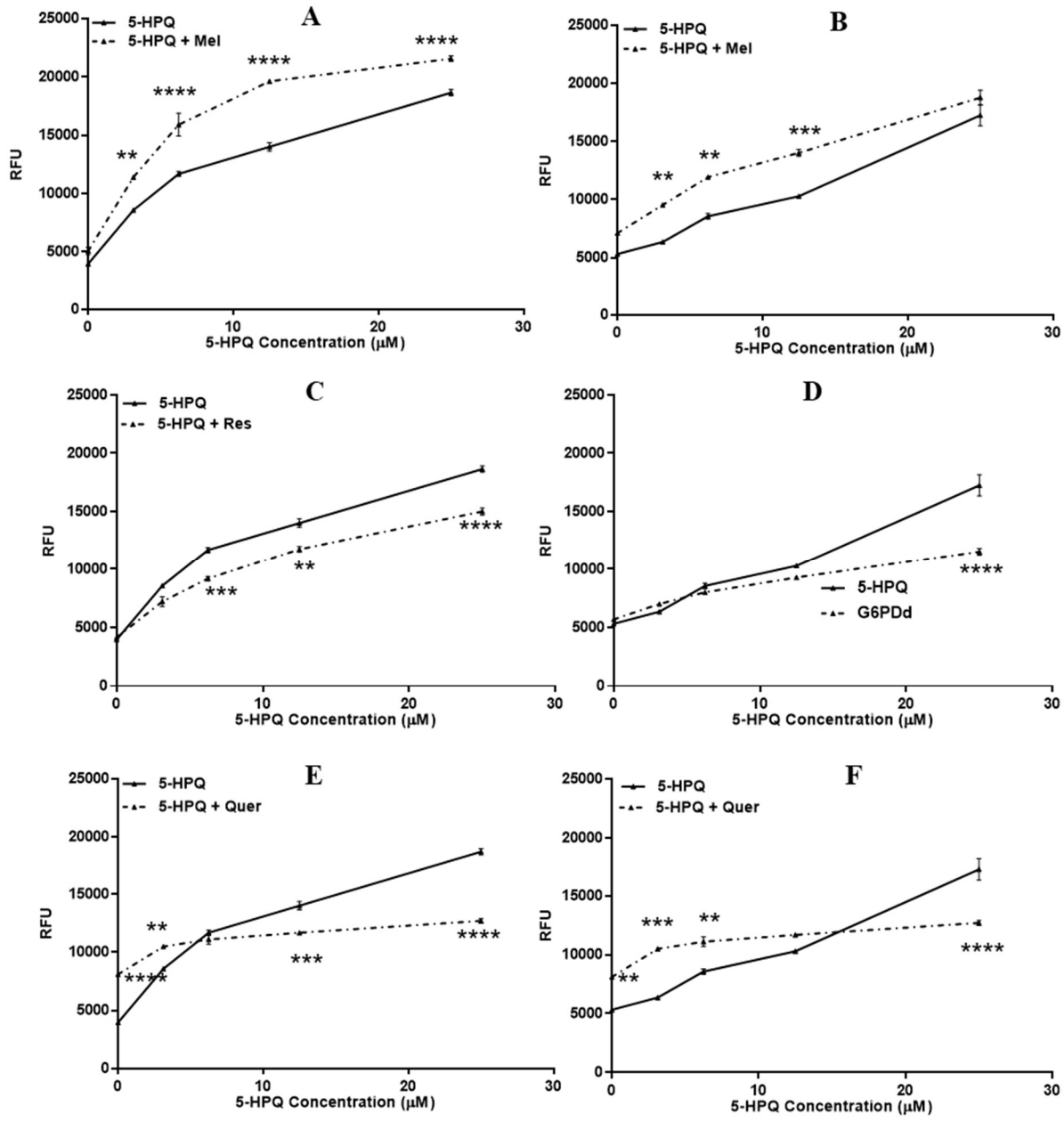

Figure 3.5: ROS generation due to treatment with 5-HPQ (A, B, C, D, E and F), 5-HPQ + Mel (A and B), 5-HPQ + Res (C and D) and 5-HPQ + Quer in (E and F) normal and (B, D and F) G6PDd human erythrocytes at 120 minutes. Each data point represents mean ± SE of at least duplicate observations. The results were statistically analyzed with GraphPad Prism® with two-way ANOVA followed by Tukey's multiple comparison test and P values <0.05 were considered as statistically significant. **p < 0.01, ***p < 0.001, ****p < 0.0001 compared with 5-HPQ-treated erythrocytes at corresponding concentration. RFU- Relative fluorescence unit.

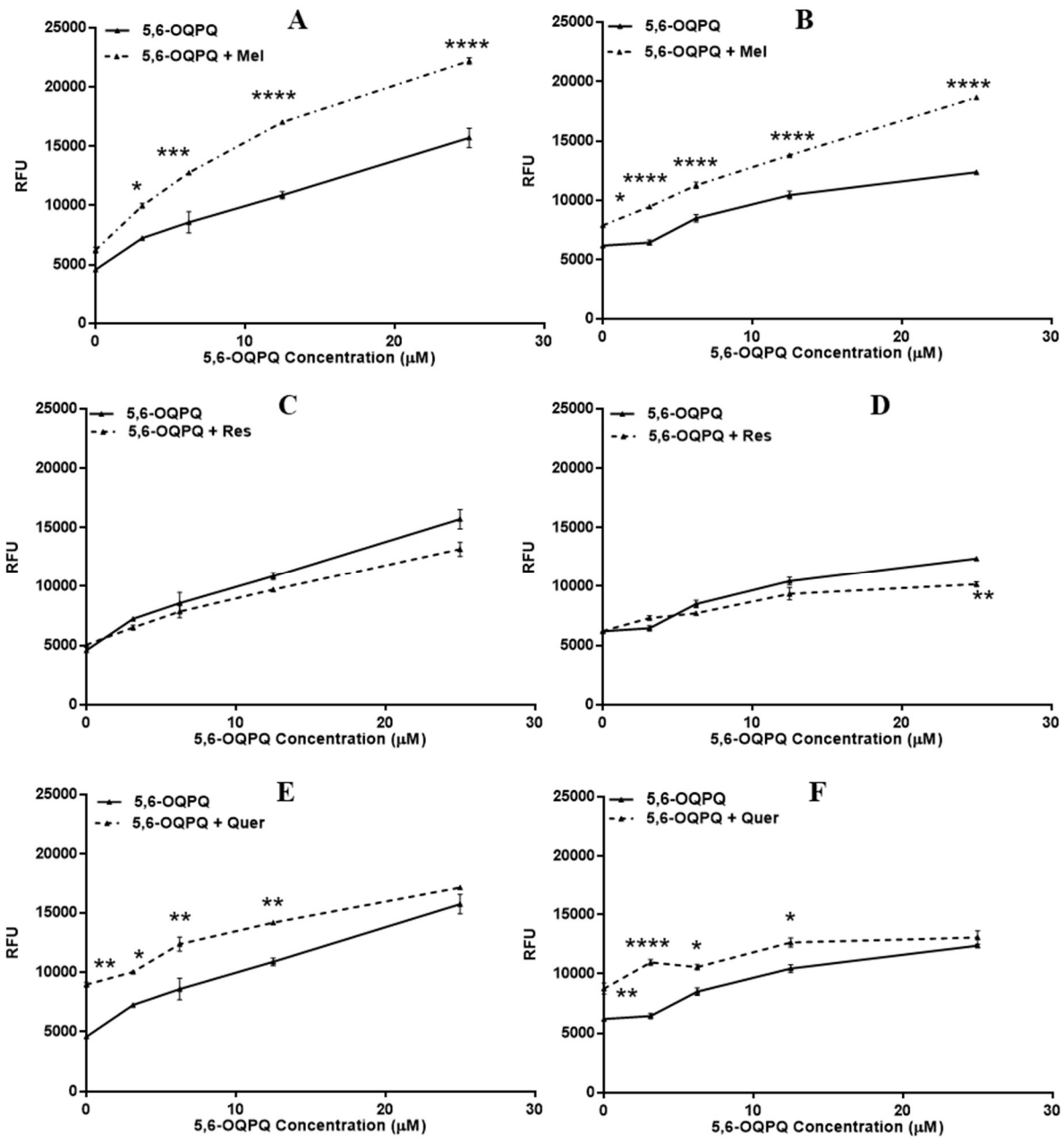

Figure 3.6: ROS generation due to treatment with 5,6-OQPQ (A, B, C, D, E and F), 5,6-OQPQ + Mel (A and B), 5,6-OQPQ + Res (C and D) 5,6-OQPQ 5-HPQ + Quer in (E and F) normal and (B, D and F) G6PDd human erythrocytes at 120 minutes. Each data point represents mean ± SE of at least duplicate observations. The results were statistically analyzed with GraphPad Prism® with two-way ANOVA followed by Tukey's multiple comparison test and P values <0.05 were considered as statistically significant. *p < 0.05, **p < 0.01, ***p < 0.001, ****p < 0.0001 compared with 5,6-OQPQ -treated erythrocytes at corresponding concentration. RFU- Relative fluorescence unit.

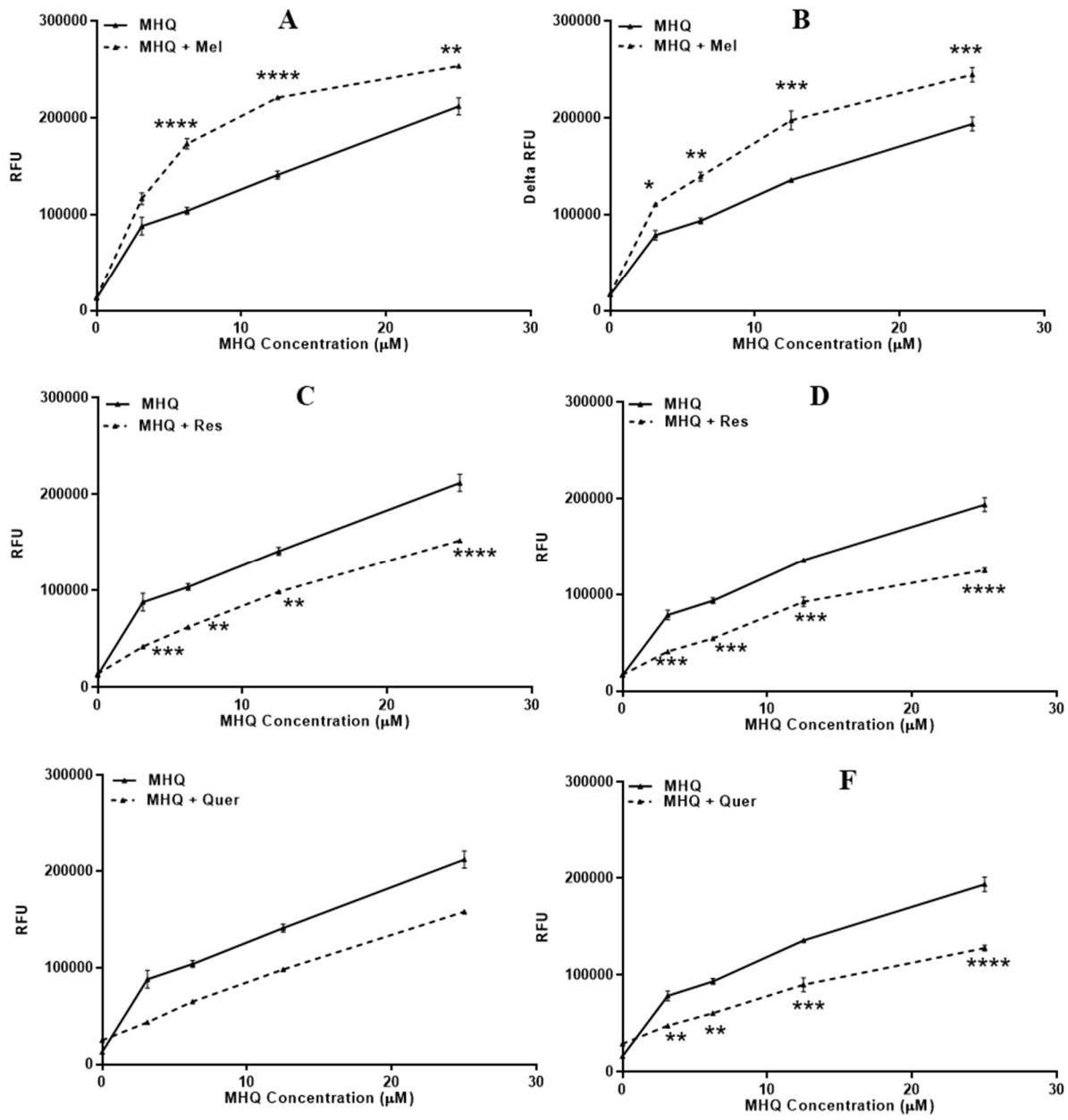

Figure 3.7: ROS generation due to treatment with MHQ (A, B, C, D, E and F), MHQ + Mel (A and B), MHQ + Res (C and D) and MHQ + Quer in (E and F) normal and (B, D and F) G6PDd human erythrocytes at 120 minutes. Each data point represents mean ± SE of at least duplicate observations. The results were statistically analyzed with GraphPad Prism® with two-way ANOVA followed by Tukey's multiple comparison test and P values <0.05 were considered as statistically significant. *$p < 0.05$, **$p < 0.01$, ***$p < 0.001$, ****$p < 0.0001$ compared with MHQ-treated erythrocytes at corresponding concentration. RFU- Relative fluorescence unit.

3.5.3. Estimation of intraerythrocytic reduced glutathione (GSH) levels.

To estimate the effect of NQO2 inhibitors (Mel, Res, and Quer) on PQ metabolite (5-HPQ, 5,6-OQPQ, and MHQ) induced-GSH depletion in normal and G6PDd human erythrocytes, an enzymatic luciferase assay was used. Co-treatment of NQO2 inhibitors (Mel, Res, and Quer) with PQ metabolites (5-HPQ, 5,6-OQPQ, and MHQ) did not have any significant effect on GSH level as compared to that of PQ metabolites (5-HPQ, 5,6-OQPQ, and MHQ) alone in normal erythrocytes (Figure 3.8, 3.9 and 3.10).

Co-treatment of NQO2 inhibitors (Mel, Res, and Quer) with 5-HPQ caused further depletion in GSH level as caused by 5-HPQ alone in G6PDd human erythrocytes. However, this effect is not significant (Figure 3.8). Similarly, co-exposure of NQO2 inhibitors (Mel, Res, and Quer) with 5,6-OQPQ caused further depletion in GSH level as caused by 5,6-OQPQ alone in G6PDd human erythrocytes. However, this effect is not significant (Figure 3.9). Though, co-exposure of NQO2 inhibitors (Mel, Res, and Quer) with MHQ did not have any significant effect on GSH level as compared to that of MHQ alone in normal erythrocytes (Figure 3.10).

These results suggest that cotreatment of NQO2 inhibitors (Mel, Res, and Quer) with PQ metabolites (5-HPQ, 5,6-OQPQ and MHQ) had no significant effect on PQ metabolites-induced depletion in GSH levels in normal and G6PDd human erythrocytes.

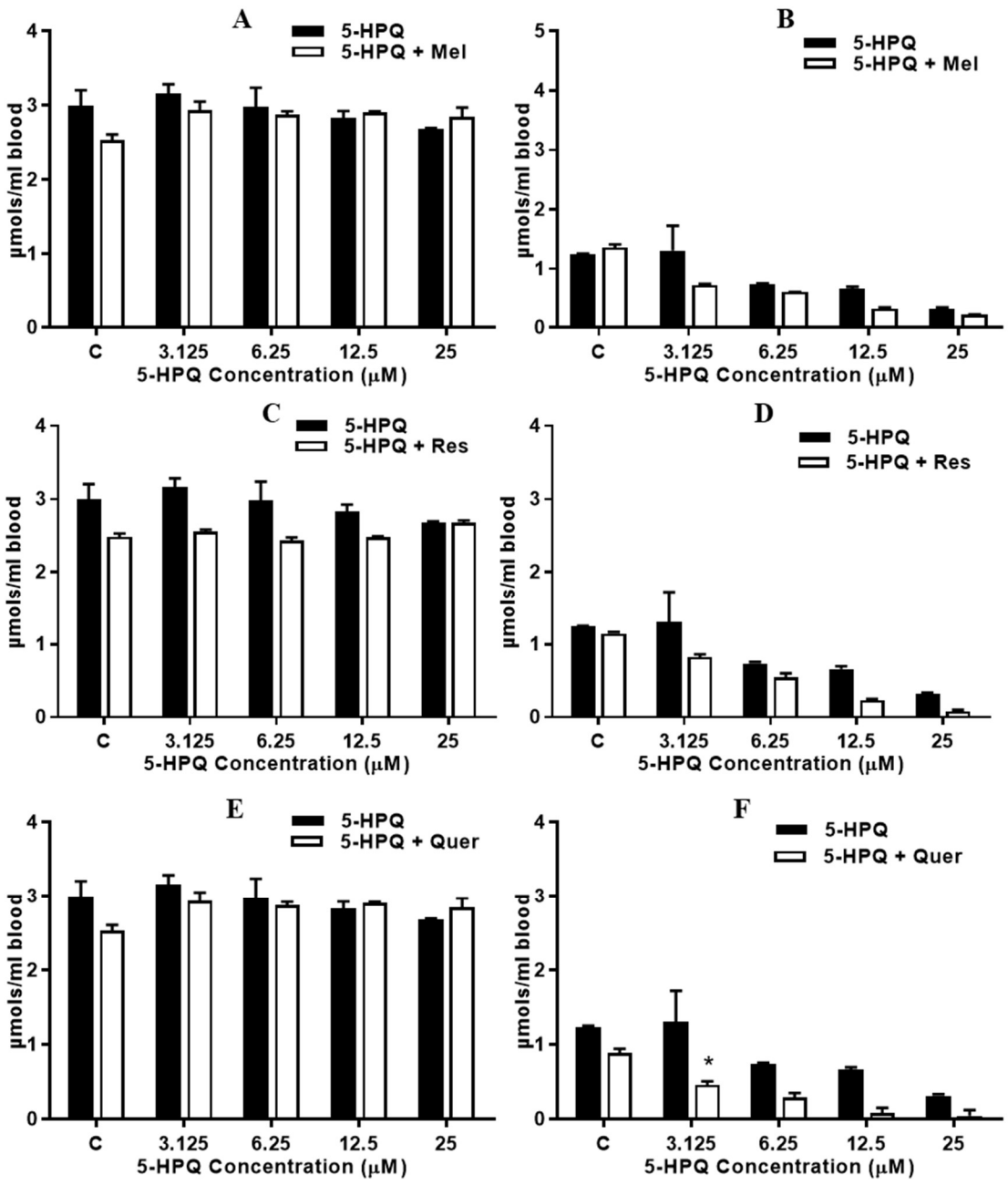

Figure 3.8: Intraerythrocytic GSH levels due to treatment with 5-HPQ (A, B, C, D, E and F), 5-HPQ + Mel (A and B), 5-HPQ + Res (C and D) and 5-HPQ + Quer in (E and F) normal and (B, D and F) G6PDd human erythrocytes. Each data point represents mean ± SE of at least duplicate observations. The results were statistically analyzed with GraphPad Prism® with two-way ANOVA followed by Tukey's multiple comparison test and P values <0.05 were considered as statistically significant. *$p < 0.05$ compared with 5-HPQ-treated erythrocytes at corresponding concentration.

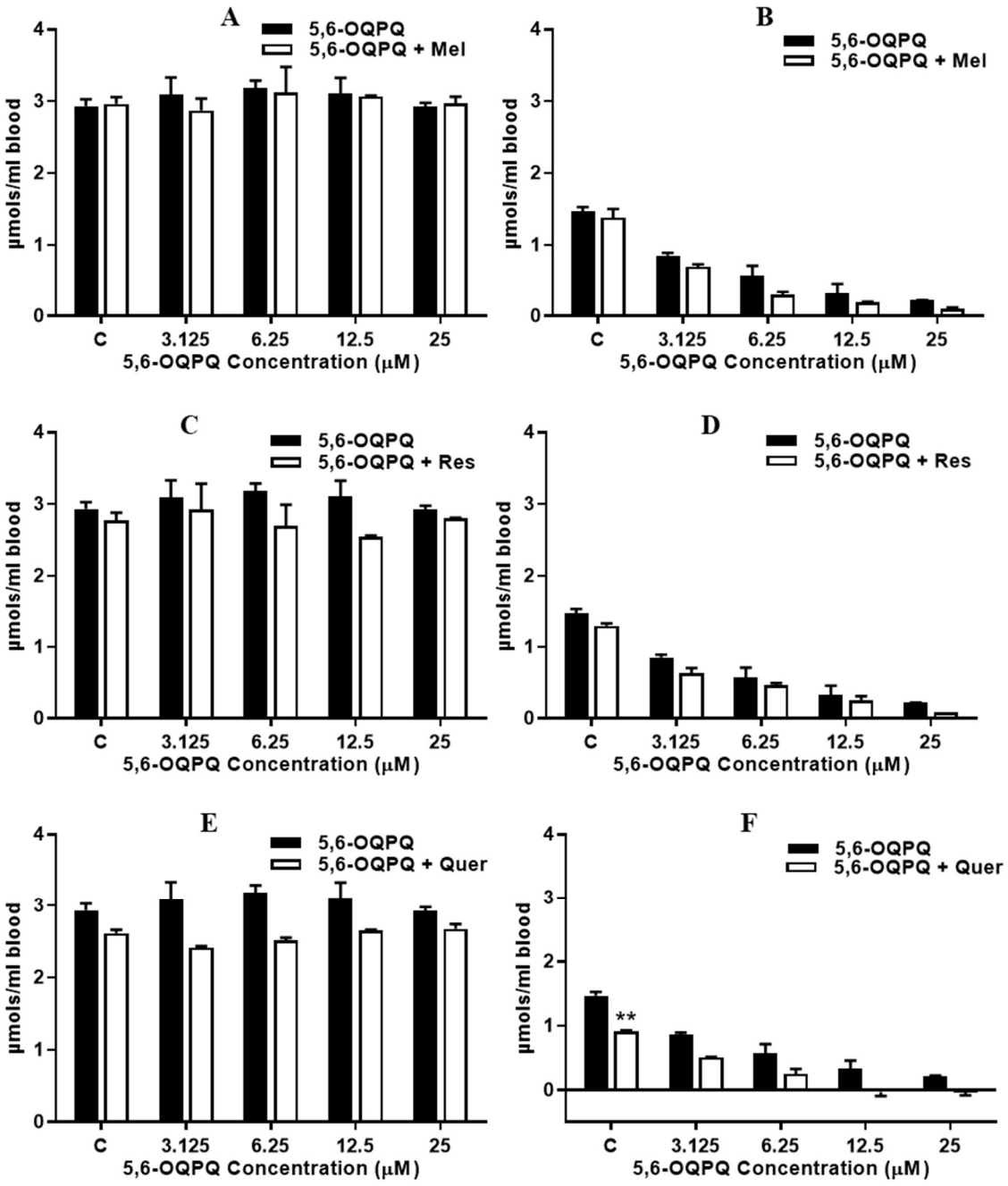

Figure 3.9: Intraerythrocytic GSH levels due to treatment with 5,6-OQPQ (A, B, C, D, E and F), 5,6-OQPQ + Mel (A and B), 5,6-OQPQ + Res (C and D) and 5,6-OQPQ + Quer in (E and F) normal and (B, D and F) G6PDd human erythrocytes. Each data point represents mean ± SE of at least duplicate observations. The results were statistically analyzed with GraphPad Prism® with two-way ANOVA followed by Tukey's multiple comparison test and P values <0.05 were considered as statistically significant. **p < 0.01 compared with vehicle control erythrocytes at corresponding concentration.

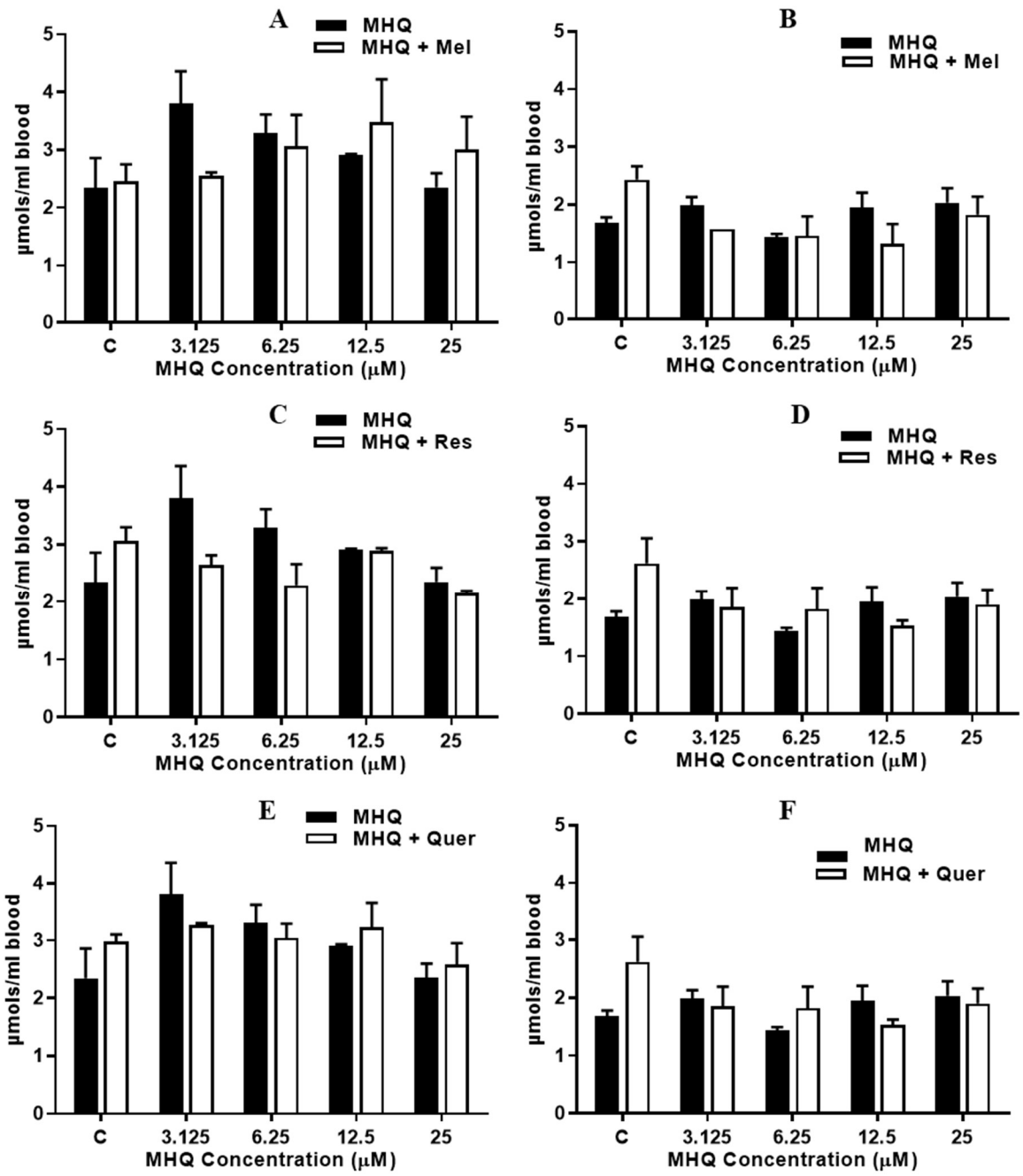

Figure 3.10: Intraerythrocytic GSH levels due to treatment with MHQ (A, B, C, D, E and F), MHQ + Mel (A and B), MHQ + Res (C and D) and MHQ + Quer in (E and F) normal and (B, D and F) G6PDd human erythrocytes. Each data point represents mean ± SE of at least duplicate observations. The results were statistically analyzed with GraphPad Prism® with two-way ANOVA followed by Tukey's multiple comparison test and P values <0.05 were considered as statistically significant.

3.5.4. Estimation of intraerythrocytic total glutathione levels.

Total intraerythrocytic glutathione level was also measured by enzymatic luciferase assay using TCEP as reducing agent to thiol (Winther and Thorpe 2014). The results showed that co-treatment of NQO2 inhibitors (Mel, Res and Quer) with PQ metabolites (5-HPQ, 5,6-OQPQ and MHQ) did not have any significant effect on total GSH level as compared to that of PQ metabolites (5-HPQ, 5,6-OQPQ and MHQ) alone in normal and G6PDd human erythrocytes (Figure 3.11 - Figure 3.13).

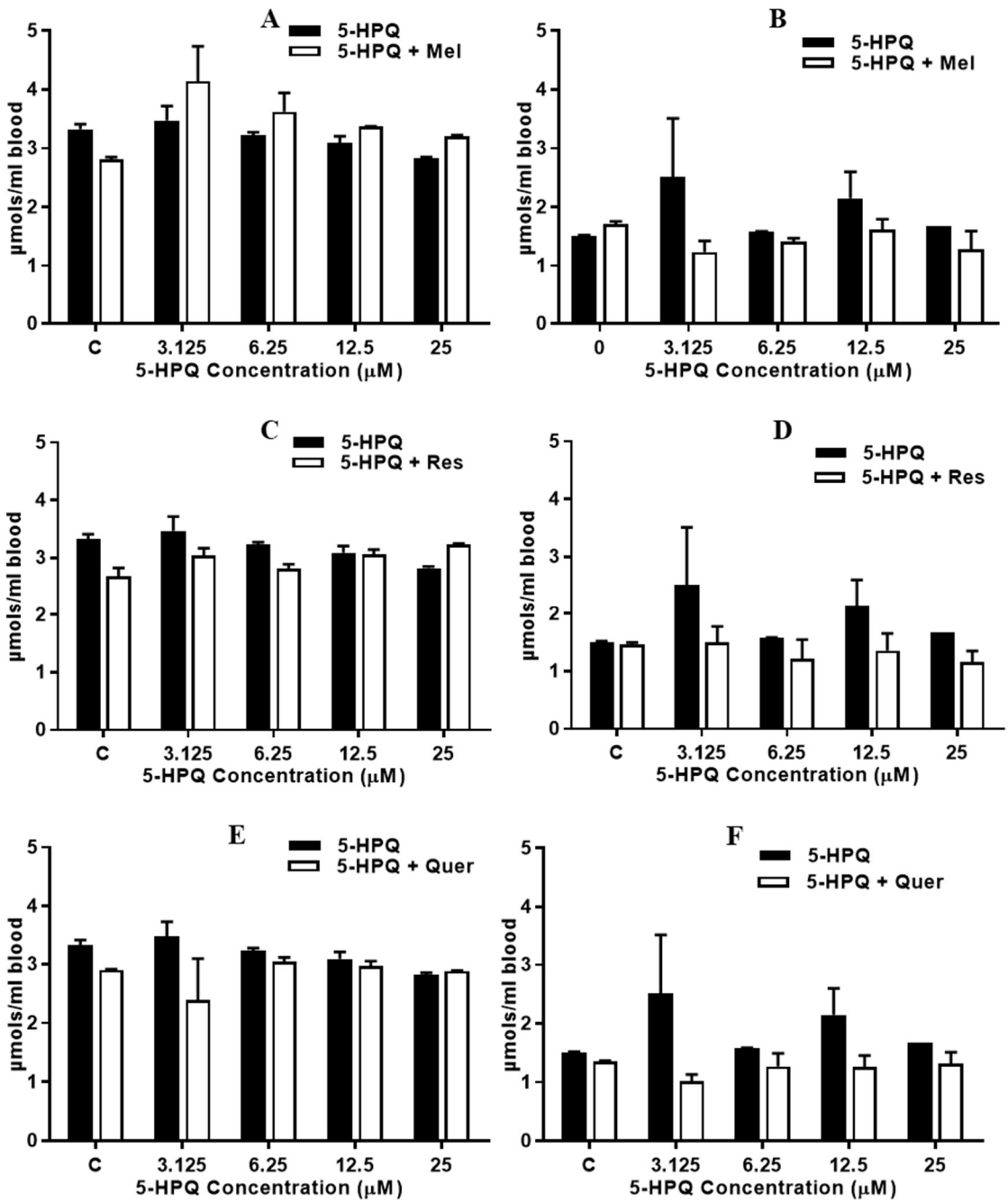

Figure 3.11: Intraerythrocytic total GSH levels due to treatment with 5-HPQ (A, B, C, D, E and F), 5-HPQ + Mel (A and B), 5-HPQ + Res (C and D) and 5-HPQ + Quer in (E and F) normal and (B, D and F) G6PDd human erythrocytes. Each data point represents mean ± SE of at least duplicate observations. The results were statistically analyzed with GraphPad Prism® with two-way ANOVA followed by Tukey's multiple comparison test and P values <0.05 were considered as statistically significant.

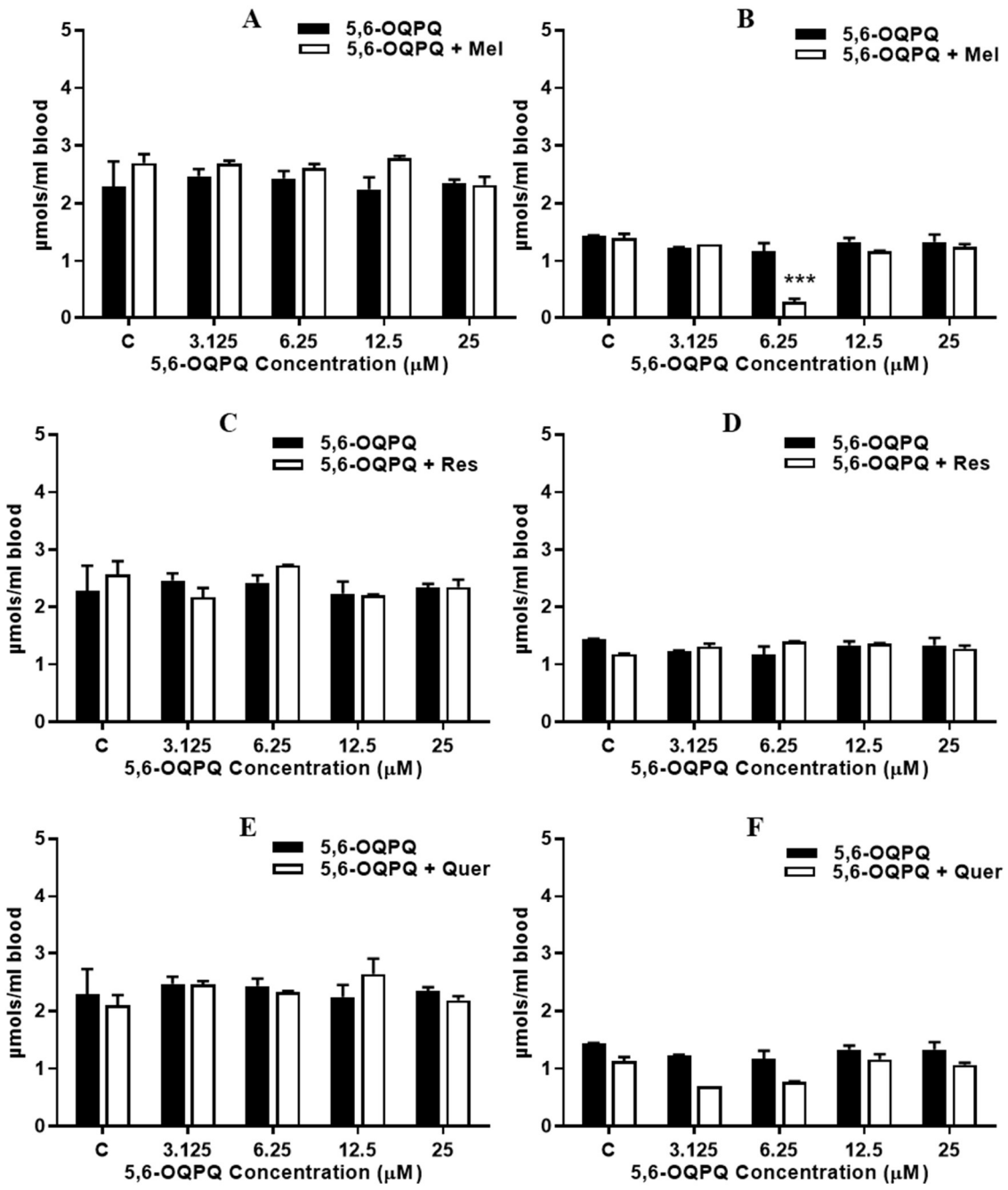

Figure 3.12: Intraerythrocytic total GSH levels due to treatment with 5,6-OQPQ (A, B, C, D, E and F), 5,6-OQPQ + Mel (A and B), 5,6-OQPQ + Res (C and D) and 5,6-OQPQ + Quer in (E and F) normal and (B, D and F) G6PDd human erythrocytes. Each data point represents mean ± SE of at least duplicate observations. The results were statistically analyzed with GraphPad Prism® with two-way ANOVA followed by Tukey's multiple comparison test and P values <0.05 were considered as statistically significant. ***$p < 0.001$ compared with 5,6-OQPQ-treated erythrocytes at corresponding concentration.

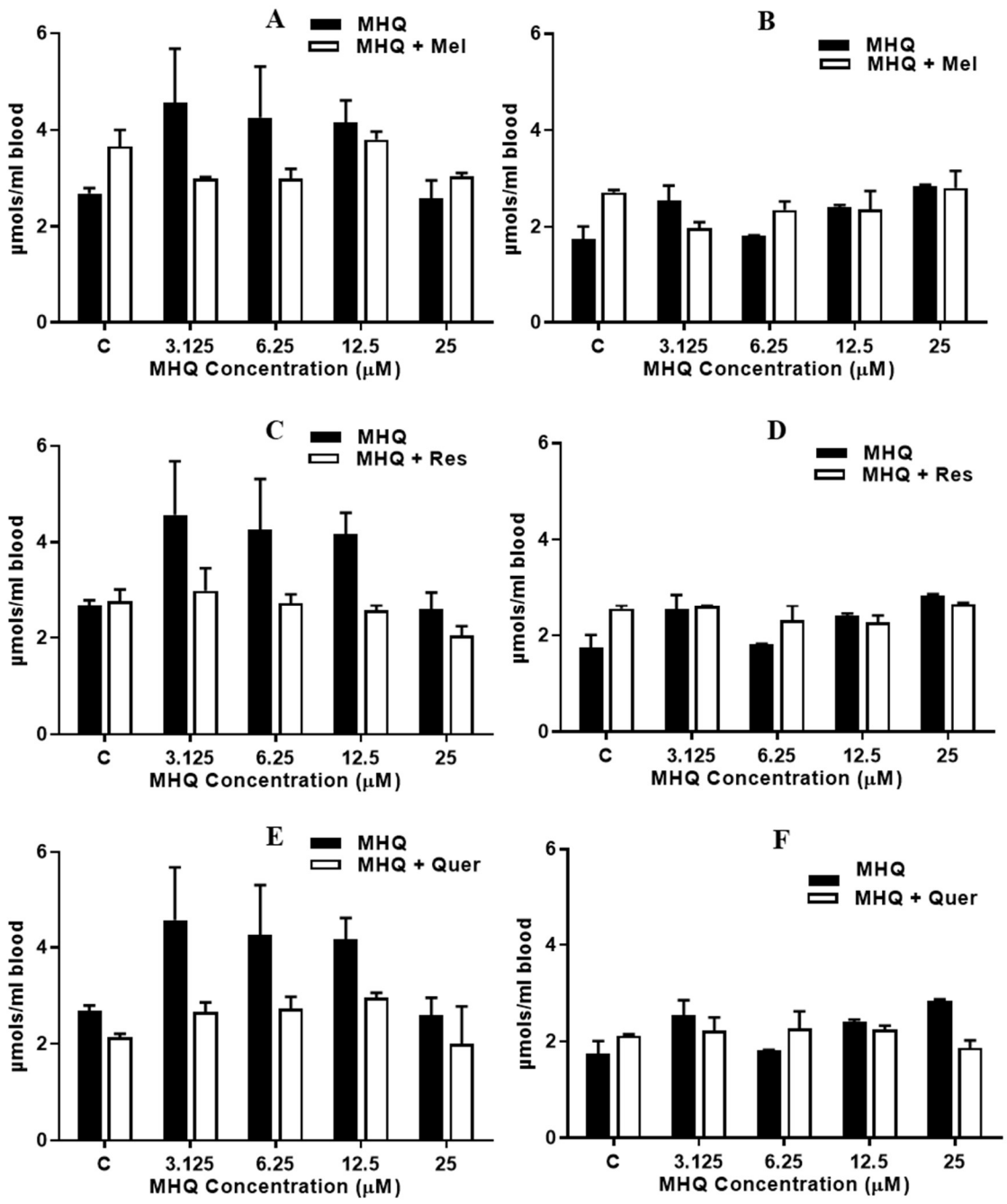

Figure 3.13: Intraerythrocytic total GSH levels due to treatment with MHQ (A, B, C, D, E and F), MHQ + Mel (A and B), MHQ + Res (C and D) and MHQ + Quer in (E and F) normal and (B, D and F) G6PDd human erythrocytes. Each data point represents mean ± SE of at least duplicate observations. The results were statistically analyzed with GraphPad Prism® with two-way ANOVA followed by Tukey's multiple comparison test and P values <0.05 were considered as statistically significant.

3.5.5. Determination of phosphatidylserine exposure in human erythrocytes.

The flow cytometric assay employing FITC Annexin V binding assay was used to determine phosphatidylserine externalization in normal and G6PDd erythrocytes. Translocation of phosphatidylserine on the outer membrane of erythrocytes due to treatment with 5,6-OQPQ (25 μM) alone and in combination with Quer (100 μM) and a comparative evaluation of translocation of phosphatidylserine in normal and G6PDd erythrocytes due to 5,6-OQPQ and 5,6-OQPQ + Quer exposure was done. Quer alone did not have any significant effect on phosphatidylserine externalization in normal and G6PDd erythrocytes (Figure 3.14). Treatment with 5,6-OQPQ and 5,6-OQPQ + Quer significantly induced phosphatidylserine externalization in both normal and G6PDd erythrocytes. Treatment with 5,6-OQPQ and 5,6-OQPQ + Quer induced significantly higher phosphatidylserine externalization in G6PDd as compared to normal erythrocytes (Figure 3.14). Thus, these results suggest that 5,6-OQPQ and 5,6-OQPQ + Quer caused externalization of phosphatidylserine on the outer surface of G6PDd human erythrocytes. Co-exposure of Quer with 5,6-OQPQ did not have any additional effect on phosphatidylserine externalization caused by 5,6-OQPQ alone in normal and G6PDd erythrocytes (Figure 3.14).

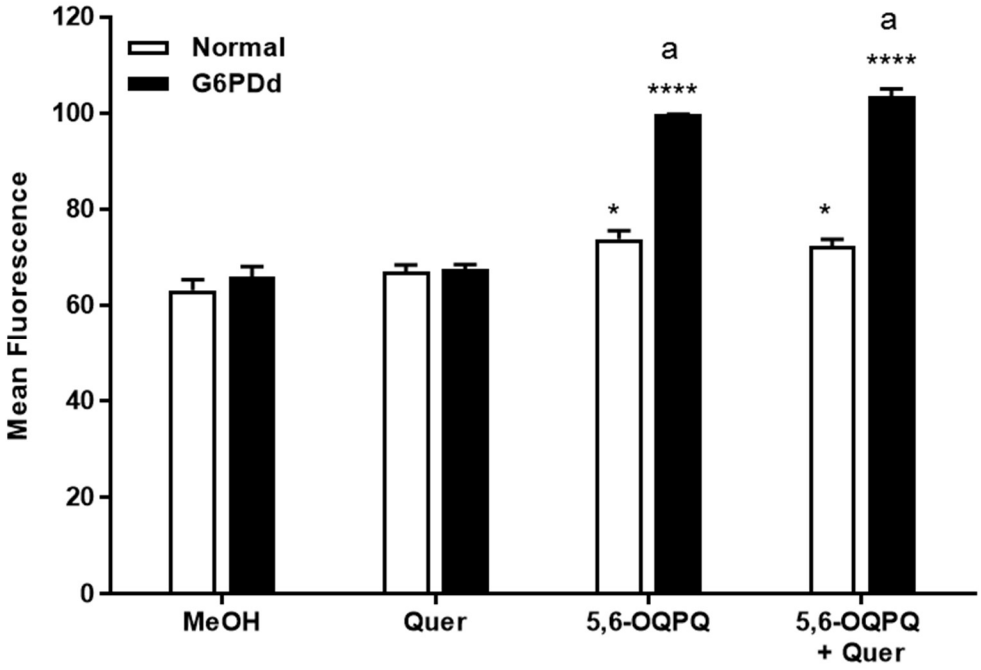

Figure 3.14: Phosphatidylserine exposure induced by 5,6-OQPQ, Quer and 5,6-OQPQ+ Quer in normal and G6PDd human erythrocytes with. Each data point represents mean ± SE of at least duplicate observations. The results were analyzed with GraphPad Prism® with two-way ANOVA followed by Tukey's multiple comparison test and P values <0.05 were considered as statistically significant. *$p < 0.05$, ****$p < 0.0001$ compared with corresponding erythrocyte and vehicle control. $^{a}p < 0.0001$ compared with normal human erythrocytes exposed to corresponding treatment (within group).

3.5.6. Computational docking.

(Leung and Shilton 2013) demonstrated the involvement and importance of water-mediated interactions of PQ with the NQO2 enzyme. Also, the presence of water molecules plays an important role in the prediction of accurate poses/orientation of ligand−protein interactions. Therefore, the water molecules in the crystal structure near 5Å of ligand binding site were kept. The docking of primaquine (PQ), PQ metabolites (5-HPQ, 5,6-OQPQ, and MHQ), menadione and melatonin using Glide employing extra precision (XP) docking method. PQ, Mel (NQO2 inhibitor), and menadione (NQO2 substrate) were used as reference compounds for this study. The docking pose of PQ in our study showed the identical binding pose as shown in NQO2-primaquine X-ray structure (4FGJ) (Figure 15). Further protein-ligand interactions study from docking confirmed that PQ occupied the identical active site pocket and interacted with the key binding site residues. The docking pose and interactions of menadione with NQO2 also matches with the 2QR2 crystal structure. This confirmed that the parameters set for Glide-XP docking mode were reliable. The Glide gscores and binding free energies of preferred binding poses of ligands with protein (4FGJ) are shown in Table 3.1. Glide gscore is a scoring function which approximates the ligand binding free energy. The more negative ligand binding free energy suggests tighter binding between ligand and protein. These computational docking results demonstrated that water molecules play an important role in the interaction between ligands and human NQO2.

Glide gscores and binding free energies of PQ (Isomers; R and S) indicates that PQ has strong binding affinity towards NQO2 compared to melatonin (Table 3.1). These results were consistent with experimental results (Ki of PQ = 1.04 μM and IC50 of Mel = 41.5 μM) (Ferry et al. 2010; Graves et al. 2002). However, the PQ metabolite, R/S-5-HPQ showed slightly better docking scores compared to R/S- PQ, which suggests R/S-5-HPQ may have slightly better binding

with NQO2 compared to PQ.

The preferred binding poses of R/S-5-HPQ, R/S-PQ, S-PQ, R/S-5,6-OQPQ and MHQ in human NQO2 are shown in Figure 3.15. A detailed observation indicates that two water participates in the interaction between R/S-5-HPQ and NQO2 protein. R/S-5-HPQ interacted via water-mediated hydrogen-bond between the nitrogen of quinoline ring with ASN161 and another water-mediated hydrogen-bond between protonated amine (side chain) of R/S-5-HPQ and GLN 122. A hydrogen bond between protonated amine (side chain) of R/S-5-HPQ and GLU 193 was also observed (Figure 3.16). The quinoline ring of R-PQ displayed π-π stacking with TRP 105 and PHE 178. The protonated amine of the side chain of R-PQ formed salt bridge interactions with GLU 193. The protonated amine of the side chain of R-PQ also formed a hydrogen bond with a water molecule. (Figure 3.17.A). The quinoline ring of S-PQ displayed π-π stacking with TRP 105. S-PQ interacted via water-mediated hydrogen- bonding between the nitrogen of quinoline ring with ASN161 and an additional water-mediated hydrogen- bonding between protonated amine (side chain) of S-PQ and GLN 122 was also observed. A hydrogen bonding between protonated amine (side chain) of S-PQ and GLU 193 was also seen (Figure 3.17.B).

The quinoline ring of R/S-5,6-OQPQ displayed π-π stacking with TRP 105. The oxygen atom present at the 6^{th} position of quinoline ring in R/S-5,6-OQPQ interacted with ASN161 via water-mediated hydrogen-bonding. The protonated amine of the side chain of R/S-5,6-OQPQ formed another water-mediated hydrogen- bonding with GLN 122 and a hydrogen bond with GLU 193 (Figure 3.18). The docking pose of Mel exhibited π-π stacking with indole ring and TRP 105, and an H-bond between the oxygen of acyl group of the side chain of Mel and backbone of GLN 121 was observed (Figure 3.19). Menadione, also known as vitamin K3, exhibited strong hydrophobic interactions with Trp105, Phe106, Phe126, and Phe178. Menadione also interacted

with ASN161 and carbonyl oxygen at the C1 position via water-mediated H-bonding (Figure 3.20). The docking pose of our study matches well with the pose reported in human quinone reductase type 2, complex with menadione (PDB ID: 4FGJ).

The superimposition of most preferred binding poses of 5-HPQ and Mel in the binding pocket of NQO2 suggest that they both bind in the similar orientation and the aromatic rings of 5-HPQ and Mel were parallel to isoalloxazine ring of FAD (Figure 3.19). Careful observation of most preferred binding poses of other PQ metabolites suggests that other PQ metabolites orient in a similar fashion as S-PQ and Mel and one of the aromatic rings of these metabolites was parallel to isoalloxazine ring of FAD (Figure. 3.15, 3.21 and 3.22). These results indicate that like PQ, these metabolites of PQ may have a stronger binding affinity towards NOQ2 enzyme.

Table 3.1: The docking scores of best binding poses of PQ, PQ metabolites, and Melatonin in a human NQO2 protein having water molecules in their binding pocket.

Ligands	Glide gscore (kcal/mol)	Prime MM-GBSA dG binding (kcal/mol)
R-5-HPQ	−8.514	−68.039
S-5-HPQ	−8.389	−69.046
R-PQ	−8.313	−68.658
S-PQ	−8.290	−69.425
S-5,6-OQPQ	−7.300	−55.127
R-5,6-OQPQ	−7.268	−55.120
MHQ	−6.564	−50.514
Melatonin	−6.431	−63.846
Menadione	−5.957	−39.439

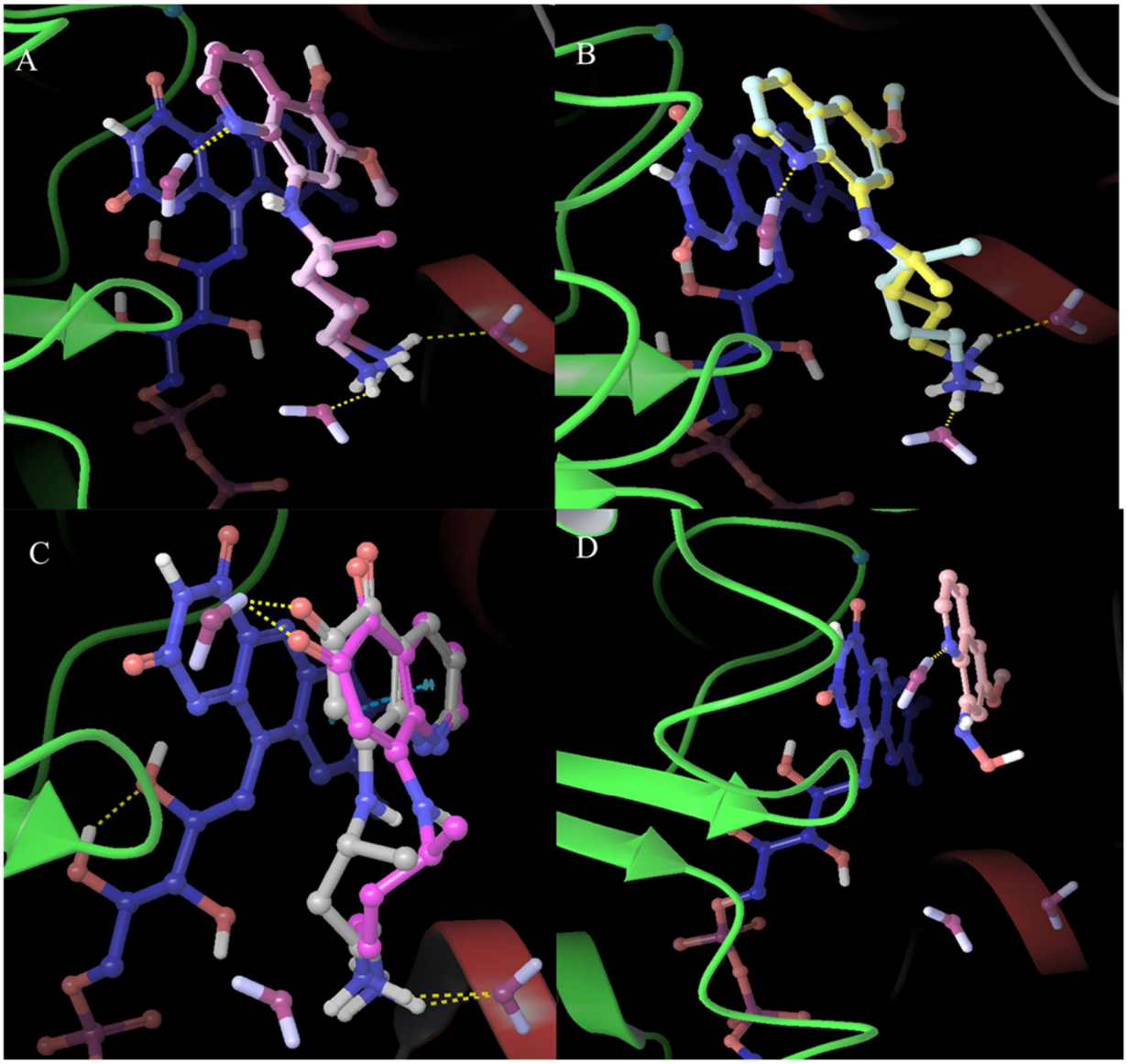

Figure 3.15: The most preferred binding poses of (A) R-5-HPQ (carbon in maroon) and S-5-HPQ (carbon in plum), (B) R-PQ (carbon in turquoise) and S-PQ (carbon in yellow) and (C) R-5,6-OQPQ (carbon in grey) and S-5,6-OQPQ (carbon in purple) and (D) MHQ (carbon in pink) with NQO2.

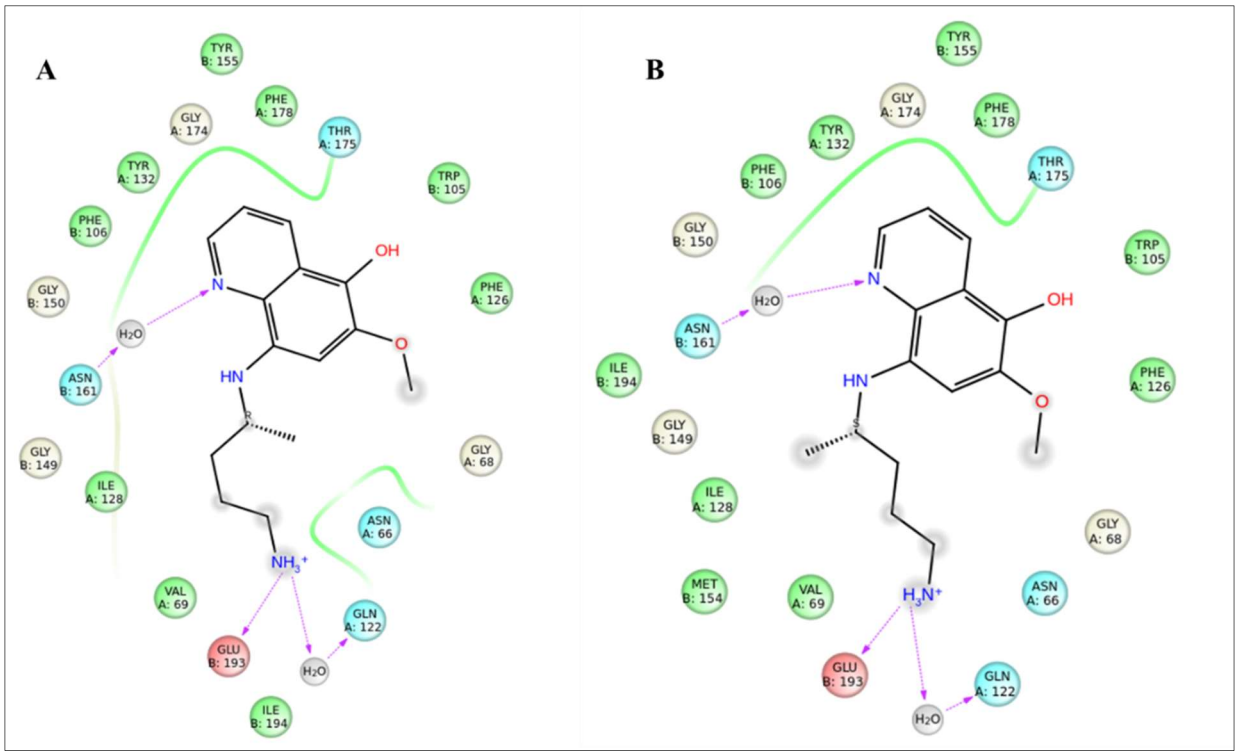

Figure 3.16: The 2D interactions of the most preferred binding pose of (A) R-5-HPQ and (B) S-5-HPQ.

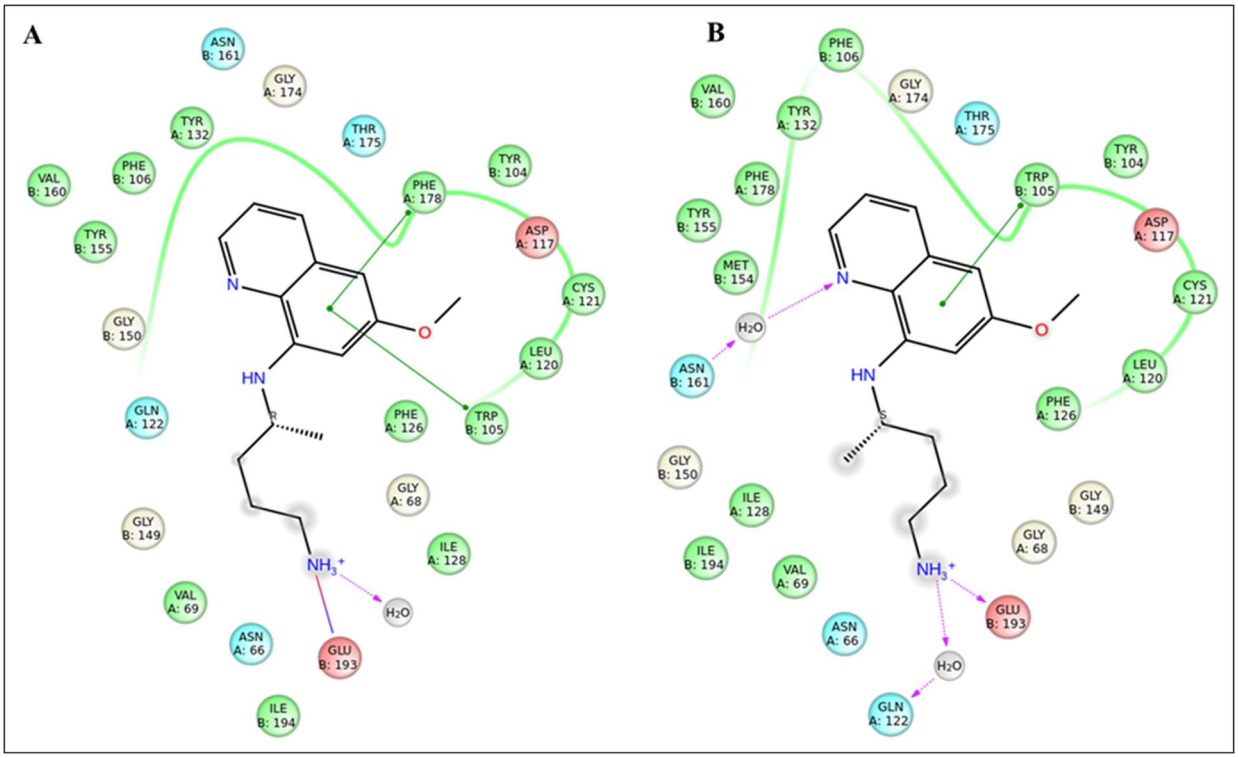

Figure 3.17: The 2D interactions of the most preferred binding pose of (A) R-PQ, and (B) S-PQ.

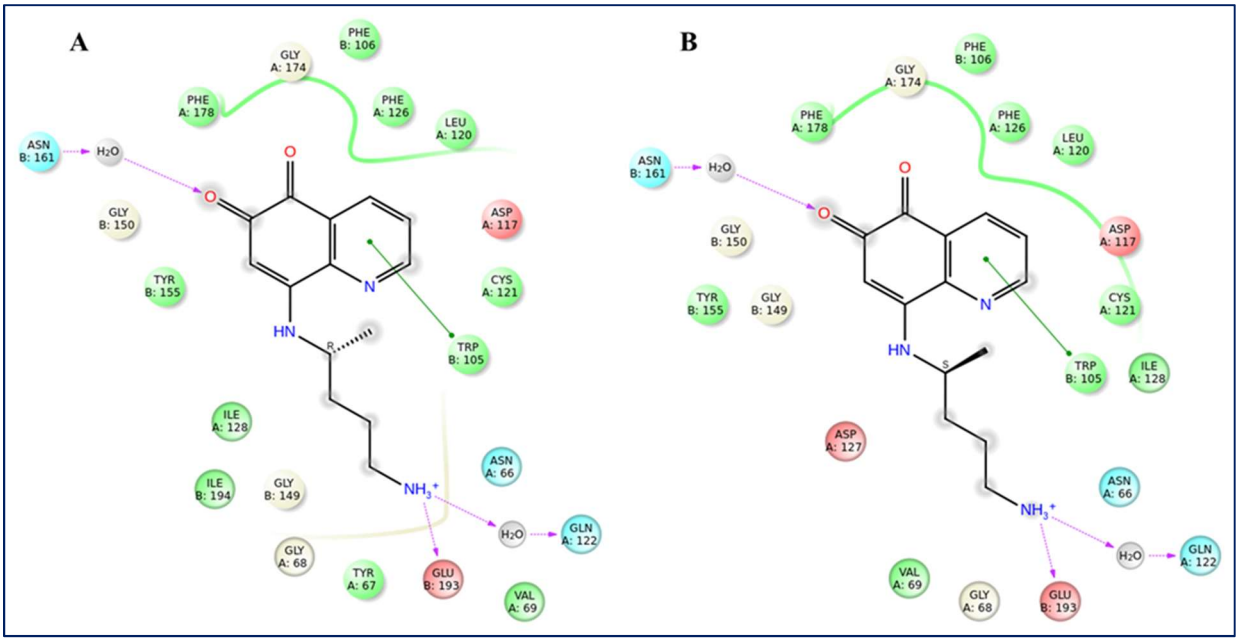

Figure 3.18: The 2D interactions of the most preferred binding pose of (A) R-5,6-OQPQ, and (B) S--5,6-OQPQ.

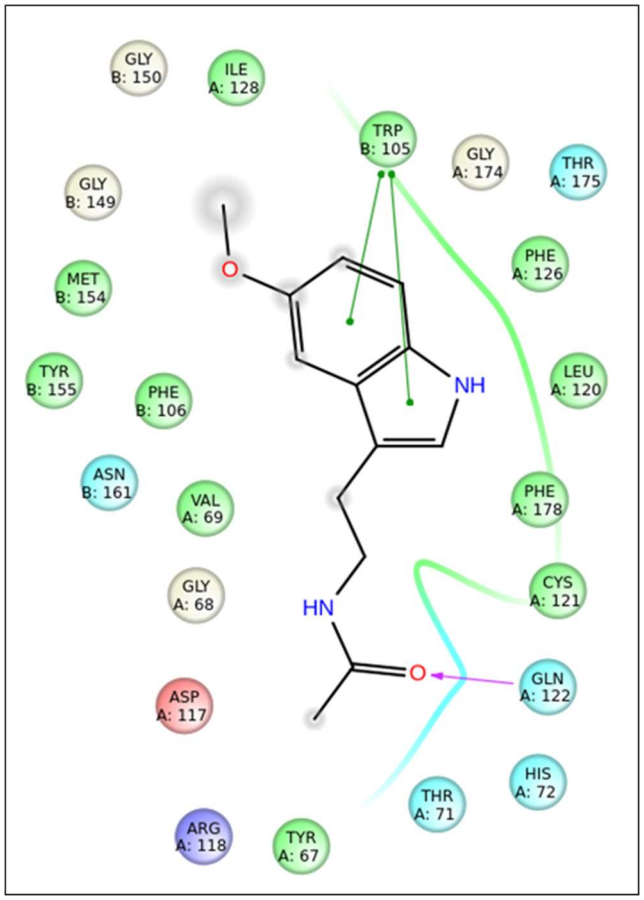

Figure 3.19: The 2D interactions diagram of the most preferred binding pose of melatonin (Mel).

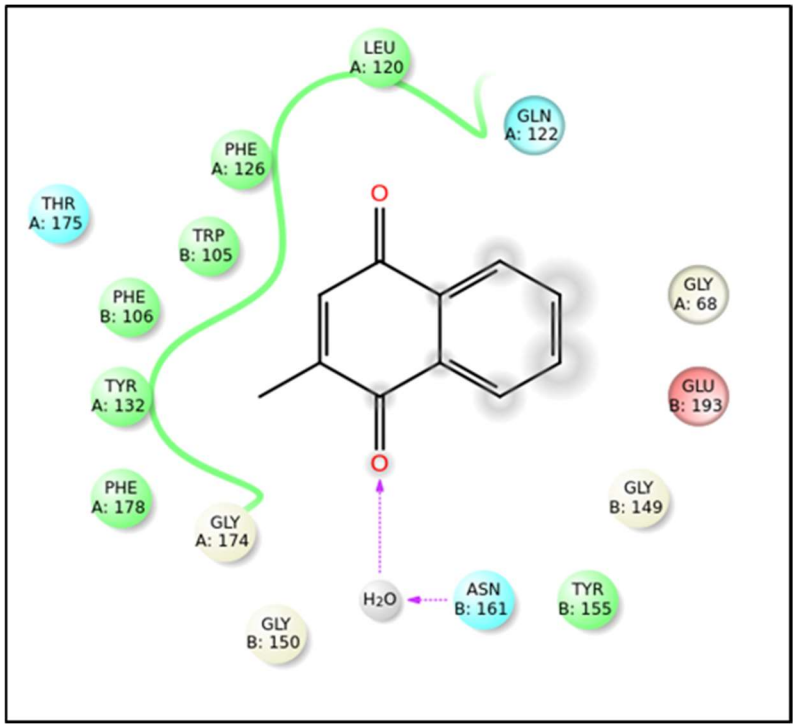

Figure 3.20: The 2D interactions diagram of the most preferred binding pose of menadione.

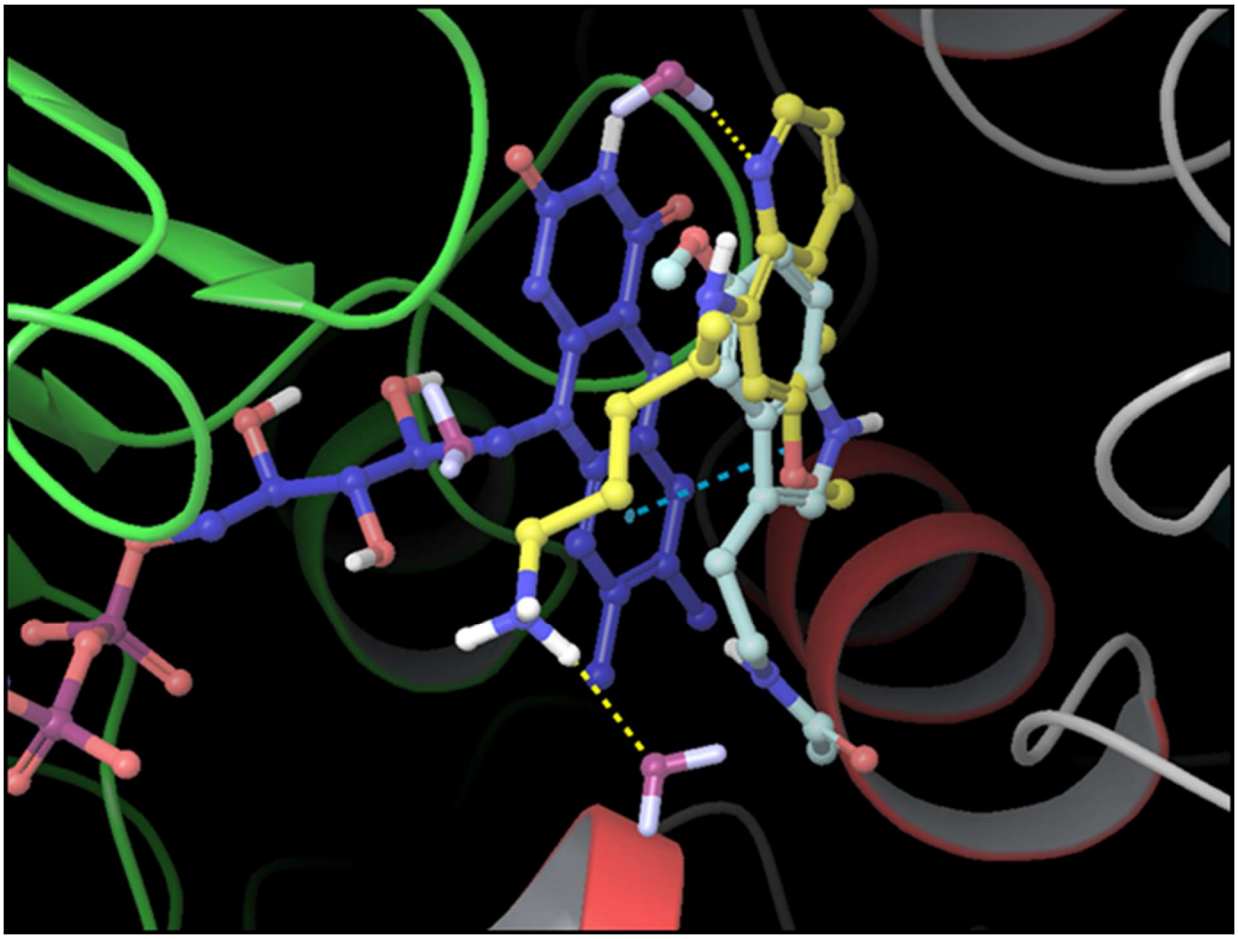

Figure 3.21: Overlay of superimposed poses of melatonin (carbon in turquoise, ball and stick model) and S-PQ (carbon in yellow, ball and stick model) after docking in NQO2 (4FGJ). FAD is shown in carbon in blue. Chain B (green) and chain A (red) are represented in cartoon representations.

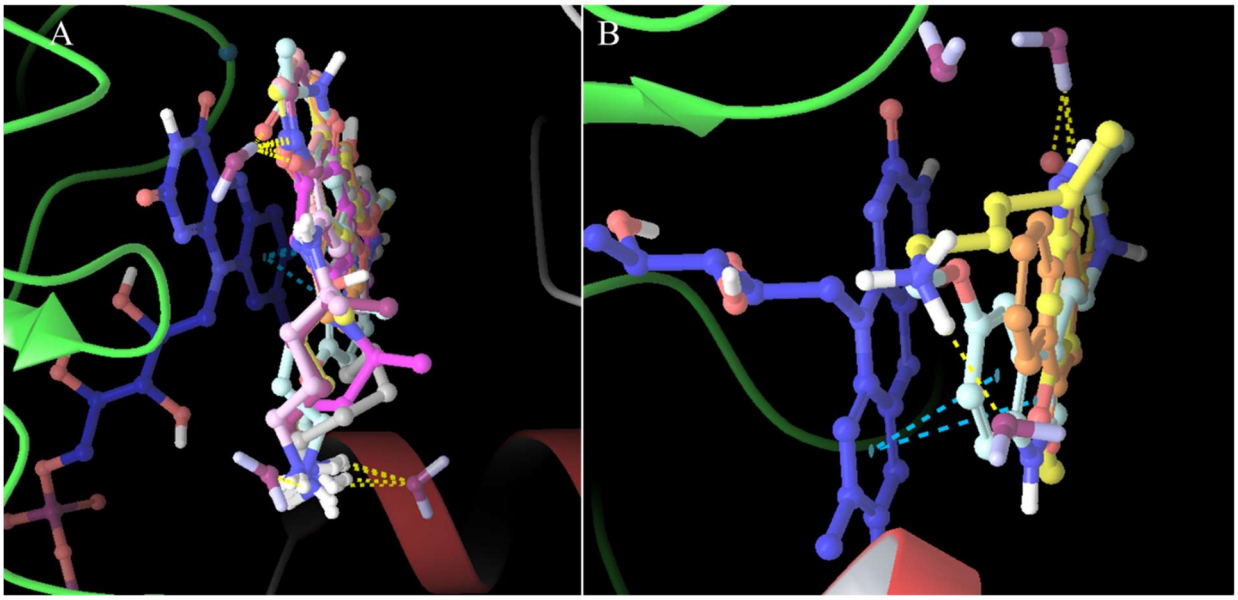

Figure 3.22: Overlay of superimposed poses of (A) R-5-HPQ (carbon in maroon), S-5-HPQ (carbon in plum), R-PQ (carbon in turquoise), S-PQ (carbon in yellow), R-5,6-OQPQ (carbon in grey), S-5,6-OQPQ (carbon in purple), and MHQ (carbon in pink) and (B) melatonin (carbon in turquoise), S-PQ (carbon in yellow) and menadione (carbon in orange) after docking in NQO2 (4FGJ). FAD is shown in carbon in blue. Chain B (green) and chain A (red) are represented in cartoon representations.

3.6. DISCUSSION

NQO2 is an FAD-linked oxidoreductive enzyme that catalyzes mandatory two-electron reductions of quinone to hydroquinones without forming highly reactive semiquinones and free radicals (Foster et al. 2000; Vella et al. 2005). The NQO2 acts as a detoxification enzyme for quinones (Graves et al. 2002). Quinones are redox active molecules and involve in a redox cycle with their semiquinone radicals. This redox cycling causes generation of superoxide radicals. Production of ROS leads to oxidative stress within the cells and causes oxidation of cellular macromolecules, including DNA, lipids, and proteins (Bolton et al. 2000). Human erythrocytic NQO2 is the only protein target identified for PQ (Ki-1.04±0.38 μM) (Graves et al. 2002; Murce et al. 2015). However, the potential implications of binding of PQ with NQO2 in efficacy and/or toxicity of PQ are not very clear. Previous kinetics studies demonstrated that PQ preferentially binds to the oxidized state of NQO2 and shows competitive inhibition against the electron donating co-factor dihydronicotinamide riboside (NRH), and FADH2 (Leung and Shilton 2013).

Current studies are focused on investigating the function of NQO2, a cytosolic flavoprotein enzyme involved in metabolic detoxification/activation of hemotoxic metabolites of PQ, in PQ-induced hemolytic anemia. In this study, the selective and potent inhibitors of NQO2 namely, melatonin (Mel) (IC_{50} = 41.5±1.5μM), resveratrol (Res) (IC_{50} = 0.143±0.05 μM) and quercetin (Quer) (IC_{50} = 1.4±0.1 μM) (Ferry et al. 2010; Boutin et al. 2005) were used as the probes to understand the hemolytic toxicity of PQ. Studies were further extended to investigate the interactions between crystal structure of human NQO2 (PBD: 4FGJ) and PQ metabolites (5-HPQ, 5,6-OQPQ, and MHQ) using computational molecular docking approach.

Mel potentiated the hemotoxicity when the human erythrocytes were cotreated with PQ metabolites and Mel. Mel cotreatment increased 5-HPQ, 5,6-OQPQ and MHQ induced

methemoglobin accumulation and oxidative stress generation in normal as well as G6PDd erythrocytes. Mel also potentiated GSH depletion caused by 5-HPQ, 5,6-OQPQ selectively in G6PDd erythrocytes only. Similarly, Res cotreatment with also augmented 5-HPQ, 5,6-OQPQ and MHQ induced methemoglobin accumulation. Res partially attenuated 5-HPQ, 5,6-OQPQ and MHQ induced oxidative stress in both normal and G6PDd erythrocytes. This effect of resveratrol may be due its antioxidant properties (Farris et al. 2013; Zhang et al. 2014). Res did not potentiate GSH depletion caused by 5-HPQ and 5,6-OQPQ selectively in G6PDd erythrocytes. Quer showed hemolytic toxicity properties. It significantly increased methemoglobin and generated oxidative stress in normal and G6PDd erythrocytes and caused depletion in GSH levels selectively in G6PDd erythrocytes. Quer co-treatmnet synergistically increased 5-HPQ, 5,6-OQPQ and MHQ induced methemoglobin accumulation and did not cause further depletion in GSH levels caused by 5-HPQ, 5,6-OQPQ alone. Quer did not significantly increase PS exposure caused by 5,6-OQPQ. Earlier investigation have shown that quercetin oxidizes oxyhemoglobin and causes lysis of human erythrocyte (Galati et al. 2002). Quer is converted to oxidant products when act as an antioxidant and scavenges free radicals (Boots et al. 2007). The oxidant quinoid product(s) further results in the formation of superoxide ions, show high reactivity toward thiols and thus arylates glutathione and protein thiol groups. This further leads to depletion of glutathione, and impairs functions of several vital enzymes like glutathione reductase (Boots et al. 2003; Boots et al. 2007; Choi et al. 2003; Galati et al. 2002; Metodiewa et al. 1999). The results of the current study suggest that co-treatment of erythrocytes with NQO2 inhibitors and PQ metabolites potentiated the hemotoxicity compared to treatment with PQ metabolites alone. Redox cycling of quinone and quinone-imine metabolites have been implicated in hemotoxicity of PQ (Marcsisin et al. 2016). This suggests the potential role of NQO2 in detoxification of reactive metabolites of PQ from erythrocytes. Thus,

inhibiting NQO2 through potent and selective inhibitors of NQO2 is likely to alter the hemolytic toxicity of PQ metabolites.

The computational docking results suggested that the presence of water molecules in the binding pocket of NQO2 played critical role in binding of PQ and its metabolites with NQO2. The importance of water molecule in binding between NQO2 enzyme and PQ has been demonstrated earlier (Leung and Shilton 2013). Mel, Menadione, PQ and PQ metabolites bind at the same binding pocket with slight variations. The glide gscores suggest that PQ and its metabolites may have a better affinity towards NQO2 as compared to Mel and menadione.

The biochemical results showed that in the presence of NQO2 inhibitors, the hemolytic toxicity caused by PQ metabolites is potentiated. The computational docking results suggest that PQ metabolites interact with NQO2 better that Mel and Menadione. Since in the presence of NQO2 inhibitors, the toxicity is increased which suggest the protective role of the NQO2 enzyme. Based on biochemical and computational docking results, we believe that PQ metabolites might act as the substrates and NQO2 may be involve in the detoxification of PQ metabolites. These studies suggest protective role of NQO2 against PQ-induced hemolytic toxicity.

CHAPTER 4

METABOLOMIC PROFILE OF NORMAL AND GLUCOSE-6-PHOSPHATE DEHYDROGENASE DEFICIENT ERYTHROCYTES TREATED WITH PRIMAQUINE METABOLITES.

4.1. INTRODUCTION & RATIONALE

Metabolites are small compounds, produced during metabolism and depict the functional readouts of cellular and biochemical states (Patti et al. 2012). The collection of metabolites within a cell, tissue, organ or biological fluid is known as metabolome (Patti et al. 2012). By analyzing the qualitative and quantitative profiles of the cellular metabolites, biochemical activity of the cell can be determined. Disease states and drug treatments alter biochemical pathways, which can be assessed through either targeted or untargeted comparative metabolomic workflows (Patti et al. 2012; Kaddurah-Daouk et al. 2008).

As mentioned earlier, the GSH-centered antioxidant functions are severely compromised in G6PDd individuals (Judith Recht 2014; Mason et al. 2007). Primaquine (PQ) generates oxidative stress in the erythrocytes, which is primarily initiated by the PQ metabolites produced through CYP-mediated pathways (Ganesan et al. 2009; Ganesan et al. 2012). However, the interplay between hemolysis, G6PD deficiency, ROS, and GSH is more complicated (Tang et al. 2015). These findings necessitate examination of the metabolomes of normal and G6PDd human erythrocytes and also PQ-mediated changes in the metabolomes of normal and G6PDd human

erythrocytes. Thus, to explore potential mechanism(s) of PQ-induced hemolysis in G6PDd human erythrocytes, in vitro experiments with normal and G6PDd human erythrocytes treated with PQ metabolites were done to mimic the in vivo conditions during hemolytic anemia induced by PQ treatment and comparative untargeted metabolomics analyses were performed.

4.2. HYPOTHESIS

PQ metabolite, 5,6-orthoquinone primaquine (5,6-OQPQ) will alter the metabolite profile in normal and G6PDd erythrocytes. These changes will mechanistically support the pathophysiology of hemolysis in G6PDd erythrocytes.

4.3. OBJECTIVE

In this study, the changes in global cellular metabolism and compensatory responses in biochemical pathways of cellular metabolism in response to 5,6-OQPQ, metabolite of PQ were assessed using an untargeted metabolomic workflow. The conventional biochemical approach often concentrates on a single metabolite, one metabolic reaction, or a limited set of linked reactions and cycles. In contrast to the conventional biochemical approach, an untargeted LC-MS based metabolomic approach involves the simultaneous collection of qualitative and (relative) quantitative data for as many metabolites as possible to obtain insight into metabolism associated with conditions of interest, including disease state and drug exposure (Kaddurah-Daouk et al. 2008). Also, metabolomics is thought to be a valuable tool for biomarker discovery, and in contrast to conventional clinical biomarkers and classical diagnostic approaches, metabolomics poses potential benefits in feasibility, specificity, and sensitivity (Kaddurah-Daouk et al. 2008). Thus, a global untargeted metabolomic approach may aid in discovery of new biomarkers for G6PD

deficiency and PQ-induced hemolysis in normal and G6PDd erythrocyte.

4.4 MATERIALS AND METHODS.

4.4.1. Chemicals

LC-MS grade methanol and water were purchased from Fisher Scientific (Waltham, MA, USA). 5,6-OQPQ was synthesized by Dr. N.P. Dhammika Nanayakkara at the National Centre for Natural Products Research (NCNPR), University of Mississippi.

4.4.2. Procurement of human blood

Blood was drawn from normal and glucose 6-phosphate dehydrogenase deficient (G6PDd) healthy volunteers in tubes containing citrate phosphate under an institutional review board (IRB) approved protocol.

To analyze metabolite profiling of normal and G6PDd human erythrocytes, blood from four different batches was used. For three batches, G6PDd blood was taken from Caucasian male containing the Ser188Phe Mediterranean mutation and for one batch, G6PDd blood was taken from African American male carrying the classic A/A- combination of electrophoretic variant (Asn126Asp) and deficiency allele (Val68Met).

To analyze the effect of 5,6-OQPQ, on global metabolomics profile of normal and G6PDd erythrocytes, G6PDd blood was taken from a Caucasian male containing the Ser188Phe Mediterranean mutation from a single batch.

4.4.3. Sample preparation for metabolomic analysis

For untargeted metabolomics experiments of normal and G6PDd human erythrocytes, the blood was centrifuged at 4500 × g at 4^0C for 10 minutes, and buffy coats were removed. The erythrocyte pellets were washed twice with phosphate buffered saline (110 mM sodium chloride, 20 mM disodium hydrogen phosphate and 4 mM potassium dihydrogen phosphate, pH 7.4). The aliquots (250 µL each) of washed erythrocytes pellets were stored at -80^0C for further processing. The erythrocytes aliquots (250 µL) were removed from -80^0C freezer and lysed with 750 µL of cold acetonitrile: methanol: ammonium Bicarbonate (0.1 M, pH 8.0) (1:1:2) lysis buffer. The pellets were vortexed for 10 seconds, froze in liquid nitrogen for 10 seconds, defrosted for 10 minutes and sonicated with a probe tip at 10 pulses. This step was repeated 3 times. Ice-cold methanol (500 µL) was added to each pellet to precipitate proteins and then incubated at -80^0C overnight. The samples were thawed, centrifuged (14000 × rpm at 4 ^{0}C for 15 minutes) and the supernatants were transferred to separate tubes. The supernatants were dried in a speed vac at low drying rate and kept at -80^0C until ready for metabolomics analysis.

To analyze the effect of 5,6-OQPQ on global metabolomic profiles of normal and G6PDd erythrocytes, the blood was centrifuged at 4500 × g at 4^0C for 10 minutes, and buffy coats were removed. The erythrocyte pellets were washed twice with phosphate buffered saline (110 mM sodium chloride, 20 mM disodium hydrogen phosphate and 4 mM potassium dihydrogen phosphate, pH 7.4). The washed erythrocytes pellets were then re-suspended at 50% hematocrit in phosphate buffered saline (PBS). Normal and G6PDd human erythrocytes were treated with the 5,6-OQPQ (50 µM) for different time periods (0, 30, 60, 120 and 480 minutes). The reaction mixture contained 200 µl erythrocytes which were suspended in PBS with 50% hematocrit, 10 µl of 5,6-OQPQ and PBS to make a final volume of reaction mixture to 800 µl. The reaction mixture with appropriate control without 5,6-OQPQ was also set up simultaneously. The reaction mixtures

were incubated for 0, 30, 60, 120 and 480 minutes at 37^{0}C in a shaking water bath. The samples were removed from the water bath and centrifuged at 15294 X g for 10 min at 4 ^{0}C. The erythrocytes' pellets were obtained from controls and 5,6-OQPQ treatments, flash frozen in liquid nitrogen for 30 seconds and then stored at -80^{0}C for further processing. The samples were thawed and 600 µL of chilled acetonitrile: methanol: ammonium bicarbonate (0.1 M, pH 8.0) (1:1:2) lysis buffer was added to the erythrocyte's pellets. The samples were vortexed for 10 seconds, frozen in liquid nitrogen for 10 seconds, defrosted for 10 minutes, again vortexed for 10 seconds and sonicated in sonicator bath, in the presence of ice for 5 minutes at a time. The protein in the samples was precipitated using ice-cold methanol and then incubated at -80^{0}C overnight. The samples were thawed, centrifuged (20817 × g at 4 ^{0}C for 15 minutes), and the supernatants were transferred to fresh tubes. The supernatants were dried in a speed vac at low drying rate and kept at -80^{0}C until ready to use.

4.4.4. UHPLC-MS analysis

The UHPLC-MS analysis was done by Dr. Alexandra Rutledge in Vanderbilt University. For LC-MS analysis, dried samples were reconstituted in 100 µl of acetonitrile/ water (80:20, v/v) and centrifuged for 5 min at 21130 X g to remove insoluble material. A quality control pool was prepared from equal volumes of each experimental sample. This sample was used as one measure of quality control during the experiment as well as for data-dependent acquisitions (DDA) for feature annotation. Full MS and DDA experiments were performed on a Q-Exactive HF hybrid quadrupole-Orbitrap mass spectrometer (Thermo Fisher Scientific, Bremen, Germany) equipped with a Vanquish UHPLC binary system and autosampler (Thermo Fisher Scientific, Germany). Extracts (5 µL injection volume) were separated on a SeQuant ZIC-p HILIC 5-µm, 2.1 mm × 150

mm column (normal versus G6PDd samples) or SeQuant ZIC-HILIC 3.5-µm, 2.1 mm × 100 mm column (Millipore Corporation, Darmstadt, Germany) (drug-dose-time course samples) held at 40°C. Liquid chromatography was performed at a 200 µl/min using solvent A (5mM Ammonium formate in 90% water, 10% acetonitrile) and solvent B (5mM Ammonium formate in 90% acetonitrile, 10% water) with the following gradient: 90% B for 2 minutes, 90-40% B over 16 minutes, 40% B held 2 minutes, and 40-90% B over 10 minutes, 90% B held 10 minutes.

Full MS analyses were acquired over a mass range of m/z 70-1050 under an ESI positive profile mode with a resolution of 120000 and scan rate at ~3.5 Hz. The automatic gain control (AGC) target was set at 1×10^6 ions, and maximum ion injection time (IT) was at 100 ms. Source ionization parameters were optimized with the spray voltage at 3.0 kV, and other parameters were as follows: transfer temperature at 280°C; S-Lens level at 40; heater temperature at 325°C; Sheath gas at 40, Aux gas at 10, and sweep gas flow at 1. Tandem spectra were acquired for quality control pool samples (described above) using a data-dependent scanning mode in which one full MS scan (m/z 70-1050) was followed by 2 MS/MS scans. MS/MS scans are acquired in profile mode using an isolation width of 1.3 m/z, stepped collision energy (NCE 20, 40, 60), and a dynamic exclusion of 6s. MS/MS spectra were collected at a resolution of 15000, with an automatic gain control (AGC) target set at 2×10^5 ions, and maximum ion injection time (IT) of 100 ms.

4.4.5. Data processing

Raw data were imported, processed, normalized, and reviewed using Progenesis QI v.2.1 (Non-linear Dynamics, Newcastle, UK). All sample runs were aligned against a QC pool reference run, and peak picking was performed on individual aligned runs to create an aggregate data set. Features (retention time and m/z pairs) were combined using both adduct and isotope

deconvolution. Data were normalized to all compounds. Principle Components Analysis (PCA) was used to visualize clustering of data groups. Significance was assessed using p-values and fold changes calculated from combined feature abundance data.

Tentative and putative annotations (Schrimpe-Rutledge et al. 2016) were made using experimental accurate mass measurements (< 5 ppm error), isotope distribution similarity, predicted formula (Compound Discoverer 2.0.0.303, Thermo) and fragmentation spectrum matching by searching mzCloud, the Human Metabolome Database (HMDB), METLIN, MassBank, Waters Metabolic Profiling CCS Library, and NIST 14 databases. Annotations were filtered for endogenous small molecules present in the HMDB database and classified into confidence levels based on supporting evidence. Level 2: putative identification match of experimental accurate mass (mass tolerance ± 5 ppm), predicted formula, and MS/MS spectrum to a spectral library, and Level 3: tentative structure match of experimental accurate mass (mass tolerance ± 5 ppm) and predicted formula to HMDB database. The workflow proposed for metabolite identification is shown in Figure 4.1 (Schrimpe-Rutledge et al. 2016).

4.4.6. Statistical analysis

For statistical analysis, ANOVA was performed in Progenesis QI v.2.1 (Non-linear Dynamics, Newcastle, UK) and a p-value of less than 0.05 was considered significant.

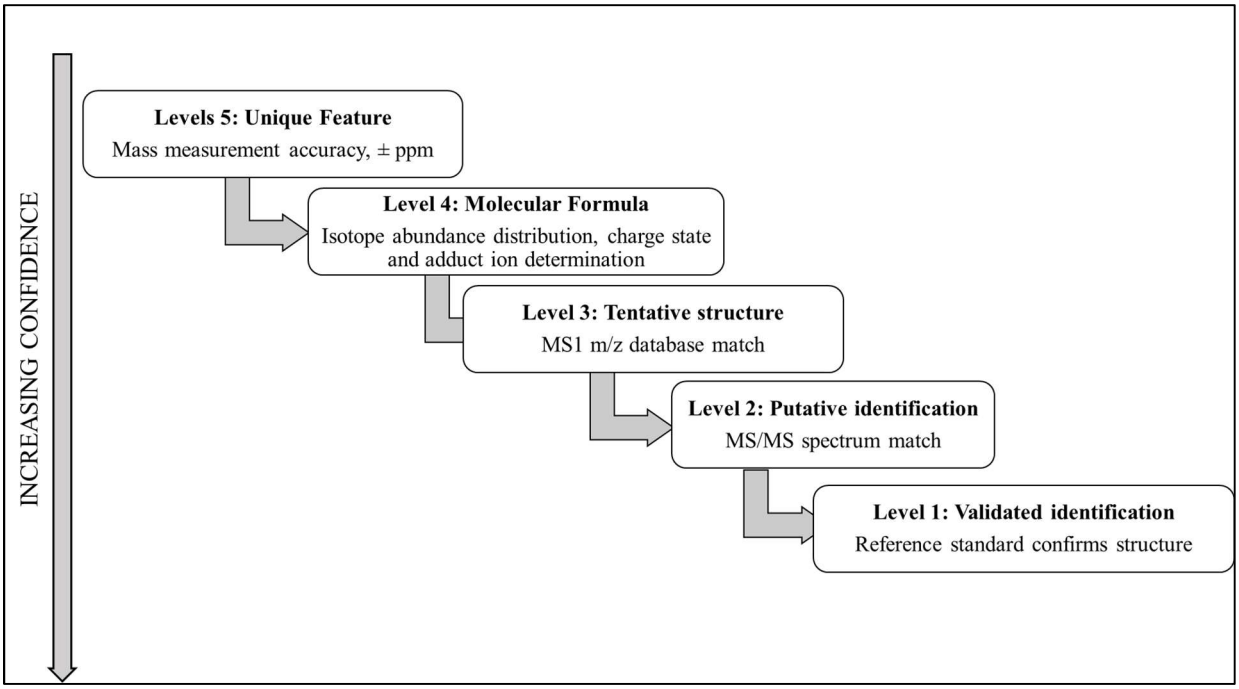

Figure 4.1: Proposed workflow for metabolite identification (Schrimpe-Rutledge et al. 2016).

4.5. RESULTS

4.5.1 Different metabolic profile of normal and G6PDd erythrocytes:

To compare global metabolomic profiles, normal and G6PDd erythrocytes, the erythrocytes were lysed and then analyzed by UHPLC-MS. Principal component analysis of the metabolomic dataset showed clustering of untreated normal and G6PDd erythrocytes sample groups (Figure 4.2). The raw data was processed and analyzed by Progenesis QI v.2. After annotation, 87 metabolites were tentatively or putatively identified (Table 4.1). Pathway analysis of these metabolites was performed using MetaboAnalyst 3.0, an open-source web application (Figure. 4.3; Table 4.2) (Xia and Wishart 2016; Xia et al. 2015). When MetaboAnalyst is used to analyze pathway of given metabolites, it matches all pathways on the basis of p values and pathway impact values. The p values and pathway impacts values are calculated from pathway enrichment analysis and pathway topology analysis respectively. In pathway analysis graphs, each circle represents a pathway. As the pathway impact values increases, the size of circle increases and as the p values increases the color of circle changes from yellow to red (yellow circle: p value less; red circle: p values higher). Among 87 metabolites there were 29 metabolites which showed fold change ≥ 1.5 in G6PDd erythrocytes as compared to normal erythrocytes (Figure. 4.4). There were 16 and 13 metabolites which were upregulated and downregulated in G6PDd erythrocytes (Figure 4.5 and Figure 4.6). The 29 metabolites which displayed fold change ≥ 1.5 in G6PDd erythrocytes as compared to normal erythrocytes were also analyzed by MetaboAnalyst 3.0 to identify the major pathways which were over-represented in G6PDd erythrocytes (Figure 4.7; Table 4.3).

Methylimidazole acetaldehyde, a histamine metabolite was significantly higher (14-fold) in G6PDd erythrocytes (Figure 4.5) (Zimatkin and Anichtchik 1999). Carnitine and its derivative

namely hydroxybutyrylcarnitine, heptadecanoylcarnitine, stearoylcarnitine, carnitine, and propionylcarnitine were significantly higher in G6PDd erythrocytes (Figure 4.5). Carnitine and derivatives of carnitine participate in lipid oxidation (Darghouth et al. 2011). Biotin amide and trigonelline levels were increased in G6PDd (Figure 4.5). Levels of amino acids including leucine, nor-leucine, aspartic acid and derivatives of amino acids namely homo-arginine, N(6)-methyllysine and alpha-N-Phenylacetyl-L-glutamine were increased in G6PDd erythrocytes (Figure 4.5). 5'-Methylthioadenosine and hypoxanthine were also upregulated in G6PDd erythrocytes (Figure 4.5). 5'-Methylthioadenosine plays an important role in methionine, and purine salvage pathways (Avila et al. 2004) and hypoxanthine is a byproduct of ATP catabolism (Farthing et al. 2015).

Metabolites that participate in GSH pathway including GSH, ophthalmic acid, and glutamic acid were significantly lower in G6PDd erythrocytes (Figure 4.6). Levels of an amino acid such as asparagine and taurine, and metabolites of amino acid, for example, pipecolic acid, a metabolite of lysine, was lower in G6PDd erythrocytes (Figure 4.6). Further, several metabolites of fatty acid (N-decanoylglycine and N-undecanoylglycine) (Cruickshank-Quinn et al. 2014) and of glycerophospholipid pathway including choline, neurine and LysoPC(16:0) were lower in abundance (Gibellini and Smith 2010; Tweedie et al. 2006; Saito et al. 2014). AMP, the precursor of ATP and ergothioneine, antioxidant and metabolite of histidine were also low in G6PDd erythrocytes (Figure 4.6).

These results suggest that the histidine, GSH-Methionine-Glutamate, purine, glycerophospholipid and fatty acid oxidation pathways were greatly affected in G6PDd erythrocytes.

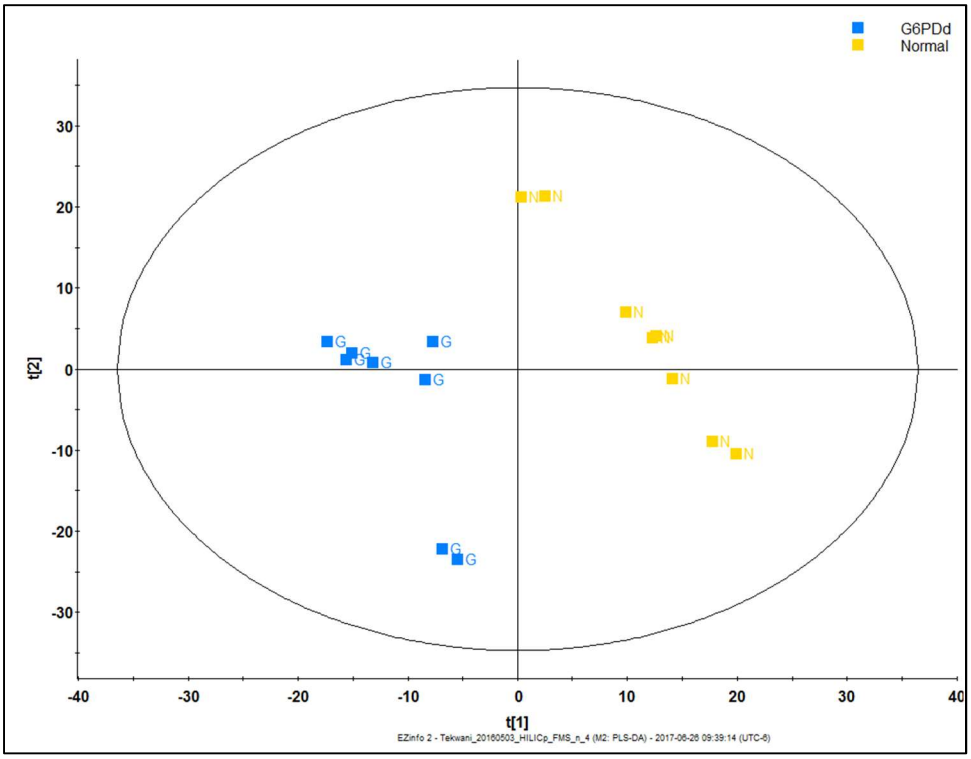

Figure 4.2: Metabolome changes in normal and G6PDd human erythrocytes in in normal-G6PDd experiment. Data were analyzed in principal component analysis plot. The score plot for normal (yellow) and G6PDd (blue) were shown (n=8). Each point represents an individual sample's data as a single unit. Clustering of the sample types shows the consistency of profiles between groups. X axis represent principal component 1 (PCA 1) and Y axis represent principal component 2 (PCA 2).

Table 4.1: The metabolites annotated (identified) in normal and G6PDd human erythrocytes in normal-G6PDd experiment.

HMDB id	Metabolite name
HMDB00034	Adenine
HMDB00043	Betaine
HMDB00045	Adenosine monophosphate
HMDB00062	L-Carnitine
HMDB00064	Creatine
HMDB00070	Pipecolic acid
HMDB00086	Glycerophosphocholine
HMDB00097	Choline
HMDB00112	Gamma-Aminobutyric acid
HMDB00125	Glutathione
HMDB00128	Guanidoacetic acid
HMDB00148	L-Glutamic acid
HMDB00157	Hypoxanthine
HMDB00158	L-Tyrosine
HMDB00159	L-Phenylalanine
HMDB00162	L-Proline
HMDB00167	L-Threonine
HMDB00168	L-Asparagine
HMDB00172	L-Isoleucine
HMDB00175	Inosinic acid
HMDB00177	L-Histidine
HMDB00187	L-Serine
HMDB00191	L-Aspartic acid
HMDB00201	L-Acetylcarnitine
HMDB00210	Pantothenic acid
HMDB00214	Ornithine
HMDB00222	L-Palmitoylcarnitine
HMDB00251	Taurine
HMDB00267	Pyroglutamic acid
HMDB00295	Uridine 5'-diphosphate
HMDB00479	3-Methylhistidine
HMDB00517	L-Arginine
HMDB00562	Creatinine
HMDB00641	L-Glutamine
HMDB00670	Homo-L-arginine
HMDB00687	L-Leucine

HMDB00696	L-Methionine
HMDB00734	Indoleacrylic acid
HMDB00824	Propionylcarnitine
HMDB00848	Stearoylcarnitine
HMDB00875	Trigonelline
HMDB00902	NAD
HMDB00904	Citrulline
HMDB00929	L-Tryptophan
HMDB00961	Farnesyl pyrophosphate
HMDB01065	2-Hydroxyphenethylamine
HMDB01173	5'-Methylthioadenosine
HMDB01325	N6,N6,N6-Trimethyl-L-lysine
HMDB01341	ADP
HMDB01406	Niacinamide
HMDB01458	Biotin amide
HMDB01488	Nicotinic acid
HMDB01511	Phosphocreatine
HMDB01645	L-Norleucine
HMDB02005	Methionine sulfoxide
HMDB02038	N(6)-Methyllysine
HMDB02064	N-Acetylputrescine
HMDB02142	Phosphoric acid
HMDB03045	Ergothioneine
HMDB03337	Oxidized glutathione
HMDB03431	L-Histidinol
HMDB03464	4-Guanidinobutanoic acid
HMDB04181	Methylimidazole acetaldehyde
HMDB04296	Acrylamide
HMDB04827	Proline betaine
HMDB05065	Oleoylcarnitine
HMDB05066	Tetradecanoylcarnitine
HMDB05765	Ophthalmic acid
HMDB06210	Heptadecanoyl carnitine
HMDB06344	Alpha-N-Phenylacetyl-L-glutamine
HMDB10382	LysoPC(16:0)
HMDB10384	LysoPC(18:0)
HMDB10386	LysoPC(18:2(9Z,12Z))
HMDB10399	LysoPC(22:1(13Z))
HMDB13127	Hydroxybutyrylcarnitine

HMDB13131	Hydroxyhexanoycarnitine
HMDB13133	Methylmalonylcarnitine
HMDB13267	N-Decanoylglycine
HMDB13286	N-Undecanoylglycine
HMDB31259	Neurine
HMDB31641	Pyrrolidine
HMDB32231	Dimethylethanolamine
HMDB32330	4-Hydroxy-2-butenoic acid gamma-lactone
HMDB41809	4-(Methylnitrosamino)-1-(3-pyridyl)-1-butanol
HMDB60067	CMP-2-aminoethylphosphonate
HMDB60363	2,5-Dichloro-4-oxohex-2-enedioate

Table 4.2: Major pathways identified using MetaboAnalyst 3.0 for 87 metabolites annotated in normal and G6PDd human erythrocytes in normal-G6PDd experiment.

.

Pathway	Total	Hits	-Log (p)	Impact
Arginine and proline	77	14	18.32	0.51
Glycine, serine and threonine	48	8	10.10	0.26
Alanine, aspartate and glutamate	24	5	8.64	0.22
Histidine	44	7	7.74	0.79
Glutathione	38	5	5.57	0.25
Cysteine and methionine	56	5	3.94	0.10
Glycerophospholipid	39	4	3.78	0.03

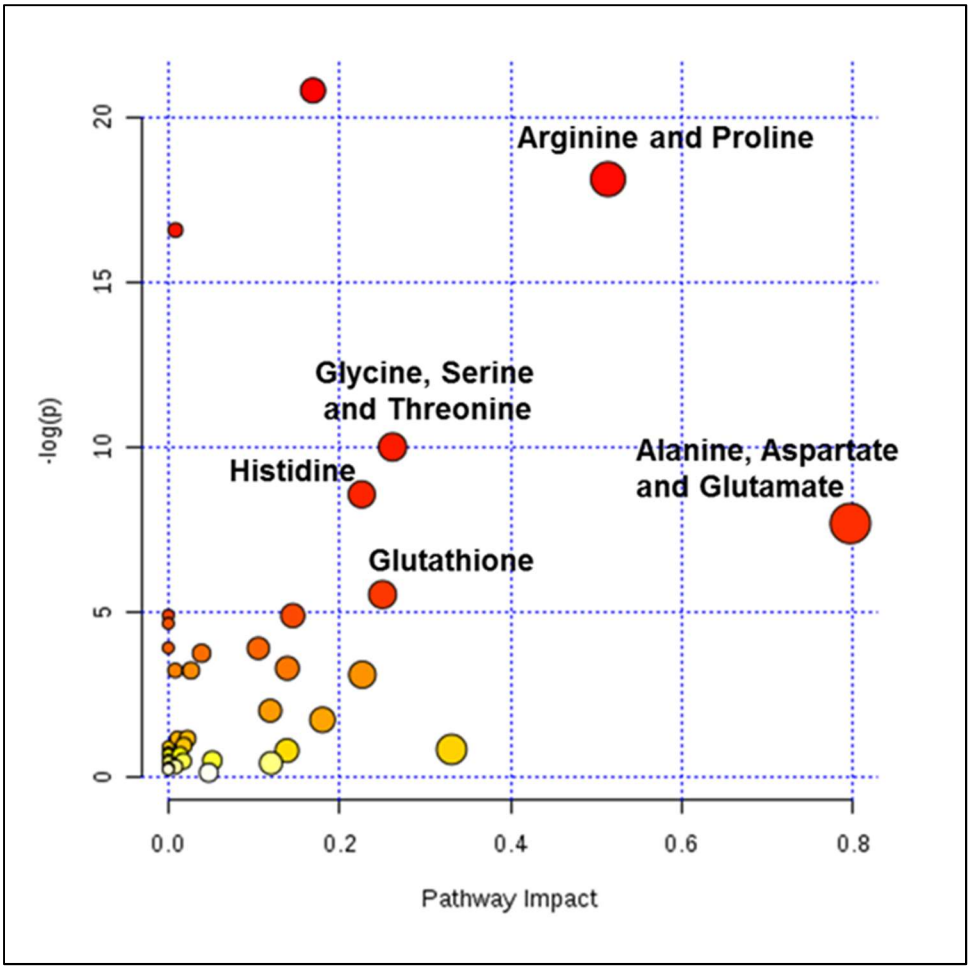

Figure 4.3: Pathway analysis of 87 metabolites identified between normal and G6PDd erythrocytes using MetaboAnalyst 3.0 in normal-G6PDd experiment.

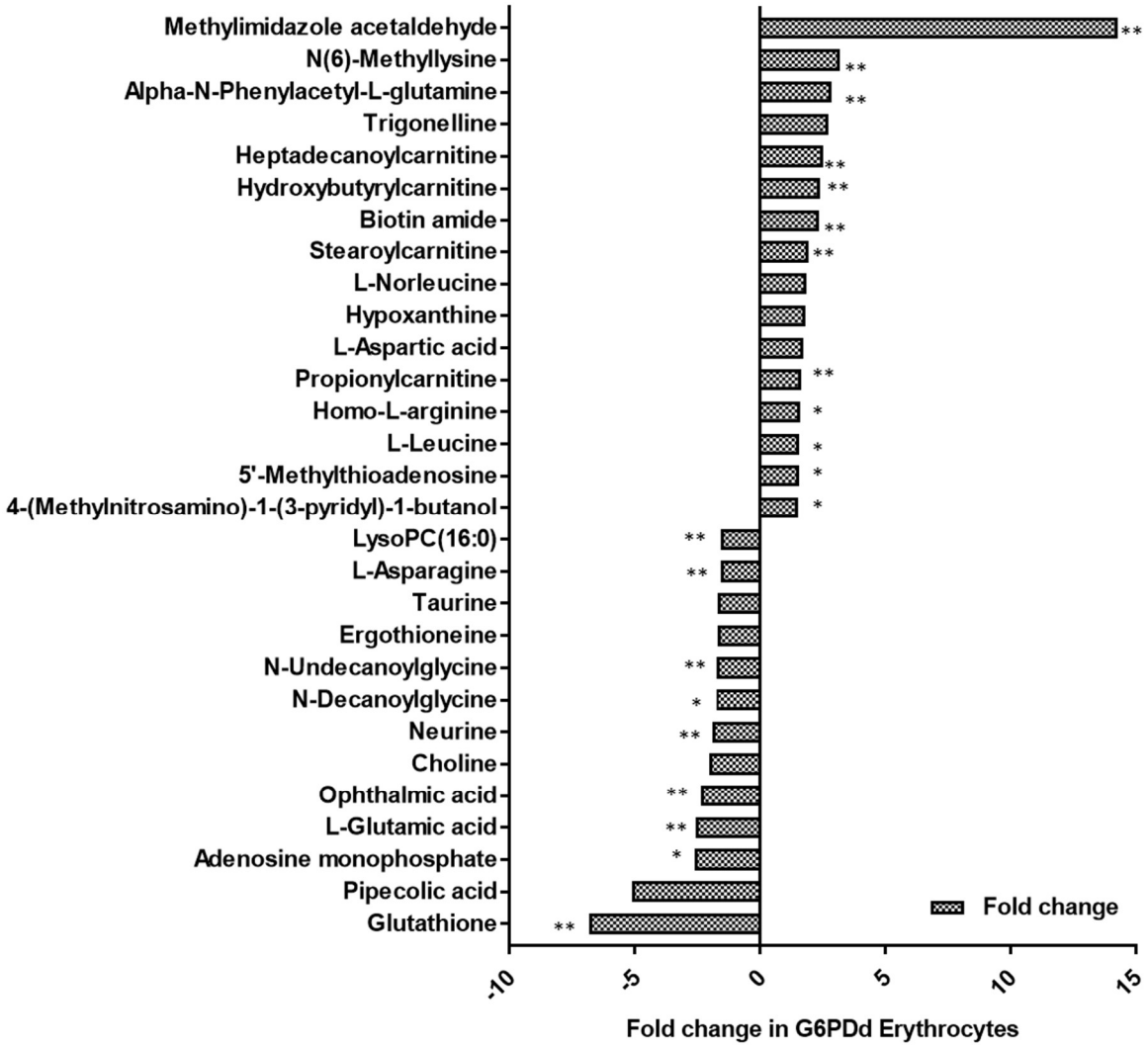

Figure 4.4: Metabolite fold change in G6PDd erythrocytes versus normal erythrocytes. n = 4. Fold change ≥ 1.5. Statistical differences between normal and G6PD-deficient cells were determined by ANOVA. P values <0.05 were considered significant ($^{*}p < 0.05$ and $^{**}p < 0.01$).

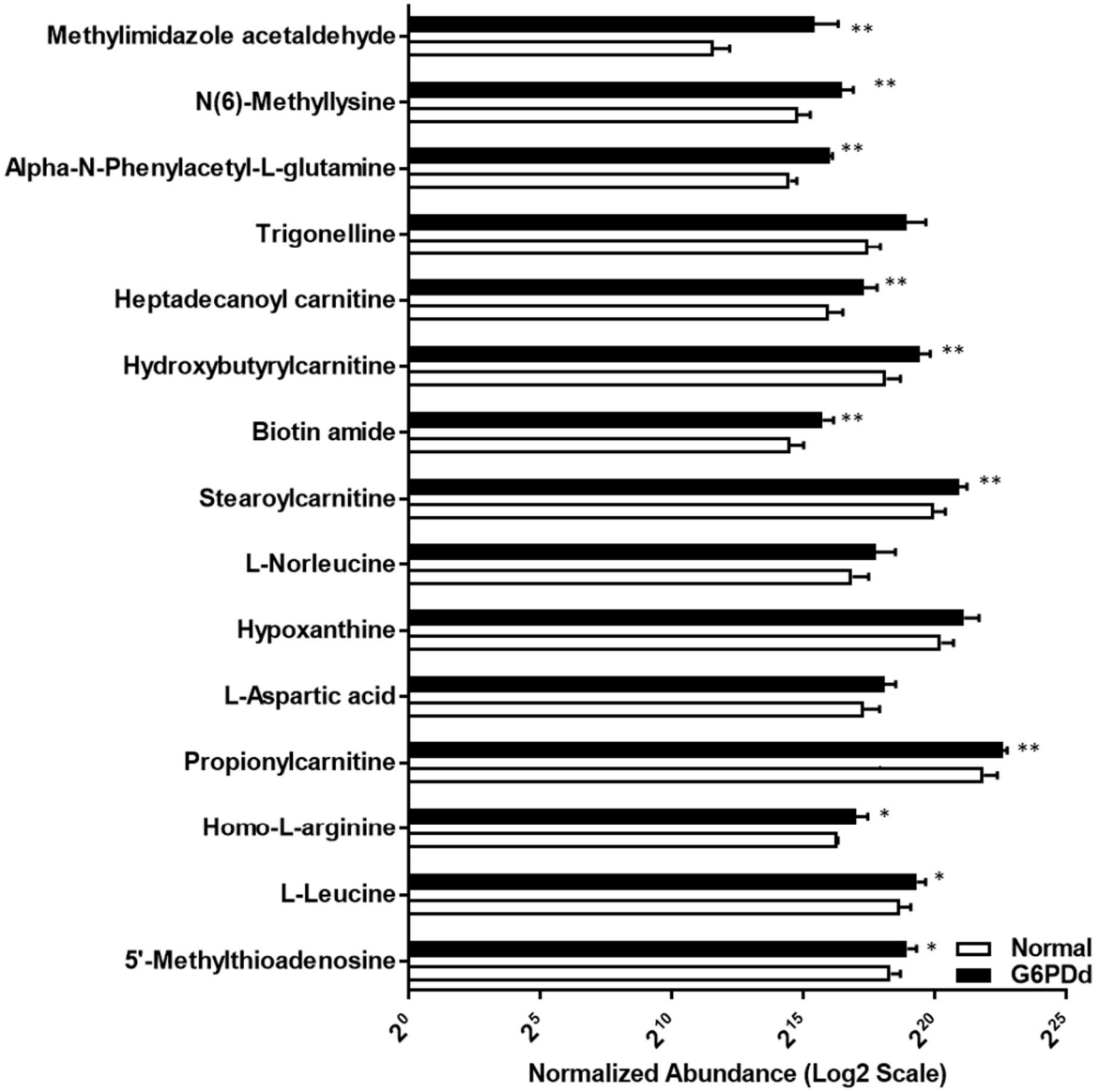

Figure 4.5: Metabolites which were upregulated (fold change ≥ 1.5) in G6PDd erythrocytes. In the figure, from top to bottom is largest fold change to smallest. Each bar represents mean of 4 experiments, and each experiment had 2 technical replicates. x-axis = Log2 normalized abundance scale. Statistical differences between normal and G6PDd erythrocytes were determined by ANOVA. p-value ≤ 0.05; Error bars represent 95% confidence; Significance values * ≤ 0.05, ** ≤ 0.01.

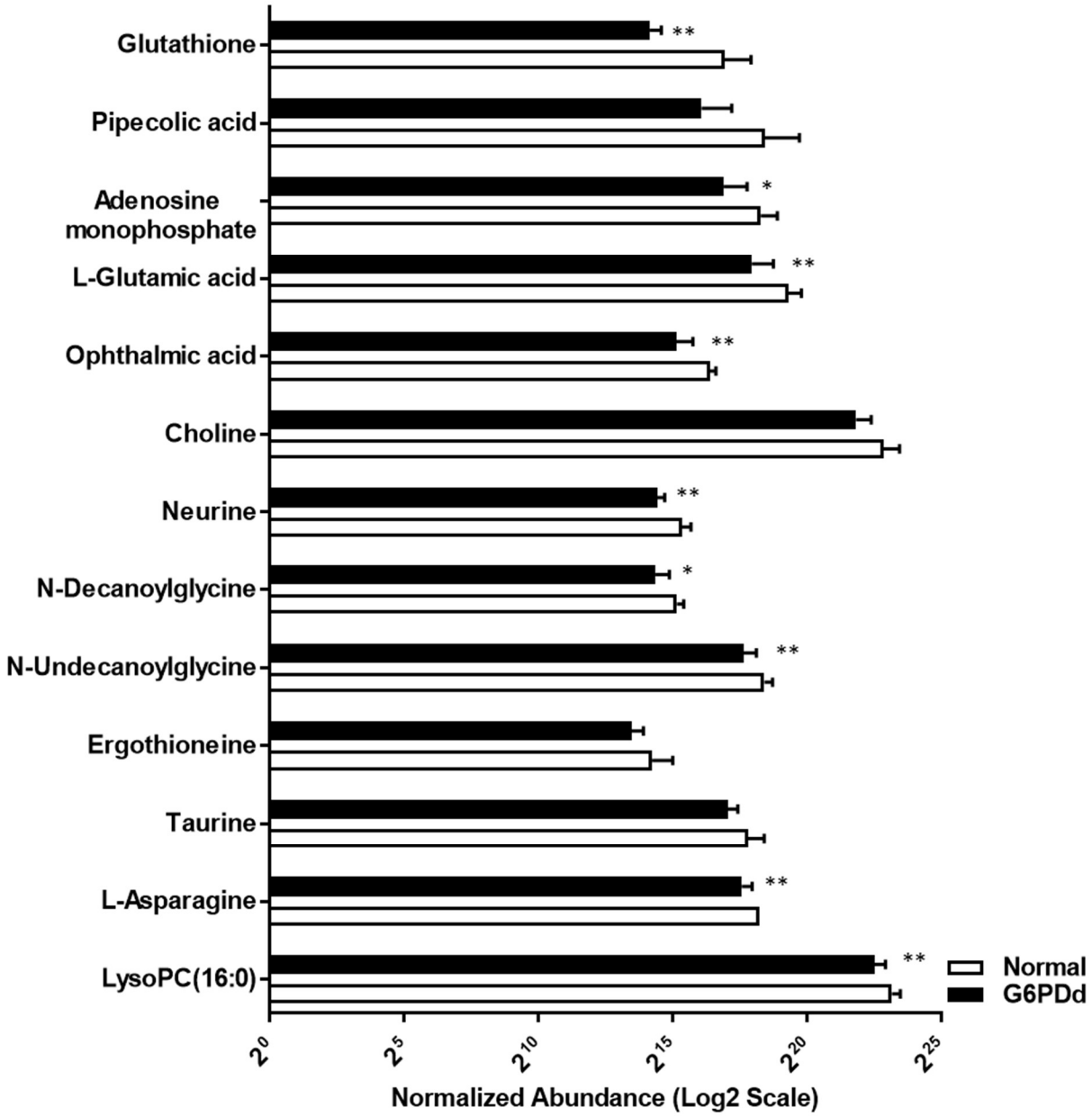

Figure 4.6: Metabolites which were downregulated (fold change ≥ 1.5) in G6PDd erythrocytes. In the figure, from top to bottom is largest fold change to smallest. Each bar represents mean of 4 experiments, and each experiment had 2 technical replicates. x-axis = Log2 normalized abundance scale. Statistical differences between normal and G6PDd erythrocytes were determined by ANOVA. p-value ≤ 0.05; Error bars represent 95% confidence; Significance values * ≤ 0.05, ** ≤ 0.01.

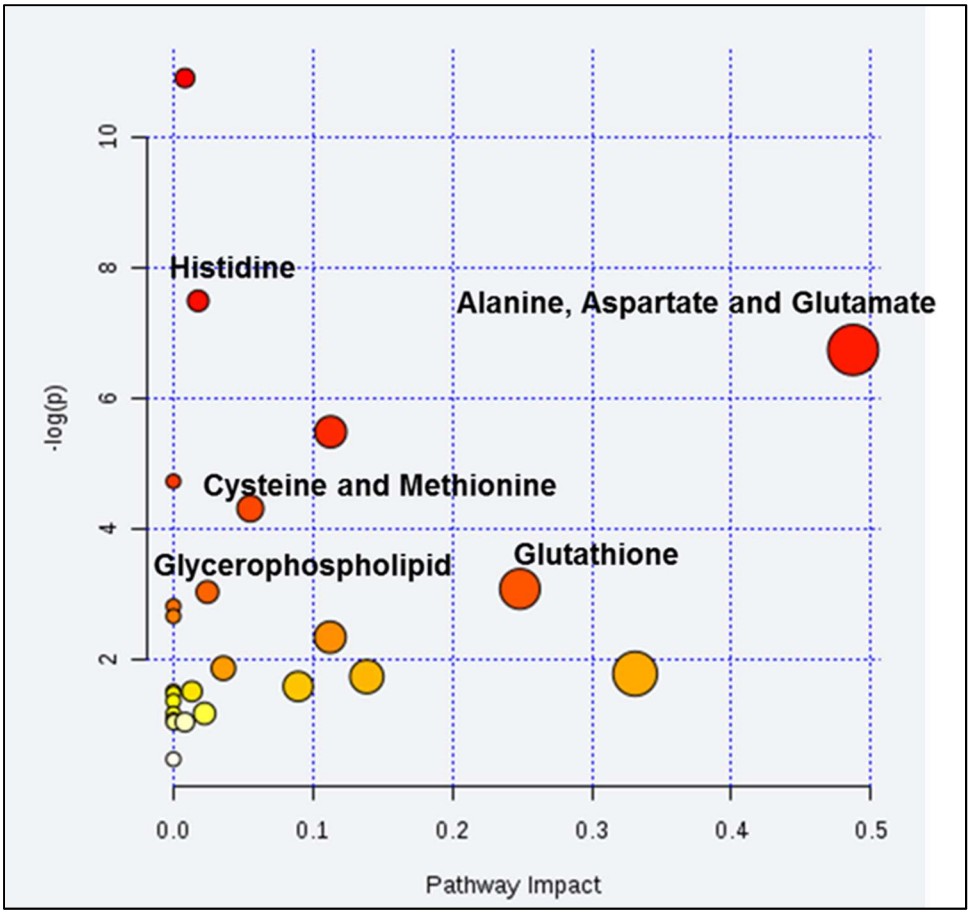

Figure 4.7: Pathway analysis of 29 metabolites that were altered more than 1.5-fold between normal and G6PDd erythrocytes using MetaboAnalyst 3.0 in normal-G6PDd experiment.

Table 4.3: Major pathways affected, identified using MetaboAnalyst 3.0 for 29 metabolites which showed fold change ≥ 1.5 in G6PDd erythrocytes as compared to normal erythrocytes in normal-G6PDd experiment.

Pathway name	Total	Hits	-Log (p)	Impact
Histidine	44	4	7.48	0.018
Alanine, aspartate and glutamate	24	3	6.73	0.48
Cysteine and methionine	56	3	4.31	0.05
Glutathione	38	2	3.07	0.24
Glycerophospholipid	39	2	3.03	0.024

4.5.2. Distinct metabolic profile of normal and G6PDd erythrocytes due to 5, 6-OQPQ treatment.

To identify changes in cellular metabolism between normal and G6PDd erythrocytes mediated by 5, 6-OQPQ treatment, both donor groups erythrocytes were treated with 25 µM 5, 6-OQPQ for 0, 30, 60, 120, and 480 minutes. The extractions of these erythrocytes were analyzed by UHPLC-MS as previously described and the raw data was processed and analyzed by Progenesis QI v.2. After annotation, total 111 metabolites were identified (Table 4.4). Further, pathway overrepresentation analysis of these 111 metabolites was performed using MetaboAnalyst 3.0, an open-source web application (Figure. 4.8; Table 4.5) (Xia and Wishart 2016; Xia et al. 2015). Among 111 metabolites there were 39 metabolites which showed a significant change in normal and G6PDd erythrocytes due to 5, 6-OQPQ treatment. The pathway analysis of these 39 metabolites was done using MetaboAnalyst 3.0, a web application (Figure. 4.9; Table 4.6). However, among these 39 the metabolites, only those metabolites which showed fold change ≥ 1.2 in normal and G6PDd erythrocytes due to treatment with corresponding time and were considered a meaningful change.

In the normal-G6PDd experiment, fold change ≥ 1.5 was used and was considered meaningful change because in this experiment, the normal and G6PDd erythrocytes were drawn from different individuals. To make sure that the changes observed were only due to genetic deficiency and not due to variation in diet or life style, the fold change parameter was increased. In drug-time-response experiment the normal and G6PDd erythrocytes were drawn from single individuals thus, the changes observed here are more because of drug-treatment and thus the fold change ≥ 1.2 is considered meaningful.

Table 4.4: The metabolites annotated (identified) in normal and G6PDd deficient human erythrocytes treated with PQ, 5,6-OQPQ (25 μM) in drug-time-response experiment.

HMDB id	Metabolite name
HMDB00214	Ornithine
HMDB00062	L-Carnitine
HMDB05765	Ophthalmic acid
HMDB00045	Adenosine monophosphate
HMDB01325	N6,N6,N6-Trimethyl-L-lysine
HMDB04827	Proline betaine
HMDB00479	3-Methylhistidine
HMDB62709	S-Adenosyl-L-methionine
HMDB00201	L-Acetylcarnitine
HMDB03431	L-Histidinol
HMDB00064	Creatine
HMDB00489	Aspartylglycosamine
HMDB00902	NAD
HMDB13127	Hydroxybutyrylcarnitine
HMDB00875	Trigonelline
HMDB00187	L-Serine
HMDB03640	Beta-Leucine
HMDB13220	Beta-Citryl-L-glutamic acid
HMDB13133	Methylmalonylcarnitine
HMDB00824	Propionylcarnitine
NA	2-Aminomethylpyrimidine
HMDB00097	Choline
HMDB00177	L-Histidine
HMDB00086	Glycerophosphocholine
HMDB01413	Citicoline
HMDB00168	L-Asparagine
HMDB01202	dCMP
HMDB00295	Uridine 5'-diphosphate
HMDB00182	L-Lysine
HMDB00961	Farnesyl pyrophosphate
HMDB03334	Symmetric dimethylarginine
HMDB00267	Pyroglutamic acid
HMDB00043	Betaine
HMDB01201	Guanosine diphosphate
HMDB60067	CMP-2-aminoethylphosphonate
HMDB00251	Taurine

HMDB01511	Phosphocreatine
HMDB00112	Gamma-Aminobutyric acid
HMDB01539	Asymmetric dimethylarginine
HMDB00033	Carnosine
HMDB00641	L-Glutamine
HMDB29198	Dimethylurea
HMDB00929	L-Tryptophan
HMDB29418	S-Cysteinosuccinic acid
HMDB00191	L-Aspartic acid
HMDB00630	Cytosine
HMDB02044	8-Hydroxyguanosine
HMDB02249	6-Methyltetrahydropterin
HMDB00079	Dihydrothymine
HMDB01406	Niacinamide
HMDB03337	Oxidized glutathione
HMDB00175	Inosinic acid
HMDB13124	Propenoylcarnitine
HMDB01341	ADP
HMDB00217	NADP
HMDB00538	Adenosine triphosphate
HMDB13131	Hydroxyhexanoycarnitine
HMDB32330	4-Hydroxy-2-butenoic acid gamma-lactone
HMDB00562	Creatinine
HMDB00939	S-Adenosylhomocysteine
HMDB02224	5-Methyldeoxycytidine
HMDB00167	L-Threonine
HMDB01125	Inositol cyclic phosphate
HMDB00157	Hypoxanthine
HMDB00050	Adenosine
HMDB00510	Aminoadipic acid
HMDB60363	2,5-Dichloro-4-oxohex-2-enedioate
HMDB00210	Pantothenic acid
NA	S-(1,2-Dicarboxyethyl) Glutathione
HMDB00159	L-Phenylalanine
HMDB06045	Dityrosine
HMDB01458	Biotin amide
HMDB00696	L-Methionine
HMDB05065	Oleoylcarnitine
HMDB00229	beta-Nicotinamide mononucleotide
HMDB00687	L-Leucine

HMDB00904	Citrulline
HMDB00172	L-Isoleucine
HMDB01173	5'-Methylthioadenosine
HMDB00148	L-Glutamic acid
HMDB02142	Phosphoric acid
HMDB13854	N4-Acetylsulfamethoxazole
HMDB10382	LysoPC (16:0)
HMDB00162	L-Proline
HMDB00222	L-Palmitoylcarnitine
HMDB01065	Phenyl ethanolamine
HMDB00125	Glutathione
HMDB00034	Adenine
HMDB00725	4-Hydroxyproline
HMDB02820	Methylimidazoleacetic acid
HMDB01545	Pyridoxal
HMDB00263	Phosphoenolpyruvic acid
HMDB32538	Triethanolamine
HMDB00517	L-Arginine
HMDB00848	Stearoylcarnitine
HMDB10384	LysoPC (18:0)
HMDB00158	L-Tyrosine
HMDB31641	Pyrrolidine
HMDB13267	N-Decanoylglycine
HMDB03045	Ergothioneine
HMDB00070	Pipecolic acid
HMDB01229	Dopaquinone
HMDB01066	S-Lactoylglutathione
HMDB13286	N-Undecanoylglycine
HMDB04437	Diethanolamine
HMDB02117	Oleamide
HMDB13279	N-Nonanoylglycine
HMDB00301	Urocanic acid
HMDB13648	Palmitoleoyl Ethanolamide
HMDB29598	Metenamine
HMDB13034	Palmitoylglycine

Table 4.5: Major pathways identified using MetaboAnalyst 3.0 for 111 metabolites annotated in drug-time-response experiment.

Pathway name	Total	Hits	-Log (p)	Impact
Arginine and proline	77	12	11.54	0.54
Histidine	44	9	11.15	0.29
Glycine, serine and threonine	48	7	6.71	0.25
Alanine, aspartate and glutamate	24	5	6.70	0.79
Glutathione	38	6	6.31	0.26
Glycerophospholipid	39	6	6.17	0.08
Nicotinate and nicotinamide	44	6	5.54	0.04
Purine	92	9	5.42	0.26
Cysteine and methionine	56	6	4.35	0.20

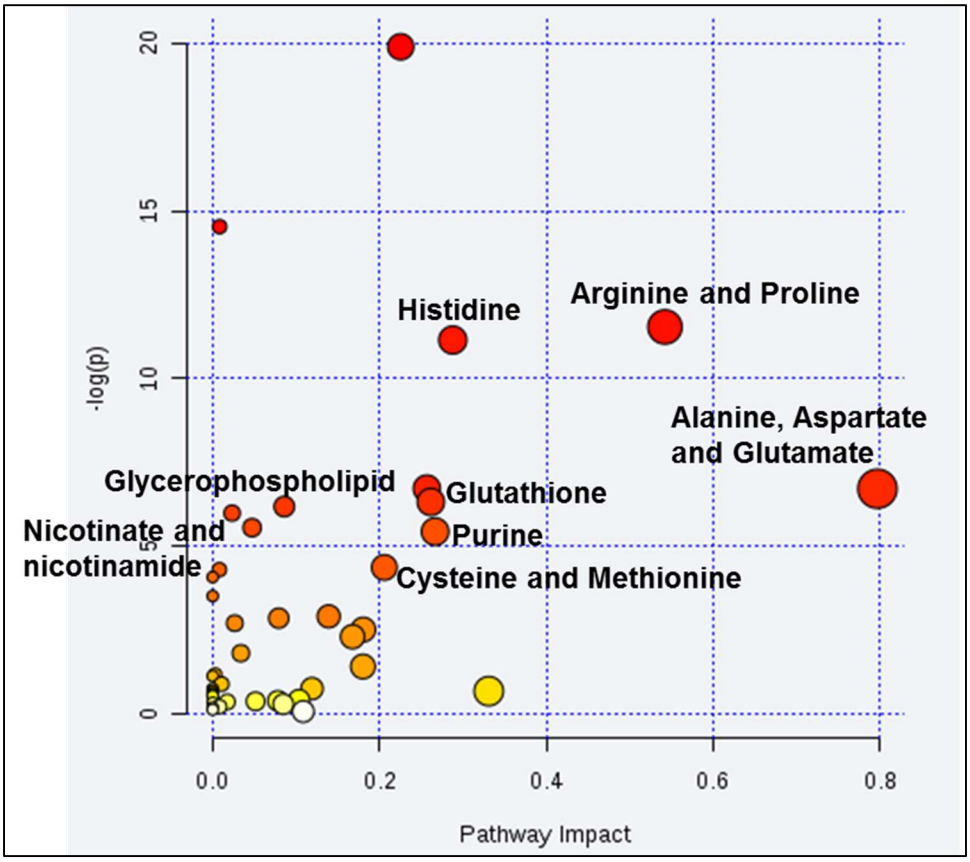

Figure 4.8: Pathway analysis of 111 metabolites identified in the drug-time-response experiment using MetaboAnalyst 3.0.

Table 4.6: Major pathways affected, identified using MetaboAnalyst 3.0 for 39 metabolites showed significantly changed in normal and G6PDd erythrocytes due to 5,6-OQPQ (25 μM) treatment as compared to untreated normal and untreated G6PDd erythrocytes with corresponding time point.

Pathway name	Total	Hits	-Log (p)	Impact
Purine	92	7	9.04	0.25
Glutathione	38	4	6.70	0.24
Arginine and proline	77	5	5.95	0.39
Cysteine and methionine	56	4	5.26	0.16
Glycerophospholipid	39	3	4.34	0.05
Histidine	44	3	4.02	0.07
Alanine, aspartate and glutamate	24	2	3.29	0.22

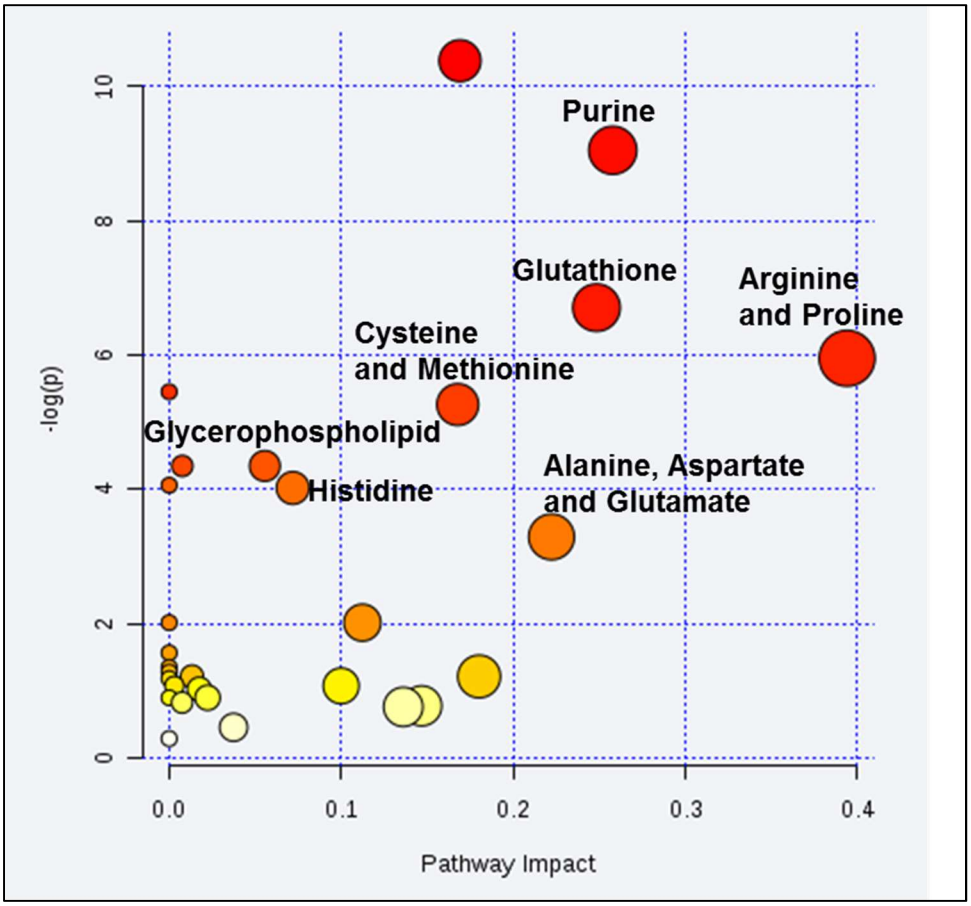

Figure 4.9: Pathway analysis of 39 metabolites showed significantly changed in normal and G6PDd erythrocytes due to 5,6-OQPQ treatment as compared to untreated normal and untreated G6PDd erythrocytes with corresponding time point.

4.5.2.1. Alterations in GSH-methionine-glutamic acid metabolism in normal and G6PDd erythrocytes due to 5, 6-OQPQ treatment.

The basal level of GSH precursor, DCE-GS (S-1,2-dicarboxyethyl-glutathione) and S-lactoylglutathione were significantly increased in G6PDd erythrocytes. DCE-GS was elevated due to treatment in both erythrocyte groups. However, there was a nonspecific increase of DCE-GS was in both erythrocytes (Figure 4.10). The basal level of oxidized glutathione and glutamic acid were significantly lower in G6PDd erythrocytes (Figure 4.10 and 4.11). Oxidized glutathione was depleted in both erythrocytes at later time points (120 and 480 minutes) due to treatment (Figure 4.10). The level of glutamic acid was depleted selectively in normal erythrocytes due to treatment at 120 and 480 minutes (Figure 4.11). The level of ophthalmic acid was significantly higher in both erythrocytes due to treatment at a corresponding time however significant accumulation of ophthalmic acid was in both erythrocytes due to incubation time (Figure 4.11). There was a depletion in SAM and 5-methylthioadenosine levels in both erythrocytes due to treatment as compared to untreated erythrocytes at a corresponding time (Figure 4.12). These results indicate that metabolites of the GSH-methionine-glutamate pathway were significantly changed in both erythrocytes due to treatment. The schematic diagram of the GSH-methionine-glutamate pathway was shown in Figure 4.13.

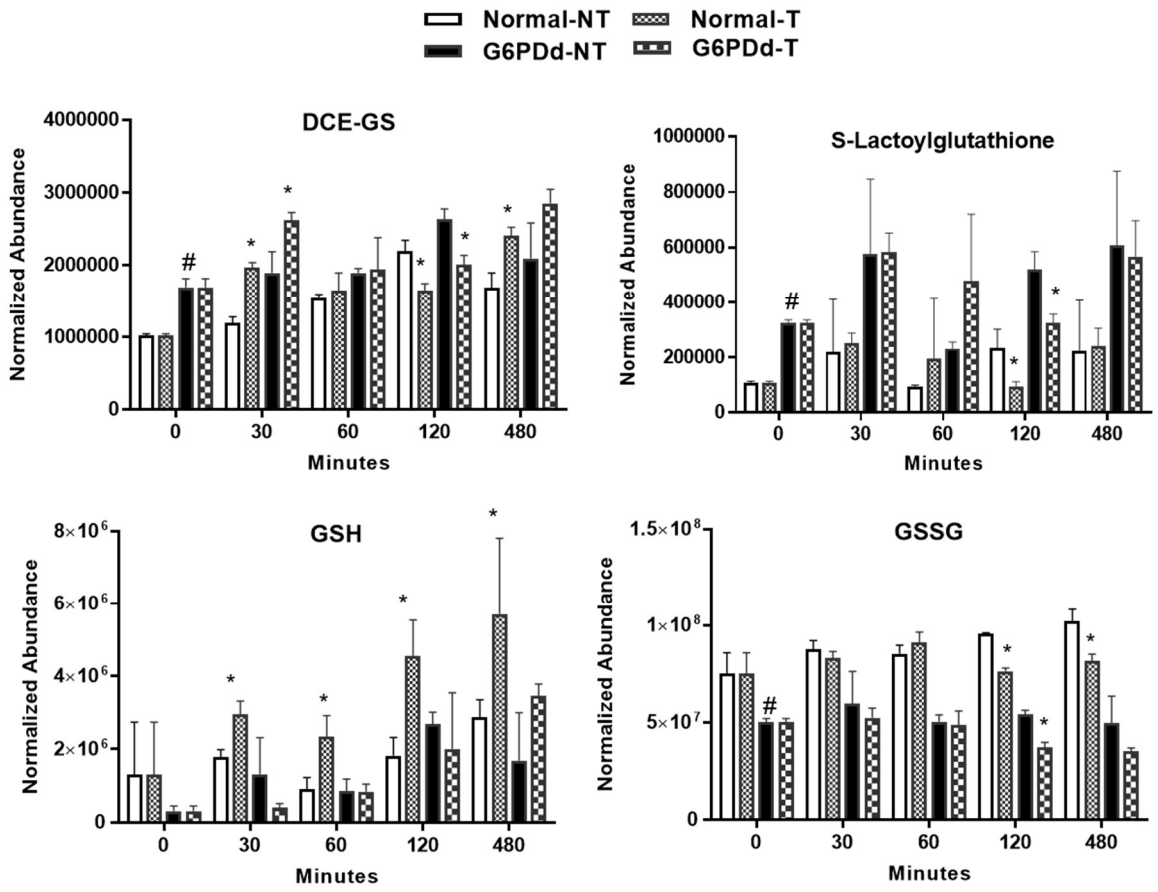

Figure 4.10: Distinct effect of 5, 6-OQPQ (25µM) on **GSH metabolic pathway** and precursors of GSH in normal and G6PDd erythrocytes at 0, 30, 60, 120, and 480 minutes, and processed with an untargeted metabolomics workflow. Metabolites were annotated as previously described, and were mapped onto the GSH metabolic pathways. The levels of metabolites are expressed (Y-axis) as normalized abundance. Each bar represents mean ± SD of at least three observations. Statistical differences between groups were determined by ANOVA; P values <0.05 were considered as statistically significant. $^{*}p < 0.05$ compared with no treatment with corresponding erythrocytes at corresponding time. $^{\#}p < 0.05$ compared with pretreatment in normal erythrocyte at 0-minute. 0-minute data represent pretreatment erythrocytes. DCE-GS- S-(1,2-Dicarboxyethyl) Glutathione; GSH- Reduced glutathione; GSSG- Oxidized glutathione.

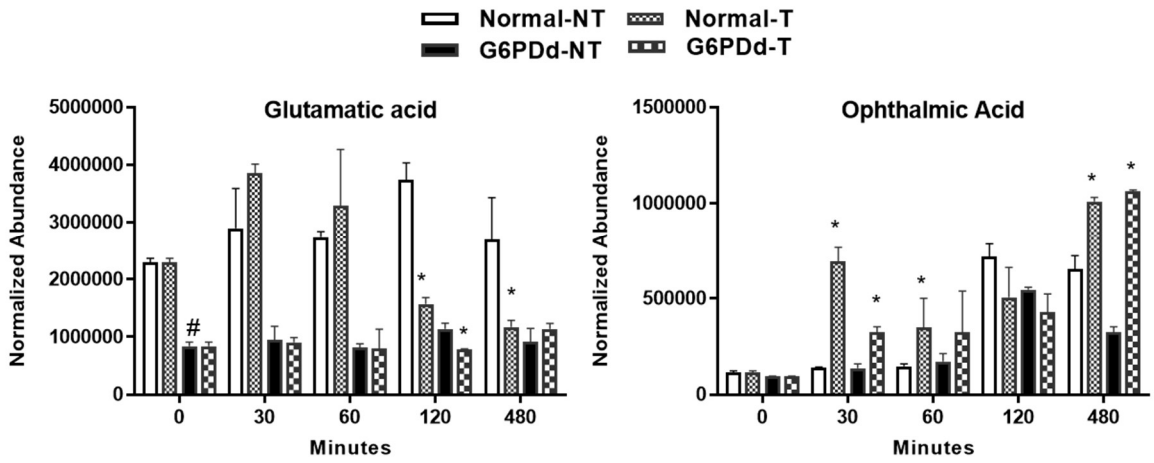

Figure 4.11: Distinct effect of 5, 6-OQPQ (25µM) on the **glutamic acid** metabolic pathway in normal and G6PDd erythrocytes at 0, 30, 60, 120, and 480 minutes, and processed with an untargeted metabolomics workflow. Metabolites were annotated as previously described, and were mapped onto the glutamic metabolic pathways. The levels of metabolites are expressed (y-axis) as normalized abundance. Each bar represents mean ± SD of at least three observations. Statistical differences between groups were determined by ANOVA; P values <0.05 were considered as statistically significant$^{*}p < 0.05$ compared with no treatment with corresponding erythrocytes at corresponding time. $^{\#}p < 0.05$ compared with pretreatment in normal erythrocyte at 0-minute. 0-minute data represent pretreatment erythrocytes. 0-minute data represent pretreated erythrocytes.

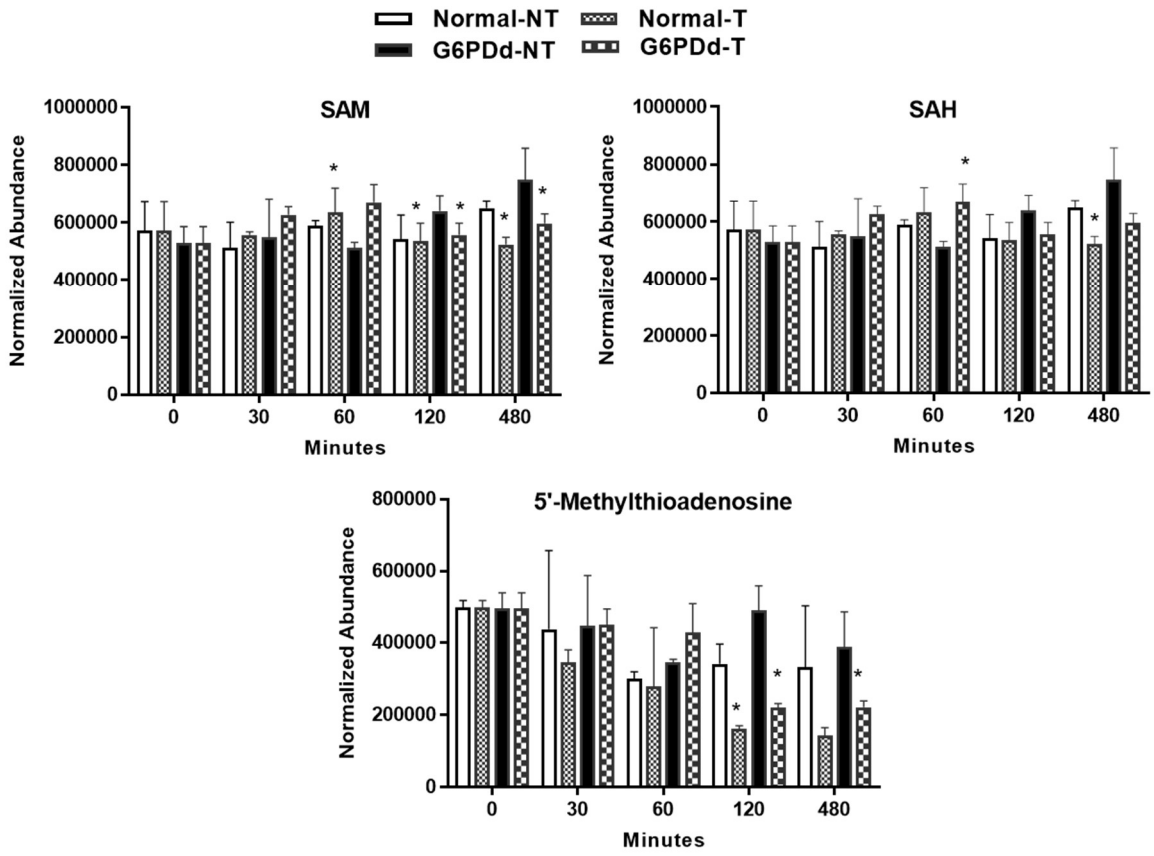

Figure 4.12. Distinct effect of 5, 6-OQPQ (25μM) on the **methionine** metabolic pathway in normal and G6PD-deficient RBCs at 0, 30, 60, 120, and 480 minutes, and processed with an untargeted metabolomics workflow. Metabolites were annotated as previously described, and were mapped onto the methionine metabolic pathways. The levels of metabolites are expressed (Y-axis) as normalized abundance. Each bar represents mean ± SD of at least three observations. Statistical differences between groups were determined by ANOVA; P values <0.05 were considered as statistically significant. $^{*}p < 0.05$ compared with no treatment with corresponding erythrocytes at corresponding time. 0-minute data represent pretreatment erythrocytes. 0-minute data represent pretreated erythrocytes. SAH: S-Adenosylhomocysteine; SAM: S-Adenosyl-methionine.

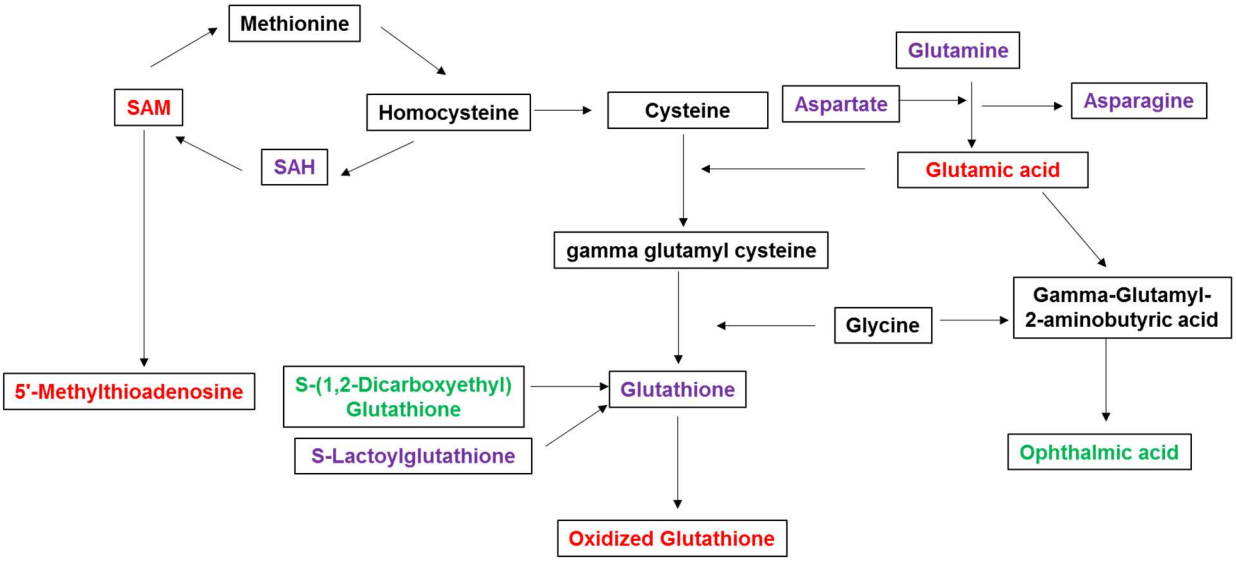

Figure 4.13: Schematic diagram of **glutathione-methionine-glutamic acid** metabolism pathway. The metabolites colored in red, green and purple were identified in normal and G6PDd erythrocytes treated with 25µM 5, 6-OQPQ for 0, 30, 60, 120, and 480 minutes. Metabolites colored in black were intermediate of the pathway and were not identified. The metabolites in purple, red and green showed no change, increase and decrease respectively due to treatment.

4.5.2.2. Alternations in arginine-proline metabolism in normal and G6PDd erythrocytes due to 5, 6-OQPQ treatment.

The basal level of proline and arginine were significantly lower and higher in G6PDd erythrocytes, respectively. The levels of proline, arginine, and ornithine levels were significantly increased due to treatment in both erythrocytes. However, there was nonspecific depletion of proline, arginine, and ornithine in both erythrocytes due to incubation (Figure 4.14). These results suggest the metabolites of arginine-proline were significantly increased due to treatment in normal and G6PDd erythrocytes.

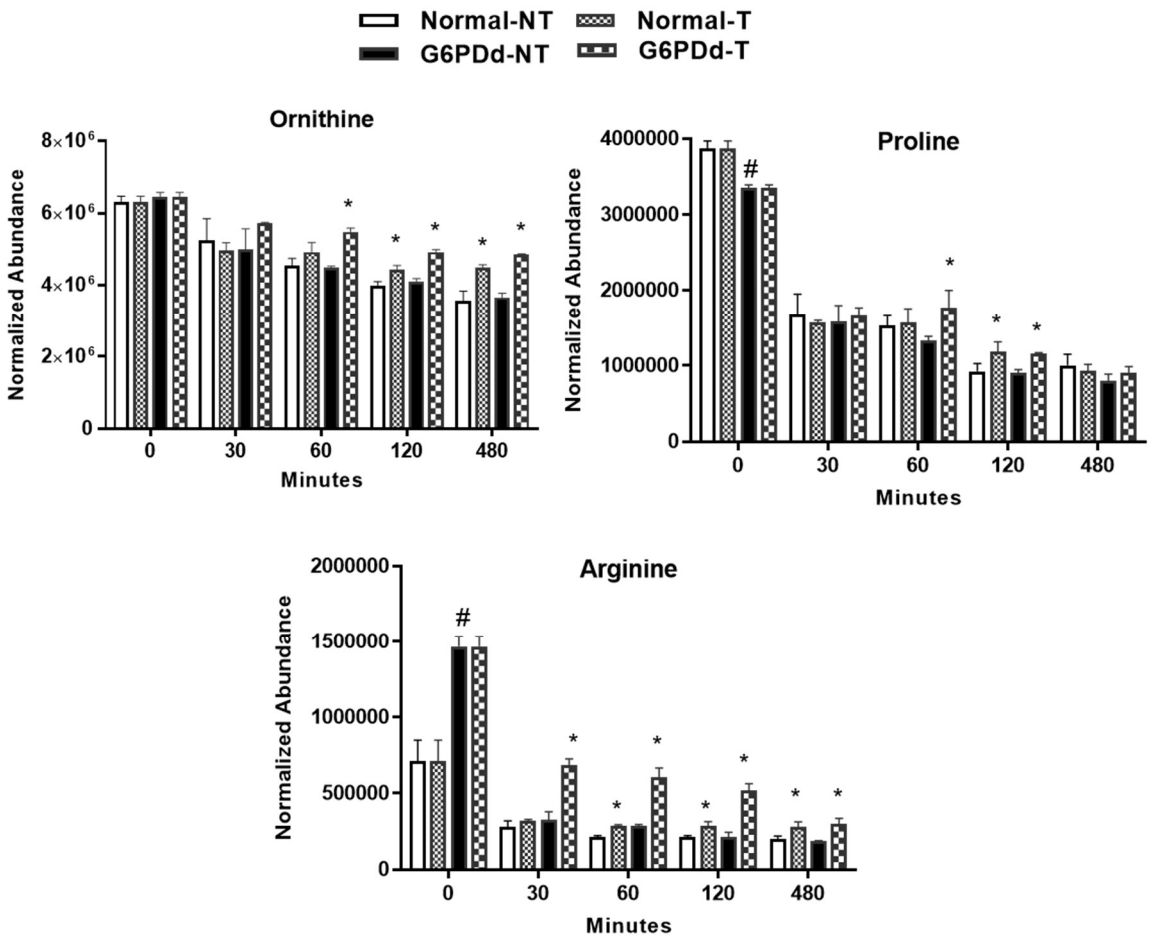

Figure 4.14: Distinct effect of 5, 6-OQPQ (25µM) on the **arginine and proline** metabolic pathway in normal and G6PDd erythrocytes at 0, 30, 60, 120, and 480 minutes, and processed with an untargeted metabolomics workflow. Metabolites were annotated as previously described, and were mapped onto the arginine and proline metabolic pathways. The levels of metabolites are expressed (Y-axis) as normalized abundance. Each bar represents mean ± SD of at least three observations. Statistical differences were determined by ANOVA; P values <0.05 were considered as statistically significant. $^{*}p < 0.05$ compared with no treatment with corresponding erythrocytes at corresponding time. $^{\#}p < 0.05$ compared with pretreatment in normal erythrocyte at 0-minute. 0-minute data represent pretreatment erythrocytes. 0-minute data represent pretreated erythrocytes.

4.5.2.3. Alternations in purine and nicotinamide metabolism in normal and G6PDd erythrocytes due to 5, 6-OQPQ treatment.

There was an accumulation of ADP (adenosine diphosphate) and AMP (adenosine monophosphate) selectively in normal erythrocytes due to treatment. However, the levels of AMP were depleted selectively in G6PDd erythrocytes due to treatment. In addition, there was a nonspecific accumulation of ADP and AMP in both erythrocytes due to incubation. Adenine levels were significantly depleted in both erythrocytes due to treatment at later time points (120 and 480 minutes) (Figure 4.15). The basal levels of IMP (inosine monophosphate) and GDP (guanosine diphosphate) were significantly lower and higher in G6PDd erythrocytes respectively. There was a depletion in IMP and GDP due to treatment in both erythrocytes. Hypoxanthine was accumulated in both erythrocytes in both erythrocytes due to treatment. There was nonspecific accumulation and depletion of IMP and hypoxanthine arginine and ornithine in both erythrocytes due to incubation (Figure 4.16). Furthermore, in the pyrimidine pathway, the NMN (nicotinamide mononucleotide) levels were significantly depleted in G6PDd erythrocytes due to treatment (Figure 4.17). These results suggest the metabolites of purine pathway were significantly altered due to treatment in normal and G6PDd erythrocytes.

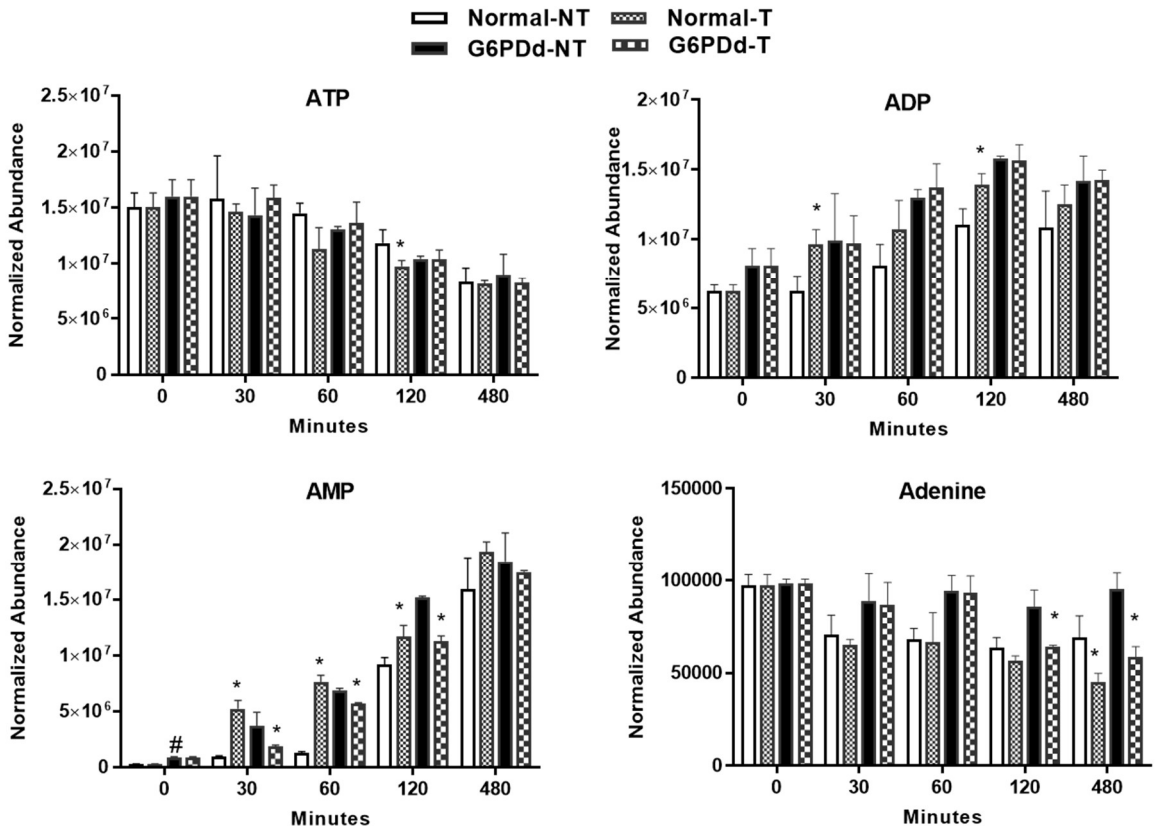

Figure 4.15: Distinct effect of 5, 6-OQPQ (25µM) on the **purine (ATP and its precursor)** metabolic pathway in normal and G6PDd erythrocytes at 0, 30, 60, 120, and 480 minutes, and processed with an untargeted metabolomics workflow. Metabolites were annotated as previously described, and were mapped onto the purine metabolic pathways. The levels of metabolites are expressed (-axis) as normalized abundance. Each bar represents mean ± SD of at least three observations. Statistical differences were determined by ANOVA; P values <0.05 were considered as statistically significant. $^{*}p < 0.05$ compared with no treatment with corresponding erythrocytes at corresponding time. $^{\#}p < 0.05$ compared with pretreatment in normal erythrocyte at 0-minute. 0-minute data represent pretreatment erythrocytes. ATP: Adenosine triphosphate. ADP: Adenosine diphosphate. AMP: Adenosine monophosphate.

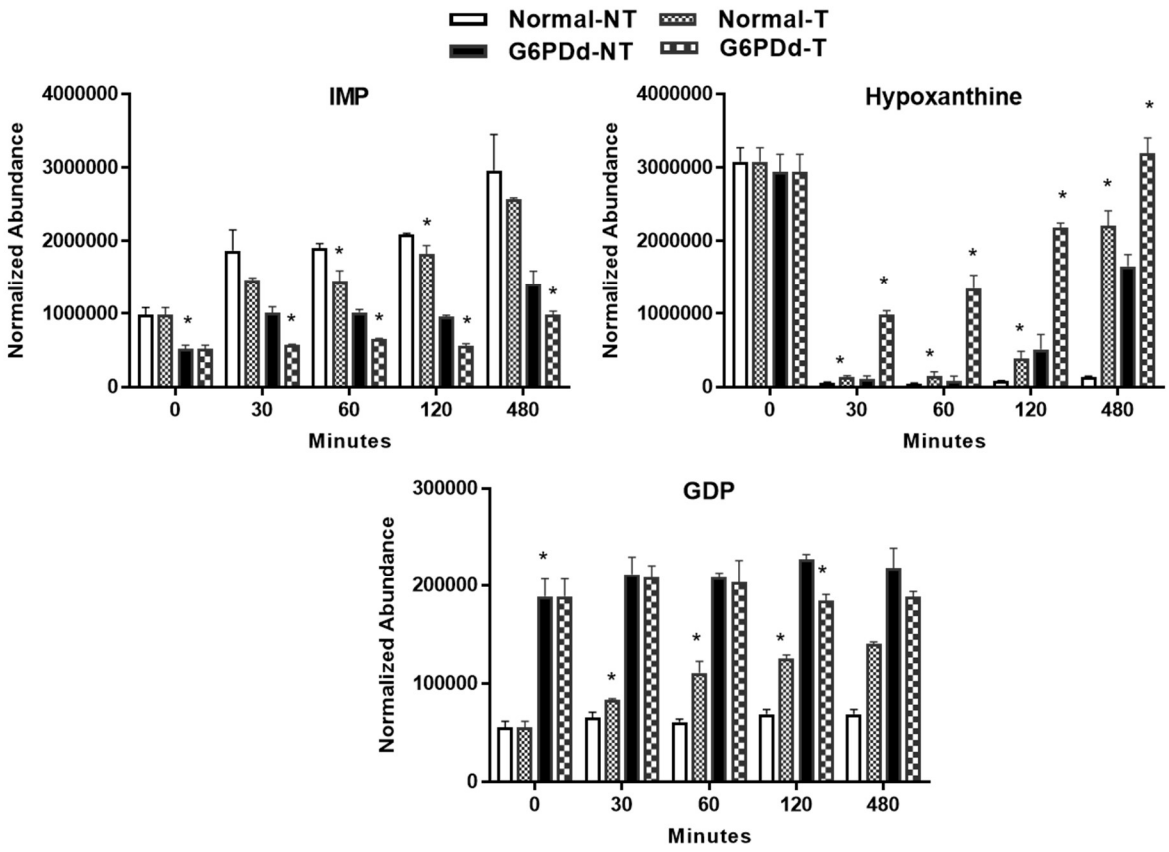

Figure 4.16: Distinct effect of 5, 6-OQPQ (25μM) on the **purine (IMP, hypoxanthine, and GDP)** metabolic pathway in normal and G6PDd erythrocytes at 0, 30, 60, 120, and 480 minutes, and processed with an untargeted metabolomics workflow. Metabolites were annotated as previously described, and were mapped onto the purine metabolic pathways. The levels of metabolites are expressed (Y-axis) as normalized abundance. Each bar represents mean ± SD of at least three observations. Statistical differences were determined by ANOVA; P values <0.05 were considered as statistically significant. $^{*}p < 0.05$ compared with no treatment with corresponding erythrocytes at corresponding time. $^{\#}p < 0.05$ compared with pretreatment in normal erythrocyte at 0-minute. 0-minute data represent pretreatment erythrocytes. IMP: Inosine monophosphate. GDP: Guanosine diphosphate.

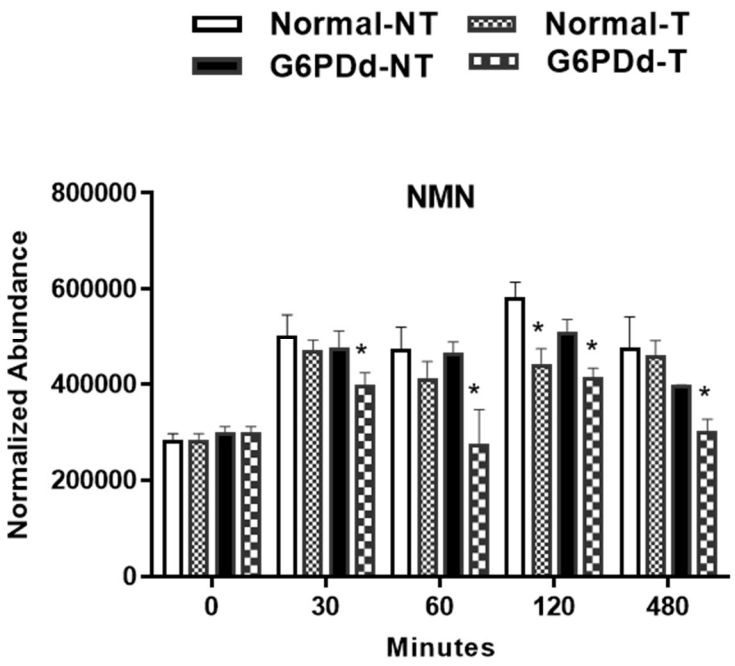

Figure 4.17: Distinct effect of 5, 6-OQPQ (25µM) on the **NMN** levels in normal and G6PDd erythrocytes at 0, 30, 60, 120, and 480 minutes, and processed with an untargeted metabolomics workflow. Metabolites were annotated as previously described. The levels of metabolites are expressed (Y-axis) as normalized abundance. Each bar represents mean ± SD of at least three observations. Statistical differences between 5, 6-OQPQ-treated normal and G6PD-deficient cells were determined by ANOVA; P values <0.05 were considered as statistically significant. $^{*}p < 0.05$ compared with no treatment with corresponding erythrocytes at corresponding time. 0-minute data represent pretreatment erythrocytes. 0-minute data represent pretreated erythrocytes. NMN: Nicotinamide mononucleotide.

4.5.2.4. Alternations in glycerophospholipid metabolism in normal and G6PDd erythrocytes due to 5, 6-OQPQ treatment.

The basal levels of GPC (glycerophosphocholine), lysophosphatidylcholines (LPC) (16:0) and lysophosphatidylcholines (18:0) were significantly lower in G6PDd erythrocytes (Figure 4.18). GPC levels were elevated in normal and G6PDd erythrocytes due to treatment. LPC (16:0) and LPC (18:0) were depleted at 120 minutes in both normal and G6PDd erythrocytes and were increased selectively in G6PDd erythrocytes at 480 minutes due to treatment (Figure 4.18). Citicoline, a biomarker of chronic hemolysis and formed from phosphocholine (Paglia et al. 1983) was selectively accumulated in G6PDd erythrocytes due to treatment at all time points (Figure 4.18). These results indicate the metabolites of glycerophospholipid pathway were significantly modified due to treatment in normal and G6PDd erythrocytes.

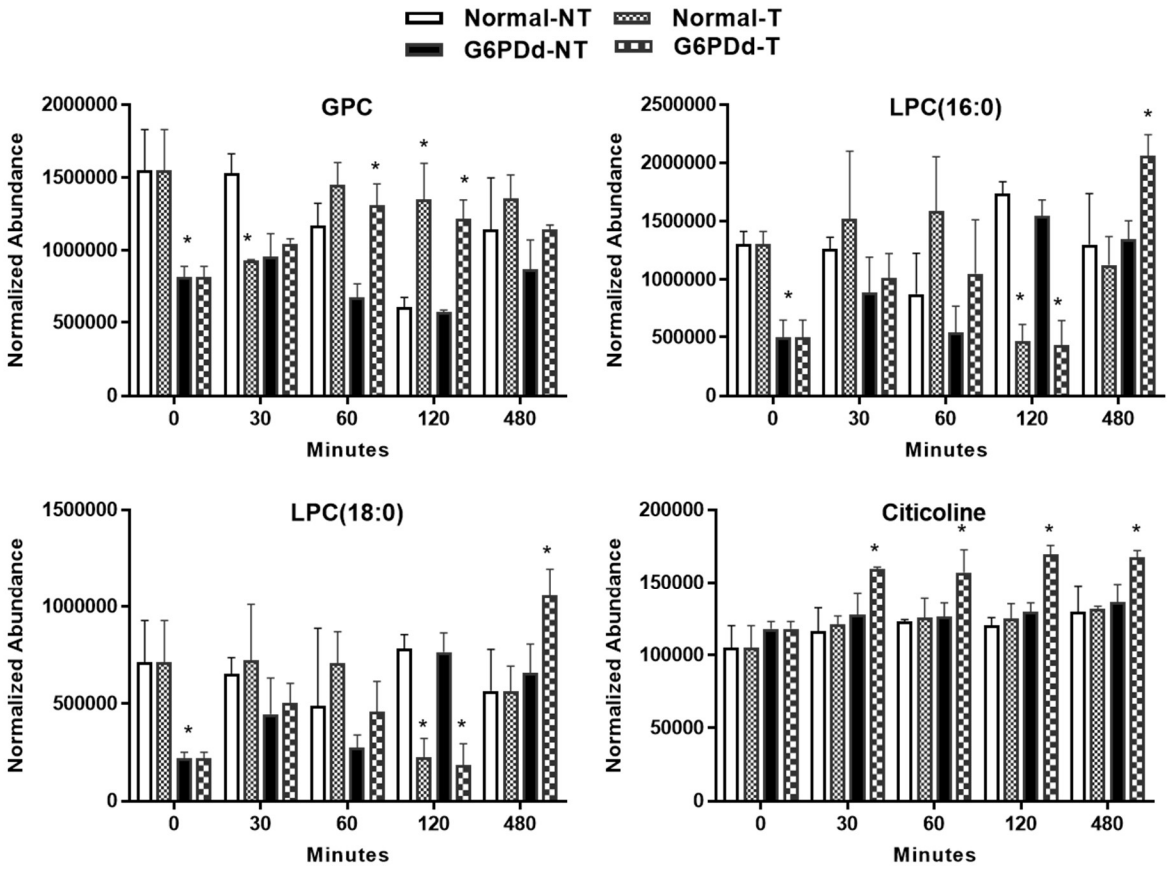

Figure 4.18: Distinct effect of 5, 6-OQPQ (25μM) on the **glycerophospholipid** metabolic pathway in normal and G6PDd erythrocytes at 0, 30, 60, 120, and 480 minutes, and processed with an untargeted metabolomics workflow. Metabolites were annotated as previously described, and were mapped onto the glycerophospholipid metabolic pathways. The levels of metabolites are expressed (Y-axis) as normalized abundance. Each bar represents mean ± SD of at least three observations. Statistical differences were determined by ANOVA; P values <0.05 were considered as statistically significant. $^{*}p < 0.05$ compared with no treatment with corresponding erythrocytes at corresponding time. $^{\#}p < 0.05$ compared with pretreatment in normal erythrocyte at 0-minute. 0-minute data represent pretreatment erythrocytes. GPC: Glycerophosphocholine; LPC (16:0): Lysophosphatidylcholines (16:0); LPC (18:0): Lysophosphatidylcholines (18:0).

4.5.2.5. Alternations in histidine metabolism in normal and G6PDd erythrocytes due to 5, 6-OQPQ treatment.

The basal level of ergothioneine, the natural metabolite of histidine metabolism and antioxidant was increased in G6PDd erythrocytes (Halliwell et al. 2016). The level of histidinol, the precursor of histidine and ergothioneine both were significantly higher in both erythrocytes due to treatment (Figure 4.19). These results showed that the precursor and metabolites of histidine were significantly elevated in erythrocytes due to treatment.

4.5.2.6. Alternations in antioxidants in normal and G6PDd erythrocytes due to 5, 6-OQPQ treatment.

The basal levels of antioxidant pantothenic acid and BCGA (beta-citryl-glutamic acid) were elevated in G6PDd erythrocytes and serine was depleted in G6PDd erythrocytes (Figure 4.20). Treatment elevated lysine, BCGA, and serine in both erythrocytes at later time point (120 and 480 minutes) suggesting that in response to treatment the antioxidant levels were increased as a compensatory mechanism. However, the levels of pantothenic acid were depleted selectively in G6PDd erythrocytes due to treatment (Figure 4.20). These results showed that treatment elevated antioxidants in both erythrocytes as a compensatory mechanism.

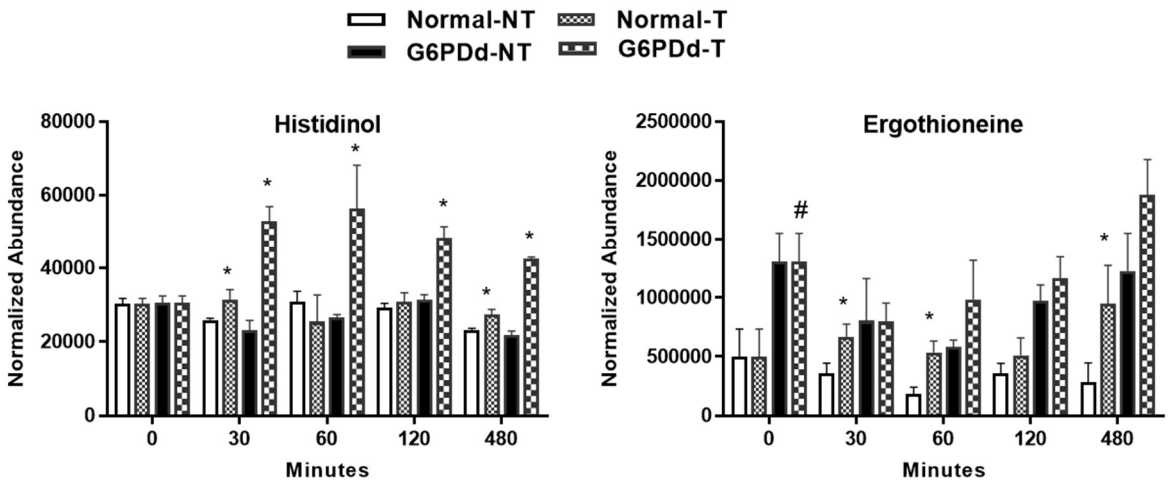

Figure 4.19: Distinct effect of 5, 6-OQPQ (25μM) on the **histidine** metabolic pathway in normal and G6PDd erythrocytes at 0, 30, 60, 120, and 480 minutes, and processed with an untargeted metabolomics workflow. Metabolites were annotated as previously described, and were mapped onto the histidine metabolic pathways. The levels of metabolites are expressed (Y-axis) as normalized abundance. Each bar represents mean ± SD of at least three observations. Statistical differences were determined by ANOVA; P values <0.05 were considered as statistically significant$^{*}p < 0.05$ compared with no treatment with corresponding erythrocytes at corresponding time. $^{\#}p < 0.05$ compared with pretreatment in normal erythrocyte at 0-minute. 0-minute data represent pretreatment erythrocytes. 0-minute data represent pretreated erythrocytes.

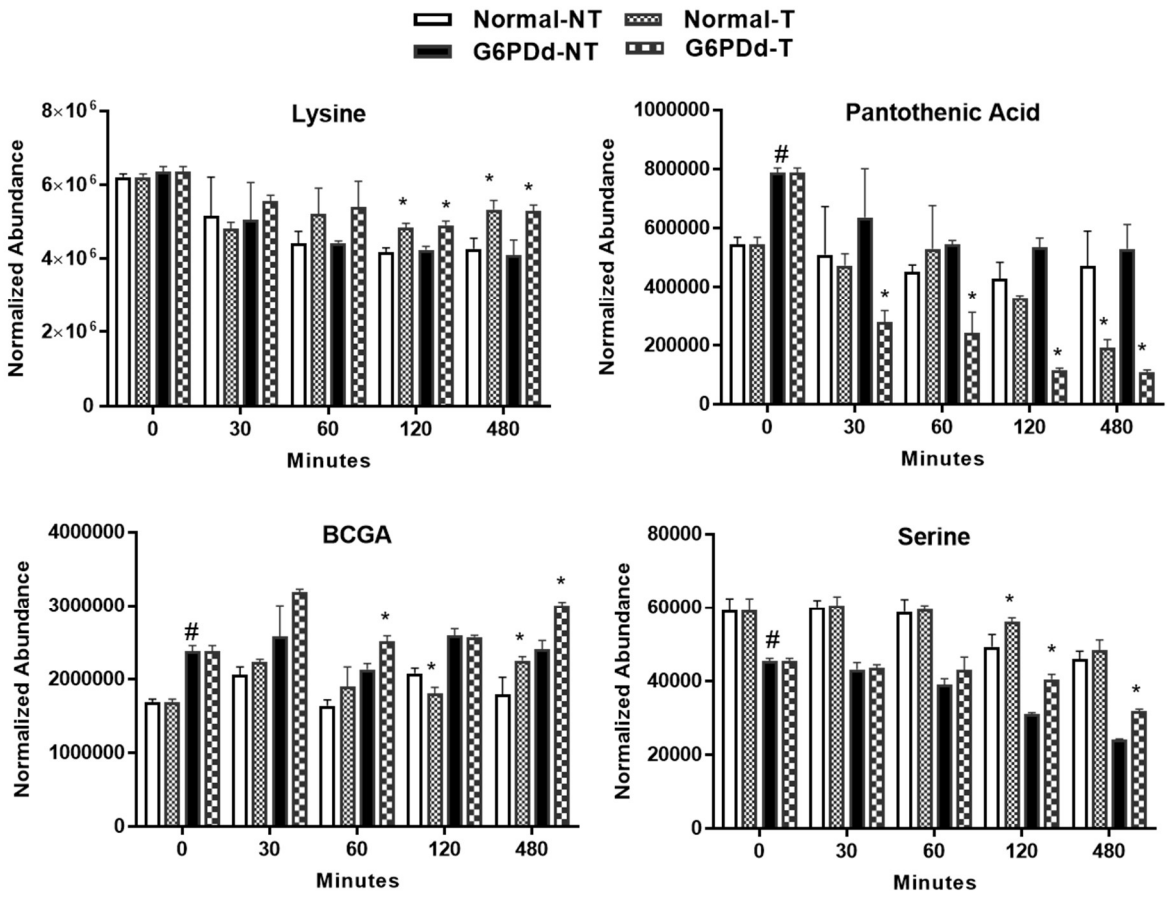

Figure 4.20: Distinct effect of 5, 6-OQPQ (25µM) on the **antioxidants** namely, lysine, pantothenic acid, BCGA (beta-citryl-glutamic acid) and serine levels in normal and G6PDd erythrocytes at 0, 30, 60, 120, and 480 minutes, and analyzed for their metabolite profiles. The levels of metabolites are expressed (Y-axis) as normalized abundance. Each bar represents mean ± SD of at least three observations. Statistical differences were determined by ANOVA; P values <0.05 were considered as statistically significant. $^{*}p < 0.05$ compared with no treatment with corresponding erythrocytes at corresponding time. $^{\#}p < 0.05$ compared with pretreatment in normal erythrocyte at 0-minute. 0-minute data represent pretreatment erythrocytes. 0-minute data represent pretreatment erythrocytes. 0-minute data represent pretreated erythrocytes.

4.5.2.7. Alternations in hemolysis and oxidative stress biomarkers in normal and G6PDd erythrocytes due to 5, 6-OQPQ treatment.

The basal levels of SDMA (symmetric dimethylarginine) and dityrosine were elevated in G6PDd erythrocytes, and ADMA (asymmetric dimethylarginine) was depleted in G6PDd erythrocytes (Figure 4.21). SDMA and ADMA were elevated due to treatment. SMDA selectively accumulated in G6PDd erythrocytes and ADMA was accumulated in both erythrocytes due to treatment. There was nonspecific depletion of SDMA and ADMA in both erythrocytes due to incubation. Dityrosine and dopaquinone were depleted in both erythrocytes due to treatment. There was the nonspecific elevation of dopaquinone in both erythrocytes due to incubation (Figure 4.21). These results showed that treatment affects hemolysis, oxidative stress and aging biomarker in both erythrocytes.

4.5.2.8. Alternations in MTH, MTC, leucine, and phosphocreatine in normal and G6PDd erythrocytes due to 5, 6-OQPQ treatment.

The basal levels of MDC (5-methyldeoxycitidine) and phosphocreatine were elevated in G6PDd erythrocytes, and leucine was depleted in G6PDd erythrocytes (Figure 4.22). Treatment elevated levels of MDC and phosphocreatine and leucine in both erythrocytes. Levels of phosphocreatine were selectively increased in G6PDd erythrocytes. Treatment decreased MDC levels in both erythrocytes. There was a non-specific decrease in leucine in both erythrocytes due to incubation (Figure 4.22).

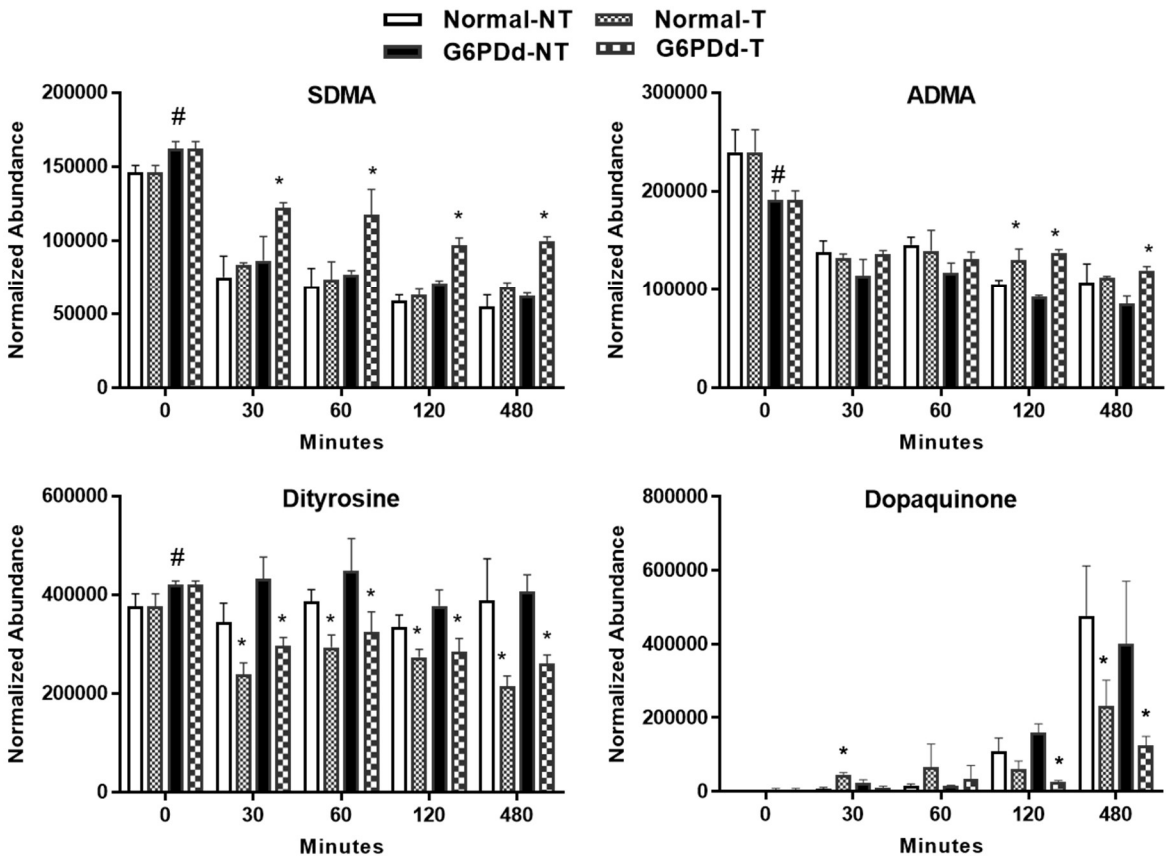

Figure 4.21. Distinct effect of 5, 6-OQPQ (25 μM) on **SDMA, ADMA, dityrosine and dopaquinone** levels in normal and G6PDd erythrocytes at 0, 30, 60, 120, and 480 minutes, and analyzed for their metabolite profiles. The levels of metabolites are expressed (Y-axis) as normalized abundance. Each bar represents mean ± SD of at least three observations. Statistical differences were determined by ANOVA; P values <0.05 were considered as statistically significant. $^{*}p < 0.05$ compared with no treatment with corresponding erythrocytes at corresponding time. $^{\#}p < 0.05$ compared with pretreatment in normal erythrocyte at 0-minute. 0-minute data represent pretreatment erythrocytes. 0-minute data represent pretreatment erythrocytes.0-minute data represent pretreated erythrocytes. SMDA: Symmetric dimethylarginine. ADMA: Asymmetric dimethylarginine.

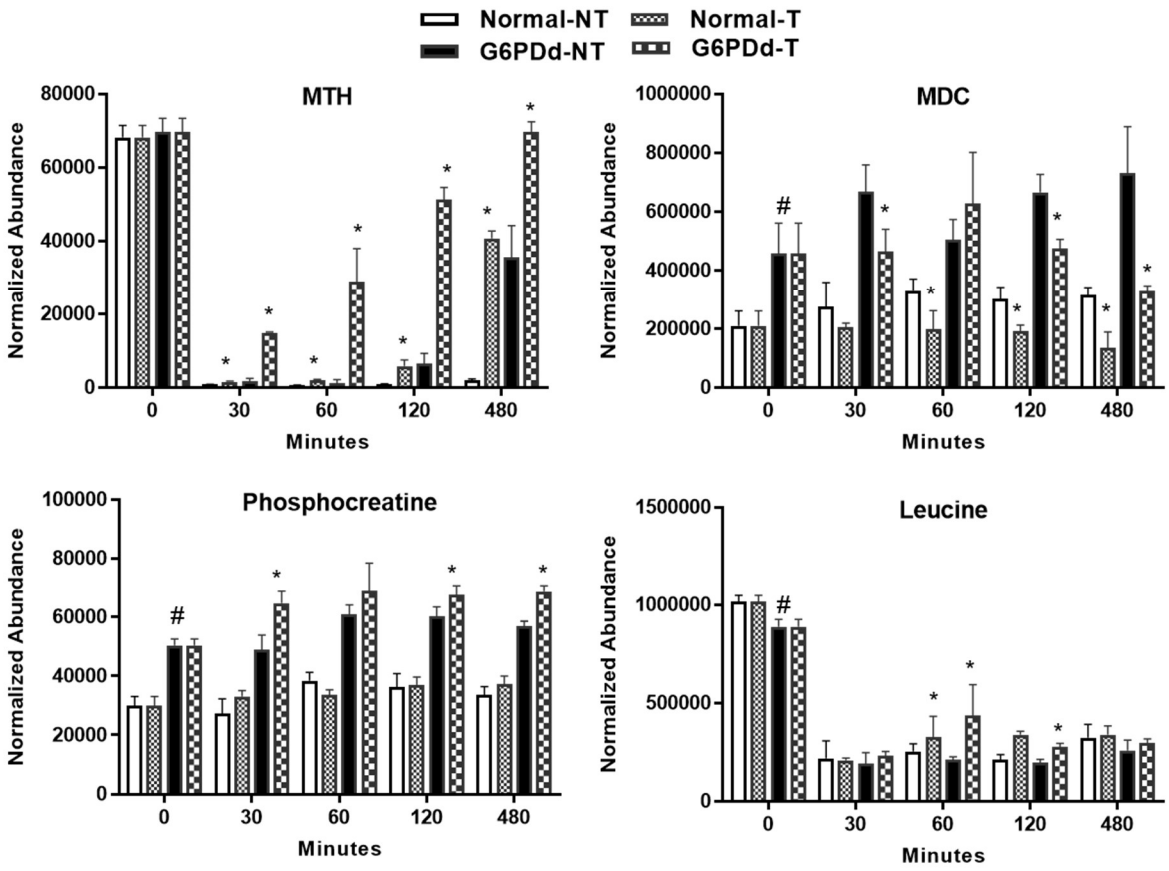

Figure 4.22: Distinct effect of 5, 6-OQPQ (25μM) on the **MTH, MDC, leucine and phosphocreatine** levels in normal and G6PDd erythrocytes at 0, 30, 60, 120, and 480 minutes, and analyzed for their metabolite profiles. The levels of metabolites are expressed (Y-axis) as normalized abundance. Each bar represents mean ± SD of at least three observations. Statistical differences were determined by ANOVA; P values <0.05 were considered as statistically significant$^{*}p < 0.05$ compared with no treatment with corresponding erythrocytes at corresponding time. $^{\#}p < 0.05$ compared with pretreatment in normal erythrocyte at 0-minute. 0-minute data represent pretreatment erythrocytes. 0-minute data represent pretreatment erythrocytes.0-minute data represent pretreated erythrocytes. MTH: 6-methyltetrahydropterin. MDC: 5-methyldeoxycytidine.

4.5.3. Common metabolites in normal-G6PDd experiment and drug-time-response experiment.

There were 66 metabolites which were commonly identified in both experiments. The detail of these metabolites with their normalized abundance was described in Table 4.7 and Table 4.8.

Table 4.7: Lists of common metabolites annotated and their normalized abundance (Mean and SD) in normal erythrocytes in both normal-G6PDd experiment and drug-time-response experiment.

	Normal-G6PDd experiment		Drug-time-response experiment	
	Normal erythrocytes		Normal erythrocytes	
Description	Mean	SD	Mean	SD
2,5-Dichloro-4-oxohex -2-enedioate	6298179.24	1656459.59	7245169.17	182649.31
3-Methylhistidine	1753733.62	1384796.28	3948042.73	180334.33
4-Hydroxy-2-butenoic acid gamma-lactone	25642.31	9832.45	8218.88	325.28
5'-Methylthioadenosine	329056.15	113843.19	496687.04	19056.17
Adenine	19622.43	3235.87	97089.07	5978.72
Adenosine monophosphate	323028.04	201345.04	265135.48	7599.72
ADP	508146.89	185127.15	6251585.95	441201.68
Betaine	9854665.06	1885975.93	13630389.61	144364.07
Biotin amide	23259.56	11741.25	46354.69	3143.65
Choline	7651067.75	4674310.49	7209640.73	82413.45
Citrulline	1100310.44	257547.15	1838015.72	135396.53
CMP-2-aminoethylphosphonate	85183.85	28629.68	228284.68	29300.48
Creatine	28659415.84	1621178.31	3794777.46	96843.13
Creatinine	4750868.75	654875.19	5927286.76	320104.43
Ergothioneine	19394.73	16446.25	496498.76	238150.14
Farnesyl pyrophosphate	448115.63	222499.17	221300.86	34919.04
Gamma-Aminobutyric acid	43100.63	5042.56	97243.91	1851.78
Glutathione	125006.72	149046.12	1300921.29	1437512.01
Glycerophosphocholine	156883.04	95245.52	1546687.16	281379.69
Hydroxybutyrylcarnitine	293870.74	153593.81	85144.68	4843.33
Hypoxanthine	1239929.47	567572.48	32164.54	441.71
Inosinic acid	206291.19	64272.42	3077085.13	189833.95
L-Acetylcarnitine	19382135.22	7017580.19	983742.98	100682.97
L-Arginine	533239.62	220127.71	8726580.48	203735.26
L-Asparagine	312131.26	62672.68	709759.86	138856.18
L-Aspartic acid	161911.30	98611.55	529903.46	26427.06
L-Carnitine	8695931.51	3725851.54	1194144.18	37337.59
L-Glutamic acid	659687.48	308042.27	13866888.96	591662.79
L-Glutamine	1960260.06	464758.90	2290404.87	75011.39
L-Histidine	238275.12	54713.43	1316890.00	92776.33

L-Histidinol	1397574.40	220727.26	10738833.53	271379.36
L-Isoleucine	371135.47	148837.84	30319.23	1421.20
L-Leucine	421042.54	161682.29	835375.28	26393.87
L-Methionine	56142.99	21370.53	1015899.57	31817.46
L-Norleucine	120161.11	76380.11	351802.04	43471.56
L-Palmitoylcarnitine	1749789.01	793668.47	209141.10	64820.65
L-Phenylalanine	386616.80	105705.49	680230.67	45358.84
L-Proline	2034823.75	278503.60	3871337.20	96310.16
L-Serine	85725.77	9614.63	59153.45	3300.20
L-Threonine	233988.78	28823.87	259938.71	8920.35
L-Tryptophan	91950.97	28817.73	312095.48	24446.90
L-Tyrosine	257470.70	102429.84	924326.87	100488.95
LysoPC(16:0)	9486034.38	2830304.04	1302394.23	111652.79
LysoPC(18:0)	6216279.52	1978632.16	712508.48	214629.73
Methylmalonylcarnitine	1192570.70	443762.38	3194952.66	335370.61
N6,N6,N6-Trimethyl-L-lysine	2269710.97	439161.40	1956589.06	182540.22
NAD	1651753.14	273296.52	3571121.70	553902.16
N-Decanoylglycine	36969.16	8185.04	259693.71	21806.22
Niacinamide	708690.92	237915.26	569419.44	59813.45
N-Undecanoylglycine	354588.37	98940.10	1357004.19	213753.25
Oleoylcarnitine	3311751.41	1366332.93	238627.04	162102.44
Ophthalmic acid	86278.81	16946.20	114041.52	9521.48
Ornithine	488951.99	61149.36	6306402.07	166234.33
Oxidized glutathione	16500582.81	4649985.88	74975807.89	10812731.40
Pantothenic acid	84864.84	81933.74	542893.97	24883.64
Phosphocreatine	24083.34	12301.67	29944.26	3073.47
Phosphoric acid	6554.04	3652.96	25247.93	958.86
Pipecolic acid	358495.03	615310.98	192634.83	24032.17
Proline betaine	7684600.13	6487641.04	2065.59	56.99
Propionylcarnitine	3791068.47	1988628.24	5201753.34	141751.18
Pyroglutamic acid	569409.76	132703.94	402319.93	23365.39
Pyrrolidine	51841.72	7925.69	125610.72	6634.00
Stearoylcarnitine	1024579.87	435731.70	192367.58	36543.47
Taurine	231738.77	142558.67	74403.01	1873.79
Trigonelline	180387.49	83212.35	411590.89	16623.84
Uridine 5'-diphosphate	69506.67	17467.74	81930.23	9207.47

Table 4.8: Lists of common metabolites annotated and their normalized abundance (Mean and SD) in G6PDd erythrocytes in both normal -G6PDd experiment and drug-time-response experiment.

	Normal-G6PDd experiment		Drug-time-response experiment	
	G6PDd erythrocytes		G6PDd erythrocytes	
Description	Mean	SD	Mean	SD
2,5-Dichloro-4-oxohex-2-enedioate	6012686.70	1031473.33	7371153.31	193531.88
3-Methylhistidine	2188241.97	1156990.24	4873143.67	242237.33
4-Hydroxy-2-butenoic acid gamma-lactone	29555.50	4709.64	12488.81	361.42
5'-Methylthioadenosine	508191.62	166106.38	493566.99	43573.48
Adenine	18154.64	2560.71	98010.74	2608.14
Adenosine monophosphate	123400.08	122174.01	868679.74	67304.35
ADP	344986.02	212749.52	8096303.80	1237492.03
Betaine	10641366.83	254947.72	14282662.76	462268.05
Biotin amide	54683.89	21769.14	266174.56	23594.82
Choline	3766634.26	2162376.67	3270526.40	71793.85
Citrulline	1173147.68	231361.76	1554602.18	48458.02
CMP-2-aminoethylphosphonate	116891.47	21765.10	234943.82	22384.23
Creatine	26272575.53	1443005.23	5028598.27	130976.01
Creatinine	4485204.43	288770.24	7785782.44	391986.21
Ergothioneine	11405.99	4879.09	1305595.50	245722.26
Farnesyl pyrophosphate	435064.96	68081.68	911107.34	88176.40
Gamma-Aminobutyric acid	44774.88	6959.44	160266.65	6295.54
Glutathione	18358.39	7455.32	306722.77	134150.23
Glycerophosphocholine	115337.55	76257.86	816714.67	73415.76
Hydroxybutyrylcarnitine	703192.14	268473.47	452286.21	9720.61
Hypoxanthine	2257187.69	1328444.08	69256.37	3842.35
Inosinic acid	209186.94	130924.29	2942326.05	236036.33
L-Acetylcarnitine	21877132.97	3250112.04	516313.07	50453.82
L-Arginine	706584.27	418116.83	12832427.97	453395.32
L-Asparagine	197779.25	70678.92	1465400.08	69583.77
L-Aspartic acid	279244.69	113722.11	331958.51	11017.02
L-Carnitine	11261154.29	887933.15	271900.82	7077.86
L-Glutamic acid	256424.32	227227.88	13555246.99	290003.92
L-Glutamine	1838946.30	396593.71	839911.76	69843.26
L-Histidine	195084.76	53015.50	1022795.23	47449.71
L-Histidinol	1112566.12	162627.25	10164007.88	394111.02

L-Isoleucine	517775.87	180949.63	30580.17	1842.49
L-Leucine	652760.21	200667.91	783227.80	39474.25
L-Methionine	44020.19	7544.24	887918.24	37725.01
L-Norleucine	220663.94	180247.31	369264.15	52420.63
L-Palmitoylcarnitine	2029483.36	507592.36	136064.23	76632.17
L-Phenylalanine	444826.15	120467.14	570330.99	22367.79
L-Proline	2018391.64	148321.90	3347829.78	43872.48
L-Serine	67302.72	25354.05	45310.99	801.17
L-Threonine	216999.93	75452.05	220117.10	13871.15
L-Tryptophan	90833.98	19872.68	253396.46	9696.50
L-Tyrosine	210335.12	23318.11	925047.09	41715.07
LysoPC(16:0)	6033925.34	2424153.21	497628.24	150042.67
LysoPC(18:0)	4176371.31	1772720.69	220413.41	30508.68
Methylmalonylcarnitine	1421867.51	710599.56	2266440.88	105833.55
N6,N6,N6-Trimethyl-L-lysine	2402360.68	597307.22	2686557.80	127204.35
NAD	2112321.73	356485.66	5644409.44	269867.18
N-Decanoylglycine	21110.31	11043.21	181709.41	60227.82
Niacinamide	1009133.24	113092.47	1084718.71	71034.64
N-Undecanoylglycine	205205.33	98666.06	1073334.59	358864.03
Oleoylcarnitine	4126495.84	1066355.15	311001.40	190306.57
Ophthalmic acid	36398.82	23198.93	94091.23	2085.54
Ornithine	413922.32	63885.86	6443207.49	130052.89
Oxidized glutathione	11613412.28	4595472.91	49992603.19	1949433.14
Pantothenic acid	111824.97	35910.25	787547.29	15169.15
Phosphocreatine	31595.71	12597.51	50346.09	2195.77
Phosphoric acid	7383.75	5920.08	28058.76	474.55
Pipecolic acid	69924.58	98177.03	131134.47	21772.37
Proline betaine	6355894.24	8003257.93	124321.43	2345.49
Propionylcarnitine	6302821.18	924522.51	4976433.48	110502.07
Pyroglutamic acid	532726.01	113901.62	332322.57	10233.05
Pyrrolidine	65963.69	11132.50	118775.30	5934.49
Stearoylcarnitine	1991111.83	541859.71	93155.39	38869.35
Taurine	137975.86	48447.48	73288.11	452.96
Trigonelline	495849.31	396151.55	608417.08	15475.09
Uridine 5'-diphosphate	67501.26	16004.26	143336.84	9870.28

4.6. DISCUSSION

G6PD deficiency is an X-linked hereditary disorder caused due to a mutation in G6PD gene (Cappellini and Fiorelli 2008; Youngster et al. 2010). G6PD enzyme participates in the pentose phosphate pathway, which is the sole source for production of NADPH, glutathione recycling in erythrocytes, and is essential for the function of catalase (Nkhoma et al. 2009; Mason et al. 2007; Cappellini and Fiorelli 2008; Judith Recht 2014). NADPH, GSH, and catalase constitute primary antioxidant defense system in human erythrocytes (Judith Recht 2014). The G6PDd erythrocytes have limited capability to regenerate NADPH and recycle GSH and thus, have lower levels of GSH (Judith Recht 2014; Mason et al. 2007). The results of the current study are consistent with the earlier reports and thus support the known data (Nkhoma et al. 2009; Mason et al. 2007; Cappellini and Fiorelli 2008; Judith Recht 2014).

In this study, the basal normal and G6PDd metabolome profiles were compared to identify the major pathways which were modified in G6PDd erythrocytes. The comparison between metabolites in normal and G6PDd revealed that GSH levels were significantly lower in G6PDd erythrocytes. The GSH-Methionine-Glutamate pathway was interconnected and together participate in GSH synthesis (Tang et al. 2015). In our study, the levels of GSH, tripeptide analog of ophthalmic acid and glutamic acid, the precursor of GSH were significantly lower in G6PDd erythrocyte. Furthermore, 5'-methylthioadenosine which plays a crucial role in methionine and purine salvage pathways (Avila et al. 2004) were higher. Moreover, the metabolites participate in glycerophospholipid pathway like choline, neurine and LysoPC (16:0) were lower (Gibellini and Smith 2010; Tweedie et al. 2006; Saito et al. 2014). Carnitine and derivatives of carnitine participate were higher and in lipid oxidation (Darghouth et al. 2011), and the metabolite of fatty acid namely, N-decanoylglycine and N-undecanoylglycine were significantly lower (Cruickshank-

Quinn et al. 2014). These findings suggest disruption of lipid/fatty acid oxidation and glycerophospholipid pathway. The glycerophospholipids phosphatidylcholine play major roles in the structure and function of those eukaryotic membranes (Gibellini and Smith 2010), and the disruption of lipid oxidation and glycerophospholipid pathway might indicate the membrane fragility seen in G6PDd erythrocytes (Johnson et al. 1994).

Another focus of the current study was to examine the metabolomes of both normal and G6PDd erythrocytes treated with a hemotoxic metabolite of PQ, 5,6-OQPQ for 30, 60, 120 and 480 minutes. The results showed that the GSH-methionine-glutamic acid pathway was highly affected due to treatment in both erythrocytes. Oxidized glutathione and precursors of GSH namely, glutamic acid (Ellinger et al. 2011), 5-methylthioadenosine, and SAM were depleted at later time points (120 and 480 minutes) of treatment in both erythrocytes. Similarly, adenine the precursor of ATP was also depleted at later time points in both erythrocytes. However, the level of serine, BCGA and lysine were considerably increased due to treatment in both erythrocytes at 120 and 480 minutes. Serine plays an important role in providing one-carbon units to the tetrahydrofolate (THF) cycle and supports ATP and NADPH generation. ATP generates by serine is used by methionine to form S-adenosyl methionine (SAM) (Maddocks et al. 2016). In addition, serine has antioxidant properties and it protects the cells from H_2O_2-induced oxidative stress (Miyazaki et al. 1992). BCGA is a derivative of glutamic acid and acts as metal ion chelator. BCGA also has antioxidant activity like the enzyme super oxide dismutase (Hamada-Kanazawa et al. 2010; Narahara et al. 2010). Like serine and BCGA, lysine also has antioxidant activities (O'Doherty et al. 2014). The change in these metabolites at 120 and 480 minutes indicates the compensatory mechanism of erythrocyte and suggest that it is almost similar in both erythrocytes.

The level of ophthalmic acid, a tripeptide analog of GSH was increased due to treatment

in both erythrocytes at early and later time points. Ophthalmic acid was formed from 2-aminobutyrate via consecutive reactions with gamma-glutamylcysteine and glutathione synthetase like glutathione formation. GSH contain a thiol group from cysteine in GSH and in ophthalmic acid the thiol group is replaced by a methyl group. The enzyme gamma-glutamylcysteine synthetase, is feedback-inhibited by GSH, and is considered as a rate-limiting step in GSH formation (Cuozzo and Kaiser 1999). GSH depletion caused by oxidative compounds like acetaminophen activates gamma-glutamylcysteine synthetase, which in turn induced ophthalmic acid formation. Though, unlike GSH, ophthalmic acid is not metabolized further and thus is accumulated (Soga et al. 2006).

The levels of citicoline, SDMA and phosphocreatine were higher selectively in G6PDd erythrocytes due to 5,6-OQPQ treatment. Phosphocreatine decreases oxidative stress (Cunha et al. 2014) and furthermore, it interacts with membrane lipids and causes modifications in membrane structure in order to protect cellular membranes against different insults (Tokarska-Schlattner et al. 2012). Citicoline is a biomarker of chronic hemolysis (Paglia et al. 1983). SDMA is pro-inflammatory and pro-oxidant in nature (Tain and Hsu 2017) and is related with oxidative stress induction (Schepers et al. 2011). Higher SDMA levels have been reported in numerous clinical conditions like coronary artery disease, diabetes mellitus, hypertension, hyperuricemia, preeclampsia, polycystic ovary syndrome, and stroke (Tain and Hsu 2017). ADMA levels were also elevated but in both erythrocytes and at later time points. Elevated ADMA levels are associated with genetic disease-related with hemolysis like sickle cell disease, thalassemia and other complications related with hemolysis like leg ulcers, cholelithiasis, and priapism (Landburg et al. 2010).

Treatment of 5,6-OQPQ elevated levels of proline and ornithine. Proline defends the cells

against hydrogen peroxide-induced stress and accumulation of proline is a compensatory response of hydrogen peroxide-induced stress. Moreover, proline takes care the intracellular GSH pool and the GSH/GSSG ratio of the cell during oxidative stress (Krishnan et al. 2008). Ornithine is a biomarker of hemolysis. During hemolysis, erythrocytes release red-cell arginase, an enzyme cause conversion of arginine to ornithine (Morris et al. 2005).

Thus, the current study suggests that histidine, GSH-Methionine-Glutamate, purine, glycerophospholipid and fatty acid oxidation pathways were greatly affected in G6PDd erythrocytes as compare to normal erythrocyte. Moreover, treatment of 5,6-OQPQ, a metabolite of PQ significantly modified GSH-methionine-glutamic acid, histidine and glycerophospholipid pathway. Furthermore, the metabolites changed at later time points suggest compensatory mechanism. The level of antioxidant like serine, lysine and BCGA were elevated in both erythrocytes due to 5,6-OQPQ treatment at later time points. Hemolysis related markers like citicoline and SDMA were also elevated selectively in G6PDd erythrocytes due to 5,6-OQPQ treatment which can be used as new hemotoxic marker related with PQ-induced.

CHAPTER 5

FUTURE STUDIES

8-aminoquinolines (8-AQs) represent an important drug class with unique antiprotozoal activities. 8-AQs are used in the treatment of leishmaniasis, pneumocystis infections, trypanosomiasis and malaria (Tekwani and Walker 2006). Primaquine (PQ) is a unique 8-AQ antimalarial drug. It is the only FDA-approved drug, which is active against the hard-to-kill liver stage of *Plasmodium vivax* and *P. ovale* and used to prevent malaria relapse (Ashley et al. 2014; Tekwani and Walker 2006). Malaria relapses significantly contribute to infection and morbidity in *P. vivax* and *P. ovale* malaria (Leslie et al. 2016). Further, PQ is the only drug having activity against mature stage V gametocytes of *P. falciparum* and thus recommended by the World Health Organization, to prevent malaria transmission (Tekwani and Walker 2006; Ashley et al. 2014).

The current in vitro studies showed that the metabolites of PQ namely, 5-HPQ, 5,6-OQPQ, and MHQ are hemotoxic and induce a concentration-dependent hemotoxicity response by generating methemoglobinemia and producing oxidative stress in normal and G6PDd human erythrocytes. The PQ metabolite 5,6-OQPQ also depletes GSH and induces the exposure of phosphatidylserine (a marker for suicidal erythrocyte death-eryptosis) on the outer membrane of erythrocytes, selectively in G6PDd human erythrocytes. Externalization of PS on the outer membrane is the final commitment of erythrocyte to be phagocytized by macrophages. The eryptotic pathway triggers the removal of damaged erythrocytes from the circulation in the G6PDd

population on exposure to PQ. Further, other biochemical and cellular markers associated with eryptosis namely, intraerythrocytic calcium levels and activation of calpain can also be evaluated to gain a better insight into the pathways and events that lead to hemolysis caused by PQ.

The role of NQO2, a cytosolic flavoprotein enzyme involved in metabolic detoxification/activation of quinones, in PQ-induced hemolytic anemia was also investigated. To acheieve this, the inhibitors of NQO2 namely, melatonin (Mel), resveratrol (Res) and quercetin (Quer) were used as the probes. The interactions between human NQO2 (PBD: 4FGJ) and PQ metabolites (5-HPQ, 5,6-OQPQ, and MHQ) were also investigated using molecular docking approach. The results of the current study suggest that co-treatment of erythrocytes with NQO2 inhibitors and PQ metabolites potentiated the hemotoxicity compared to PQ metabolites alone. These results suggest potential role of NQO2 in detoxification of reactive metabolites of PQ and protection of erythrocytes from PQ-induced hemolysis. The computational docking results suggest that Mel, menadione, PQ and PQ metabolites bind at the same binding pocket of the NQO2 with a slightly different orientations; however, the glide gscores results suggest that PQ and its metabolites may have a better affinity towards NQO2 as compared to Mel and menadione. Additional experiments may be done to understand the functional interactions (substrate or inhibitor) of PQ metabolites with human NQO2.

Finally, the changes in metabolite levels and biochemical pathways in normal and G6PDd erythrocytes due to 5,6-OQPQ treatments were examined. A battery of metabolites (citicoline, SDMA and phosphocreatine) are selectively changed in the G6PDd erythrocytes. These metabolites can be evaluated as the markers of PQ-induced hemolysis. Changes in some metabolites like serine, BCGA, lysine, glutamic acid suggest compensatory mechanism of PQ-

induced toxicity in normal and G6PDd erythrocytes. The knowledge regarding compensatory mechanisms can be used to formulate the strategy for attenuation of PQ-induced toxicity, without compromising with the therapeutic activity

The study provides a better insight into the pathways and biomarkers of toxicity involved with the PQ-treatment. Further, the knowledge regarding the interaction of PQ metabolites with NQO2 enzyme is clearer now and suggests the potential target related to the PQ-toxicity. In summary, the data obtained in this study provide the knowledge to understand the mechanism, pathway and target associated with PQ toxicity and would help to improved therapeutic value of PQ. Also, the knowledge generated through proposed studies will allow multiple avenues of development of 8-AQ analogs with improved safety and therapeutic profiles for malaria control and elimination campaigns.

REFERENCES

Aguilar-Dorado IC, Hernandez G, Quintanar-Escorza MA, Maldonado-Vega M, Rosas-Flores M, Calderon-Salinas JV (2014) Eryptosis in lead-exposed workers. Toxicol Appl Pharmacol 281 (2):195-202. doi:10.1016/j.taap.2014.10.003

Albuquerque RV, Malcher NS, Amado LL, Coleman MD, Dos Santos DC, Borges RS, Valente SA, Valente VC, Monteiro MC (2015) In Vitro Protective Effect and Antioxidant Mechanism of Resveratrol Induced by Dapsone Hydroxylamine in Human Cells. PLoS One 10 (8):e0134768. doi:10.1371/journal.pone.0134768

Ali NA, al-Naama LM, Khalid LO (1999) Haemolytic potential of three chemotherapeutic agents and aspirin in glucose-6-phosphate dehydrogenase deficiency. East Mediterr Health J 5 (3):457-464

Aracena P, Lazo-Hernandez C, Molina-Berrios A, Sepulveda DR, Reinoso C, Larrain JI, Navarro J, Letelier ME (2014) Microsomal oxidative stress induced by NADPH is inhibited by nitrofurantoin redox biotranformation. Free Radic Res 48 (2):129-136. doi:10.3109/10715762.2013.836695

Arruda MM, Mecabo G, Rodrigues CA, Matsuda SS, Rabelo IB, Figueiredo MS (2013) Antioxidant vitamins C and E supplementation increases markers of haemolysis in sickle cell anaemia patients: a randomized, double-blind, placebo-controlled trial. Br J Haematol 160 (5):688-700. doi:10.1111/bjh.12185

Ashley EA, Recht J, White NJ (2014) Primaquine: the risks and the benefits. Malar J 13:418. doi:10.1186/1475-2875-13-418

Aufrere MB, Hoener BA, Vore M (1978) Reductive metabolism of nitrofurantoin in the rat. Drug Metab Dispos 6 (4):403-411

Avila MA, Garcia-Trevijano ER, Lu SC, Corrales FJ, Mato JM (2004) Methylthioadenosine. Int J

Biochem Cell Biol 36 (11):2125-2130. doi:10.1016/j.biocel.2003.11.016

Barclay JA, Ziemba SE, Ibrahim RB (2011) Dapsone-induced methemoglobinemia: a primer for clinicians. Ann Pharmacother 45 (9):1103-1115. doi:10.1345/aph.1Q139

Barkan G, Goldsmith L (1946) Antibacterial action of an oxidation product of sulfanilamide. J Am Chem Soc 68:733

Biswas S, Bhattacharyya J, Dutta AG (2005) Oxidant induced injury of erythrocyte-role of green tea leaf and ascorbic acid. Mol Cell Biochem 276 (1-2):205-210. doi:10.1007/s11010-005-4062-4

Blum A, Ghaben W, Slonimsky G, Simsolo C (2011) Metformin-induced hemolytic anemia. Isr Med Assoc J 13 (7):444-445

Bolchoz LJ, Budinsky RA, McMillan DC, Jollow DJ (2001) Primaquine-induced hemolytic anemia: formation and hemotoxicity of the arylhydroxylamine metabolite 6-methoxy-8-hydroxylaminoquinoline. J Pharmacol Exp Ther 297 (2):509-515

Bolchoz LJ, Gelasco AK, Jollow DJ, McMillan DC (2002a) Primaquine-induced hemolytic anemia: formation of free radicals in rat erythrocytes exposed to 6-methoxy-8-hydroxylaminoquinoline. J Pharmacol Exp Ther 303 (3):1121-1129. doi:10.1124/jpet.102.041459

Bolchoz LJ, Morrow JD, Jollow DJ, McMillan DC (2002b) Primaquine-induced hemolytic anemia: effect of 6-methoxy-8-hydroxylaminoquinoline on rat erythrocyte sulfhydryl status, membrane lipids, cytoskeletal proteins, and morphology. J Pharmacol Exp Ther 303 (1):141-148. doi:10.1124/jpet.102.036921

Bolton JL, Trush MA, Penning TM, Dryhurst G, Monks TJ (2000) Role of quinones in toxicology. Chem Res Toxicol 13 (3):135-160

Boots AW, Kubben N, Haenen GR, Bast A (2003) Oxidized quercetin reacts with thiols rather than with ascorbate: implication for quercetin supplementation. Biochem Biophys Res Commun 308 (3):560-565

Boots AW, Li H, Schins RP, Duffin R, Heemskerk JW, Bast A, Haenen GR (2007) The quercetin paradox. Toxicol Appl Pharmacol 222 (1):89-96. doi:10.1016/j.taap.2007.04.004

Boutin JA, Chatelain-Egger F, Vella F, Delagrange P, Ferry G (2005) Quinone reductase 2 substrate specificity and inhibition pharmacology. Chem Biol Interact 151 (3):213-228. doi:10.1016/j.cbi.2005.01.002

Bowman ZS, Jollow DJ, McMillan DC (2005a) Primaquine-induced hemolytic anemia: role of splenic macrophages in the fate of 5-hydroxyprimaquine-treated rat erythrocytes. J Pharmacol Exp Ther 315 (3):980-986. doi:10.1124/jpet.105.090407

Bowman ZS, Morrow JD, Jollow DJ, McMillan DC (2005b) Primaquine-induced hemolytic anemia: role of membrane lipid peroxidation and cytoskeletal protein alterations in the hemotoxicity of 5-hydroxyprimaquine. J Pharmacol Exp Ther 314 (2):838-845. doi:10.1124/jpet.105.086488

Bowman ZS, Oatis JE, Jr., Whelan JL, Jollow DJ, McMillan DC (2004) Primaquine-induced hemolytic anemia: susceptibility of normal versus glutathione-depleted rat erythrocytes to 5-hydroxyprimaquine. J Pharmacol Exp Ther 309 (1):79-85. doi:10.1124/jpet.103.062984

Bucklin MH, Groth CM (2013) Mortality following rasburicase-induced methemoglobinemia. Ann Pharmacother 47 (10):1353-1358. doi:10.1177/1060028013501996

Buzard JA, Kopko F, Paul MF (1960) Inhibition of glutathione reductase by nitrofurantoin. The Journal of laboratory and clinical medicine 56:884-890

Cappellini MD, Fiorelli G (2008) Glucose-6-phosphate dehydrogenase deficiency. Lancet 371

(9606):64-74. doi:10.1016/s0140-6736(08)60073-2

Cha YS, Kim H, Kim J, Kim OH, Kim HI, Cha K, Lee KH, Hwang SO (2016) Incidence and patterns of hemolytic anemia in acute dapsone overdose. Am J Emerg Med 34 (3):366-369. doi:10.1016/j.ajem.2015.09.021

Chan MC, Wong HB (1975) Letter: Glucose-6-phosphate dehydrogenase deficiency and co-trimoxazole. Lancet 1 (7903):410

Chan TK (1972) G.-6-P.D. deficiency, typhoid, and co-trimoxazole. Lancet 2 (7789):1258

Chan TK, McFadzean JS (1974) Haemolytic effect of trimethoprim-sulphamethoxazole in G-6-PD deficiency. Trans R Soc Trop Med Hyg 68 (1):61-62

Chan TY (1997) Co-trimoxazole-induced severe haemolysis: the experience of a large general hospital in Hong Kong. Pharmacoepidemiol Drug Saf 6 (2):89-92. doi:10.1002/(sici)1099-1557(199703)6:2<89::aid-pds261>3.0.co;2-8

Cheah CY, Lew TE, Seymour JF, Burbury K (2013) Rasburicase causing severe oxidative hemolysis and methemoglobinemia in a patient with previously unrecognized glucose-6-phosphate dehydrogenase deficiency. Acta Haematol 130 (4):254-259. doi:10.1159/000351048

Chisholm-Burns MA, Patanwala AE, Spivey CA (2010) Aseptic meningitis, hemolytic anemia, hepatitis, and orthostatic hypotension in a patient treated with trimethoprim-sulfamethoxazole. Am J Health Syst Pharm 67 (2):123-127. doi:10.2146/ajhp080558

Choi EJ, Chee KM, Lee BH (2003) Anti- and prooxidant effects of chronic quercetin administration in rats. Eur J Pharmacol 482 (1-3):281-285

Claro LM, Leonart MS, Comar SR, do Nascimento AJ (2006) Effect of vitamins C and E on oxidative processes in human erythrocytes. Cell Biochem Funct 24 (6):531-535.

doi:10.1002/cbf.1255

Clayman CB, Arnold J, Hockwald RS, Yount EH, Jr., Edgcomb JH, Alving AS (1952) Toxicity of primaquine in Caucasians. J Am Med Assoc 149 (17):1563-1568

Colgan R, Williams M (2011) Diagnosis and treatment of acute uncomplicated cystitis. Am Fam Physician 84 (7):771-776

Cornwell JR, Bartek JK (1996) Phenazopyridine hydrochloride: information for patient teaching. Urol Nurs 16 (4):153-154

Cruickshank-Quinn CI, Mahaffey S, Justice MJ, Hughes G, Armstrong M, Bowler RP, Reisdorph R, Petrache I, Reisdorph N (2014) Transient and persistent metabolomic changes in plasma following chronic cigarette smoke exposure in a mouse model. PLoS One 9 (7):e101855. doi:10.1371/journal.pone.0101855

Cunha MP, Martin-de-Saavedra MD, Romero A, Egea J, Ludka FK, Tasca CI, Farina M, Rodrigues AL, Lopez MG (2014) Both creatine and its product phosphocreatine reduce oxidative stress and afford neuroprotection in an in vitro Parkinson's model. ASN Neuro 6 (6). doi:10.1177/1759091414554945

Cuozzo JW, Kaiser CA (1999) Competition between glutathione and protein thiols for disulphide-bond formation. Nat Cell Biol 1 (3):130-135. doi:10.1038/11047

Curry S (1982) Methemoglobinemia. Ann Emerg Med 11 (4):214-221

Darghouth D, Koehl B, Madalinski G, Heilier JF, Bovee P, Xu Y, Olivier MF, Bartolucci P, Benkerrou M, Pissard S, Colin Y, Galacteros F, Bosman G, Junot C, Romeo PH (2011) Pathophysiology of sickle cell disease is mirrored by the red blood cell metabolome. Blood 117 (6):e57-66. doi:10.1182/blood-2010-07-299636

Deps P, Guerra P, Nasser S, Simon M (2012) Hemolytic anemia in patients receiving daily dapsone

for the treatment of leprosy. Lepr Rev 83 (3):305-307

Dershwitz M, Ts'ao CH, Novak RF (1985) Metabolic and morphologic effects of the antimicrobial agent nitrofurantoin on human erythrocytes in vitro. Biochem Pharmacol 34 (11):1963-1970

Dhaliwal G, Cornett PA, Tierney LM, Jr. (2004) Hemolytic anemia. Am Fam Physician 69 (11):2599-2606

Elinoff JM, Salit RB, Ackerman HC (2011) The tumor lysis syndrome. N Engl J Med 365 (6):571-572; author reply 573-574. doi:10.1056/NEJMc1106641#SA1

Ellinger JJ, Lewis IA, Markley JL (2011) Role of aminotransferases in glutamate metabolism of human erythrocytes. J Biomol NMR 49 (3-4):221-229. doi:10.1007/s10858-011-9481-9

Farris P, Krutmann J, Li YH, McDaniel D, Krol Y (2013) Resveratrol: a unique antioxidant offering a multi-mechanistic approach for treating aging skin. J Drugs Dermatol 12 (12):1389-1394

Farthing DE, Farthing CA, Xi L (2015) Inosine and hypoxanthine as novel biomarkers for cardiac ischemia: from bench to point-of-care. Exp Biol Med (Maywood) 240 (6):821-831. doi:10.1177/1535370215584931

Fasinu PS, Tekwani BL, Nanayakkara NP, Avula B, Herath HM, Wang YH, Adelli VR, Elsohly MA, Khan SI, Khan IA, Pybus BS, Marcsisin SR, Reichard GA, McChesney JD, Walker LA (2014) Enantioselective metabolism of primaquine by human CYP2D6. Malar J 13:507. doi:10.1186/1475-2875-13-507

Fernandez E, Cardenas AM (1990) The mechanism of photohaemolysis by photoproducts of nalidixic acid. J Photochem Photobiol B 4 (3):329-333

Fernandez E, Cardenas AM, Martinez G (1987) Phototoxicity from nalidixic acid: oxygen

dependent photohemolysis. Farmaco Sci 42 (9):681-690

Ferry G, Hecht S, Berger S, Moulharat N, Coge F, Guillaumet G, Leclerc V, Yous S, Delagrange P, Boutin JA (2010) Old and new inhibitors of quinone reductase 2. Chem Biol Interact 186 (2):103-109. doi:10.1016/j.cbi.2010.04.006

Fibach E, Rachmilewitz E (2008) The role of oxidative stress in hemolytic anemia. Curr Mol Med 8 (7):609-619

Foster CE, Bianchet MA, Talalay P, Faig M, Amzel LM (2000) Structures of mammalian cytosolic quinone reductases. Free Radic Biol Med 29 (3-4):241-245

Friesner RA, Murphy RB, Repasky MP, Frye LL, Greenwood JR, Halgren TA, Sanschagrin PC, Mainz DT (2006) Extra precision glide: docking and scoring incorporating a model of hydrophobic enclosure for protein-ligand complexes. J Med Chem 49 (21):6177-6196. doi:10.1021/jm051256o

Gait JE (1990) Hemolytic reactions to nitrofurantoin in patients with glucose-6-phosphate dehydrogenase deficiency: theory and practice. DICP 24 (12):1210-1213

Galati G, Sabzevari O, Wilson JX, O'Brien PJ (2002) Prooxidant activity and cellular effects of the phenoxyl radicals of dietary flavonoids and other polyphenolics. Toxicology 177 (1):91-104

Galun E, Oren R, Glikson M, Friedlander M, Heyman A (1987) Phenazopyridine-induced hemolytic anemia in G-6-PD deficiency. Drug Intell Clin Pharm 21 (11):921-922

Ganesan S, Chaurasiya ND, Sahu R, Walker LA, Tekwani BL (2012) Understanding the mechanisms for metabolism-linked hemolytic toxicity of primaquine against glucose 6-phosphate dehydrogenase deficient human erythrocytes: evaluation of eryptotic pathway. Toxicology 294 (1):54-60. doi:10.1016/j.tox.2012.01.015

Ganesan S, Sahu R, Walker LA, Tekwani BL (2010) Cytochrome P450-dependent toxicity of dapsone in human erythrocytes. J Appl Toxicol 30 (3):271-275. doi:10.1002/jat.1493

Ganesan S, Tekwani BL, Sahu R, Tripathi LM, Walker LA (2009) Cytochrome P(450)-dependent toxic effects of primaquine on human erythrocytes. Toxicol Appl Pharmacol 241 (1):14-22. doi:10.1016/j.taap.2009.07.012

Garg A, Prasad B, Takwani H, Jain M, Jain R, Singh S (2011) Evidence of the formation of direct covalent adducts of primaquine, 2-tert-butylprimaquine (NP-96) and monohydroxy metabolite of NP-96 with glutathione and N-acetylcysteine. J Chromatogr B Analyt Technol Biomed Life Sci 879 (1):1-7. doi:10.1016/j.jchromb.2010.10.029

Garratty G (2012) Immune hemolytic anemia caused by drugs. Expert Opin Drug Saf 11 (4):635-642. doi:10.1517/14740338.2012.678832

Gibellini F, Smith TK (2010) The Kennedy pathway--De novo synthesis of phosphatidylethanolamine and phosphatidylcholine. IUBMB Life 62 (6):414-428. doi:10.1002/iub.337

Gordon-Smith EC (1980) Drug-induced oxidative haemolysis. Clin Haematol 9 (3):557-586

Goth L (2008) [Rasburicase therapy may cause hydrogen peroxide shock]. Orv Hetil 149 (34):1587-1590. doi:10.1556/oh.2008.28422

Graves PR, Kwiek JJ, Fadden P, Ray R, Hardeman K, Coley AM, Foley M, Haystead TA (2002) Discovery of novel targets of quinoline drugs in the human purine binding proteome. Mol Pharmacol 62 (6):1364-1372

Grinter SZ, Zou X (2014) Challenges, applications, and recent advances of protein-ligand docking in structure-based drug design. Molecules 19 (7):10150-10176. doi:10.3390/molecules190710150

Grossman S, Budinsky R, Jollow D (1995) Dapsone-induced hemolytic anemia: role of glucose-6-phosphate dehydrogenase in the hemolytic response of rat erythrocytes to N-hydroxydapsone. J Pharmacol Exp Ther 273 (2):870-877

Grossman SJ, Jollow DJ (1988) Role of dapsone hydroxylamine in dapsone-induced hemolytic anemia. J Pharmacol Exp Ther 244 (1):118-125

Grossman SJ, Simson J, Jollow DJ (1992) Dapsone-induced hemolytic anemia: effect of N-hydroxy dapsone on the sulfhydryl status and membrane proteins of rat erythrocytes. Toxicol Appl Pharmacol 117 (2):208-217

Gupta K, Hooton TM, Naber KG, Wullt B, Colgan R, Miller LG, Moran GJ, Nicolle LE, Raz R, Schaeffer AJ, Soper DE (2011) International clinical practice guidelines for the treatment of acute uncomplicated cystitis and pyelonephritis in women: A 2010 update by the Infectious Diseases Society of America and the European Society for Microbiology and Infectious Diseases. Clin Infect Dis 52 (5):e103-120. doi:10.1093/cid/ciq257

Halliwell B, Cheah IK, Drum CL (2016) Ergothioneine, an adaptive antioxidant for the protection of injured tissues? A hypothesis. Biochem Biophys Res Commun 470 (2):245-250. doi:10.1016/j.bbrc.2015.12.124

Hamada-Kanazawa M, Kouda M, Odani A, Matsuyama K, Kanazawa K, Hasegawa T, Narahara M, Miyake M (2010) beta-Citryl-L-glutamate is an endogenous iron chelator that occurs naturally in the developing brain. Biol Pharm Bull 33 (5):729-737

Heeres PA, Zondag HA (1961) [Hemolytic anemia caused by sulfanilamide as a result of glucose-6-phosphate-dehydrogenase deficiency: an x-chromosomal hereditary disease]. Folia Med Neerl 4:121-131

Hockwald RS, Arnold J, Clayman CB, Alving AS (1952) Toxicity of primaquine in Negroes. J

Am Med Assoc 149 (17):1568-1570

Hoener B, Patterson SE (1981) Nitrofurantoin disposition. Clin Pharmacol Ther 29 (6):808-816

Hong YL, Pan HZ, Scott MD, Meshnick SR (1992) Activated oxygen generation by a primaquine metabolite: inhibition by antioxidants derived from Chinese herbal remedies. Free Radic Biol Med 12 (3):213-218

Huang SY, Zou X (2010) Advances and challenges in protein-ligand docking. Int J Mol Sci 11 (8):3016-3034. doi:10.3390/ijms11083016

Huang YC, Chang TK, Fu YC, Jan SL (2014) C for colored urine: acute hemolysis induced by high-dose ascorbic acid. Clin Toxicol (Phila) 52 (9):984. doi:10.3109/15563650.2014.954124

Ibrahim IH, Sallam SM, Omar H, Rizk M (2006) Oxidative hemolysis of erythrocytes induced by various vitamins. Int J Biomed Sci 2 (3):295-298

Ibrahim U, Saqib A, Mohammad F, Atallah JP, Odaimi M (2017) Rasburicase-induced methemoglobinemia: The eyes do not see what the mind does not know. J Oncol Pharm Pract:1078155217701295. doi:10.1177/1078155217701295

Johnson RM, Ravindranath Y, ElAlfy MS, Goyette G, Jr. (1994) Oxidant damage to erythrocyte membrane in glucose-6-phosphate dehydrogenase deficiency: correlation with in vivo reduced glutathione concentration and membrane protein oxidation. Blood 83 (4):1117-1123

Jonen HG (1980) Reductive and oxidative metabolism of nitrofurantoin in rat liver. Naunyn Schmiedebergs Arch Pharmacol 315 (2):167-175

Judith Recht EAaNW (2014) Safety of 8-aminoquinoline antimalarial medicines. World Health Organisation,

Kaddurah-Daouk R, Kristal BS, Weinshilboum RM (2008) Metabolomics: a global biochemical approach to drug response and disease. Annu Rev Pharmacol Toxicol 48:653-683. doi:10.1146/annurev.pharmtox.48.113006.094715

Kamakshi RV (2014) Drug-Induced Hematologic Disorders. McGraw-Hill Education,

Kelner MJ, Alexander NM (1985) Methylene blue directly oxidizes glutathione without the intermediate formation of hydrogen peroxide. J Biol Chem 260 (28):15168-15171

Khutornenko AA, Roudko VV, Chernyak BV, Vartapetian AB, Chumakov PM, Evstafieva AG (2010) Pyrimidine biosynthesis links mitochondrial respiration to the p53 pathway. Proc Natl Acad Sci U S A 107 (29):12828-12833. doi:10.1073/pnas.0910885107

Kirkiz S, Yarali N, Arman Bilir O, Tunc B (2014) Metformin-induced hemolytic anemia. Med Princ Pract 23 (2):183-185. doi:10.1159/000356149

Kramer PA, Glader BE, Li TK (1972) Mechanism of methemoglobin formation by diphenylsulfones. Effect of 4-amino-4'-hydroxyaminodiphenylsulfone and other p-substituted derivatives. Biochem Pharmacol 21 (9):1265-1274

Krishnan N, Dickman MB, Becker DF (2008) Proline modulates the intracellular redox environment and protects mammalian cells against oxidative stress. Free Radic Biol Med 44 (4):671-681. doi:10.1016/j.freeradbiomed.2007.10.054

Kwiek JJ, Haystead TA, Rudolph J (2004) Kinetic mechanism of quinone oxidoreductase 2 and its inhibition by the antimalarial quinolines. Biochemistry 43 (15):4538-4547. doi:10.1021/bi035923w

Landburg PP, Teerlink T, Biemond BJ, Brandjes DP, Muskiet FA, Duits AJ, Schnog JB (2010) Plasma asymmetric dimethylarginine concentrations in sickle cell disease are related to the hemolytic phenotype. Blood Cells Mol Dis 44 (4):229-232.

doi:10.1016/j.bcmd.2010.02.005

Lang E, Lang F (2015) Mechanisms and pathophysiological significance of eryptosis, the suicidal erythrocyte death. Semin Cell Dev Biol 39:35-42. doi:10.1016/j.semcdb.2015.01.009

Lang F, Lang E, Foller M (2012) Physiology and pathophysiology of eryptosis. Transfus Med Hemother 39 (5):308-314. doi:10.1159/000342534

Lang F, Lang KS, Lang PA, Huber SM, Wieder T (2006) Mechanisms and significance of eryptosis. Antioxid Redox Signal 8 (7-8):1183-1192. doi:10.1089/ars.2006.8.1183

Leslie T, Nahzat S, Sediqi W (2016) Epidemiology and Control of Plasmodium vivax in Afghanistan. Am J Trop Med Hyg. doi:10.4269/ajtmh.16-0172

Leung KK, Shilton BH (2013) Chloroquine binding reveals flavin redox switch function of quinone reductase 2. J Biol Chem 288 (16):11242-11251. doi:10.1074/jbc.M113.457002

Lexomboon U, Unkurapiana N (1978) Co-trimoxazole in the treatment of typhoid fever in children with glucose-6-phosphate dehydrogenase deficiency. Southeast Asian J Trop Med Public Health 9 (4):576-580

Li XQ, Bjorkman A, Andersson TB, Gustafsson LL, Masimirembwa CM (2003) Identification of human cytochrome P(450)s that metabolise anti-parasitic drugs and predictions of in vivo drug hepatic clearance from in vitro data. Eur J Clin Pharmacol 59 (5-6):429-442. doi:10.1007/s00228-003-0636-9

Long DJ, 2nd, Jaiswal AK (2000) NRH:quinone oxidoreductase2 (NQO2). Chem Biol Interact 129 (1-2):99-112

Macczak A, Cyrkler M, Bukowska B, Michalowicz J (2016) Eryptosis-inducing activity of bisphenol A and its analogs in human red blood cells (in vitro study). J Hazard Mater 307:328-335. doi:10.1016/j.jhazmat.2015.12.057

Maddocks OD, Labuschagne CF, Adams PD, Vousden KH (2016) Serine Metabolism Supports the Methionine Cycle and DNA/RNA Methylation through De Novo ATP Synthesis in Cancer Cells. Mol Cell 61 (2):210-221. doi:10.1016/j.molcel.2015.12.014

Marcsisin SR, Reichard G, Pybus BS (2016) Primaquine pharmacology in the context of CYP 2D6 pharmacogenomics: Current state of the art. Pharmacol Ther 161:1-10. doi:10.1016/j.pharmthera.2016.03.011

Mason PJ, Bautista JM, Gilsanz F (2007) G6PD deficiency: the genotype-phenotype association. Blood Rev 21 (5):267-283. doi:10.1016/j.blre.2007.05.002

McDonagh EM, Bautista JM, Youngster I, Altman RB, Klein TE (2013) PharmGKB summary: methylene blue pathway. Pharmacogenet Genomics 23 (9):498-508. doi:10.1097/FPC.0b013e32836498f4

McMillan DC, Jensen CB, Jollow DJ (1998) Role of lipid peroxidation in dapsone-induced hemolytic anemia. J Pharmacol Exp Ther 287 (3):868-876

McMillan DC, Powell CL, Bowman ZS, Morrow JD, Jollow DJ (2005) Lipids versus proteins as major targets of pro-oxidant, direct-acting hemolytic agents. Toxicol Sci 88 (1):274-283. doi:10.1093/toxsci/kfi290

McMillan DC, Simson JV, Budinsky RA, Jollow DJ (1995) Dapsone-induced hemolytic anemia: effect of dapsone hydroxylamine on sulfhydryl status, membrane skeletal proteins and morphology of human and rat erythrocytes. J Pharmacol Exp Ther 274 (1):540-547

Meir A, Kleinman Y, Rund D, Da'as N (2003) Metformin-induced hemolytic anemia in a patient with glucose-6- phosphate dehydrogenase deficiency. Diabetes Care 26 (3):956-957

Metodiewa D, Jaiswal AK, Cenas N, Dickancaite E, Segura-Aguilar J (1999) Quercetin may act as a cytotoxic prooxidant after its metabolic activation to semiquinone and quinoidal

product. Free Radic Biol Med 26 (1-2):107-116

Mitra AK, Thummel KE, Kalhorn TF, Kharasch ED, Unadkat JD, Slattery JT (1995) Metabolism of dapsone to its hydroxylamine by CYP2E1 in vitro and in vivo. Clin Pharmacol Ther 58 (5):556-566. doi:10.1016/0009-9236(95)90176-0

Mitsides N, Green D, Middleton R, New D, Lamerton E, Allen J, Redshaw J, Chadwick PR, Subudhi CP, Wood G (2014) Dapsone-induced methemoglobinemia in renal transplant recipients: more prevalent than previously thought. Transpl Infect Dis 16 (1):37-43. doi:10.1111/tid.12161

Miyazaki Y, Hara-Hotta H, Matsuyama T, Yano I (1992) Hemolysis of phosphatidylcholine-containing erythrocytes by serratamic acid from Serratia marcescens. Int J Biochem 24 (7):1033-1038

Morais Mda S, Augusto O (1993) Peroxidation of the antimalarial drug primaquine: characterization of a benzidine-like metabolite with methaemoglobin-forming activity. Xenobiotica 23 (2):133-139

Morris CR, Kuypers FA, Kato GJ, Lavrisha L, Larkin S, Singer T, Vichinsky EP (2005) Hemolysis-associated pulmonary hypertension in thalassemia. Ann N Y Acad Sci 1054:481-485. doi:10.1196/annals.1345.058

Munday R, Fowke EA (1994) Generation of superoxide radical and hydrogen peroxide by 2,3,6-triaminopyridine, a metabolite of the urinary tract analgesic phenazopyridine. Free Radic Res 21 (2):67-73

Murce E, Cuya-Guizado TR, Padilla-Chavarria HI, Franca TC, Pimentel AS (2015) Structure-based de novo design, molecular docking and molecular dynamics of primaquine analogues acting as quinone reductase II inhibitors. J Mol Graph Model 62:235-244.

doi:10.1016/j.jmgm.2015.10.001

Naiman KM (1964) RED CELL GLUCOSE-6-PHOSPHATE DEHYDROGENASE DEFICIENCY--A NEWLY RECOGNIZED CAUSE OF NEONATAL JAUNDICE AND KERNICTERUS IN CANADA. Can Med Assoc J 91 (1243):1243-1249

Narahara M, Hamada-Kanazawa M, Kouda M, Odani A, Miyake M (2010) Superoxide scavenging and xanthine oxidase inhibiting activities of copper-beta-citryl-L-glutamate complex. Biol Pharm Bull 33 (12):1938-1943

Ng JS, Edwards EM, Egelund TA (2012) Methemoglobinemia induced by rasburicase in a pediatric patient: a case report and literature review. J Oncol Pharm Pract 18 (4):425-431. doi:10.1177/1078155211429385

Nkhoma ET, Poole C, Vannappagari V, Hall SA, Beutler E (2009) The global prevalence of glucose-6-phosphate dehydrogenase deficiency: a systematic review and meta-analysis. Blood Cells Mol Dis 42 (3):267-278. doi:10.1016/j.bcmd.2008.12.005

Noonan HM, Kimbrell M, Johnson WB, Reuler JB (1983) Phenazopyridine-induced hemolytic anemia. Urology 21 (6):623-624

O'Doherty PJ, Lyons V, Tun NM, Rogers PJ, Bailey TD, Wu MJ (2014) Transcriptomic and biochemical evidence for the role of lysine biosynthesis against linoleic acid hydroperoxide-induced stress in Saccharomyces cerevisiae. Free Radic Res 48 (12):1454-1461. doi:10.3109/10715762.2014.961448

Owusu SK (1972) Acute haemolysis complicating co-trimoxazole therapy for typhoid fever in a patient with G.-6-P.D. deficiency. Lancet 2 (7781):819

Packer CD, Hornick TR, Augustine SA (2008) Fatal hemolytic anemia associated with metformin: a case report. J Med Case Rep 2:300. doi:10.1186/1752-1947-2-300

Paglia DE, Valentine WN, Nakatani M, Rauth BJ (1983) Selective accumulation of cytosol CDP-choline as an isolated erythrocyte defect in chronic hemolysis. Proc Natl Acad Sci U S A 80 (10):3081-3085

Pamba A, Richardson ND, Carter N, Duparc S, Premji Z, Tiono AB, Luzzatto L (2012) Clinical spectrum and severity of hemolytic anemia in glucose 6-phosphate dehydrogenase-deficient children receiving dapsone. Blood 120 (20):4123-4133. doi:10.1182/blood-2012-03-416032

Pandey KB, Rizvi SI (2010) Markers of oxidative stress in erythrocytes and plasma during aging in humans. Oxid Med Cell Longev 3 (1):2-12. doi:10.4161/oxim.3.1.10476

Patti GJ, Yanes O, Siuzdak G (2012) Innovation: Metabolomics: the apogee of the omics trilogy. Nat Rev Mol Cell Biol 13 (4):263-269. doi:10.1038/nrm3314

Potter BM, Xie LH, Vuong C, Zhang J, Zhang P, Duan D, Luong TL, Bandara Herath HM, Dhammika Nanayakkara NP, Tekwani BL, Walker LA, Nolan CK, Sciotti RJ, Zottig VE, Smith PL, Paris RM, Read LT, Li Q, Pybus BS, Sousa JC, Reichard GA, Marcsisin SR (2015) Differential CYP 2D6 metabolism alters primaquine pharmacokinetics. Antimicrob Agents Chemother 59 (4):2380-2387. doi:10.1128/aac.00015-15

Pui CH (2002) Rasburicase: a potent uricolytic agent. Expert Opin Pharmacother 3 (4):433-442. doi:10.1517/14656566.3.4.433

Pybus BS, Marcsisin SR, Jin X, Deye G, Sousa JC, Li Q, Caridha D, Zeng Q, Reichard GA, Ockenhouse C, Bennett J, Walker LA, Ohrt C, Melendez V (2013) The metabolism of primaquine to its active metabolite is dependent on CYP 2D6. Malar J 12:212. doi:10.1186/1475-2875-12-212

Pybus BS, Sousa JC, Jin X, Ferguson JA, Christian RE, Barnhart R, Vuong C, Sciotti RJ, Reichard

GA, Kozar MP, Walker LA, Ohrt C, Melendez V (2012) CYP450 phenotyping and accurate mass identification of metabolites of the 8-aminoquinoline, anti-malarial drug primaquine. Malar J 11:259. doi:10.1186/1475-2875-11-259

Rees DC, Kelsey H, Richards JD (1993) Acute haemolysis induced by high dose ascorbic acid in glucose-6-phosphate dehydrogenase deficiency. BMJ 306 (6881):841-842

Reinke CM, Thomas JK, Graves AH (1995) Apparent hemolysis in an AIDS patient receiving trimethoprim/sulfamethoxazole: case report and literature review. J Pharm Technol 11 (6):256-262; quiz 293-255

Rossi L, Silva JM, McGirr LG, O'Brien PJ (1988) Nitrofurantoin-mediated oxidative stress cytotoxicity in isolated rat hepatocytes. Biochem Pharmacol 37 (16):3109-3117

Ruggiero NA, Kish TD, Lee ML (2016) Metformin-Induced Hemolytic Anemia in a Patient With Glucose-6-Phosphate Dehydrogenase Deficiency. Am J Ther 23 (2):e575-578. doi:10.1097/mjt.0000000000000194

Saito K, Maekawa K, Ishikawa M, Senoo Y, Urata M, Murayama M, Nakatsu N, Yamada H, Saito Y (2014) Glucosylceramide and lysophosphatidylcholines as potential blood biomarkers for drug-induced hepatic phospholipidosis. Toxicol Sci 141 (2):377-386. doi:10.1093/toxsci/kfu132

Sastry GM, Adzhigirey M, Day T, Annabhimoju R, Sherman W (2013) Protein and ligand preparation: parameters, protocols, and influence on virtual screening enrichments. J Comput Aided Mol Des 27 (3):221-234. doi:10.1007/s10822-013-9644-8

Schepers E, Barreto DV, Liabeuf S, Glorieux G, Eloot S, Barreto FC, Massy Z, Vanholder R (2011) Symmetric dimethylarginine as a proinflammatory agent in chronic kidney disease. Clin J Am Soc Nephrol 6 (10):2374-2383. doi:10.2215/cjn.01720211

Schrimpe-Rutledge AC, Codreanu SG, Sherrod SD, McLean JA (2016) Untargeted Metabolomics Strategies-Challenges and Emerging Directions. J Am Soc Mass Spectrom 27 (12):1897-1905. doi:10.1007/s13361-016-1469-y

Schrödinger (2016a) Schrödinger Release 2016-1: Maestro S. Schrödinger, New York, NY

Schrödinger (2016b) Schrödinger Release 2016-2: LigPrep S. Schrödinger

New York, NY

Scott JM, Weir DG (1980) Drug-induced megaloblastic change. Clin Haematol 9 (3):587-606

Shakti L, Veeraraghavan B (2015) Advantage and limitations of nitrofurantoin in multi-drug resistant Indian scenario. Indian J Med Microbiol 33 (4):477-481. doi:10.4103/0255-0857.167350

Sills MR, Zinkham WH (1994) Methylene blue-induced Heinz body hemolytic anemia. Arch Pediatr Adolesc Med 148 (3):306-310

Skold A, Cosco DL, Klein R (2011) Methemoglobinemia: pathogenesis, diagnosis, and management. South Med J 104 (11):757-761. doi:10.1097/SMJ.0b013e318232139f

Soga T, Baran R, Suematsu M, Ueno Y, Ikeda S, Sakurakawa T, Kakazu Y, Ishikawa T, Robert M, Nishioka T, Tomita M (2006) Differential metabolomics reveals ophthalmic acid as an oxidative stress biomarker indicating hepatic glutathione consumption. J Biol Chem 281 (24):16768-16776. doi:10.1074/jbc.M601876200

Tain YL, Hsu CN (2017) Toxic Dimethylarginines: Asymmetric Dimethylarginine (ADMA) and Symmetric Dimethylarginine (SDMA). Toxins (Basel) 9 (3). doi:10.3390/toxins9030092

Tang HY, Ho HY, Wu PR, Chen SH, Kuypers FA, Cheng ML, Chiu DT (2015) Inability to maintain GSH pool in G6PD-deficient red cells causes futile AMPK activation and irreversible metabolic disturbance. Antioxid Redox Signal 22 (9):744-759.

doi:10.1089/ars.2014.6142

Tekwani BL, Walker LA (2006) 8-Aminoquinolines: future role as antiprotozoal drugs. Curr Opin Infect Dis 19 (6):623-631. doi:10.1097/QCO.0b013e328010b848

Terrell JR, Spruill WJ, Parish RC, Jenkins FH (1988) Phenazopyridine-induced methemoglobinemia. Drug Intell Clin Pharm 22 (11):915

Tishler M, Abramov A (1983) Phenazopyridine-induced hemolytic anemia in a patient with G6PD deficiency. Acta Haematol 70 (3):208-209

Tokarska-Schlattner M, Epand RF, Meiler F, Zandomeneghi G, Neumann D, Widmer HR, Meier BH, Epand RM, Saks V, Wallimann T, Schlattner U (2012) Phosphocreatine interacts with phospholipids, affects membrane properties and exerts membrane-protective effects. PLoS One 7 (8):e43178. doi:10.1371/journal.pone.0043178

Tweedie D, Brossi A, Chen D, Ge YW, Bailey J, Yu QS, Kamal MA, Sambamurti K, Lahiri DK, Greig NH (2006) Neurine, an acetylcholine autolysis product, elevates secreted amyloid-beta protein precursor and amyloid-beta peptide levels, and lowers neuronal cell viability in culture: a role in Alzheimer's disease? J Alzheimers Dis 10 (1):9-16

Udomratn T, Steinberg MH, Campbell GD, Jr., Oelshlegel FJ, Jr. (1977) Effects of ascorbic acid on glucose-6-phosphate dehydrogenase-deficient erythrocytes: studies in an animal model. Blood 49 (3):471-475

Vasquez-Vivar J, Augusto O (1992) Hydroxylated metabolites of the antimalarial drug primaquine. Oxidation and redox cycling. J Biol Chem 267 (10):6848-6854

Vasquez-Vivar J, Augusto O (1994) Oxidative activity of primaquine metabolites on rat erythrocytes in vitro and in vivo. Biochem Pharmacol 47 (2):309-316

Vella F, Ferry G, Delagrange P, Boutin JA (2005) NRH:quinone reductase 2: an enzyme of

surprises and mysteries. Biochem Pharmacol 71 (1-2):1-12. doi:10.1016/j.bcp.2005.09.019

Vilter RW (1980) Nutritional aspects of ascorbic acid: uses and abuses. West J Med 133 (6):485-492

Wang Y, Gray JP, Mishin V, Heck DE, Laskin DL, Laskin JD (2008) Role of cytochrome P450 reductase in nitrofurantoin-induced redox cycling and cytotoxicity. Free Radic Biol Med 44 (6):1169-1179. doi:10.1016/j.freeradbiomed.2007.12.013

Winterbourn CC (1985) Free-radical production and oxidative reactions of hemoglobin. Environ Health Perspect 64:321-330

Winther JR, Thorpe C (2014) Quantification of thiols and disulfides. Biochim Biophys Acta 1840 (2):838-846. doi:10.1016/j.bbagen.2013.03.031

Wolf R, Tuzun B, Tuzun Y (2000) Dapsone: unapproved uses or indications. Clin Dermatol 18 (1):37-53

Wright RO, Lewander WJ, Woolf AD (1999) Methemoglobinemia: etiology, pharmacology, and clinical management. Ann Emerg Med 34 (5):646-656

Xia J, Sinelnikov IV, Han B, Wishart DS (2015) MetaboAnalyst 3.0--making metabolomics more meaningful. Nucleic Acids Res 43 (W1):W251-257. doi:10.1093/nar/gkv380

Xia J, Wishart DS (2016) Using MetaboAnalyst 3.0 for Comprehensive Metabolomics Data Analysis. Curr Protoc Bioinformatics 55:14 10 11-14 10 91. doi:10.1002/cpbi.11

Xuan J, Chen S, Ning B, Tolleson WH, Guo L (2016) Development of HepG2-derived cells expressing cytochrome P450s for assessing metabolism-associated drug-induced liver toxicity. Chem Biol Interact 255:63-73. doi:10.1016/j.cbi.2015.10.009

Youngster I, Arcavi L, Schechmaster R, Akayzen Y, Popliski H, Shimonov J, Beig S, Berkovitch M (2010) Medications and glucose-6-phosphate dehydrogenase deficiency: an evidence-

based review. Drug Saf 33 (9):713-726. doi:10.2165/11536520-000000000-00000

Yu CH, Wang CH, Chang CC (2011) Chocolate-colored blood with normal artery oxygen: methemoglobinemia related to phenazopyridine. Am J Med Sci 341 (4):337. doi:10.1097/MAJ.0b013e3181df9369

Zhang Z, Gao L, Cheng Y, Jiang J, Chen Y, Jiang H, Yu H, Shan A, Cheng B (2014) Resveratrol, a natural antioxidant, has a protective effect on liver injury induced by inorganic arsenic exposure. Biomed Res Int 2014:617202. doi:10.1155/2014/617202

Zimatkin SM, Anichtchik OV (1999) Alcohol-histamine interactions. Alcohol Alcohol 34 (2):141-147

VITA

JAGRATI JAIN (M.S.)
Graduate Research Assistant,
National Centre for Natural Products,
Department of BioMolecular Sciences,
School of Pharmacy, University of Mississippi,
University, MS-38677, USA.

Educational Qualification:

Degree	Emphasis	University
Ph.D. in Pharmaceutical Sciences (August 2013-Present)	Pharmacology	University of Mississippi, USA
Master of Science (2008-10)	Biotechnology	Jiwaji University, India
Bachelor of Science (2005-08)	Chemistry; Industrial Microbiology	Bundelkhand University, India

Experience:

2013-Present: Research Assistant, National Center for Natural Products Research, University of Mississippi, University, MS.

2010-2011: Project Trainee, Development, and Maintenance of Clinical Candidate Database, GVK Biosciences Private Ltd, Hyderabad, India.

2010: MS dissertation, GVK Biosciences Private Ltd, Hyderabad, India.

Honors:

2016: 1st place in poster presentation, 4th Malaria Symposium, University of Mississippi, University, USA.

2015: Young Investigator Honorable Mention, 64th Annual ASTMH Meeting,

Philadelphia, USA.

2015: Graduate student travel fellowship, 3rd Metabolomics Workshop, University of Alabama, Birmingham, USA.

2015: 2nd place in poster presentation, 3rd Malaria Symposium, University of Mississippi, University, USA.

2015: 3rd place in poster presentation, 15th Annual ICSB meeting, Oxford, USA.

2008: Highest marks in M.S. Degree in Department of Life Sciences, GICTS College, Gwalior, India.

2004: 1st place in Science Question Forum in Rashtriya Vigyan Divas Samaroh (National Science Day celebration), District Science Club, Jhansi, India.

2003: 3rd place in Science Model Exhibition in Janpad Istareey Baal Vigyan Mahotsav (District level children science festival), District Science Club, Jhansi, India.

2002: 2nd place in Environmental Management Model in Regional Science Exhibition, Jhansi, India.

2002-2003: Ekikrat Scholarship of Uttar Pradesh government for two years.

Professional Societies and Committee Responsibilities:

2016-2017: Senate (Pharmacology Division, Department of BioMolecular Sciences), Graduate Student Council, University of Mississippi.

2016-2017: Secretary in Public Relation, Indian Student Association (ISA), University of Mississippi.

2015: Phi Kappa Phi Honor Society

2015: American Association of Pharmaceutical Scientists (AAPS)

2015: Golden Key International Honor Society

2015: American Society of Tropical Medicine & Hygiene (ASTMH) Society

2015-2016: Vice President, Indian Student Association (ISA), University of Mississippi.

Published Abstracts:

1. **Metabolic conversion of carboxy-primaquine, a major metabolite of primaquine, to potential hemotoxic intermediates.** Jagrati Jain, Narayan D Chaurasiya, Bharathi Avula, NP Dhammika Nanayakkara, James D McChesney, Ikhlas A. Khan, Larry A Walker and Babu L Tekwani. Abstract Number 850. 65th Annual Meeting, American Society of Tropical Medicine & Hygiene (ASTMH), 2016.

2. **Quercetin potentiates the toxicity of hemolytic drugs in G6PD deficient human erythrocytes.** Jagrati Jain, Narayan D Chaurasiya, NP Dhammika Nanayakkara, James D McChesney, Larry A Walker and Babu L Tekwani. Planta Med 2016; 82 - PB17

3. **NRH: Quinone Reductase 2 (NQO2) Protects Against Hemolytic Toxicity Induced by Primaquine Antimalarial in G6PD Deficient Human Erythrocytes.** Jagrati Jain, Narayan D Chaurasiya, NP Dhammika Nanayakkara, James D McChesney, Larry A Walker and Babu L Tekwani. Abstract Number 970. 64th Annual Meeting, American Society of Tropical Medicine & Hygiene (ASTMH), 2015.

4. **Effect of Quinone Reductase 2 (NQO2) Inhibitor Melatonin on Primaquine-Induced Hemolysis.** J Jain, ND Chaurasiya, R Sahu, NP Dhammika Nanayakkara, LA Walker, BL Tekwani. Planta Med 2015; 81 - PP4. DOI: 10.1055/s-0035-1545221.

5. **Inhibitors of ubiquitin E3 ligase as potential new antimalarial drug leads.** Jagrati Jain, Rajnish Sahu, Larry A Walker, Babu L Tekwani. Abstract Number 295. 63rd Annual Meeting, American Society of Tropical Medicine & Hygiene (ASTMH), 2014.

Published Research Paper:

1. Ubiquitin E3 ligase inhibitors' as potential new antimalarial drug leads. Jain J, Jain SK, Walker LA, Tekwani BL. BMC Pharmacol Toxicol. 2017 Jun 2;18(1):40.

Pending Research Papers:

1. Quercetin potentiates hemotoxic effect of hemolytic drugs in human erythrocytes. (Draft given to advisor).

2. Protective role of Quinone Reductase 2 (NQO2) in primaquine-induced hemotoxicity in human erythrocytes. (Tentative title).

3. Metabolome changes in normal and G6PD deficient human erythrocytes in response to primaquine metabolite. (Tentative title).

4. Drug-induced oxidative hemolysis (review)

Poster Presentations:

1. **Metabolic conversion of carboxy-primaquine, a major metabolite of primaquine, to potential hemotoxic intermediates.** Jagrati Jain, Narayan D Chaurasiya, Bharathi Avula, NP Dhammika Nanayakkara, James D McChesney, Ikhlas A. Khan, Larry A Walker and Babu L Tekwani. Abstract Number 850. 65th Annual Meeting, American Society of Tropical Medicine & Hygiene (ASTMH), 2016.

2. **Hemolytic Drug Metabolites Produce Eryptotic Response in G6PD Deficient Human Erythrocytes.** Jagrati Jain, Narayan D Chaurasiya, Bharathi Avula, NP Dhammika Nanayakkara, James D McChesney, Larry A Walker and Babu L Tekwani. 4th Malaria Symposium. April 25th, 2016.

3. **Metabolism and Toxicity of Carboxy-Primaquine, the Major Plasma Metabolite of Primaquine.** Jagrati Jain, Narayan D Chaurasiya, Bharathi Avula, NP Dhammika Nanayakkara, James D McChesney, Larry A Walker and Babu L Tekwani. 4th Malaria Symposium. April 25th, 2016.

4. **Quercetin potentiates eryptotic response of hemolytic drugs in G6PD deficient human erythrocytes.** Jagrati Jain, Narayan D Chaurasiya, NP Dhammika Nanayakkara, James D McChesney, Larry A Walker and Babu L Tekwani. 6th Graduate Student Council Symposium. April 15th, 2016.

5. **Quercetin potentiates the toxicity of hemolytic drugs in G6PD deficient human erythrocytes.** Jagrati Jain, Narayan D Chaurasiya, NP Dhammika Nanayakkara, James D McChesney, Larry A Walker and Babu L Tekwani. 16th Annual Oxford International Conference on the Science of Botanicals (ICSB) Meeting. April 11th - 14th, 2016.

6. **NRH: Quinone Reductase 2 (NQO2) Protects Against Hemolytic Toxicity Induced by Primaquine Antimalarial in G6PD Deficient Human Erythrocytes.** Jagrati Jain, Narayan D Chaurasiya, NP Dhammika Nanayakkara, James D McChesney, Larry A Walker and Babu L Tekwani. Abstract Number 970. 64th Annual Meeting, American Society of Tropical Medicine & Hygiene (ASTMH), 2015. October 25th – 29th, 2015.

7. **Protective role of NRH: Quinone Reductase 2 (NQO2) in Primaquine-induced hemolytic toxicity.** Jagrati Jain, Narayan D Chaurasiya, NP Dhammika Nanayakkara, James D McChesney, Larry A Walker and Babu L Tekwani. Drug Discovery and Development Colloquium (DDDC). June 22nd-24th, 2015.

8. **Investigating the mechanism of Primaquine-induced hemolytic toxicity with natural product inhibitors of NRH: Quinone Reductase 2 (NQO2).** Jagrati Jain, Narayan D Chaurasiya, NP Dhammika Nanayakkara, James D McChesney, Larry A Walker and Babu L Tekwani. 42nd Annual Meeting, Medicinal Chemistry-Pharmacognosy Meeting-Miniature (MALTO). May 17th-19th, 2014.

9. **Inhibitors of Ubiquitin E3 ligase arrest the growth of *Plasmodium falciparum* at**

trophozoite stage. Jagrati Jain, Larry A. Walker, Babu L. Tekwani. 3rd Malaria Symposium. April 22nd, 2015.

10. **Effect of Quinone Reductase 2 (NQO2) Inhibitor on Primaquine-Induced Hemolytic Toxicity.** Jagrati Jain, Narayan D Chaurasiya, NP Dhammika Nanayakkara, James D McChesney, Larry A Walker and Babu L Tekwani. 3rd Malaria Symposium. April 22nd, 2015.

11. **Effect of Quinone Reductase 2 (NQO2) Inhibitor Melatonin on Primaquine-Induced Hemolysis.** Jagrati Jain, Narayan D Chaurasiya, NP Dhammika Nanayakkara, Larry A Walker and Babu L Tekwani. 15th Annual Oxford International Conference on the Science of Botanicals (ICSB). April 13th - 16th, 2015.

12. **Inhibitors of ubiquitin E3 ligase as potential new antimalarial drug leads.** Jagrati Jain, Rajnish Sahu, Larry A. Walker, Babu L. Tekwani. Abstract Number 295. 63rd Annual Meeting, American Society of Tropical Medicine & Hygiene (ASTMH). November 3rd, 2014.

13. **Inhibitors of ubiquitin e3 ligase as potential new antimalarial drug leads.** Jagrati Jain, Rajnish Sahu, Larry A. Walker, Babu L. Tekwani. 41st Annual Meeting, Medicinal Chemistry-Pharmacognosy Meeting-Miniature (MALTO). May 18th-20th, 2014.

Podium Presentations:

1. **Biochemical and molecular assessment of toxicity of Primaquine (PQ) metabolites on human erythrocytes.** Prospectus defense. February 7th, 2017. School of Pharmacy, University of Mississippi.

2. **Unraveling pathways for hemolytic toxicity of nitrofurantoin in human erythrocytes.** Original research proposal (ORP) defense. May 4th, 2016. School of Pharmacy, University of Mississippi

3. **Targeting ubiquitin-dependent protein degradation pathway of *Plasmodium falciparum*: Evaluation of the antimalarial activity of the inhibitors of ubiquitin E3 ligase.** Jagrati Jain, Rajnish Sahu, Larry A. Walker, Babu L. Tekwani. 2nd Malaria Symposium. April 24th, 2014.

Conferences Attended:

1. **American Society of Tropical Medicine & Hygiene (ASTMH),** 65th Annual Meeting, November 13th-17th, 2016 at Atlanta Marriott Marquis and Hilton Atlanta, Atlanta, Georgia USA.

2. **4th Malaria Symposium.** April 25th, 2016. E. F. Yerby Conference Center, Grove Loop, University, MS USA.

3. **Oxford International Conference on the Science of Botanicals (ICSB)** 16th Annual Meeting. April 11th - 14th, 2016. Oxford Conference Center, Oxford, MS USA.

4. **American Society of Tropical Medicine & Hygiene (ASTMH)**, 64th Annual Meeting, October 25th – 29th, 2015 at Philadelphia Marriott Downtown, Philadelphia, Pennsylvania, USA.

5. **Drug Discovery and Development Colloquium (DDDC),** June 22nd-24th, 2015. Thad Cochran Research Center, University, Mississippi, USA.

6. Medicinal Chemistry-Pharmacognosy Meeting-Miniature **(MALTO)** 42nd Annual Meeting, May 17th-19th, 2014 – University of Mississippi, University, Mississippi, USA.

7. **3rd Malaria Symposium**. April 22nd, 2015. E. F. Yerby Conference Center, Grove Loop, University, Mississippi, USA.

8. **Oxford International Conference on the Science of Botanicals (ICSB)** 15th Annual Meeting. April 13th - 16th, 2015. Oxford Conference Center, Oxford, Mississippi, USA.

9. **Southern Central Chapter of the Society of Toxicology Meeting**, 2014 Fall Annual Meeting. October 23th-24th, 2014. University of Mississippi, University, Mississippi, USA.

10. **American Society of Tropical Medicine & Hygiene (ASTMH)**, 63rd Annual Meeting, November 2th-6th, 2014, Sheraton New Orleans and the New Orleans Marriott, New Orleans, Louisiana, USA.

11. **The American Society of Pharmacognosy (ASP)**, 55th Annual Meeting, August 2nd-6th, 2014, Oxford Conference Center, Oxford, Mississippi, USA.

12. **Medicinal Chemistry-Pharmacognosy Meeting-Miniature (MALTO)** 41st Annual Meeting, May 18th-20th, 2014. The University of Tennessee Health Science Center, Memphis, Tennessee, USA.

13. **2nd Malaria Symposium**. April 24th, 2014. E. F. Yerby Conference Center, Grove Loop, University, Mississippi, USA.

14. **1st Malaria Symposium**. April 2013. E. F. Yerby Conference Center, Grove Loop,

University, Mississippi, USA.

Technical/Scientific Workshops Attended:

1. **Metabolomics Workshop**. June 14th- 18th, 2015. University of Alabama, Birmingham, Tennessee, USA.

2. **EuPathDB Workshop**. June 17th- 20th, 2012. University of Georgia, Athens, Georgia, USA.